Design

of Steel-to-Concrete Joints

Design Manual I

František Wald
Jan Hofmann
Ulrike Kuhlmann
et al

Design
of Steel-to-Concrete Joints

Design Manual I

Design of steel-to-concrete joints, Design manual I

Contents

Symbols

<u>Lower case</u>

a   factor considering the shoulder width, length

b   length

c   minimum edge distance, effective width, length

$c_{cr,N}$ critical edge distance, $c_{cr,N} = 1.5\ h_{ef}$

c_w drag coefficient

d   diameter

d_b diameter of the bolt

d_h diameter of the head of headed stud

d_s diameter of the shaft of headed stud

$d_{s,re}$ diameter of the stirrup

$d_{s,nom}$ nominal diameter of the anchor shaft

d_w diameter of the washer

$e_{x,y}$ length between the bolt axis and the edge of the plate

e   eccentricity

f_{bd} design bond strength according to EN1992-1-1:2004

f_{cd} design strength of concrete

f_{ck} characteristic strength of concrete

$f_{ck,cube}$ characteristic square strength of concrete

f_u strength of structural steel

f_{ub} strength of the bolt

f_{uk} characteristic strength of steel

f_y nominal yield strength of steel

f_{ya} average yield strength

f_{yb} nominal value of yield strength of the bolt

f_{yd} design yield strength of steel

$f_{yd,re}$ design yield strength of the stirrups

f_{yk} characteristic yield strength of steel

h   height

h_{ef} effective embedment depth according to product specifications

k   coefficient depending on the type of forming

k_1 factor for concrete cone strength in case of headed studs

k_2 factor for the headed studs for component P

k_A factor considering the cross-section

k_a form factor at porous edge sections

k_b stiffness of the bolt

$k_{b,re}$ bond stiffness due to supplementary reinforcement, stirrups

k_{C1} stiffness due to the displacement of the anchorage in case of concrete cone failure with supplementary reinforcement, combination C1

k_{C2} stiffness due to the displacement of the head, due to the pressure under the head on the concrete, and steel elongation, combination C2

$k_{c,de}$ stiffness of the descending branch for component CC

$k_{c,soft}$ stiffness of the concrete cone in the softening branch

k_j concentration factor

k_p stiffness coefficient of the plate

$k_{p,de}$ stiffness of the descending branch for component P

k_s stiffness of the anchor shaft for component S

$k_{s,re}$ steel stiffness due to supplementary reinforcement, stirrups

k_v empirical value depending on the type of anchor

l_1 anchorage length

l_{ep} elongated length

l_{eff} effective length of T-stub, defined in accordance with EN1993 1-8:2006

$l_{v,eff}$ effective length of shear area

m   distance between threaded and headed studs

m_{pl} plastic moment resistance per unit, defined as $m_{pl} = \frac{0.25 \cdot t_f^2 \cdot f_y}{\gamma_{M0}}$

n   location of the prying force, number

n_{re} total number of legs of stirrups

p   internal pressure

r   radius of the fillet of a rolled profile

s   actual spacing of anchors

$s_{cr,N}$	critical spacing for anchors
t	thickness
t_f	thickness of the T-stub, flange
t_w	thickness of T-stub, column
t_{p1}	thickness of the anchor plate
t_{p2}	thickness of the base plate
w_{fic}	fictive effective width
x	distance between the anchor and the crack on the concrete surface assuming a crack propagation from the stirrup of the supplementary reinforcement to the concrete surface with an angle of 35°
z	distance of tension/compressed part

Upper case

A	cross section area
A_{c0}	loaded area
A_{c1}	maximum spread area
$A_{c,N}$	actual projected area of concrete cone of the anchorage at the concrete surface, limited by overlapping concrete cones of adjacent anchors ($s < s_{cr,N}$), as well as by edges of the concrete member ($c < c_{cr,N}$)
$A_{c,N}^0$	reference area of the concrete cone of an individual anchor with large spacing and edge distance projected on the concrete surface
A_{eff}	effective area
A_h	area on the head of the headed stud
A_{net}	net cross section area
A_s	tensile stress area in the bolt
$A_{s,nom}$	nominal cross section area of all shafts
$A_{s,re}$	nominal cross section area of all legs of the stirrups
$B_{t,Rd}$	design tension resistance of a single bolt-plate assembly $$B_{t,Rd} = 0.9 \cdot f_{ub} \cdot A_s / \gamma_{Mb}$$
D	diameter of column
E	modulus of elasticity the steel $E = 210\,000$ MPa
F	force or load
$F_{c.Rd}$	resistance of compressed part

F_d	design load
F_k	characteristic load
F_{memb}	axial force
$F_{t.Ed}$	external tensile force
$F_{t.Rd}$	external ultimate resistance
$F_{T.Rd}$	resistance of tension part
I	moment of inertia
I_t	torsion constant
K	general stiffness
L	length
L_b	length of anchor bolt
L_{cr}	buckling length
L_D	the elongation length of the bolt, which may be taken as the total grip length (thickness of material plus washers) plus half the sum of the height of the bolt head and the height of the nut
L_h	length of the anchor shaft
$I_{p,bp}$	equivalent moment of inertia
$M_{c,Rd}$	bending moment capacity
$M_{j,Rd}$	design moment resistance of a joint
$M_{N,Rd}$	interaction resistance bending with compression
$M_{pl.Rd}$	plastic moment resistance defined as $M_{pl,Rd} = l_{eff} \cdot m_{pl}$
$M_{t,Rd}$	torsion capacity
N_{act}	actual load on the anchor
$N_{b,Rd}$	design buckling resistance
N_{cr}	critical buckling load
N_{Ed}	tension/compression load
N_{ETA}	tension load for which the displacements are derived in the product specifications
$N_{pl,Rd}$	design capacity in tension/compression
N_{Rd}	design capacity
$N_{Rd,b,re}$	design tension resistance for bond failure of stirrups
$N_{Rd.C3}$	design failure load or the combined model
$N_{Rd,c}$	design tension resistance for concrete cone failure of headed stud

$N_{Rd,cs}$	design failure load for the concrete strut	
$N_{Rd,p}$	design tension resistance for pull out failure of headed stud	
$N_{Rd,re}$	design failure load for the supplementary reinforcement	
$N_{Rd,s}$	design tension resistance for steel failure of headed stud	
$N_{Rd,s,re}$	design tension resistance for steel failure of stirrups	
$N_{Rk,c}^0$	characteristic resistance of a single anchor without edge and spacing effects	
N_u	ultimate resistance	
N_y	yielding resistance	
Q	prying force	
R_d	design capacity	
R_k	characteristic resistance	
S_i	elastic stiffness	
$S_{j,ini}$	initial stiffness	
V_{ETA}	shear load for which the displacements are derived in the product specifications	
$V_{pl,Rd}$	shear capacity	
V_{Rd}	design failure load for the anchor under shear	
$V_{Rd,c}$	design shear resistance for concrete cone failure	
$V_{Rd,cp}$	design shear resistance for concrete pryout	
$V_{Rd,p}$	design shear resistance for pullout	
$V_{Rd,s}$	design shear resistance for steel failure	
W_e	external work	
W_{eff}	section modulus of effective area	
W_{el}	elastic section modulus	
W_i	internal work	
W_{pl}	plastic section modulus	

Greek symbols

α	factor according to EN1992:2006 for hook effect and large concrete cover
α_c	factor of component concrete break out in tension
α_p	factor for the component head pressing
α_s	factor of component stirrups
β_j	material coefficient
γ_F	partial safety factor for actions
γ_M	material safety factor
γ_{Mb}	partial safety factor for bolts $\gamma_{Mb} = 1.25$
γ_{Mc}	partial safety factor for concrete $\gamma_{Mc} = 1.5$
γ_{Ms}	partial safety factor for steel $\gamma_{Ms} = 1.15$
γ_{MV}	partial safety factor for shear resistance of studs $\gamma_{MV} = 1.25$
γ_{Mw}	partial safety factor for welds $\gamma_{Mw} = 1.25$
γ_{M0}	partial safety factor for resistance of Class 1, 2 or 3 cross-sections $\gamma_{M0} = 1.0$
γ_{M1}	partial safety factor for resistance of a member to buckling $\gamma_{M1} = 1.0$
γ_{M2}	partial safety factor resistance of net section at bolt holes $\gamma_{M2} = 1.25$
δ	deformation, displacement
δ_{act}	displacement corresponding to N_{act}
δ_c	displacement corresponding to N_{act} for concrete cone
δ_f	corresponding displacement at failure load $N_{Rd,sre}$ or $N_{Rd,bre}$
$\delta_{N,ETA}$	displacement given in the product specifications for a corresponding tension load
$\delta_{Rd,b,re}$	deformation corresponding to design resistance for bond failure of stirrups
$\delta_{Rd,c}$	deformation corresponding to design resistance for concrete cone failure
$\delta_{Rd,p}$	deformation corresponding to design resistance for pull out failure
$\delta_{Rd,s}$	deformation corresponding to N_{Rd}
$\delta_{Rd,s}$	deformation corresponding to design resistance for steel failure
$\delta_{Rd,s,re}$	deformation corresponding to design resistance for steel failure of stirrups

$\delta_{Rd,sy}$	deformation corresponding to design yield resistance for steel failure		cr	critical
			d	design
δ_u	elongation		e	external
$\delta_{V,ETA}$	displacement given in the product specifications for a corresponding shear load		eff	effective
			ETA	European technical approval
			g	grout
$\epsilon_{bu,re}$	strain limit for the stirrups due to bond		h	head
ϵ_{su}	ultimate design strain limit for steel		i	internal
$\epsilon_{su,re}$	strain limit for the stirrups under tension		k	characteristic
			lim	limit
$\epsilon_{su,re}$	strain limit for the stirrups under tension		Mc	material concrete
ϵ_u	ultimate strain		Ms	material steel
θ	angle		N	tension
λ	slenderness of member		nom	nominal
μ	coefficient of friction		po	pullout
ν	Poisson`s ratio, $\nu = 0.30$		p	plate
σ	stress		pl	plastic
c	reduction factor		Rd	resistance design
$\psi_{A,N}$	factor accounting for geometric effects in anchor group, $\psi_{A,N} = A_{c,N}/A_{c,N}^0$		Rk	characteristic resistance
			re	failure
			rec	reinforcement
$\psi_{re,N}$	factor accounting for negative effect of closely spaced reinforcement in the concrete member on strength of anchors with $h_{ef} < 100$ mm		Sd	internal design
			s	shaft of anchor, stud
			soft	softening
$\psi_{s,N}$	factor accounting for the influence of edges of the concrete member on the distribution of stresses in the concrete $\psi_{s,N} = 0.7 + 0.,3 \cdot c/c_{cr,N} \leq 1.0$		supp	support
			T	tension part
			t	tension
ψ_{supp}	support factor considering the confinement of the stirrups $\psi_{supp} = 2.5 - x/h_{ef} \geq 1.0$		tot	total
			p	plate
			p1	anchor plate
Φ	rotation		p2	base plate
			u	ultimate

Subscripts

A	area		uk	characteristic ultimate
act	actual		V	shear
b	bolt, bond		w	column web
bd	design bond		x, y	directions
c	column, concrete		y	yield
cb	concrete block		yd	design yield
ck	characteristic concrete		yk	characteristic yield
cp	concrete pry out			
cs	concrete strut			

1 INTRODUCTION

The mixed building technology allows to utilise the best performance of all structural materials available such as steel, concrete, timber and glass. Therefore the building are nowadays seldom designed from only one structural material. Engineers of steel structures in practice are often faced with the question of economical design of steel to concrete joints, because some structural elements, such as foundations, stair cases and fire protection walls, are optimal of concrete. A gap in knowledge between the design of fastenings in concrete and steel design was abridged by standardized joint solutions developed in the INFASO project, which profit from the advantage of steel as a very flexible and applicable material and allow an intelligent connection between steel and concrete building elements. The requirements for such joint solutions are easy fabrication, quick erection, applicability in existing structures, high loading capacity and sufficient deformation capacity. One joint solution is the use of anchor plates with welded headed studs or other fasteners such as post-installed anchors. Thereby a steel beam can be connected by butt straps, cams or a beam end plate connected by threaded bolts on the steel plate encased in concrete. Examples of typical joint solutions for simple steel-to-concrete joints, column bases and composite joints are shown in Fig. 1.1.

a)   b)   c)
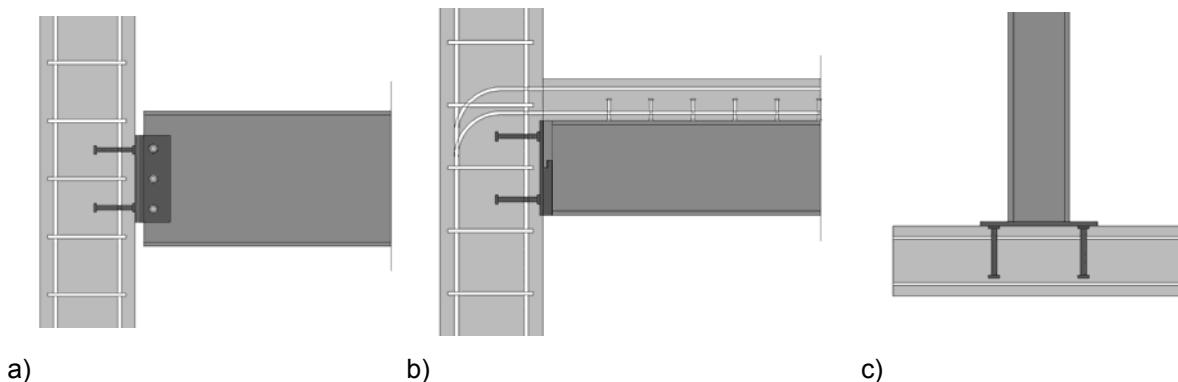
Fig. 1.1 Examples for steel-to-concrete joints,
a) simple joint, b) composite joint, c) column bases

The Design Manual I gives an overview of the existing design rules and introduces components developed. To present the use of the developed design rules, worked examples are given within the Design Manual I. More detailed information about the background documents, the experiments and development of the new design rules might be found in the final report, (Kuhlman et al 2013) and in Design manual II. This manual is focused to more complex worked examples, the application of a software tool for design, sensitivity study of proposed analytical models and its boundary conditions as well as design tables of optimal solutions.

Chapter 2 gives a general overview about the component method and presents the existing models for steel-to-concrete joints. It also includes a short summary of the joint models and components developed in the project. In Chapter 3 and Chapter 4 the concrete and the steel components for the modelling of steel-to-concrete joints are described in more detail. The components already described in the codes as well as components of the newly derived models are introduced. Values for stiffness and resistance are presented. In Chapter 5 the single components are assembled to evaluate the overall joint resistance. Chapter 6 shows how the joint stiffness can be derived due to the stiffness's of the single components. For the global analysis of a structure the joint behaviour/stiffness may have an influence. The effects of the joint modelling on the global analysis are explained in Chapter 7. The tolerances for steel-to-concrete joints and their effect on the construction are discussed in Chapter 8. In the Chapter 9 worked examples for the whole range of the steel-to-concrete joints are prepared. This examples are demonstrating the possibilities of the new design rules and allow an easy

access for the engineers in practice. The references are given to this Design manual I (DM I) and to Eurocodes (EN199x-1-x). Chapter 10 summarises the offered opportunity for innovations.

Chapters 1 and 2 were prepared by U. Kuhlman and J. Ruopp, Chapter 3 by J. Hofmann and A. Sharma, Chapters 4, 5 and 6 by F. Wald, Bečková Š. and Schwarz I., Chapter 7 by da Silva L. Simoes, H. Gervásio and J. Henriques and F. Gentili and Chapter 8 by M. Krimpmann. The worked examples 9.1 to 9.3 were set by Š. Bečková and I. Schwarz, 9.4 by Š. Bečková, I. Schwarz and M. Krimpmann, 9.5 by J. Ruopp, 9.6 and 9.7 by J. Henriques and F. Gentili, with help of the headed studs design models by A. Sharma.

2 COMPONENT METHOD FOR STEEL TO CONCRETE JOINTS

2.1 Design method

In the past decades, the component method has been set as a unified approach for the efficient analysis of steel and composite joints, see (Da Silva 2008). The basic principle of the component method consists of determining the complex non-linear joint response through the subdivision into basic joint components. The joint can be regarded as a set of individual basic components that contribute to its structural behaviour by means of resistance, stiffness and deformation capacity. The component method allows designers to take options more efficiently because the contribution of each component to the joint behaviour may be optimized according to the limiting components. Thus, one of the main advantages of the component method is that the analysis of an individual component can be done independently of the type of joint. In a second calculation step the single components are assembled by the designers according to the joint configuration.

Joint components may be divided by the type of loading. Accordingly, three groups of components are usually identified: components for tension, compression and shear. Additionally, a second division may be done according to their location: panel zone or connecting zone. In Fig. 2.1 these two definitions are illustrated based on a double sided composite joint.
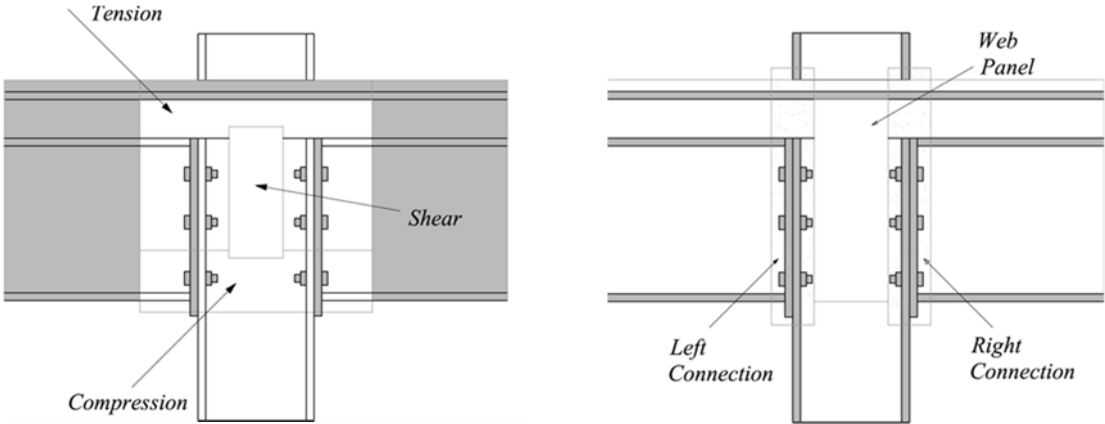

Fig. 2.1 Division of joint into groups and zones

In practice these components are modelled by translational springs with non-linear force-deformation response that are exposed to internal forces. The joint may then be represented by a spring model as illustrated in Fig. 2.2.
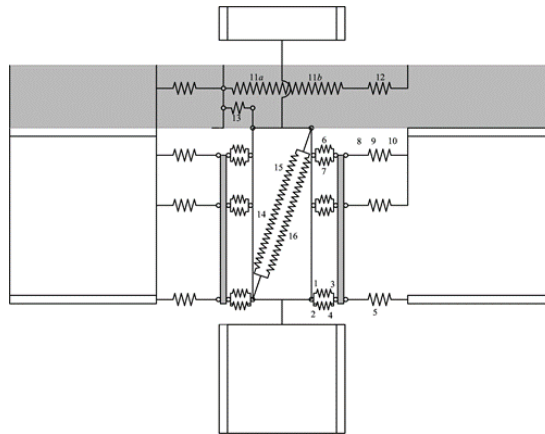
Fig. 2.2 Component model for composite joint with separated the panel zone in shear

The component method is given by EN1993-1-8:2006 and EN1994-1-1:2010 for the analysis of steel and composite joints. The application of the method requires following steps:

1. Identification of the basic joint components
2. Characterization of the structural properties of the basic joint components
3. Assembly of the component properties

In the referred codes, a list of basic joint components is provided for the most common joint configurations. Basic joint components are then characterized in terms of strength, stiffness and deformation capacity allowing to obtain the F-δ curve, see Fig. 2.3, reproducing its behaviour. Finally, through the assembly procedure the joint properties are determined. The joint behaviour may be later reproduced by an M-Φ curve, see Fig. 2.4, in the structural analysis.
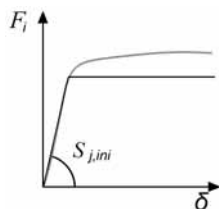
Fig. 2.3 Component force deformation, F-δ, curve, experiment in black and model in grey line
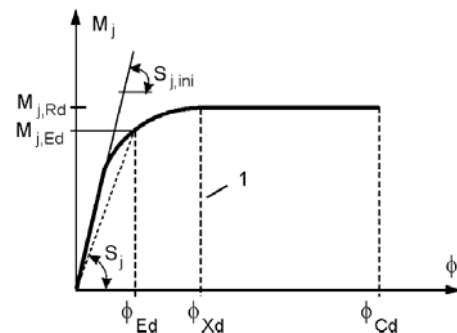
Fig. 2.4 Joint moment rotation, M-Φ, curve experiment in black and model in grey line

2.2 Classification of joints

2.2.1 Global analyses

The classification of the joints is prepared to examine the extent to which the stiffness or strength have to be considered in the calculation according the design accuracy. In total there are three different calculation methods which require different joint properties. These calculation methods and the joint properties are compared within Tab. 2.1Tab. 2.1 Relation between method of global analysis and considered joint behaviour

Method of global analysis	Considered joint behaviour
Elastic	
Rigid plastic	
Elastic plastic	

Elastic method

If the elastic calculation method is applied, only the joint stiffness S_j is considered. S_j is implemented in the structural calculation as spring element or one-dimensional beam element in order to determine the internal forces. If the bending moment does not exceed 2/3 of the moment resistance of the joint the initial stiffness $S_{j,ini}$ can be used to describe the elastic behaviour. For calculations, where the plastic moment capacity is reached, the joint stiffness can be calculated with the secant stiffness $S_{j,ini}/\mu$. The joints are classified for this method by taking into consideration the rotational stiffness.

Rigid plastic method

In the second calculation method the elastic behaviour of the joint is neglected. Internal forces of the structural calculation are calculated from 1st order plastic hinge theory only satisfying equilibrium conditions. Within this method only the plastic moment capacity is considered, but the joints must have sufficient deformation capacity to allow full plastic redistribution. In this case the joints are classified by the resistance.

Elastic plastic method

If the third method is applied the overall moment-rotation-relationship of the joint has to be considered. This relationship is used within the joint modelling of the structural calculation. For simplification a bilinear approach of the moment rotation curve may be used. Typically the reduced secant stiffness is applied. If the elastic plastic method is used, the joint has to be classified by stiffness and strength.

The advantages of this method are shown in the following example. In Fig. 2.5 a steel frame with horizontal and vertical loading is shown. Instead of modelling the column bases as a pinned joint as it is common in practice, the column bases may be classified as semi-rigid and modelled with a rotational spring. Thereby the column bases may stabilise the structure and reduce the bending moment in the steel-to-steel beam to column joints. So a classification of the column bases as semi-rigid instead of pinned makes the steel structure more safe and economical.

14
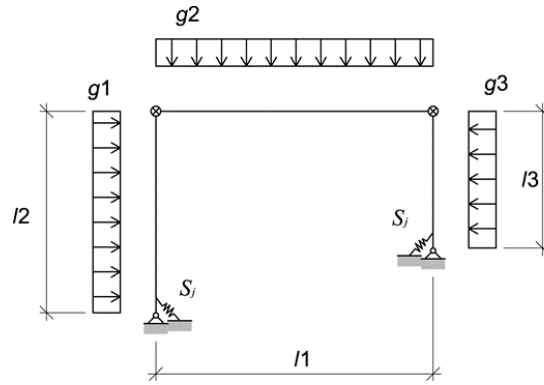
Fig. 2.5 Considering the rotation stiffness of joints with springs

It is also important not to underestimate the stiffness of the column bases, because big rotational stiffness might cause unexpected high bending moments in the joints which may lead to failure. The classification of the joints, may be found in cl 5 of EN1993-1-8:2006 and is explained in the following section.

2.2.2 Stiffness

The first part of this chapter deals with the classification of beam to column/wall and beam to beam joints, the second part with the classification of column bases. Depending on its initial rotational stiffness $S_{j,ini}$ a joint may be classified as pinned, rigid or semi-rigid. Normally pinned joints can transfer axial and shear force. Rotation of the joint does not cause significant bending moments. If a joint cannot be classified as normally pinned or rigid it is classified as semi-rigid. Rigid joints have a rotational stiffness which legitimise to treat the joint as rigid in the global analysis.
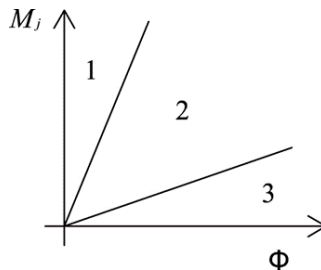
Fig. 2.6 Classification due to stiffness

Joints classified according to the connecting beams

Rigid joints, in Fig. 2.6 zone 1, is classified as rigid if

$$S_{j,ini} \geq K_b \ E \ I_b / L_b \tag{2.1}$$

If a bracing system reduces the horizontal displacement more than 80 %, then $K_b = 8$. For other frames provided that in every storey the following equation (2.2) is valid, then $K_b = 25$.

$$\frac{K_b}{K_c} \geq 0.1 \tag{2.2}$$

<u>Semi-rigid joints</u>, in Fig. 2.6 zone 2, are all joints which are not classified as pinned or rigid. For frames where Eq. 2.3 applies the joints should be classified as semi rigid and not as rigid.

$$\frac{K_b}{K_c} < 0.1 \tag{2.3}$$

<u>Nominally pinned joints</u>, in Fig. 2.6 zone 3, are expecting to have a limited bending stiffness compared to the bending stiffness of the connected beam.

$$S_{j,ini} \leq 0.5 \cdot E \cdot I_b / L_b \tag{2.4}$$

where

K_b is mean value of I_b / L_b for all the beams at the top of that storey
K_c is mean value of I_c / L_c for all columns of that storey
I_b is the second moment of area of beam
I_c is the second moment of area of column
L_b is the span of beam
L_c is the storey height of a column

<u>Column bases classified according to the connecting column</u>

Column bases are classified as rigid if the following conditions are satisfied. There are two possible cases which have to be considered. If there is an additional bracing in a frame and the additional bracing reduces the horizontal movement at least by 80 %, then the column base affects the accuracy of the column design, which depends on the column relative slenderness. This column base might be assumed as rigid according to EN1993-1-8:2006 cl. 5.2a, if

$$\bar{\lambda}_0 \leq 0.5 \tag{2.5}$$

for

$$0.5 < \bar{\lambda}_0 < 3.93 \text{ is } S_{j,ini} \geq 7 \left(2\,\bar{\lambda}_0 - 1\right) E\,I_c / L_c \tag{2.6}$$

and for

$$\bar{\lambda}_0 \geq 3.93 \text{ and } S_{j,ini} \geq 48\,E\,I_c / L_c \tag{2.7}$$

where

$\bar{\lambda}_0$ is the relative slenderness of a column in which both ends are assumed as pinned.

For all other constructions, the cases where the storey´s sway is not prevented, the column base might be classified according to cl. 5.2d in EN1993-1-8:2006 as rigid if

$$S_{j,ini} \geq 30\,EI_c / L_c \tag{2.8}$$

2.2.3   Strength

A joint is classified for strength as pinned, full-strength or partial-strength, see Tab. 2.1 and Fig. 2.7. The classification by strength may be found in EN1993-1-8:2006 cl 5.2.3. <u>Nominally pinned joint </u>should have a design moment resistance less than 25 % of the design moment resistance, which would be required for a full-strength joint. They must have sufficient rotational capacity. A <u>Partial-strength joint</u> is a joint, which cannot be classified as pinned or full-strength.

16

The design moment resistance of a <u>full-strength joint</u> is bigger than the design moment resistance of the beam or column connected to it.
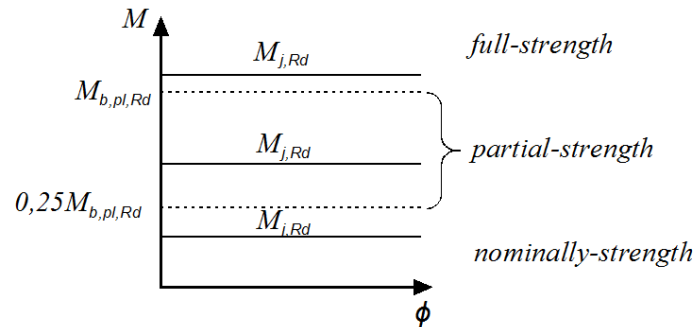

Fig. 2.7 Classification due to resistance

If the design resistance of the beam $M_{b,pl,Rd}$ is smaller than the design resistance of the column $M_{c,pl,Rd}$, $M_{b,pl,Rd}$ is replaced for connections at the top of a column by $M_{c,pl,Rd}$ see Fig. 2.7. If the design resistance of the beam $M_{b,pl,Rd}$ is smaller than the double design resistance of the column $M_{c,pl,Rd}$ than in the figure above $M_{b,pl,Rd}$ is replaced for connections within the column height by $2\,M_{c,pl,Rd}$.

2.2.4 Deformation capacity

In EN1993-1-8:2006 an explicit classification for deformation or rotational capacity of the joint is not implemented. The complexity on classification according to deformation capacity is in the lack of knowledge of the upper values of material properties by designers, which do not allow a safe prediction of the failing component. In EN 1993-1-8 cl 6.4 design rules for the rotation capacity are given based on best engineering practice. If the system is calculated with a plastic global analysis a sufficient rotation capacity is needed. No investigation of the rotation capacity of the joint is necessary, if the moment resistance of the joint $M_{j,Rd}$ is at least 20 % bigger than the plastic moment resistance $M_{pl,Rd}$ of the connected beam, see (2.9). Then the plastic hinge appears in the beam and the rotational capacity has to be satisfied by the beam section.

$$M_{j,Rd} \geq 1.2 \cdot M_{pl,Rd} \tag{2.9}$$

If the moment resistance of the joint is not 1.2 times the plastic moment resistance of the connected beam and a plastic hinge is assumed in the joint, minimum rotational capacities for bolted and welded joints have to be checked.

Bolted joints

The rules for bolted joints may be found in EN1993-1-8:2006 cl 6.4.2. A bolted joint is assumed to have a sufficient rotation capacity if following conditions can be applied:

If the failure load $M_{j,Rd}$ is determined by the resistance of the column web panel and for this panel $d/t_w \leq 69\,\varepsilon$

where

d is the nominal bolt diameter and
t_w is the thickness of the web

If the thickness of the flange of the column or the beam end plate is sufficiently thin to satisfy the following formula.

$$t \leq 0.36 \, d \sqrt{f_{ub}/f_y} \tag{2.10}$$

where
f_{ub} is ultimate strength of the bolts
f_y is yield strength of the flange or the end plate

Welded joints

The rules for welded joints may also be found in EN1993-1-8:2006 cl 6.4. For a welded beam to column connection the rotation capacity $\emptyset_{Cd}$ may be calculated with the following equation. In this case the web has to be stiffened in the compression area but not in the tension are and the moment resistance is not determined by the resistance of the column web panel.

$$\emptyset_{Cd} = 0.025 \, h_c/h_b \tag{2.11}$$

where
h_c is the depth of the column
h_b is the depth of the beam

For a welded beam to column connection where the compression and the tension area in the column are not stiffened, the rotation capacity may be assumed to be at least 0.015 rad.

2.3   Steel-to-concrete joints

2.3.1   Available models

Design models for steel-to-concrete joints are currently available in the three standard documents:

EN1993-1-8:2006 includes values for stiffness and resistance for all steel components and values for stiffness and resistance for concrete components in compression. There are no rules for concrete components in tension or shear.

EN1994-1-1:2010 enhancement of the rules from EN 1993-1-8 on composite joints such as the connection of composite girder to steel columns.

CEN/TS 1992-4-1:2009 summarises values for the design resistance of fasteners in concrete. But no values for stiffness and ductility are available.

2.3.2   Steel and composite structures

Design rules in the Eurocode are given for different joint configurations. The model for the column bases is described in the EN1993-1-8:2006 and the model for the composite joint in EN1994-1-1:2010.

Column bases with base plates

The analytical prediction model for column base with base plate is described in the EN1993-1-8:2006. With these design rules column bases loaded by axial force and bending moments are calculated. The model is only including concrete components for the compression forces.

For the tension force only steel components are considered. The design resistance of column bases with steel base plates is described in EN1993-1-8:2006, cl 6.2.8. First according to the eccentricity of the axial force e and the geometry of the column base one of the four loading types is chosen, and the lever arm z is calculated. For this see Tab. 2.2. Then the loading of the tension and the compression components are calculated. The failure load is determined by the weakest activated component. These components are for:

Tension

Base plate in bending under tension	cl 6.2.6.11 in EN1993-1-8
Anchor bolt in tension	cl 6.2.6.12 in EN1993-1-8
Column web in tension	cl 6.2.6.8 in EN1993-1-8

Compression

Base plate in bending under compression	cl 6.2.6.10 in EN1993-1-8
Concrete in compression	cl 6.2.6.9 in EN1993-1-8
Column web and flange in compression	cl 6.2.6.7 in EN1993-1-8

Shear

Anchor bolts in shear	cl 6.2.2.6 to 6.2.2.9 in EN1993-1-8

According to procedure in EN1993-1-8:2006 cl 6.3.4 one of the four cases of the loading and geometry is chosen, see Tab.2.2. Then the rotational stiffness is calculated. One complexity creates change of the loading type depending on the loading cases. From this different rotational stiffness values for different combinations of bending moment and axial forces are resulting. The design of the embedded column base according to Eurocodes was developed by (Pertold et al, 2000) based on set of tests and finite element modelling. This model is prepared to approve resistance to combine base plate with embedding.
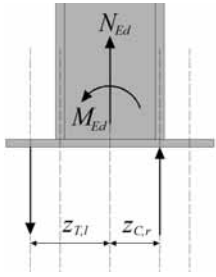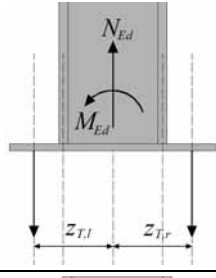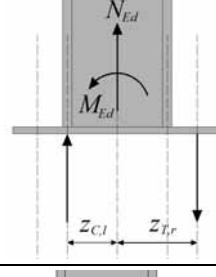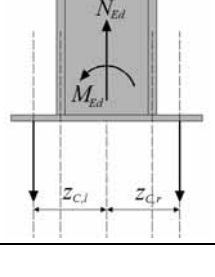
Composite joints

The composite joint is described in the Section 8 in EN1994-1-1:2010. The composite joint may be used for the connection of composite beams to steel columns. The design rules are an enhancement of the rules according to EN1993-1-8:2006 and new components are added. These additional components are:

- Longitudinal steel reinforcement in tension	cl. 8.4.2.1 EN1994-1-1:2010
- Steel contact plate in compression	cl 8.4.2.2 EN1994-1-1:2010
- Column web in transverse compression	cl 8.4.3 EN1994-1-1:2010
- Reinforced components	cl 8.4.4 EN1994-1-1:2010
- Column web panel in shear	cl 8.4.4.1 EN1994-1-1:2010
- Column web in compression	cl 8.4.4.2 EN1994-1-1:2010

For all other components EN1993-1-8:2006 is applied.

Tab. 2.2 The loading situations for the definition of the lever arm

Number	Description of loading	Sketch	Explanation
1	Left side in tension Right side in compression $z = z_{T,l} + z_{C,r}$		Bending moment is dominating
2	Left side in tension Right side in tension $z = z_{T,l} + z_{T,r}$		Tensile force is dominating
3	Left side in compression Right side in tension $z = z_{C,l} + z_{T,r}$		Bending moment is dominating
4	Left side in compression Right side in compression $z = z_{C,l} + z_{C,r}$		Compression force is dominating
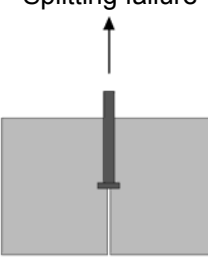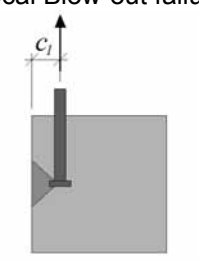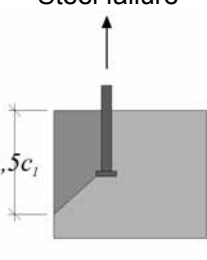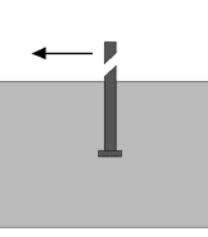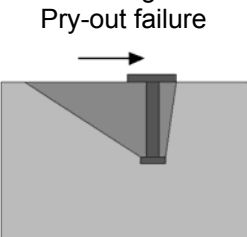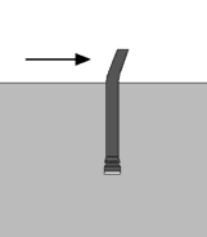
Fig. 2.8 Composite joint

Tab. 2.3 Failure modes observed for anchors in concrete

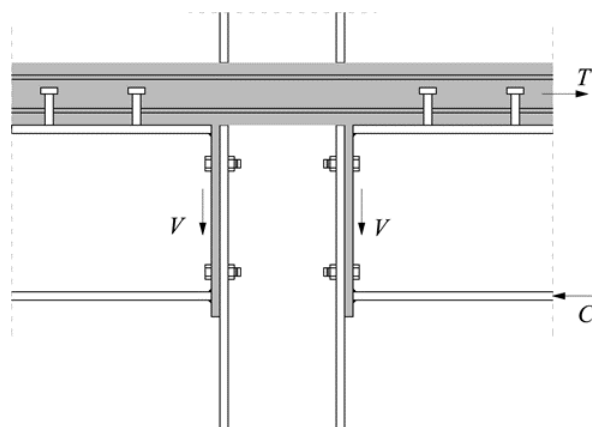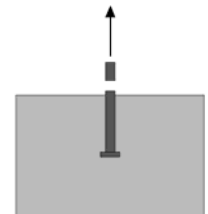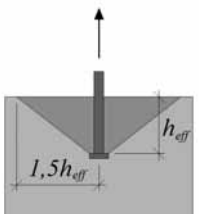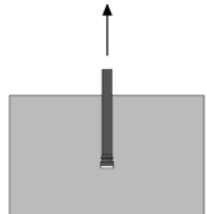| Loading	Failure modes		
Tension	Steel failure Concrete cone failure h_{eff} $1,5h_{eff}$ Pull-out / Pull-through Splitting failure Local Blow-out failure c_1 Steel failure $1,5c_1$		
Shear	Steel failure Concrete edge failure Pry-out failure Pull-out failure		

2.3.3 Concrete structures

In CEN/TS1992-4-1:2009 the design of fastenings in concrete is given. In these rules the failure modes of the fasteners and the concrete are described in a detailed way. For tension and shear loading various failure modes exist. Failure modes are given according to CEN/TS 1992-4-1:2009, see Tab. 2.3.. All possible failure modes are determined. The smallest resistance defines the design resistance of the joint. The design rules for the resistance include different types of geometries. Also edge effects, concrete with and without cracks and different kinds of fasteners are considered. However for stiffness no design rules are given and the use of additional stirrups is covered in a very conservative way.

2.3.4 Components for joints with anchor plate

Headed studs in tension / Headed studs with stirrups in tension

Load-displacement-curves of test specimens have shown, that in cases were additional reinforcement is used, also other components besides the reinforcement have a contribution on the overall load bearing capacity of the fixture. If, for instance, the reinforcement starts to yield, compression struts may develop and a small concrete cone failure can be the decisive component. With the design model the interaction of the concrete cone and the stirrups is considered. This allows the increase of the design resistance and the determination of the stiffness of the two combined components concrete cone and stirrups in tension in cases, where both of them are interacting. In Fig. 2.9 a headed stud with additional reinforcement and the assembly of single components is shown.

21

Headed stud failure in tension

Pull-out failure

Concrete cone failure with stirrups in tension
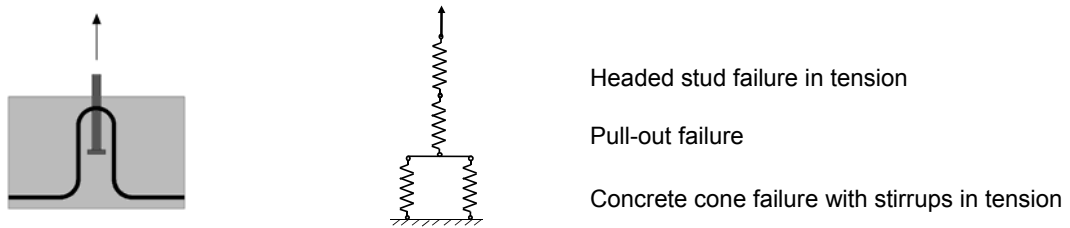
Fig. 2.9 Component headed studs with stirrups in tension

Embedded plate in tension

Ductile behaviour and a larger rotation capacity of column bases can be initiated with a thin anchor plate in combination with a base plate welded to the end of the column. In Fig. 2.10 three different kinds of geometries of embedded plates are shown, see Kuhlman et al, 2013.
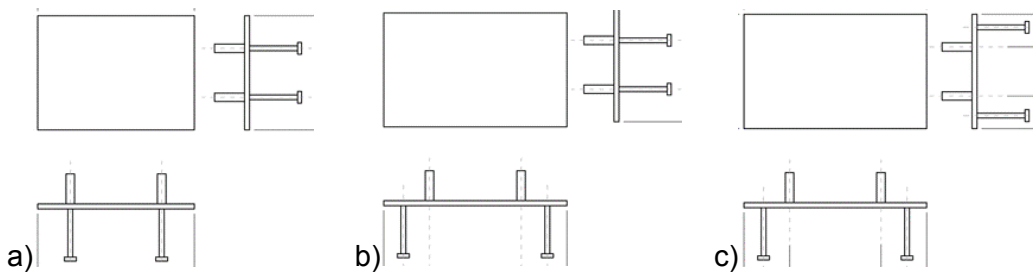
Fig. 2.10 Example of different positions of headed and treaded studs,
a) above, b) in distance in one major direction, c) in distance in general

The headed studs are welded on the bottom side of the base plate to connect the thin plate to the concrete. The column base plate is connected to the anchor plate by the threaded bolts. If the threaded bolts and the headed studs are in one line like, see Fig. 2.10, the anchor plate has no influence on the behaviour of the joint. If the threaded bolts and the headed studs are not in one line the anchor plate is activated. The model of the embedded plate represents an additional failure mode for the T-stub in tension. If the T-stub reaches its limit state, the thin base plate may still increase its capacity due to the membrane effect. The component embedded plate in tension shows a ductile behaviour as large deformations occur before failure. A detailed explanation of this component is given in Chapter 7.

The Tab. 2.4 summarises the components, which are used to model the simple and rigid steel beam to concrete column/wall joints and column bases using anchor plates.

Tab. 2.4 Components for joints with anchor plates

Component	Headed stud in tension	Concrete breakout in tension	Stirrups in tension	Pull-out failure of the headed stud	Headed stud in shear
Figure					
Chapter	3.1.1	3.1.2	3.1.4	3.1.5	3.1.6

Component	Friction	Concrete in compression	Concrete panel in shear	Longitudinal steel	Slip of the composite beam

				reinforcement in tension	
Figure					
Chapter	3.3.7	3.4	3.5	3.6	3.7

Component	Threaded studs in tension/ shear	Punching of the anchor plate	Anchor plate in bending and tension	Colum/beam flange and web in compression	Steel contact plate
Figure					
Chapter	4.7	4.3	4.4	4.5	4.6

3 COMPONENTS IN CONCRETE

3.1 Component model for headed studs

For components embedded in concrete the displacement behaviour and therefore the F-δ–curve is influenced by the concrete properties itself and the interaction between the anchorage and the concrete. The influence of concrete on the behaviour of anchorages in tension have to be considered. The scatter in concrete is much larger than that observed for the material steel, see (Pallarés and Hajjar, 2009).

For design, a material safety factor for concrete according to EN1992-1-1:2004 of $\gamma_{Mc} = 1.5$ is used. The characteristic values for the resistances are derived by assuming a normal distribution and a probability of 90 % for the 5 % fractal that corresponds to the characteristic value. The given displacements and stiffness's are mean values and can scatter with coefficient of variation up to 50 %.

The complete F-δ–curve for the design of a headed stud in tension is described by a rheological model using and combining different components for the headed stud. The individual components for anchorages with supplementary reinforcement are:

Component S   Steel failure of the headed stud ($\delta_{Rd,s}$ / $N_{Rd,s}$)
Component CC   Concrete cone failure ($\delta_{Rd,c}$ / $N_{Rd,c}$)
Component RS   Steel failure of the stirrups ($\delta_{Rd,s,re}$ / $N_{Rd,s,re}$)
Component RB   Bond failure of the stirrups ($\delta_{Rd,b,re}$ / $N_{Rd,b,re}$)
Component P   Pull out failure of the headed stud ($\delta_{Rd,p}$ / $N_{Rd,p}$)

The combination is given in Fig. 3.1.

a) with supplementary reinforcement   b) without supplementary reinforcement
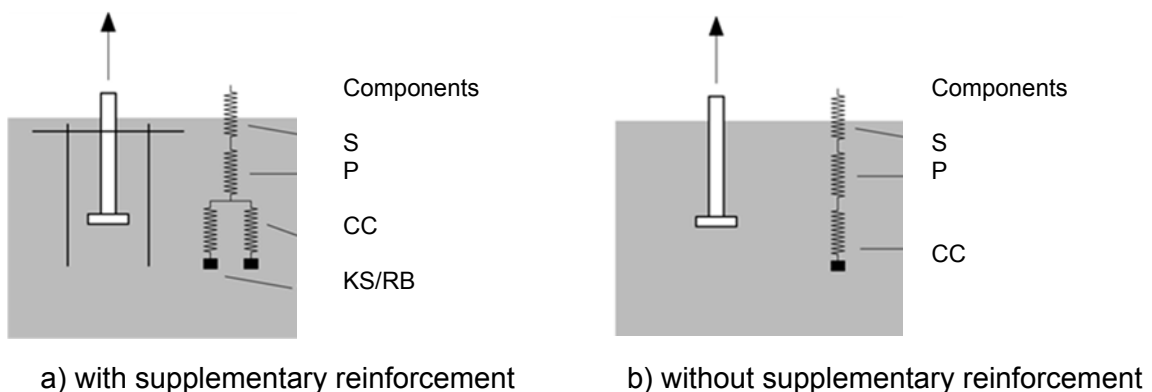
Fig. 3.1 Spring models for the different components of anchorages embedded in concrete

3.1.1 Headed studs in tension, component S

If a headed stud is loaded in tension, the load is first transferred from the loading point at the base plate to the bearing areas of the headed stud. Therefore the shaft will elongate up to the design yielding strength $f_{yd} = f_{yk}/\gamma_{Ms}$. For design the behaviour is assumed as linear elastic up to the yielding load of the headed stud. The corresponding elongation due to the introduced stress is calculated with the equation using the Hooke´s law. The elongation corresponding to the yield load is given by

$$\delta_{Rd,sy} = \frac{N_{Rd,s} \, L_h}{A_{s,nom} \, E_s} = \frac{\sigma_{Rd,s} \, L_h}{E_s} \; [mm] \tag{3.1}$$

where

L_h is length of the anchor shaft [mm]
$N_{Rd,s}$ is design tension resistance of the headed stud [N]
E_s is elastic modulus of the steel, $E_s = 210\,000$ N/mm² [N/mm²]
$A_{s,nom}$ is nominal cross section area of all shafts

$$A_{s,nom} = \frac{\pi \, d_{s,nom}^2}{4} \; [mm²] \tag{3.2}$$

where

$d_{s,nom}$ is nominal diameter of the shaft [mm]

The design load at steel yielding failure is calculated as given below

$$N_{Rd,s} = A_{s,nom} \, \frac{f_{uk}}{\gamma_{Ms}} = n \, \pi \left(\frac{d_{s,nom}^2}{4} \right) \frac{f_{uk}}{\gamma_{Ms}} \; [N] \tag{3.3}$$

where

f_{uk} is characteristic ultimate strength of the shaft material of the headed stud [N/mm²]
n is number of headed studs in tension [-]
γ_{Ms} is partial safety factor for steel [-]

Exceeding the design steel yielding strength f_{yd}, the elongation will strongly increase without a significant increase in load up to a design strain limit ε_{su}. For the design, this increase of strength is neglected on the safe side and the stiffness is assumed to be zero, $k_s = 0$ N/mm. Depending on the product the failure shall be assumed at the yielding point. In general, fasteners as headed studs are deemed to have an elongation capacity of at least $\varepsilon_{su} = 0.8$ %. This limit shall be used to determine the response of the fasteners unless it is proven by means of tests that they have a higher elongation capacity.

Therefore the stiffness k_s is described as given below depending on the displacement or load

$$k_{s1} = \frac{A_{s,nom} \, E_s}{L_h} \text{ for } N_{act} < N_{Rd,sy} \; [N/mm] \tag{3.4}$$

$$k_{s2} = 0 \text{ for } \delta \geq \delta_{Rd,sy} \leq e_{su} \text{ and } N_{act} = N_{Rd,sy} \; [N/mm] \tag{3.5}$$

where

$\delta_{Rd,sy}$ is displacement at yielding of the shaft, see Eq. (3.1) [mm]
ε_{su} is maximum elongation capacity of the shaft, 0.8 % [-]

3.1.2 Headed studs in tension, component CC

The component concrete breakout in tension is described using the design load $N_{Rd,c}$ for concrete cone failure and the displacement in the softening branch after failure. Up to the design load the component can´t be assumed as absolutely rigid without any displacement. The displacement corresponding to design load is given by

$$\delta_{Rd,c1} = \frac{N_{Rd,c}}{k_{c,pp}} \text{ [mm]} \tag{3.6}$$

The design load at concrete cone failure is calculated as

$$N_{Rd,c} = N_{Rk,c}^0 \, \psi_{A,N} \, \psi_{s,N} \, \frac{\psi_{re,N}}{\gamma_{Mc}} \text{ [N]} \tag{3.7}$$

where
$N_{Rk,c}^0$ is characteristic resistance of a single anchor without edge and spacing effects

$$N_{Rk,c}^0 = k_1 \, h_{ef}^{1.5} \, f_{ck}^{0.5} \text{ [N]} \tag{3.8}$$

where
k_1 is basic factor 8.9 for cracked concrete and 12.7 for non-cracked concrete [-]
h_{ef} is embedment depth given according to the product specifications [mm]
f_{ck} is characteristic concrete strength according to EN206-1:2000 [N/mm²]
$\psi_{A,N}$ is factor accounting for the geometric effects of spacing and edge distance [-]

$$\psi_{A,N} = \frac{A_{c,N}}{A_{c,N}^0} \text{ [-]} \tag{3.9}$$

where

$\psi_{s,N}$ is factor accounting for the influence of edges of the concrete member on the distribution of stresses in the concrete

$$\psi_{s,N} = 0.7 \, + \, 0.3 \, \frac{c}{c_{cr,N}} \leq 1 \, [-] \tag{3.10}$$

where
$\psi_{re,N}$ is factor accounting for the negative effect of closely spaced reinforcement in the concrete member on the strength of anchors with an embedment depth $h_{ef} < 100$ mm
$0.5 + h_{ef} / 200$ for $s < 150$ mm (for any diameter) [-]
                             or $s < 100$ mm (for $d_s \leq 10$ mm)
1.0   for $s \geq 150$ mm (for any diameter) [-]
γ_{Mc} is 1.5 for concrete [-]
$A_{c,N}^0$ is reference area of the concrete cone of an individual anchor with large spacing and edge distance projected on the concrete surface [mm²]. The concrete cone is idealized as a pyramid with a height equal to h_{ef} and a base length equal to $s_{cr,N}$ with

$$s_{cr,N} \, = \, 3.0 \, h_{ef} \text{ [mm]} \tag{3.11}$$

$$c_{cr,N} \, = \, 0.5 \, s_{cr,N} \, = \, 1.5 \, h_{ef} \text{ [mm]} \tag{3.12}$$

where
$A_{c,N}$ is actual projected area of concrete cone of the anchorage at the concrete surface, limited by overlapping concrete cones of adjacent anchors, $s < s_{cr,N}$, as well as by edges of the concrete member, $c < c_{cr,N}$. It may be deduced from the idealized failure cones of single anchors [mm²]

To avoid a local blow out failure the edge distance shall be larger than $0.5 \, h_{ef}$. Due to sudden and brittle failure, the initial stiffness for concrete cone is considered as infinity, i.e. till the actual load, N_{act} is less than or equal to the design tension resistance for concrete cone, the

displacement δ_c is zero. Once the design load is exceeded, the displacement increases with decreasing load, descending branch. Thus, the load-displacement behaviour in case of concrete cone breakout is idealized as shown in Fig. 3.2.
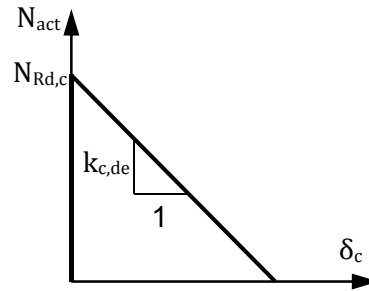
Fig. 3.2 Idealized load-displacement relationship for concrete cone breakout in tension

The stiffness of the descending branch $k_{c,de}$ for the design is described with the following function

$$k_{c,de} = \alpha_c \sqrt{f_{ck}\, h_{ef}} \cdot \psi_{A,N} \cdot \psi_{s,N} \cdot \psi_{re,N} \text{ [N/mm]} \qquad (3.13)$$

where

α_c is factor of component concrete break out in tension, currently $\alpha_c = -537$
h_{ef} is embedment depth of the anchorage [mm]
f_{ck} is characteristic concrete compressive strength [N/mm²]
$A_{c,N}$ is projected surface of the concrete cone [mm²]
$A^0_{c,N}$ projected surface of the concrete cone of a single anchorage [mm²]

The displacement δ_c as a function of the acting load N_{act} is described using the design resistance and the stiffness of the descending branch.

For ascending part

$$N_{act} \leq N_{Rd,c} \text{ and } \delta_c = 0 \qquad (3.14)$$

For descending branch

$$\delta_c > 0 \text{ mm and } \delta_c = \frac{N_{act} - N_{Rd,c}}{k_{c,de}} \qquad (3.15)$$

3.1.3   Stirrups in tension, component RS

The component stirrups in tension was developed based on empirical studies. Therefore the tests results were evaluated to determine the displacement of the stirrups depending on the load N_{act} acting on the stirrup. The displacement is determined like given in the following equation

$$\delta_{Rd,s,re} = \frac{2\, N^2_{Rd,s,re}}{\alpha_s\, f_{ck}\, d^4_{s,re}\, n^2_{re}} \text{ [mm]} \qquad (3.16)$$

where

27

α_s is factor of the component stirrups, currently $\alpha_s = 12\ 100$ [-]

$N_{Rd,s,re}$ is design tension resistance of the stirrups for tension failure [N]

$d_{s,re}$ is nominal diameter of thereinforcement leg [mm]

f_{ck} is characteristic concrete compressive strength [N/mm²]

n_{re} is total number of legs of stirrups [-]

The design load for yielding of the stirrups is determined as given

$$N_{Rd,s,re} = A_{s,re} f_{yd,re} = n_{re}\ \pi\ \left(\frac{d_{s,re}^2}{4}\right) f_{yd,re} \text{ [N]} \qquad (3.17)$$

where

$A_{s,re}$ is nominal cross section area of all legs of the stirrups [mm²]

$d_{s,re}$ is nominal diameter of the stirrups [mm]

f_{yd} is design yield strength of the shaft material of the headed stud [N/mm²]

n_{re} is total number of legs of stirrups [-]

Exceeding the design steel yielding strength $f_{yd,re}$ the elongation will increase with no significant increase of the load up to a strain limit $\varepsilon_{su,re}$ of the stirrups. For the design this increase of strength is neglected on the safe side. In general reinforcement steel stirrups shall have an elongation capacity of at least $\varepsilon_{su,re} = 2,5$ %. So the design strain limit $\varepsilon_{su,re}$ is assumed to be 2.5 %. The displacement as a function of the acting load is determined as

$$k_{s,re1} = \frac{\sqrt{n_{re}^2\ \alpha_s\ f_{ck}\ d_{s,re}^4}}{\sqrt{2\ \delta}} \quad \text{for } \delta < \delta_{Rd,s,re} \text{ [N/mm]} \qquad (3.18)$$

$$k_{s,re2} = 0 \quad \text{for } \delta \geq \delta_{Rd,s,re} \leq \varepsilon_{su,re} \text{ [N/mm]} \qquad (3.19)$$

3.1.4 Stirrups in tension - bond failure, component RB

The displacement of the concrete component stirrups in tension is determined under the assumption that bond failure of the stirrups will occur. This displacement is calculated with equation (3.19) as

$$\delta_{Rd,b,re} = \frac{2\ N_{Rd,b,re}^2}{\alpha_s\ f_{ck}\ d_{s,re}^4\ n_{re}^2} \text{ [mm]} \qquad (3.20)$$

where

α_s is factor of the component stirrups, currently $\alpha_s = 12\ 100$ [-]

$N_{Rd,b,re}$ is design tension resistance of the stirrups for bond failure [N]

$d_{s,re}$ is nominal diameter of the stirrups [mm]

f_{ck} is characteristic concrete compressive strength [N/mm²]

The design anchorage capacity of the stirrups according CEN/TS-model [5] is determined the design tension resistance of the stirrups for bond failure

$$N_{Rd,b,re} = \sum n_{s,re}\ \left(\frac{l_1\ \pi\ d_{s,re}\ f_{bd}}{\alpha}\right) \text{ [N]} \qquad (3.21)$$

where

$n_{s,re}$ is number of legs [-]

l_1 is anchorage length [mm]
$d_{s,re}$ is nominal diameter of the stirrups [mm]
f_{bd} is design bond strength according to EN1992-1-1:2004 [N/mm²]
α is factor according to EN1992-1-1:2004 for hook effect and large concrete cover, currently $0.7 \cdot 0.7 = 0.49$ [-]

$$k_{b,re1} = \frac{\sqrt{n_{re}^2 \; \alpha_s \; f_{ck} \; d_{s,re}^4}}{\sqrt{2 \, \delta}} \quad \text{for } \delta < \delta_{Rd,b,re} \;\; [\text{N/mm}] \tag{3.22}$$

$$k_{b,re2} = 0 \quad \text{for } \delta \geq \delta_{Rd,b,re} \leq \varepsilon_{su,re} \;\; [\text{N/mm}] \tag{3.23}$$

3.1.5   Headed studs in tension, component P

The pull out failure of the headed studs will take place if the local stresses at the head are larger than the local design resistance. Up to this level the displacement of the headed stud will increase due to the increasing pressure under the head.

$$\delta_{Rd,p,1} = k_p \cdot \left(\frac{N_{Rd,c}}{A_h \cdot f_{ck} \cdot n} \right)^2 \; [\text{mm}] \tag{3.24}$$

$$\delta_{Rd,p,2} = 2 \, k_p \cdot \left(\frac{\min \, (N_{Rd,p}; N_{Rd,re})}{A_h \cdot f_{ck} \cdot n} \right)^2 - \delta_{Rd,p,1} \; [\text{mm}] \tag{3.25}$$

$$k_p = \alpha_p \cdot \frac{k_a \cdot k_A}{k_2} \; [-] \tag{3.26}$$

where
A_h is area on the head of the headed stud [mm²]

$$A_h = \frac{\pi}{4} \cdot (d_h^2 - d_s{}^2) \tag{3.27}$$

where
k_a is form factor at porous edge sections [-]

$$k_a = \sqrt{5/a} \geq 1 \tag{3.28}$$

where
a_p is factor considering the shoulder width [mm]

$$a_p = 0.5 \cdot (d_h - d_s) \tag{3.29}$$

where
k_A is factor considering the cross section depending on factor k_a [-]

$$k_A = 0.5 \cdot \sqrt{d_s^2 + m \cdot \left(d_h^2 - d_s^2 \right)} - 0.5 \cdot d_h \tag{3.30}$$

where
n   is number of the headed studs [-]

α_p is factor of the component head pressing, currently is $\alpha_p = 0.25$ [-]

k_2 is factor for the headed studs in non-cracked concrete, currently 600 [-]

       is factor for the headed studs in cracked concrete, currently 300 [-]

m   is pressing relation, $m = 9$ for headed studs [-]

d_h is diameter of the head [mm]

d_s is diameter of the shaft [mm]

$N_{Rd,p}$ is design load at failure in cases of pull out

$$N_{Rd,p} = n \, p_{uk} \, A_h / \gamma_{Mc} \tag{3.31}$$

where

p_{uk} is characteristic ultimate bearing pressure at the headed of stud [N/mm²]

$N_{Rd,c}$ is design load for concrete cone failure without supplementary reinforcement

$$N_{Rd,c} = N_{Rk,c}^0 \, \psi_{A,N} \, \psi_{s,N} \, \frac{\psi_{re,N}}{\gamma_{Mc}} \ \text{[N]} \tag{3.32}$$

where

$N_{Rd,re}$ design load at failure of the supplementary reinforcement minimum value of

$$N_{Rd,s,re} = A_{s,re} \, f_{yd,re} = n \, \pi \, \frac{d_{s,re}^2}{4} \, f_{yd,re} \ \text{and} \ N_{Rd,b,re} = \sum_{n_{s,re}} \frac{l_1 \cdot \pi \cdot d_{s,re} \cdot f_{bd}}{\alpha} \ \text{[N]} \tag{3.33}$$

The stiffness as a function of the displacement is determined as

$$k_{p,1} = \sqrt{\frac{(A_h \, f_{ck} \, n)^2}{\delta_{act} \, k_p}} \ \text{[N/mm]} \tag{3.34}$$

$$k_{p,2} = \sqrt{\frac{(A_h \, f_{ck} \, n)^2 \, (\delta + \delta_{Rd,p1})}{2 \, \delta_{act}^2 \, k_p}} \ \text{[N/mm]} \tag{3.35}$$

$$k_{p,3} = \min(N_{Rd,p}; N_{Rd,re})/\delta + k_{p,pp}[1 - \delta_{Rd,p,2}/\delta] \ \text{[N/mm]} \tag{3.36}$$

The stiffness $k_{p,de}$ depends on the failure modes. If the supplementary reinforcement fails by yielding ($N_{Rd,s,re} < N_{Rd,b,re}$ and $N_{Rd,s,re} < N_{Rd,p}$) the design stiffness $k_{p,de}$ is assumed as 10^4 N/mm², negative due to descending branch.

In all other cases (e.g. $N_{Rd,s,re} > N_{Rd,b,re}$ or $N_{Rd,s,re} > N_{Rd,p}$) $k_{p,de}$ shall be assumed as infinite due to brittle failure. The stiffness in case of pull out failure is calculated using the minimum value of the stiffness's calculated with equation (3.34) to (3.36).

$$k_{p,de} = \min(k_{p,1}; k_{p,2}; k_{p,3}) \ \text{[N/mm]} \tag{3.37}$$

3.1.6   Headed studs in shear, component V

The load-displacement behaviour mainly depends on the pressure to the concrete near the surface of the concrete member. Due to concrete crushing at the surface of the concrete member, the displacement under shear loading varies very large with a coefficient of variation about 40 % to 50 %. However a semi-empirical calculation shows that the displacement at failure mainly depends on the acting loading, the diameter of the anchors and the embedment

depth. Therefore the displacement under shear loading for a given load level is calculated, see (Hofmann 2005), using the following equation only as an estimation

$$\delta_{Rd,v} = k_v \; \frac{\sqrt{V_{Rd}}}{d} \; h_{ef}^{0.5} \; [mm] \qquad (3.38)$$

where
k_v empirical value depending on the type of anchor [-], for headed studs k_v = 2 to 4
V_{Rd} design failure load as the minimum of the design failure loads calculated for the different failure modes ($V_{Rd,s}$, $V_{Rd,cp}$, $V_{Rd,c}$, $V_{Rd,p}$) given according to the technical product specification CEN/TS 1992-4-1 or (FIB Bulletin 58, 2011)

The displacement at ultimate load up three times larger than the displacement at the design load level due to the assumption, that the concrete near the surface is not fully crushed at design load level.

3.2   Combination of components

To come up with the total stiffness of the connection with headed studs anchored in concrete with or without supplementary reinforcement, the stiffness's must be combined. The combination depends on whether the components are acting in parallel, equal displacements, or in serial, equal load. Three combinations are given, see (Hofmann, 2005):

Combination C1
Concrete cone failure with or without supplementary reinforcement, $k_{s,re}$ = 0 and $k_{b,re}$ = 0

Combination C2
Displacement due to steel elongation and head pressure, pull out

Combination C3
Total connection of headed studs anchored in concrete with supplementary reinforcement
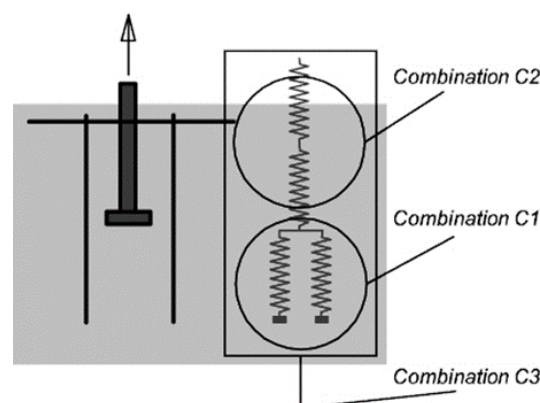

Fig. 3.3 Combinations of different single components
for an anchorage with supplementary reinforcement

3.2.1   Combination of concrete cone and stirrups, C1 = CC + RS/RB

If both components are summarized, the load is calculated using the sum of the loads at the same displacement δ due to the combination of the components using a parallel connection

from the rheological view. Two ranges must be considered. The first range is up to the load level at concrete failure $N_{Rd,c}$ the second up to a load level of failure of the stirrups $N_{Rd,s,re}$ or $N_{Rd,b,re}$.

$$k_{C1.1} = k_{c1} + k_{s,re} = \infty \text{ for } N_{act} \leq N_{Rd,c} \text{ [N/mm]}$$ (3.39)

This leads to the following equation

$$k_{C1.1} = \frac{\sqrt{n_{re}^2 \, \alpha_s \, f_{ck} \, d_{s,re}^4}}{\sqrt{2 \, \delta}} \text{ for } N_{act} \leq N_{Rd,c} \text{ [N/mm]}$$ (3.40)

In the second range the load is transferred to the stirrups and the stiffness decreases. The stiffness is calculated if N_{act} is larger than $N_{Rd,c}$ with the following equation

$$k_{C1.2} = k_{c2} + k_{s,re} \text{ for } N_{act} > N_{Rd,c} \text{ [N/mm]}$$ (3.41)

This leads to a relative complex equation

$$k_{C1.2} = \frac{N_{Rd,c}}{\delta} + k_{c,de} - k_{c,de} \frac{\delta_{Rd,c1}}{\delta} + \frac{\sqrt{n_{re}^2 \, \alpha_s \, f_{ck} \, d_{s,re}^4}}{\sqrt{2 \, \delta}}$$ (3.42)

$$\text{for } N_{act} < N_{Rd,s,re} < N_{Rd,b,re} \text{ [N/mm]}$$

If the load exceeds the ultimate load given by $N_{Rd,s,re}$ or $N_{Rd,b,re}$ the stiffness of the stirrups are negligible. Therefore the following equation applies:

$$k_{C1.3} = k_c + k_{s,re} = 0 \text{ for } N_{act} = N_{Rd,s,re} \geq N_{Rd,b,re} \text{ [N/mm]}$$ (3.43)

3.2.2   Combination of steel and pullout, C2 = S + P

If both components are summarized the load is calculated using the sum of the displacements at the same load N_{act} due to the combination of the components using a serial connection from the rheological view. This is done by summing up the stiffness's as given below

$$k_{C2} = \left(\frac{1}{k_s} + \frac{1}{k_p}\right)^{-1} \text{ [N/mm]}$$ (3.44)

This loads to the following equation

$$k_{C2} = \left(\frac{L_h}{A_{s,nom} \, E_s} + \frac{1}{k_p}\right)^{-1} = \left(\frac{L_h}{A_{s,nom} \, E_s} + \frac{1}{\min(k_{p1}; k_{p2}; k_{p3})}\right)^{-1} \text{ [N/mm]}$$ (3.45)

where
k_p is the minimum stiffness in case of pullout failure as the minimum of k_{p1}, k_{p2} and k_{p3}

32

3.2.3 Combination of all components, C3 = CC + RS/RB + P +S

To model the whole load- displacement curve of a headed stud embedded in concrete with a supplementary reinforcement the following components are combined:

concrete and stirrups in tension, components CC and RB/RS, as combination C1,
shaft of headed stud in tension, component S, and
pull-out failure of the headed stud component P as Combination 2.

The combinations C1 and C2 is added by building the sum of displacements. This is due to the serial function of both components. That means that these components are loaded with the same load but the response concerning the displacement is different. The combination of the components using a serial connection leads to the following stiffness of the whole anchorage in tension:

$$1/k_{C3} = 1/k_{C1} + 1/k_{C2} \text{ [N/mm]} \tag{3.46}$$

where
k_{C1} is the stiffness due to the displacement of the anchorage in case of concrete cone failure with supplementary reinforcement, see combination C1 [N/mm], if no supplementary reinforcement is provided k_{C1} is equal to k_c
k_{C2} is the stiffness due to the displacement of the head, due to the pressure under the head on the concrete, and steel elongation, see combination C2 [N/mm]

3.2.4 Design failure load

In principle two failure modes are possible to determine the design failure load $N_{Rd,C3}$ for the combined model. These modes are failure of

the concrete strut $N_{Rd,cs}$,

the supplementary reinforcement $N_{Rd,re}$.

The design failure load in cases of concrete strut failure is calculated using the design load in case of concrete cone failure and an increasing factor to consider the support of the supplementary reinforcement, angle of the concrete strut,

$$N_{Rd,cs} = \psi_{supp} \, N_{Rd,c} \text{ [N]} \tag{3.47}$$

where
$N_{Rd,c}$ is design failure load in case of concrete cone failure, see Eq. 3.7 [N]
$\Psi_{support}$ is support factor considering the confinement of the stirrups

$$2.5 - \frac{x}{h_{ef}} \geq 1 \text{ [-]} \tag{3.48}$$

where
x is distance between the anchor and the crack on the concrete surface assuming a crack propagation from the stirrup of the supplementary reinforcement to the concrete surface with an angle of 35° [mm]
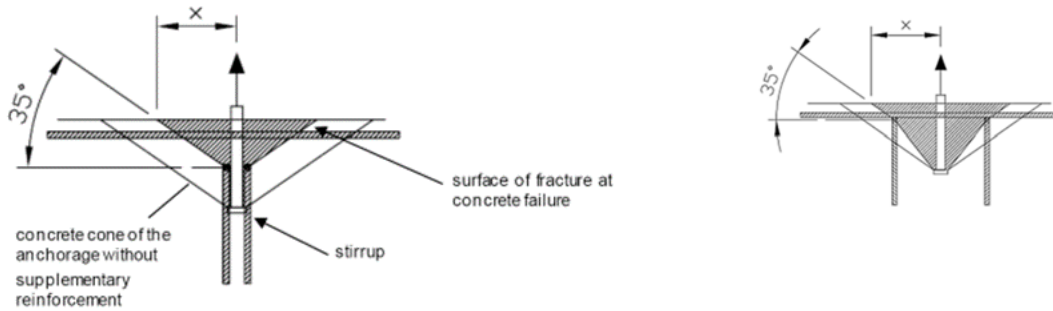
Fig. 3.4 Distance between the anchor and the crack on the concrete surface

The load is transferred to the stirrups and the concrete cone failure load is reached. Depending on the amount of supplementary reinforcement the failure of the stirrups can decisive $N_{Rd,re} < N_{Rd,cs}$. Two failure modes are possible:

steel yielding of stirrups $N_{Rd,s,re}$, see equation (3.16),

anchorage failure of stirrups $N_{Rd,b,re}$, see equation (3.20).

The corresponding failure load is calculated according to equation (3.49) summarizing the loads of the corresponding components

$$N_{Rd,re} = \min(N_{Rd,s,re}; N_{Rd,b,re}) + N_{Rd,c} + \delta_f \cdot k_{c,de} \text{ [N]} \tag{3.49}$$

where
$N_{Rd,c}$ is design failure load in case of concrete cone failure, see equation (3.7), [N]
$N_{Rd,s,re}$ is design failure load in case of yielding of the stirrups of the supplementary reinforcement, see equation (3.16) [N]
$N_{Rd,b,re}$ is design failure load in case of bond failure of the stirrups of the supplementary reinforcement, see equation (3.20) [N]
$k_{c,de}$ is stiffness of the concrete cone in the descending branch, see equation (3.13) [N/mm]
δ_f is corresponding displacement at failure load $N_{Rd,s,re}$ or $N_{Rd,b,re}$ [mm]

3.2.5 Combination of tension and shear components

The displacements in tension and shear is calculated by the sum of the displacement vectors.

3.3 Simplified stiffness's based on technical specifications

3.3.1 Headed stud in tension without supplementary reinforcement

For simplification the displacements and the stiffness of headed studs or anchorages is estimated using technical product specifications. The elongation δ_{Rd} is estimated up to the design load N_{Rd} using the displacements given in the technical product specification. The displacement is estimated by the following equation

$$\delta_{Rd,N} = \frac{\delta_{N,ETA}}{N_{ETA}} \, N_{Rd} \tag{3.50}$$

where
$\delta_{N,ETA}$ is displacement given in the product specifications for a corresponding load
N_{ETA} is tension load for which the displacements are derived in the product specifications

N_{Rd} is design tension resistance

The stiffness of the anchorage is calculated with the following equation

$$k_{Rd,N} = \frac{\delta_{N,ETA}}{N_{ETA}}$$ (3.51)

where
$\delta_{N,ETA}$ is displacement given in the product specifications for a corresponding load
N_{ETA} is tension load for which the displacements are derived in the product specifications

3.3.2 Headed stud in shear

For the design the displacement δ_v is estimated up to the design load V_{Rd} using the displacements given in the technical product specification. The displacement is estimated using the displacements far from the edge $\delta_{v,ETA}$ for short term and long term loading. The displacement is estimated by the following equation

$$\delta_{Rd,v} = \frac{\delta_{v,ETA}}{V_{ETA}} \ V_{Rd}$$ (3.52)

where
$\delta_{V,ETA}$ is displacement given in the product specifications for a corresponding load
V_{ETA} is shear load for which the displacements are derived in the product specifications
$V_{Rd,c}$ is design shear resistance

The stiffness of the anchorage is calculated with the following equation

$$k_{Rd,v} = \frac{\delta_{v,ETA}}{V_{ETA}}$$ (3.53)

where
$\delta_{V,ETA}$ is displacement given in the product specifications for a corresponding load
V_{ETA} is shear load for which the displacements are derived in the product specifications

3.3.3 Concrete breakout in tension

The characteristic load corresponding to the concrete cone breakout in tension for a single headed stud without edge influence is given by equation

$$N_{Rk,c}^0 = k_1 \ h_{ef}^{1,5} \ \sqrt{f_{ck}}$$ (3.54)

where
k_1 is basic factor for concrete cone breakout, which is equal to 8.9 for cracked concrete and 12.7 for non-cracked concrete, for headed studs, [-]
h_{ef} is effective embedment depth given according to the product specifications [mm] [-]
f_{ck} is characteristic concrete strength according to EN206-1:2000 [N/mm²]

The design load for concrete cone breakout for a single anchor, $N_{Rd,c}^0$ is obtained by applying partial safety factor of concrete γ_{Mc} to the characteristic load as

$$N_{Rd,c}^0 = \frac{N_{Rk,c}^0}{\gamma_{Mc}} \qquad (3.55)$$

For concrete, the recommended value of is γ_{Mc} = 1.5.

For a group of anchors, the design resistance corresponding to concrete cone breakout is given by equation (3.56), which is essentially same as equation (3.7)

$$N_{Rd,c} = N_{Rk,c}^0 \; \psi_{A,N} \; \psi_{s,N} \; \psi_{re,N}/\gamma_{Mc} \qquad (3.56)$$

where
$N_{Rk,c}^0$ is characteristic resistance of a single anchor without edge and spacing effects
$\psi_{A,N}$ is factor accounting for the geometric effects of spacing and edge distance
given as $\psi_{A,N} = \frac{A_{c,N}}{A_{c,N}^0}$
$A_{c,N}^0$ is reference area of the concrete cone for a single anchor with large spacing and edge distance projected on the concrete surface [mm²].
The concrete cone is idealized as a pyramid with a height equal to h_{ef} and a base length equal to $s_{cr,N}$ with $s_{cr,N} = 3.0 \; h_{ef}$, thus $A_{c,N}^0 = 9 \; h_{ef}^2$.
$A_{c,N}^0$ is reference area of the concrete cone of an individual anchor with large spacing and edge distance projected on the concrete surface [mm²].
The concrete cone is idealized as a pyramid with a height equal to h_{ef} and a base length equal to $s_{cr,N}$ with $s_{cr,N} = 3,0 \; h_{ef}$ [mm]
$A_{c,N}$ is actual projected area of concrete cone of the anchorage at the concrete surface, limited by overlapping concrete cones of adjacent anchors $s < s_{cr,N}$,
as well as by edges of the concrete member $c < c_{cr,N}$.
It may be deduced from the idealized failure cones of single anchors [mm²]
c is minimum edge distance $c = 1.5 \; h_{ef}$ [mm]
$c_{cr,N}$ is critical edge distance $c_{cr,N} = 1.5 \; h_{ef}$ [mm]
$\psi_{re,N}$ is factor accounting for the negative effect of closely spaced reinforcement in the concrete member on the strength of anchors with an embedment depth $h_{ef} < 100$ mm
$0.5 + h_{ef} / 200$ for $s < 150$ mm, for any diameter [-]
  or $s < 100$ mm, for $d_s \le 10$ mm
1.0 for $s \ge 150$ mm (for any diameter) [-]
γ_{Mc} is 1.5 for concrete [-]

3.3.4 Pull out failure of the headed studs

The design load corresponding to the pull out failure of the headed stud, $N_{Rd,p}$ is given by

$$N_{Rd,p} = p_{uk} \; A_h/\gamma_{Mc} \qquad (3.57)$$

where
p_{uk} is characteristic ultimate bearing pressure at the head of stud [N/mm²]
A_h is area on the head of the headed stud [mm²]

$$A_h = \frac{\pi}{4} \cdot (d_h^2 - d_s^2) \qquad (3.57b)$$

d_h is diameter of the head [mm]
d_s is diameter of the shaft [mm]
γ_{Mc} is 1.5 for concrete [-]

3.3.5 Interaction of components for concrete and stirrups

In case of headed stud anchored in concrete with supplementary reinforcement, stirrups, the stirrups do not carry any load till the concrete breakout initiates, i.e. till N_{act} is less than or equal to $N_{Rd,c}$. Once, the concrete breakout occurs, the load shared by concrete decreases with increasing displacement as depicted in Fig. 3.4. The load shared by concrete $N_{act,c}$ corresponding to a given displacement δ is therefore given by equation

$$N_{act,c} = N_{Rd,c} + k_{c,de}\, \delta \tag{3.57}$$

where $k_{c,de}$ is the slope of descending branch of Fig. 3.4, negative value, given by Eq. (3.7). Simultaneously, in case of concrete with supplementary reinforcement, the stirrups start to carry the load. The load carried by the stirrups corresponding to a given displacement δ is given by equation

$$N_{act,re} = n_{re}\, d_{s,re}^2 \sqrt{\frac{\alpha_s\, f_{ck}\, \delta}{2}} \tag{3.58a}$$

where
α_s is factor of the component stirrups, currently is α_s = 12 100 [-]
$d_{s,nom}$ is nominal diameter of the stirrups [mm]
f_{ck} is characteristic concrete compressive strength [N/mm²]
n_{re} is total number of legs of stirrups [-]

The total load N_{act} carried by concrete cone and stirrups corresponding to any given displacement δ is therefore given as the sum of the two components:

$$N_{act} = N_{act,c} + N_{act,re} = N_{Rd,c} + k_{c,de}\, \delta + \min\left(n_{re}\, d_{s,re}^2 \sqrt{\frac{\alpha_s\, f_{ck}\, \delta}{2}};\ N_{Rd,s,re};\ N_{Rd,b,re}\right) \tag{3.59}$$

The displacement corresponding to peak load of the system is obtained by differentiating the right hand side of Eq. (3.60) and equating it to zero. If the bond failure or steel failure of stirrups is not reached at an earlier displacement then the design peak load carried by the system $N_{u,c+s}$ is given by

$$N_{u,c+s} = N_{Rd,c} + \frac{3}{8}\, \frac{n_{re}^2\, d_{s,re}^4\, \alpha_s\, f_{ck}}{k_{c,de}} \tag{3.60}$$

where
$N_{Rd,c}$ is design load at concrete cone failure given by equation (3.7)
α_s is factor of the component stirrups, currently is α_s = 12 100 [-]
$d_{s,re}$ is Nominal diameter of the stirrups [mm]
f_{ck} is characteristic concrete compressive strength [N/mm²]
n_{re} is total number of legs of stirrups [-]
$k_{c,de}$ is stiffness of descending branch for concrete cone failure, given by eq. (3.13)

In a relatively rare case of all studs loaded in tension, both the legs of the hanger reinforcement are not uniformly loaded and the distribution of forces is difficult to ascertain. Due to this reason and also to avoid the problems with serviceability requirements, it is recommended that in such a case, the contribution of hanger reinforcement is ignored.

3.3.6 Determination of the failure load

The failure load N_u is given by the minimum of the failure load corresponding to each considered failure mode

3.3.7 Friction

For base plates the friction is defined in EN1993-1-8 cl 6.2.2. For the resistance the resistance values of friction and bolts may be added as long as the bolt holes are not oversized. For the friction between a base plate and the grout underneath the plate the following calculation may be used.

$$F_{f,Rd} = C_{f,d}\, N_{c,Ed} \qquad (3.61)$$

where
$C_{f,d}$ is coefficient for friction, for sand-cement mortar $C_{f,d} = 0.2$
$N_{c,Ed}$ is axial compressive force of the column

In this design manual the friction is not only applied to compression forces caused by axial forces but also for compression forces generated by bending moments. This principle is applied in EN1993-1-8:2006 for beam to the column end joints with end plates in cl 3.9.2(3).

3.4 Base plate in bending and concrete block in compression

3.4.1 Concrete 3D strength

The components concrete in compression and base plate in bending represent the behaviour of the compressed part of a steel to concrete connection. The resistance of these components depends primarily on the bearing resistance of the concrete block under the flexible base plate, see (Melchers, 1992). The resistance of concrete is influenced by flexibility of base plate. In case of loading by an axial force, the stresses in concrete are not uniformly distributed, they are concentrated around the footprint of the column under the plate according to its thickness, see (Dewolf, Sarisley, 1980). For the design the flexible base plate is replaced by reducing the effective fully rigid plate. The grout layer between the base plate and concrete block influences the resistance and stiffness of the component. That is why this layer is also included into this component, see (Penserini, Colson, 1989). Other important factors which influence the resistance are the concrete strength, the compression area, the location of the plate on the concrete foundation, the size of the concrete block and its reinforcement.

The stiffness behaviour of column base connection subjected to bending moment is influenced mostly by elongation of anchor bolts. The Component concrete in compression is mostly stiffer in comparison to the component anchor bolts in tension. The deformation of concrete block and base plate in compression is important in case of dominant axial compressive force.

The strength of the component $F_{Rd,u}$, expecting the constant distribution of the bearing stresses under the effective area, is given by

$$F_{Rd,u} = A_{c0}\, f_{jd} \qquad (3.62)$$

The design value of the bearing strength f_{jd} in the joint loaded by concentrated compression, is determined as follows. The concrete resistance is calculated according to cl. 6.7(2) in EN1992-1-1:2004 see Fig. 3.6 is

$$F_{Rd,u} = A_{c0}\, f_{cd}\, \sqrt{\frac{A_{c1}}{A_{c0}}} \leq 3.0\, A_{c0}\, f_{cd} \tag{3.63}$$

where

$$A_{c0} = b_1\, d_1 \quad \text{and}\ A_{c1} = b_2\, d_2 \tag{3.64}$$

where A_{c0} is the loaded area and A_{c1} the maximum spread area. The influence of height of the concrete block to its 3D behaviour is introduced by

$$h \ \geq b_2 - b_1 \text{ and } h \ \geq d_2 - d_1$$
$$3\, b_1 \ \geq b_2 \text{ and } 3\, d_1 \ \geq d_2 \tag{3.65}$$
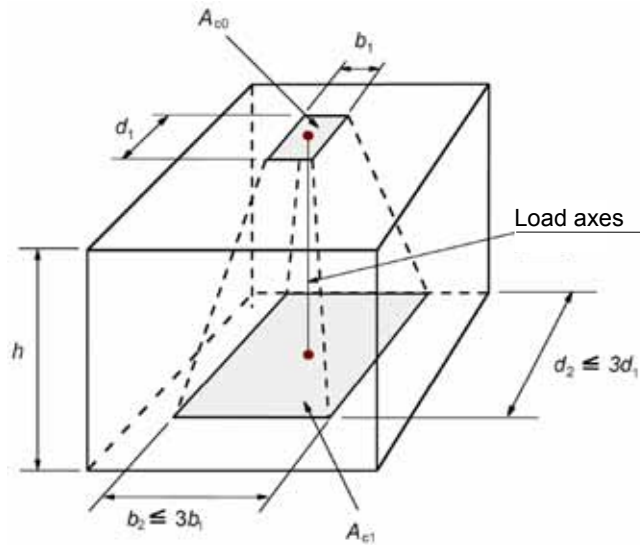
Fig. 3.5 Concrete compressive strength for calculation of 3D concentration

From this geometrical limitation the following formulation is derived

$$f_{jd} = \frac{\beta_j\, F_{Rd,u}}{b_{eff}\, l_{ef}} = \frac{\beta_j\, A_{c0}\, f_{cd}\sqrt{\frac{A_{c1}}{A_{c0}}}}{A_{c0}} = \beta_j\, f_{cd}\, k_j \leq \frac{3\, A_{c0}\, f_{cd}}{A_{c0}} = 3.0\, f_{cd} \tag{3.66}$$

The factor β_j represents the fact that the resistance under the plate might be lower due to the quality of the grout layer after filling. The value 2/3 is used in the case of the characteristic resistance of the grout layer is at least 0.2 times the characteristic resistance of concrete and thickness of this layer is smaller than 0.2 times the smallest measurement of the base plate. In different cases, it is necessary to check the grout separately. The bearing distribution under 45° is expected in these cases, see (Steenhuis et al, 2008) and Fig. 3.5 Concrete compressive strength for calculation of 3D concentration

Fig. 3. The design area A_{c0} is conservatively considered as the full area of the plate A_p.
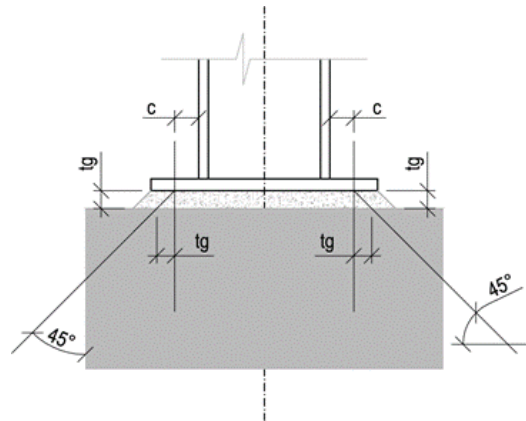
Fig. 3.6 Modelling of grout

3.4.2 Base plate flexibility

In case of the elastic deformation of the base plate is expected homogenous stress distribution in concrete block is expected under the flexible base plate based on the best engineering practice. The formula for the effective width c is derived from the equality of elastic bending moment resistance of the base plate and the bending moment acting on the base plate, see (Astaneh et al., 1992). Acting forces are shown in Fig. 3.7.
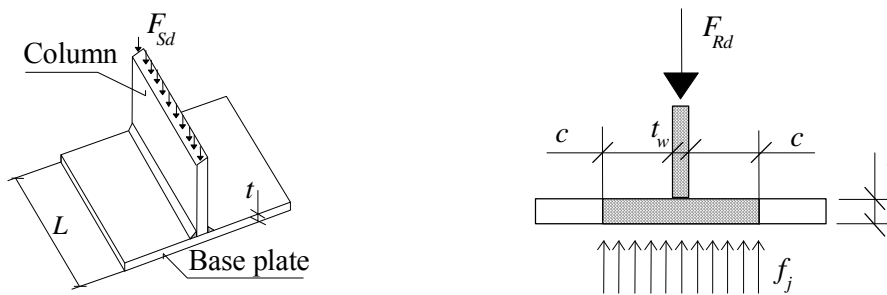

Fig. 3.7 Base plate as a cantilever for check of its elastic deformation only

Elastic bending moment of the base plate per unit length is

$$M' = \frac{1}{6} t^2 \frac{f_y}{\gamma_{M0}}$$

(3.69)

and the bending moment per unit length on the base plate of span c and loaded by distributed load is

$$M' = \frac{1}{2} f_j c^2$$

(3.70)

where f_j is concrete bearing strength and from Eq. (3.69) and (3.70) is

$$c = t \sqrt{\frac{f_y}{3 \cdot f_{jd} \cdot \gamma_{M0}}}$$

(3.71)

The flexible base plate, of the area A_p, is replaced by an equivalent rigid plate with area A_{eq}, see Fig. 3.8. Then the resistance of the component, expecting the constant distribution of the bearing stresses under the effective area is given by

$$F_{Rd,u} = A_{eq} \cdot f_{jd} \tag{3.72}$$

The resistance F_{Rd} should be higher than the loading F_{Ed}
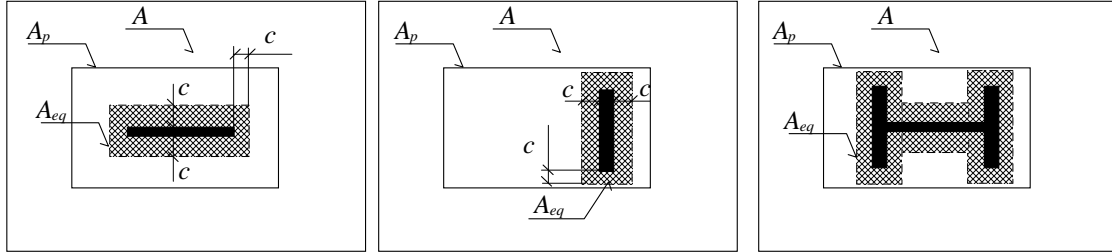
$$F_{Ed} \le F_{Rd,u} \tag{3.73}$$

Fig. 3.8 Effective area under the base plate

3.4.3 Component stiffness

The proposed design model for stiffness of the components base plate in bending and concrete in compression is given also in (Steenhuis et al, 2008). The stiffness of the component is influenced by factors: the flexibility of the plate, the Young´s modulus of concrete, and the size of the concrete block. By loading with force, a flexible rectangular plate could be pressed down into concrete block. This flexible deformation is determined by theory of elastic semi-space

$$\delta_r = \frac{F \; \alpha \; a_r}{E_c \; A_p} \tag{3.74}$$

where
F   is acting load
α is shape factor of the plate
a_r is width of equivalent rigid plate
E_c is elastic modulus of concrete
A_p is area of the plate

The factor α depends on the material characteristics. The Tab. 3.1 gives values of this factor dependent on the Poison's ratio, for concrete is $v \approx 0.15$. The table shows also the approximate value of factor α, that is $0.58 \cdot \sqrt{L/a_r}$.

Tab. 3.1 Factor α and its approximation for concrete

l / a_r	α	Approximation as $\alpha = 0.58 \cdot \sqrt{L/a_r}$.
1	0.90	0.85
1.5	1.10	1.04
2	1.25	1.20
3	1.47	1.47
5	1.76	1.90
10	2.17	2.69

For steel plate laid on concrete block it is

$$\delta_r = \frac{0.85\,F}{E_c\sqrt{l \cdot a_r}}$$ (3.75)

where
σ_r is deformation under the rigid plate
l is length of the plate

The model for the elastic stiffness behaviour of component is based on a similar interaction between concrete block and steel plate. The flexible plate is expressed as an equivalent rigid plate based on the same deformation, modelled in Fig. 3.9.
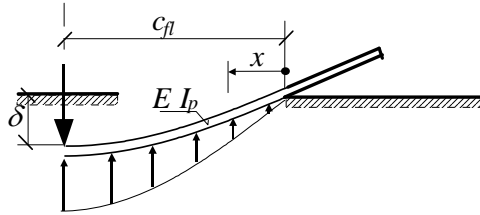

Fig. 3.9 A flange of flexible T-stub

Independent springs support the flange of a unit width. Then, the deformation of the plate is a sine function.

$$\delta_{(x)} = \delta \sin (\tfrac{1}{2}\,\pi\,x\,/\,c_{fl})$$ (3.76)

The uniform stress on the plate is rewritten by the fourth differentiate and multiplied by $E\,I'_p$

$$\delta_{(x)} = E\,I'_p\,(\tfrac{1}{2}\,\pi/c_{fl})^4\,\delta \sin\left(\tfrac{1}{2}\,\pi\,\frac{x}{c_{fl}}\right) = E\,\frac{t^3}{12}\left(\tfrac{1}{2}\,\frac{\pi}{c_{fl}}\right)^4\,\delta \sin (\tfrac{1}{2}\,\pi\,x\,/c_{fl})$$ (3.77)

where
E is elastic modulus of steel
I'_p is moment of inertia per unit length of the steel plate ($I'_p = t^3\,/\,12$)
t is thickness of the plate

$$\delta_{(x)} = \sigma_{(x)}\,h_{ef}/E_c$$ (3.78)

where
h_{ef} is equivalent concrete height of the portion under the steel plate

Assume that

$$h_{ef} = \xi\,c_{fl}$$ (3.79)

Factor ξ expresses the rotation between h_{ef} and c_{fl}. Hence

$$\delta_{(x)} = \sigma_{(x)}\,\xi\,c_{fl}/E_c$$ (3.80)

After substitution and using other expressing it is

$$c_{fl} = t \sqrt[3]{\frac{(\pi/2)^4}{12} \xi \frac{E}{E_c}} \tag{3.81}$$

The flexible length c_{fl} may be replaced by an equivalent rigid length

$$c_r = c_{fl} \, 2 \, / \, \pi \tag{3.82}$$

The factor ξ shows the ratio between h_{eq} and c_{fl}. The value a_r represents height h_{eq}. Factor α is approximated to $1.4 \cdot a_r = t_w + 2c_r$ and $t_w = 0.5 \, c_r$. Then it is written

$$h_{eq} = 1.4 \cdot (0.5 + 2) \, c_r = 1.4 \cdot 2.5 \cdot c_{fl} \cdot \frac{2}{\pi} = 2.2 \, c_{fl} \tag{3.83}$$

Hence $\xi = 2.2$.

For practical joints is estimated by $E_c \cong 30\ 000$ N / mm^2 and $E \cong 210\ 000$ N / mm^2, what leads to

$$c_{fl} = t \sqrt[3]{\frac{(\pi/2)^4}{12} \xi \frac{E}{E_c}} = t \sqrt[3]{\frac{(\pi/2)^4}{12} 2.2 \frac{210000}{30000}} = 1.98 \, t \tag{3.84}$$

or

$$c_r = c_{fl} \frac{2}{\pi} = 1.98 \cdot \frac{2}{\pi} \cdot t = 1.25 \, t \tag{3.85}$$

The equivalent width a_r is in elastic state replace with

$$a_{eq,el} = t_w + 2.5 \, t = 0.5 \, c_r + t \tag{3.86}$$

or

$$a_{eq,el} = 0.5 \cdot 1.25 \, t + 2.5 \, t = 3.125 \, t \tag{3.87}$$

From the deformation of the component and other necessary values which are described above, the formula to calculate the stiffness coefficient is derived

$$k_c = \frac{F}{\delta \, E} = \frac{E_c \, \sqrt{a_{eq,el} \, L}}{1.5 \cdot 0.85 \, E} = \frac{E_c \, \sqrt{a_{eq,el} \, L}}{1.275 \, E} = \frac{E_c \cdot \sqrt{t \cdot L}}{0.72 \cdot E} \tag{3.88}$$

where
$a_{eq,el}$ is equivalent width of the T-stub
L is length of the T-stub

3.5   Concrete panel

The resistance and deformation of the reinforced concrete wall in the zone adjacent to the joint is hereby represented by a joint link component, see (Huber and Cermeneg, 1998). Due to the nature of this joint, reinforced concrete, the developed model is based on the strut-and-tie method, commonly implemented in the analysis of reinforced concrete joints. The problem is 3D, increasing its complexity, as the tension load is introduced with a larger width than the

compression, which may be assumed concentrated within an equivalent dimension of the anchor plate, equivalent rigid plate as considered in T-stub in compression. Thus, a numerical model considering only the reinforced concrete wall and an elastic response of the material has been tested to identify the flow of principal stresses. These show that compression stresses flow from the hook of the longitudinal reinforcement bar to the anchor plate. In this way the strut-and-tie model (STM) represented in Fig. 10a is idealized. Subsequently, in order to contemplate the evaluation of the deformation of the joint, a diagonal spring is idealized to model the diagonal compression concrete strut, as illustrated in Fig. 10. The ties correspond to the longitudinal steel reinforcement bars. The properties of this diagonal spring are determined for resistance and stiffness.

The <u>resistance</u> is obtained based on the strut and nodes dimension and admissible stresses within these elements. The node at the anchor plate is within a tri-axial state. Therefore, high stresses are attained as confinement effect. In what concerns the strut, because of the 3D nature, stresses tend to spread between nodes. Giving the dimensions of the wall of infinite width, the strut dimensions should not be critical to the joint. Thus, the node at the hook of the bar is assumed to define the capacity of the diagonal spring. The resistance of the spring is then obtained according to the dimensions of this node and to the admissible stresses in the node and in the strut. For the latter, the numerical model indicates the presence of transverse tension stresses which have to be taken into consideration.

The <u>deformation</u> of the diagonal spring is obtained by assuming a non-linear stress-strain relation for the concrete under compression, as defined in (Henriques, 2012). The maximum stress is given by the limiting admissible stress as referred above. Then, deformation is calculated in function of the length of the diagonal strut and the concrete strain.

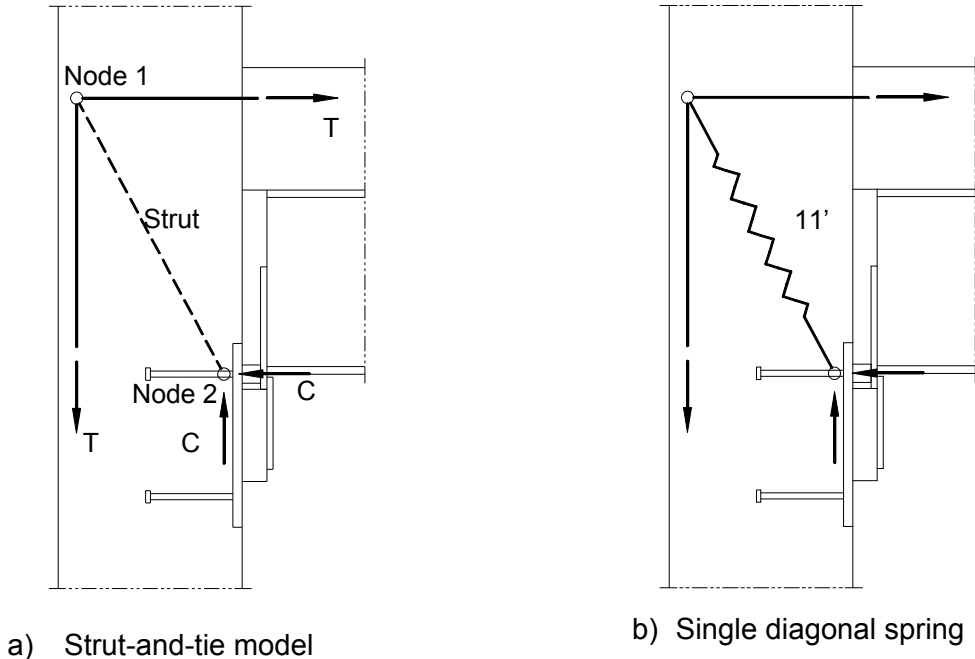a)   Strut-and-tie model

b) Single diagonal spring

Fig. 3.10 Joint link modelling

Tab. 3.2 provides the stresses for nodes and struts according to EN1992-1-1:2004. Node 1 is characterized by the hook longitudinal reinforcement bar. The represented dimension is assumed as defined in CEB-FIP Model Code 1990. In what concerns the width of the node, based on the numerical observations, it is considered to be limited by the distance between the external longitudinal reinforcement bars within the effective width of the slab. The numerical model demonstrates that the longitudinal reinforcement bars are sufficiently close, as no relevant discontinuity in the stress field is observed. Though, this is an issue under further

investigation and depending on the spacing of the reinforcing bars, this assumption may or may not be correct (Henriques, 2013).

Tab. 3.2 Stresses in strut-and-tie elements according to EN1992-1-1:2004

Element	Limiting stresses	
Node 1	$0.75 \, \nu \, f_{cd}$	
Node 2	$3 \, \nu \, f_{cd}$	
Strut	$0.6 \, \nu \, f_{cd}$	with $\nu = 1 - f_{ck}/250$
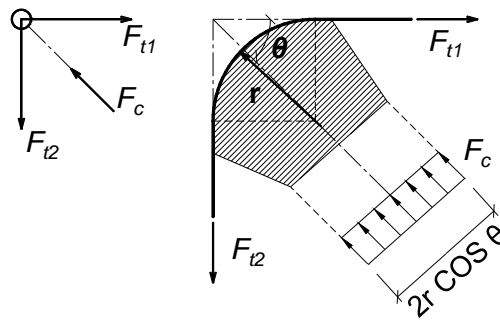
Fig. 3.11 Definition of the dimension related to the hook
of the longitudinal reinforcement bar in Node 1, according to the CEB Model Code

Finally, to simplify the assembling of the joint model, the diagonal spring representing the joint link component is converted into a horizontal spring. The properties of the horizontal spring are directly obtained from the diagonal spring determined as a function of the angle of the diagonal spring.

3.6   Longitudinal steel reinforcement in tension

In the composite joint configuration under consideration, the longitudinal reinforcement in tension is the only component able to transfer tension forces introduced by the bending moment to the supporting member e.g. a reinforced concrete wall. This component determines the behaviour of the joint. According to EN1994-1 the longitudinal steel reinforcement may be stressed to its design yield strength. It is assumed that all the reinforcement within the effective width of the concrete flange is used to transfer forces. The resistance capacity of the component may then be determined as in Eq. (3.89). Regarding the deformation of the component, the code provides stiffness coefficients for two composite joint configurations, single and double-sided joints. The stiffness coefficient for single-sided joints may be estimated as in Eq. (3.90). This stiffness coefficient depends essentially on the elongation length of the longitudinal reinforcement contributing to the deformation of the component. Analogous to the code provisions, the dimension h involved in Eq. (3.90) is assumed as shown in Fig. 3.12.

$$F_{s,r} = A_{s,r} \, f_{yr} \tag{3.89}$$

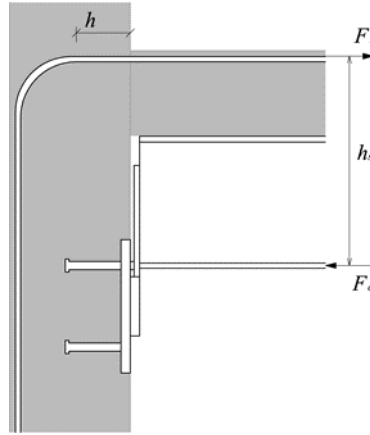$$k_{s,r} = \frac{A_{s,r}}{3.6 \, h} \tag{3.90}$$

Fig. 3.12 Dimension h for elongation length

The tension component of the joint is calculated according to

$$F_t = -M_{y,Ed}/h_s \tag{3.91}$$

3.7 Slip of the composite beam

The slip of composite beam does not directly influence the resistance of the joint. However, the level of interaction between concrete slab and steel beam defines the maximum load the longitudinal reinforcement can achieve. Therefore in such joint configuration, where reinforcement is the only tension component, the level of interaction affects the joint resistance. In the EN1994-1-1:2008, the influence of the slip of composite beam is taken into account. The stiffness coefficient of the longitudinal reinforcement, see Eq. (3.92) should be multiplied with the reduction factor k_{slip} determined as follows:

$$k_{slip} = \frac{1}{1 + \dfrac{E_s\ k_{sr}}{k_{sc}}} \tag{3.92}$$

$$K_{SC} = \frac{N\ k_{sc}}{\vartheta - \left(\dfrac{\vartheta - 1}{1 + \xi}\right)\dfrac{h_s}{d_s}} \tag{3.93}$$

$$\vartheta = \sqrt{\frac{(1 + \xi)\ N\ k_{sc}\ l\ d_s^2}{E_a\ I_a}} \tag{3.94}$$

$$\xi = \frac{E_a\ I_a}{d_s^2\ E_s\ A_s} \tag{3.95}$$

where

h_s is the distance between the longitudinal reinforcing bars and the centre of compression of the joint, that may be assumed as the midpoint of the compression flange of the steel beam

d_s is the distance between the longitudinal reinforcing bars and the centroid of the steel beam section, see Fig. 13

I_a is the second moment area of the steel beam section

l is the length of the beam in hogging bending adjacent to the joint, in the case of the tested specimens is equal to the beam's length

N is the number of shear connectors distributed over the length l

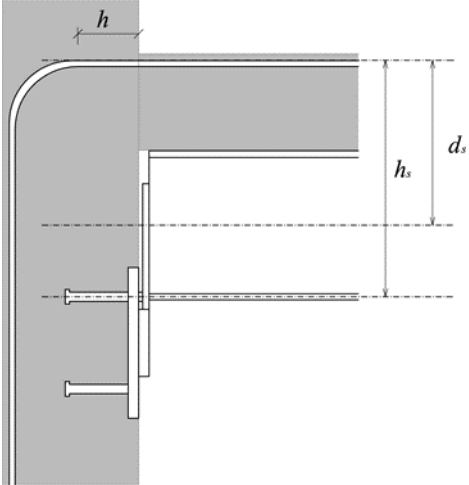k_{sc} is the stiffness of one shear connector

Fig. 3.13 Dimensions h_s and d_s

4   STEEL COMPONENTS

4.1   T-stub in tension

The base plate in bending and anchor bolts in tension is modelled by the help of T-stub model based on the beam to column end plate connection model. Though in its behaviour there are some differences. Thickness of the base plate is bigger to transfer compression into the concrete block. The anchor bolts are longer due to thick pad, thick base plate, significant layer of grout and flexible embedding into concrete block. The influence of a pad and a bolt head may be higher.
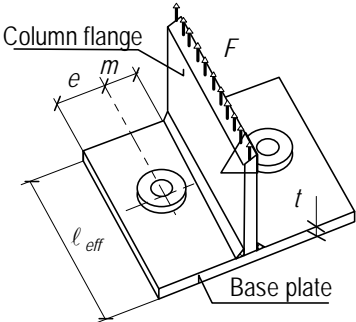

Fig. 4.1 The T stub - anchor bolts in tension and base plate in bending

Due to longer free lengths of bolts, bigger deformations could arise. The anchor bolts, compare to bolts, are expecting to behave ductile. When it is loaded by tension, the base plate is often separated from the concrete surface. This case is shown in (Wilkinson et al, 2009). By bending moment loading different behaviour should be expected. The areas of bolt head and pad change favourably distribution of forces on T-stub. This influence is not so distinctive during calculation of component stiffness. The all differences from end plate connections are involved

in the component method, see EN1993-1-8:2006. The design model of this component for resistance as well for stiffness is given in (Wald et al, 2008).
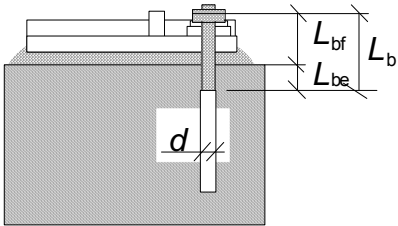

Fig. 4.2 Length of anchor bolt

4.1.1 Model

When the column base is loaded by bending moment as it is shown in Fig. 4.3, anchor bolts transfer tensile forces. This case of loading leads to elongation of anchor bolts and bending of the base plate. Deformed bolts can cause failure as well as reaching of the yield strength of the base plate. Sometimes failure in this tensile zone is caused by both, see (Di Sarno et al, 2007).
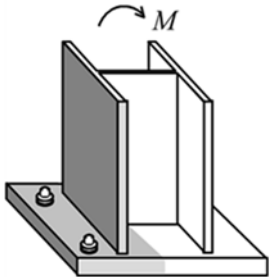

Fig. 4.3 Tensile zone and equivalent T-stub in case of loading by bending moment

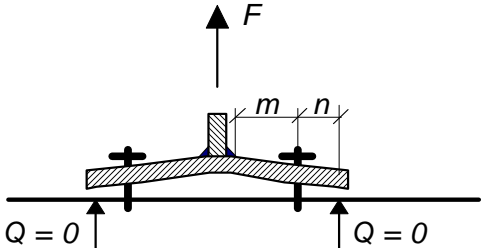Column with connected base plate taken, as it is shown in Fig. 4.4, into model of T-stub.

Fig. 4.4 T-stub separated from the concrete block with no prying force

There are two models of deformation of the T-stub of the base plate according to presence of prying. In the case the base plate separated from the concrete foundation, there is no prying force Q, see Fig. 4.4. In other case, the edge of the plate is in contact with concrete block, the bolts are loaded by additional prying force Q. This force is balanced just by the contact force at the edge of the T-stub, see Fig. 4.5.

When there is contact between the base plate and the concrete block, beam theory is used to describe deformed shape of the T-stub.
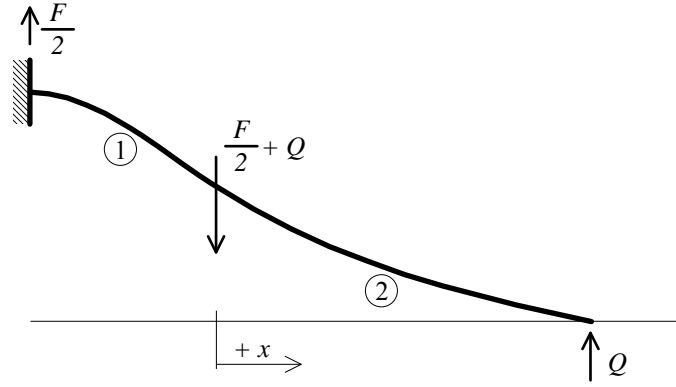
Fig. 4.5 Beam model of T-stub and prying force Q

Deformed shape of the curve is described by differential equation

$$E \, I \, \delta'' = -M \tag{4.1}$$

After writing the above equation for both parts of the beam model 1 and 2, application of suitable boundary conditions, the equations could be solved. The prying force Q is derived just from these solved equations as

$$Q = \frac{F}{2} \cdot \frac{3(m^2 \, n \, A - 2 \, L_b \, I)}{2 \, n^2 \, A \, (3 \, m + n) + 3 \, L_b \, I} \tag{4.2}$$

When the base plate is in contact with concrete surface, the prying of bolts appears and on the contrary no prying forces occur in the case of separated base plate from the concrete block due to the deformation of long bolts. This boundary, between prying and no prying has to be determined. Providing that $n = 1.25 \, m$ it may be expressed as

$$L_{b,min} = \frac{8.82 \, m^3 A_s}{l_{eff} t^3} < L_b \tag{4.3}$$

where
A_s is the area of the bolt
L_b is equivalent length of anchor bolt
l_{eff} is equivalent length of T-stub determined by the help of Yield line method, presented in following part of work

For embedded bolts length L_b is determined according to Fig. 4.2 as

$$L_b = L_{bf} + L_{be} \tag{4.4}$$

where
L_{be} is $8 \, d$ effective bolt length

When the length of bolt $L_b > L_{b,min}$ there is no prying. Previous formulae is expressed for boundary thickness $t_{lim,}$ see (Wald et al, 2008), of the base plate as

$$t_{lim} = 2.066 \, m \cdot \sqrt[3]{\frac{A_s}{l_{eff} \, L_b}} \tag{4.5}$$

If the base plate are loaded by compression force and by bending moment and not by tensile force it is recommended to neglect these prying forces. In other cases it needs to be checked.

4.1.2 Resistance

The design resistance of a T-stub of flange in tension of effective length ℓ_{eff} is determined as minimum resistance of three possible plastic collapse mechanisms. For each collapse mechanism there is a failure mode. Following collapse modes, shown in Fig. 4.6, is used for T-stub in contact with the concrete foundation, see in EN1993-1-8:2006.
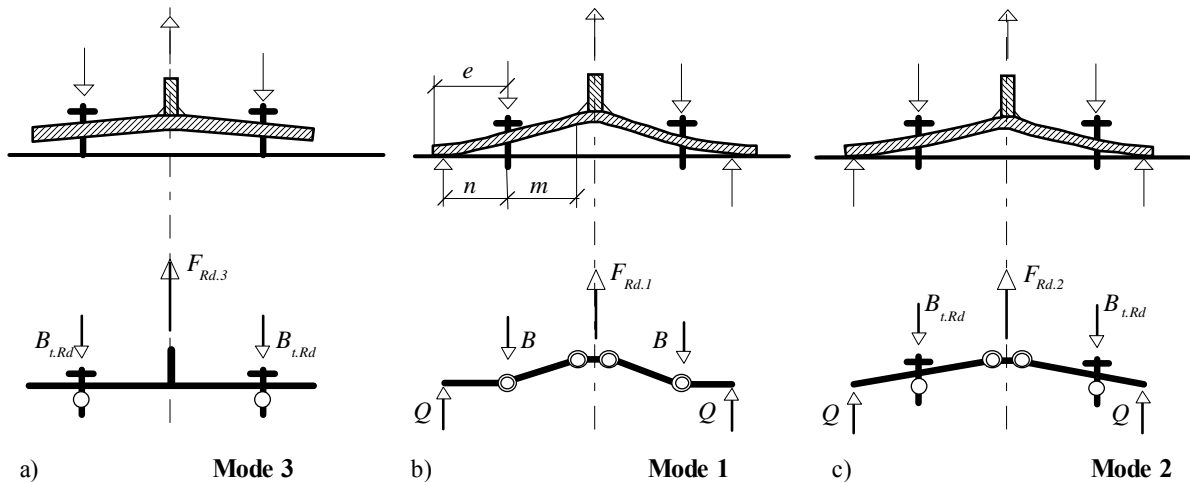

Fig. 4.6 Failure modes of the T-stub in contact with the concrete foundation

Mode 1

According to this kind of failure the T-stub with thin base plate and high strength anchor bolts is broken. In the base plate plastic hinge mechanism with four hinges is developed.

$$F_{1,Rd} = \frac{4\ l_{eff}\ m_{pl,Rd}}{m} \tag{4.6}$$

Mode 2

This mode is a transition between failure Mode 1 and 3. At the same time two plastic hinges are developed in the base plate and the limit strength of the anchor bolts is achieved.

$$F_{2,Rd} = \frac{2\ l_{eff}\ m_{pl,Rd} + \Sigma\ B_{t,Rd} \cdot n}{m + n} \tag{4.7}$$

Mode 3

Failure mode 3 occurs by the T-stub with thick base plate and weak anchor bolts. The collapse is caused by bolt fracture.

$$F_{3,Rd} = \Sigma\ B_{t,Rd} \tag{4.8}$$

The design strength F_{Rd} of the T-stub is derived as the smallest of these three possible modes:

$$F_{Rd} = \min\left(F_{1,Rd}, F_{2,Rd}, F_{3,Rd}\right) \tag{4.9}$$

Because of the long anchor bolts and thick base plate different failure mode arises compare to an end plate connection. When the T-stub is uplifted from the concrete foundation, there is no prying, new collapse mode is obtained, see Fig. 4.7. This particular failure mode is named Mode 1-2.
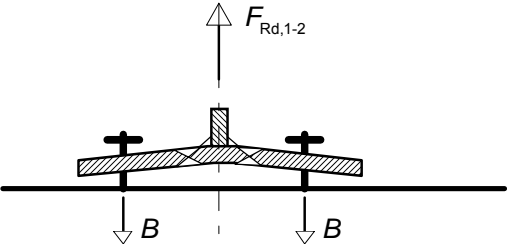

Fig. 4.7 T-stub without contact with the concrete foundation, Mode 1-2

Mode 1-2

The failure results either from bearing of the anchor bolts in tension or from the yielding of the plate in bending, where a two hinges mechanism develops in the T-stub flange. This failure does not appear in beam to column connection because of the small deformation of the bolts in tension, see (Wald et al, 2008).

$$F_{1-2,Rd} = \frac{2 \; l_{eff} \; m_{pl,Rd}}{m} \tag{4.10}$$

The relationship between Mode 1-2 and modes of T-stub in contact with concrete is shown in Fig. 4.8.
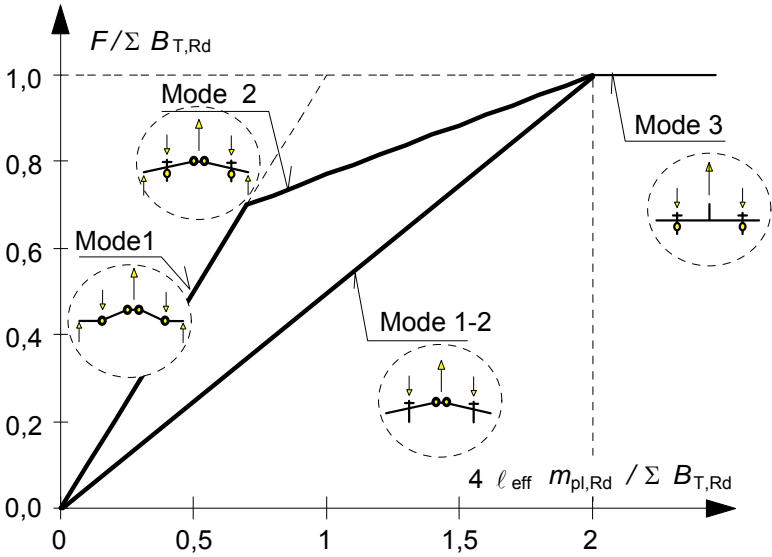

Fig. 4.8 Failure mode 1-2

The boundary between the mode 1-2 and others is given in the same way like the boundary of prying and no prying – according to the limiting bolt length $L_{b,min}$.

During the Mode 1-2 large deformations of the base plate can develop. Finally these deformations could lead to contact between the concrete block and the edge of the T-stub (prying forces can arise even in this case). After loading Modes 1 or 2 should be obtained like the first. But for reaching this level of resistance, which is necessary to obtain these modes, very large deformations are required. And so high deformations are not acceptable for design. In conclusion, in cases where no prying forces develop, the design resistance of the T-stub is taken as

$$F_{Rd} = \min \left(F_{1-2,Rd}, F_{3,Rd} \right) \qquad (4.11)$$

where

$$F_{3,Rd} = \Sigma B_{t,Rd} \qquad (4.12)$$

The equivalent length of T-stub l_{eff}, which is very important for the resistance determination, is calculated by the help of the yield line method, which is explained in the following part of the work.

Yield line method

Although numerical methods, based on extensive use of computers, are potentially capable of solving the most difficult plate problems, yield-line analysis is such an alternative computational technique (Thambiratnam, Paramasivam, 1986). It provides such an alternative design method for plates. This simple method, which uses concepts and techniques familiar to structural engineers, provides realistic upper bounds of collapse loads even for arbitrary shapes and loading conditions. The advantages of the yield-line method are: simplicity and economy, information is provided on the real load-carrying capacity of the slab, the basic principles used are familiar to structural engineers, the method also gives acceptable estimates for the ultimate load-carrying capacity of structural steel plates, and resulting designs are often more economical. On the other hand, the present limitations of the method are: the method fails in vibration analysis and cannot be used in the case of repeated static or dynamic loads (but is applied effectively for suddenly applied one-time loads), and theoretically, the law of superposition is not valid. The yield-line method offers, especially for the practicing engineer, certain advantages over the elastic stress analysis approaches.

Assumptions

The correct failure pattern is known, the critical load is obtained either from virtual work or from equilibrium considerations. Both approaches use the following basic assumptions: at impending collapse, yield lines are developed at the location of the maximum moments, the yield lines are straight lines, along the yield lines, constant ultimate moments m_u are developed, the elastic deformations within the slab segments are negligible in comparison with the rigid body motions, created by the large deformations along the yield lines, from the many possible collapse mechanisms, only one, pertinent to the lowest failure load, is important. In this case the yield-line pattern is optimum, when yield lines are in the optimum position, only ultimate bending moments, but no twisting moments or transverse shear forces are present along the yield lines. The location and orientation of yield lines determine the collapse mechanism. The Fig. 4.9 introduces an example of yield line.
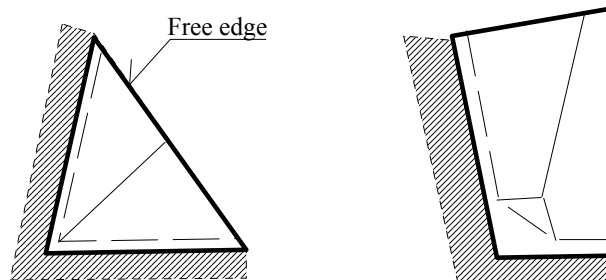

Fig. 4.9 Possible yield line patterns

The work method

The work method, see (Johansen, 1949), gives an upper-bound solution to the critical load at which the slab, with a certain ultimate resisting moment, fails. A particular configuration is searched, from a family of possible yield-line patterns which gives the lowest value of the ultimate load. The solution is based on the principle of virtual work.

The effective length of T-stub

The effective length l_{eff} of a T-stub is influenced by the failure mode of the T-stub. When there are more than one possible failure modes, it means more than one effective length, the calculation is done with the smallest (shortest) length, see EN1993-1-8:2006. The Fig. 4.10 shows, that two groups of yield line patterns can arise circular yield line and non-circular yield line. The main difference between these two types is related to contact between the T-stub and concrete foundation. By the non-circular patterns prying forces are developed. In this work there are taken into account only the modes without the contact of the edge of the base plate to the concrete foundation, it means without prying forces in bolts.

a) Circular pattern, $\ell_{eff.cp}$ b) Non-circular pattern, $\ell_{eff.np}$
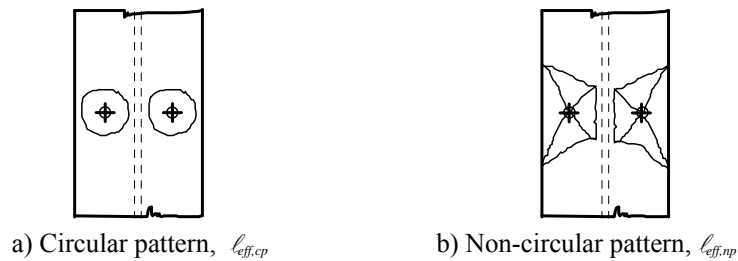
Fig. 4.10 The yield line patterns

As it was written in previous paragraphs, the effective length could be determined by the yield line method. Hence the yield line of the base plate must be designed. The collapse Mode 1 of the plate, which is shown in Fig. 4.11, is expected.
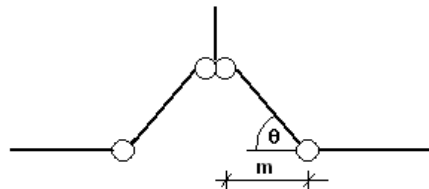
Fig. 4.11 Expected collapse mode

For this collapse mode there are following formulas:

$$m_{pl,Rd} = \frac{1}{4} t^2 f_{yd} \tag{4.13}$$

$$\tan \theta = \frac{\delta}{m} \approx \theta \tag{4.14}$$

$$F_{pl} = \frac{4 l_{eff} \, m_{pl,Rd}}{m} \tag{4.15}$$

where
$m_{pl,Rd}$ is plastic bending moment resistance of the base plate per unit length
F_{pl} is force acting in the bolt position

The assumptions to determine the yield line of the base plate are following the yield line is a straight line, this line is perpendicular to a line which pass through the bolt and tangent to the column, or this line is tangent to the column and parallel to the edge of the base plate. With these assumptions are determined. Following calculation procedure of the effective length of the T-stub in plate corner is given in (Wald et al, 2000) and (Heinisuo et al, 2012).
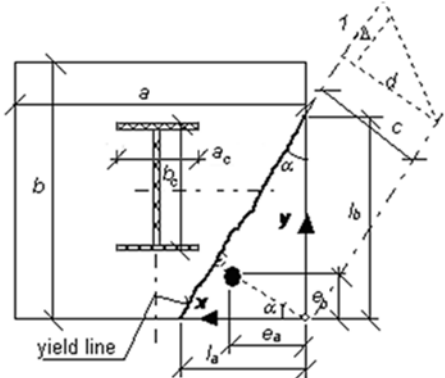

Fig. 4.12 The yield line parameters

α represents the angle between the yield line and the edge and c the minimal distance between the corner of the plate and the yield line. With the previous geometrical relation, the following relations is obtained

$$\tan \alpha = \frac{x}{y} \tag{4.16}$$

where
x, y are coordinates of the bolt, which could vary

For the design of the parameter c, the work method of the yield line theory is used. The internal work is

$$W_i = \sum_n [\overline{\theta}_j; \overline{m_{uj}}; 1] = m_{pl} \left(\frac{1}{y}x + \frac{1}{x}y\right) \tag{4.17}$$

The external work is

$$W_e = P_u \Delta = F_{pl} \Delta \tag{4.18}$$

where Δ represents the deformation of the plate in the bolt position, see Fig. 4.13.
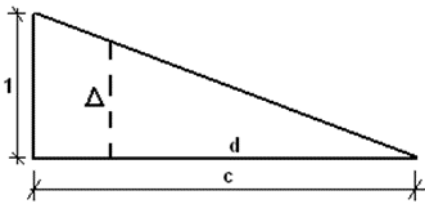

Fig. 4.13 The deformation of the plate represented by value Δ

According to previous figure is Δ replaced with

$$\frac{\Delta}{1} = \frac{d}{c} = \frac{\sqrt{x^2 + y^2}}{c} \tag{4.19}$$

After replacement Δ in the formula of the external work and putting it into equality with the internal work as

$$\frac{\sqrt{x^2 + y^2}}{c} F_{pl} = m_{pl} \left(\frac{x}{y} + \frac{y}{x} \right) \tag{4.20}$$

and then the effective length of the T-stub is

$$l_{eff} = \frac{c\, m}{4} \frac{\sqrt{x^2 + y^2}}{c} \tag{4.21}$$

The ultimate load is given by

$$F_{pl} = c\, m_{pl} \frac{\sqrt{x^2 + y^2}}{x\, y} \tag{4.22}$$

$$\frac{\partial F_{pl}}{\partial c} = m_{pl} \frac{\sqrt{x^2 + y^2}}{x\, y} = cst \tag{4.23}$$

With the yield line assumption the characteristics of the different possible failure models could be designed.

The effective length of T-stub

Two groups of yield line patterns called circular and non-circular yield lines are distinguished in EN1993-1-8:2006. The major difference between circular and non-circular patterns is related to contact between the T-stub and rigid foundation. The contact may occur only for non-circular patterns and prying force will develop only in this case. This is considered in the failure modes as follows:

Mode 1

The prying force does not have influence on the failure and development of plastic hinges in the base plate. Therefore, the formula (4.2) applies to both circular and non-circular yield line patterns.

Mode 2

First plastic hinge forms at the web of the T-stub. Plastic mechanism is developed in the base plate and its edges come into contact with the concrete foundation. As a result, prying forces develop in the anchor bolts and bolt fracture is observed. Therefore, Mode 2 occurs only for non-circular yield line patterns, which allow development of prying forces.
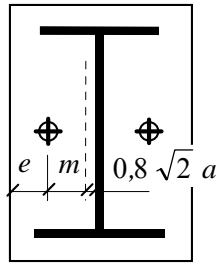
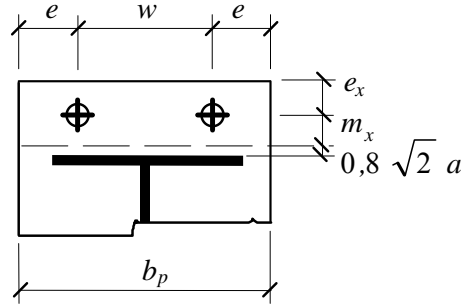Fig. 4.14a The effective length of T-stub for bolts inside the flanges

Fig. 4.14b The effective length of T-stub for bolts outside the flanges

Mode 3

This mode does not involve any yielding of the plate and applies therefore to any T-stub. In the design procedure, the appropriate effective length of the T-stub should be used for Mode 1

$$l_{eff,1} = \min(l_{eff,cp}; l_{eff,np})$$ (4.24)

and for Mode 2

$$l_{eff,2} = \min(l_{eff,np})$$ (4.25)

The design resistance of the T-stub is given by the formula (4.8). Tab. 4.1 and Tab. 4.2 indicate the values of l_{eff} for typical base plates in cases with and without contact. See Fig. 4.14 for the used symbols.

Tab. 4.1 The effective length l_{eff} of a T-stub with bolts inside the flanges (Wald et al, 2008)

Prying case	No prying case
$l_1 = 2\,\alpha\,m - (4\,m - 1{,}25\,e)$	$l_1 = 2\,\alpha\,m - (4\,m + 1{,}25\,e)$
$l_2 = 2\,\pi\,m$	$l_2 = 4\,\pi\,m$
$l_{eff,1} = \min(l_1; l_2)$	$l_{eff,1} = \min(l_1; l_2)$
$l_{eff,2} = l_1$	$l_{eff,2} = l_1$

Tab. 4.2 Effective length l_{eff} for bolts outside the flanges (Wald et al, 2008)

Prying case	No prying case
$l_1 = 4\,\alpha\,m_x + 1{,}25\,e_x$	$l_1 = 4\,\alpha\,m_x + 1.25\,e_x$
$l_2 = 2\,\pi\,m_x$	$l_2 = 2\,\pi\,m_x$
$l_3 = 0.5 b_p$	$l_3 = 0.5\,b_p$
$l_4 = 0.5\,w + 2\,m_x + 0.625\,e_x$	$l_4 = 0.5\,w + 2\,m_x + 0.625\,e_x$
$l_5 = e + 2\,m_x + 0.625\,e_x$	$l_5 = e + 2\,m_x + 0.625\,e_x$
$l_6 = \pi\,m_x + 2\,e$	$l_6 = 2\,\pi\,m_x + 4\,e$
$l_7 = \pi\,m_x + w$	$l_7 = 2\,(\pi\,m_x + w)$
$l_{eff,1} = \min(l_1; l_2; l_3; l_4; l_5; l_6; l_7)$	$l_{eff,1} = \min(l_1; l_2; l_3; l_4; l_5; l_6; l_7)$
$l_{eff,2} = \min(l_1; l_2; l_3; l_4; l_5)$	$l_{eff,2} = \min(l_1; l_2; l_3; l_4; l_5)$

4.1.3 Stiffness

The prediction of the base plate stiffness is based on (Steenhuis et al, 2008). The stiffness of the component analogous to the resistance of the T-stub is influenced by the contact of the base plate and the concrete foundation (Wald et al, 2008). The formula for deformation of the base plate loaded by the force in bolt F_b is

$$\delta_p = \frac{1}{2}\frac{F_b m^3}{3EI} = \frac{2F_b m^3}{E \cdot l_{eff} t^3} = \frac{2F_b}{E \cdot k_p} \tag{4.26}$$

and deformation of the bolt is

$$\delta_p = \frac{F_b L_b}{E_b A_b} = \frac{F_b}{E_b k_b} \tag{4.27}$$

The stiffness of the T-stub is written as

$$k_T = \frac{F_b}{E\left(\delta_p + \delta_b\right)} \tag{4.28}$$

In following conditions cases prying force are appearing in the T-stub

$$\frac{A_s}{L_b} \geq \frac{l_{eff,ini}\, t^3}{8.82\, m^3} \tag{4.29}$$

Formulas for stiffness coefficient of the base plate and of the bolt are

$$k_p = \frac{l_{eff,ini}\, t^3}{m^3} = \frac{0.85\, l_{eff} t^3}{m^3} \tag{4.30}$$

$$k_b = 1.6\frac{A_s}{L_b} \tag{4.31}$$

In case of no prying, it means when

$$\frac{A_s}{L_b} \leq \frac{l_{eff,ini}\, t^3}{8.82\, m^3} \tag{4.32}$$

Formulas are as following:

$$k_p = \frac{F_p}{E\, \delta_p} = \frac{l_{eff,ini}\, t^3}{2\, m^3} = \frac{0.425\, l_{eff}\, t^3}{m^3} \tag{4.33}$$

$$k_b = \frac{F_p}{E\delta_p} = 2.0\,\frac{A_s}{L_b} \tag{4.34}$$

The stiffness of the component of base plate in bending and bolts in tension is summarised from above simplified predictions as

$$\frac{1}{k_T} = \frac{1}{k_{b,i}} + \frac{1}{k_{p,i}} \tag{4.35}$$

For base plates are used the bolt pads under the bolt nut to help to cover the tolerances. The impact of an area of the bolt pad/nut changes the geometrical characteristics of T-stub. The influence is taken into account by the help of equivalent moment of inertia $I_{p,bp}$ and addition of stiffness k_w to the previous stiffness k_p. By practical design this influence is neglected for simplicity, see (Hofmann, 2005), even if it may be significant for resistance.

4.2 Threaded stud in tension

The threaded studs are efficient connectors welded by fabricator or on side with high level of automation, see (Metric studs 2009,2013 and Pitrakkos and Tizani, 2013) . The tension resistance of a threaded stud may be limited by

yielding resistance

$$N_{y,s} = n_a A_s f_{yk} \qquad (4.36)$$

ultimate resistance

$$N_{u,s} = n_a A_s f_{uk} \qquad (4.37)$$

initial stiffness

$$S_{i,s} = n_a \frac{E A_s}{l_{eff}} \qquad (4.38)$$

where

n_a is the number of threaded studs in a row

A_s is the area in tension of one threaded stud

l_{eff} is the effective length of the threaded stud

f_{yk} is the yield stress of the threaded stud

f_{uk} is the ultimate stress of the threaded stud

This solution procedure is applied to the headed stud connection the anchor plate to concrete block.

4.3 Punching of the anchor plate

The anchor plate under the threaded stud or above the headed stud may reach its load capacity due to shear resistance

$$F_{ap,Rd} = \frac{A_{p1,eff} \cdot f_{y,k}}{\gamma_{M0}} \qquad (4.39)$$

The stress area $A_{p1,eff}$ is determined from the thickness of the anchor plate t_{p1} and effective length $l_{v1,eff}$ of the sheared area

$$A_{ap,eff} = l_{v1,eff} \cdot t_{p1} \qquad (4.40)$$

Due to high bending of the threaded stud under the large deformations of the thin plate is assumed the effective length of shear area as half of the circumference only

$$l_{v1,eff} = 2\pi \cdot \left(a_w + \frac{d_{ts}}{2}\right)$$ (4.41)

where

a_w is throat thickness of weld of threaded stud [mm]

d_{ts} is diameter of the headed/threaded stud [mm]

This failure is assumed at all places, where a stud loaded by tension force is welded directly to a steel plate. The endless stiffness of this component should be assumed in calculations as no visible significant deformation performs due to punching trough steel plate during loading.

4.4 Anchor plate in bending and tension

The anchor plate is designed as a thin steel plate located at the top of concrete block and loaded predominantly in compression and shear. By loading the column base by the bending or tension is the anchor plate exposed to the tensile force from the treaded studs. If the threaded studs are not located directly under the headed studs, which are embedded in concrete, the anchor plate is exposed to bending, see Fig. 2.15. After the plastic hinges of the T-stub are developed, the anchor plate between the plastic hinges is elongates by tensile force.

Base plate and anchor plate   T stub plastic deformation under threaded stud

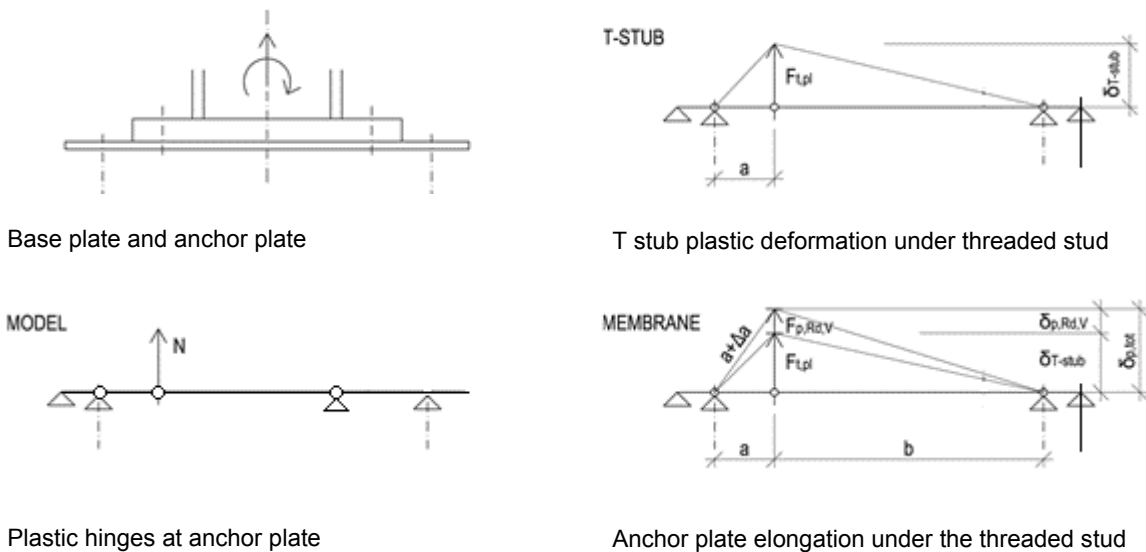Plastic hinges at anchor plate   Anchor plate elongation under the threaded stud

Fig. 4.15 Model of the anchor plate in bending and tension

The resistance of the component, see (Kuhlman et al, 2012), is not restricted to plastic mechanism only. The deformed shape with the elongated anchored plate between the threaded and headed studs is caring the additional load and may be taken into account. The behaviour, till the plastic hinges are developed, is modelled as the based plate in bending with help of T stub model, see Chapter 3.4. The anchor plate in tension resistance is

$$F_{t,ap,Rd} = A_{ap,1} \cdot \frac{f_{yk}}{\gamma_{M0}} = t_{p1} \cdot b_{ap,eff} \cdot \frac{f_{yk}}{\gamma_{M0}} \qquad (4.42)$$

where

t_{p1} is the thickness of the anchor plate

$b_{ap,eff} = n_1 \cdot \left(d_1 + 2 \cdot \sqrt{2} \cdot a_w\right)$ is the anchor plate effective width

a_w is throat thickness of weld of threaded stud

n_1 is the number of treaded studs

d_1 is the diameter of treaded stud

As the tensile force is developing in anchor plate the headed and threaded studs are exposed to horizontal force, see in Fig. 4.16. The elastic-plastic deformation at the stage of full plastification of the T stub is evaluated, see in Fig 4.17, by model of beam with four supports and three plastic hinges, see Fig. 4.15. The elongation of the anchor plate allows the uplift of the threaded stud. The model assumes that the supports, i.e. the headed and threaded studs, don't move in the horizontal direction and the headed stud in the vertical direction. E.g. the horizontal force depends linearly to the vertical one, see Fig. 4.18 and Fig. 4.19. The resulting horizontal force from tension in anchor plate is taken into account for evaluation of resistance of the components in shear and for the interaction of shear and tensile resistances.
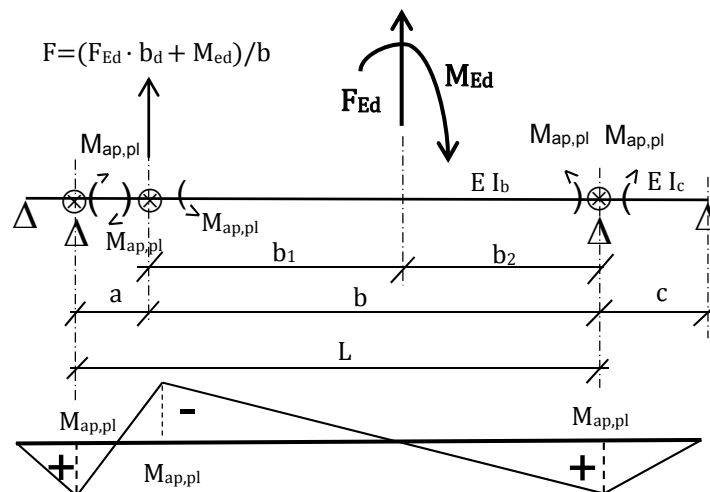

Fig. 4.16 Plastic hinges and bending moments in the anchor plate

In case of activation of the membrane action in anchor plate is verified the resistance of the related components in tension in vertical direction and in shear in horizontal direction. In the procedure is derived:

- the bending resistance of the anchor plate,
- the tensile resistance of the anchor plate,
- the bending and tensile deformation of the anchor plate.

and further is limited the resistance of the component anchor plate in bending and tension by

- the vertical resistance of the threaded stud (tensile and punching resistance) and the headed studs (tensile resistance, concrete cone failure, stirrups failure, bond failure).
- the horizontal resistance of the threaded stud (shear and bearing resistance) and the headed studs (shear and pry out resistance).

- the interaction in the threaded stud (tension and shear resistances) and the headed studs (tension and shear resistances).

The plastic resistance of the anchor plate is

$$M_{ap,pl} = \frac{l_{eff,1} \cdot t_{p1}^2}{4} \cdot \frac{f_{yk}}{\gamma_{M0}}$$

(4.43)

where

t_{p1} is thickness of the anchor plate [mm]

$l_{eff,1}$ is the effective width of the anchor plate [mm]

The effective width of the anchor plate is minimum of the

$$l_{eff,1} = \min \begin{cases} 4 \ m_1 + 1.25 \ e_{a1} \\ 2 \ \pi \ m_1 \\ 5 \ n_1 \ d_1 \cdot 0.5 \\ 2 \ m_1 + 0.625 \ e_{a1} + 0.5 \ p_1 \\ 2 \ m_1 \ + 0.625 \ e_{a1} + e_{b1} \\ \pi \ m_1 + 2 \ e_{b1} \\ \pi \ m_1 + p_1 \end{cases}$$

(4.44)

where $5 \ h_1 \ d_1$ is the effective width of the T stub between the headed and threaded studs.

The vertical deformation of the anchor plate under bending may be assumed for a beam with four supports and three plastic hinges as

$$\delta_T = \frac{1}{E \ I_b} \cdot \frac{1}{6} \cdot b^2 \cdot M_{ap,pl} + \frac{1}{E \ I_c} \cdot \frac{1}{3} \cdot b \cdot c \cdot M_{ap,pl}$$

(4.45a)

The elastic part of the deformation is

$$\delta_{T,el} = \frac{2}{3} \cdot \delta_T$$

(4.45b)

The elastic-plastic part of the deformation, see Fig. 4.17, is

$$\delta_{T,pl} = 2.22 \ \delta_{T,el}$$

(4.45c)

The force at the bending resistance of the anchor plate is evaluated from equilibrium of internal forces

$$N_{pl} \cdot \delta_T \cdot \frac{b_2}{b} + M_{Ed} \cdot \frac{\delta_T}{b} = 2 \cdot M_{ap,pl} \cdot \frac{\delta_T}{a} + 2 \cdot M_{ap,pl} \cdot \frac{\delta_T}{b}$$

(4.45)

$$N_{pl} \cdot b_2 + M_{Ed} = 2 \cdot M_{ap,pl} \cdot b \cdot \left(\frac{1}{a} + \frac{1}{b}\right)$$

(4.46)

$$\text{for } M_{Ed} = N_{Rd} \cdot e$$

$$\text{is } N_{pl} \cdot b_2 + N_{Rd} \cdot e = 2 \cdot M_{ap,pl} \cdot b \cdot \left(\frac{1}{a} + \frac{1}{b}\right)$$

(4.47)

$$N_{pl} = 2 \cdot M_{ap,pl} \cdot b \cdot \frac{\left(\frac{1}{a} + \frac{1}{b}\right)}{(b_2 + e)} \tag{4.48}$$

The vertical resistance of the component anchor plate in tension is limited by the resistance of the components: threaded stud in tension, punching of the threaded stud and tensile resistance of the anchor plate. For the thin anchor plate is decisive the punching of the threaded stud. The deformed length of the anchor plate between the threaded and headed studs at the resistance in punching of the anchor plate under the threaded stud is

$$a_{ap} = a + \Delta a = a + \frac{a \cdot F_{ap,Rd}}{t_{p1} \cdot b_{ap,eff} \cdot E} \tag{4.49}$$
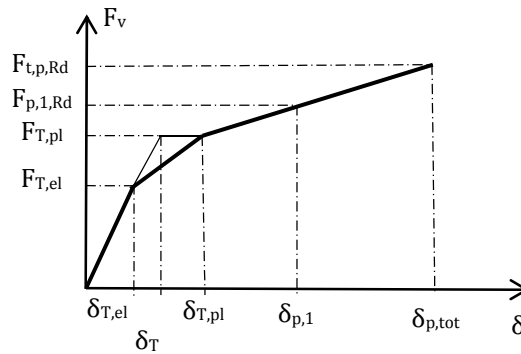
Fig. 4.17 Linear relation of acting vertical forces F_v and vertical deformation δ_v

The component of vertical deformation by the elongation of the anchor plate, see Fig. 4.14, is

$$\delta_{p,tot} = \delta_{T,pl} + \sqrt{a_{ap}^2 - a^2} \tag{4.50}$$

The component of the horizontal force at the resistance in punching of the anchor plate under the threaded stud, see Fig. 4.18, is

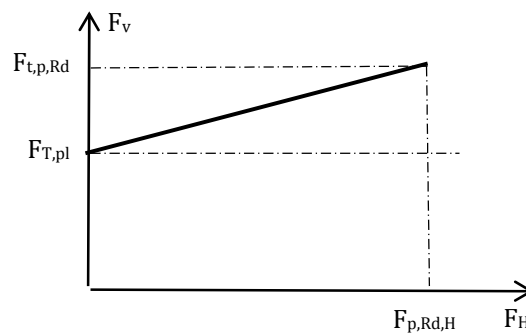$$F_{p,Rd,H} = \frac{a}{\delta_{p,tot}} \cdot F_{t,p,Rd} \tag{4.51}$$

Fig. 4.18 Linear relation of vertical F_v and horizontal forces F_H

The horizontal force $F_{ap,v}$ is limited by shear resistance of the threaded and headed studs V_{Rd}, see in Figs 4.19. The resistance to vertical force is

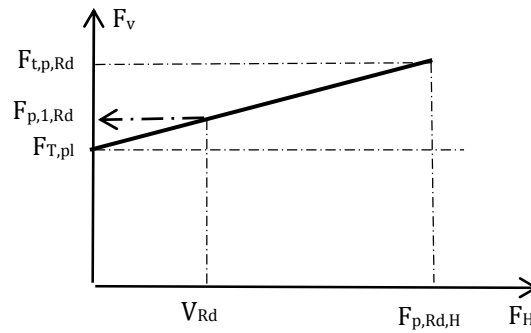$$F_{p,1,Rd} = F_{T,pl} + \frac{F_{t,p,Rd} - F_{T,pl}}{F_{p,Rd,H}} \cdot V_{Rd} \qquad (4.52)$$

Fig. 4.19 Linear relation of vertical F_v and horizontal forces F_H at resistance

The interaction of the tensile and shear forces is verified for the threaded and headed studs, see Tab. 3.4 in EN1993-1-8:2006 by

$$\frac{F_{v,Ed}}{F_{v,Rd}} + \frac{F_{t,Ed}}{1.4 \cdot F_{t,Rd}} \le 1 \qquad (4.53)$$

The interaction of tensile and shear forces is verified for the headed stud anchoring to concrete, see Chapter 3.2.5 by

$$\left(\frac{F_{v,Ed}}{F_{v,Rd}}\right)^{\frac{3}{2}} + \left(\frac{F_{t,Ed}}{F_{t,Rd}}\right)^{\frac{3}{2}} \le 1 \qquad (4.54)$$

4.5   Column/beam flange and web in compression

The resistance of the column flange and web in compression may be expected as for the beam flange, see Chapter 6.2.6.7 in EN1993-1-8:2006. In this model the column/beam web has its full plastic resistance on the lever arm of column/beam flanges

$$F_{c,f,Rd} = \frac{M_{c,Rd}}{(h - t_f)} \qquad (4.55)$$

in EN1993-1-8:2006 Eq. (4.1), where

$M_{c,Rd}$ is the design moment resistance of the beam cross-section, see EN1993-1-1:2004

h is the depth of the connected column/beam

t_f is the column/beam flange thickness

If the height of the column/beam including the haunch exceeds 600 mm the contribution of the beam web to the design compression resistance should be limited to 20%. If a beam is reinforced with haunches the proposal for design is in cl 6.2.6.7(2). The stiffness of this component in compression is expected to be negligible.

4.6   Steel contact plate

The resistance of the steel contact plate in joint may be taken as its full plastic resistance

$$F_{cp} = f_{y,cp} \, A_{cp} \qquad (4.56)$$

where

$f_{y,cp}$ is the yield strength of the steel contact plate

A_{cp} is the effective area of the contact plate under compression

A height or breadth of the contact plate exceeds the corresponding dimension of the compression flange of the steel section, the effective dimension should be determined assuming dispersion at 45° through the contact plate. It should be assumed that the effective area of the contact plate in compression may be stressed to its design yield strength f_{yd}, see EN1994-1-1:2010. The stiffness of the component the steel contact plate is negligible

4.7   Anchor bolts in shear

In most cases the shear force is transmitted via friction between the base plate and the grout. The friction capacity depends on the compressive normal force between the base plate and the grout and the friction coefficient, see Chapter 3.3.7. At increasing horizontal displacement the shear force increases till it reaches the friction capacity. At that point the friction resistance stays constant with increasing displacements, while the load transfer through the anchor bolts increases further. Because the grout does not have sufficient strength to resist the bearing stresses between the bolts and the grout, considerable bending of the anchor bolts may occur, as is indicated in Fig. 4.20, see (Bouwman et al, 1989). The tests shows the bending deformation of the anchor bolts, the crumbling of the grout and the final cracking of the concrete. Based on the work (DeWolf and Sarisley, 1980) and (Nakashima,1998) and of tests (Bouwman et al, 1989) the analytical model for shear resistance of anchor bolts was derived in EN1993-1-8 cl 6.2.2, see (Gresnight at al, 2008). Also, the preload in the anchor bolts contributes to the friction resistance. However, because of its uncertainty, e.g. relaxation and interaction with the column normal force, it was decided to neglect this action in current standard.

Fig. 4.20 Test specimen loaded by shear force and tensile force

The design shear resistance $F_{v,Rd}$ may be derived as follows

$$F_{v,Rd} = F_{f,Rd} + n \, F_{vb,Rd} \qquad (4.57)$$

where

$F_{f,Rd}$ is the design friction resistance between base plate and grout layer

$$F_{f.Rd} = C_{f,d}\, N_{c,Ed_{v,Rd}} \tag{4.58}$$

$C_{f,d}$ is the coefficient of friction between base plate and grout layer. The following values may be used for sand-cement mortar $C_{f,d} = 0.20$, see Chapter 3.3.7.

$N_{c,Sd}$ is the design value of the normal compressive force in the column. If the normal force in the column is a tensile force $F_{f,Rd} = 0$

n is the number of anchor bolts in the base plate

$F_{vb,Rd}$ is the smallest of $F_{1.vb.Rd}$ and $F_{2.vb.Rd}$

$F_{1.vb.Rd}$ is the shear resistance of the anchor bolt and

$$F_{2,vb,Rd} = \frac{\alpha_b\, f_{ub}\, A_s}{\gamma_{M2}} \tag{4.59}$$

A_s is the tensile stress area of the bolt or of the anchor bolt

α_{bc} is a coefficient depending on the yield strength f_{yb} the anchor bolt

$$\alpha_{bc} = 0.44 - 0.0003\, f_{yb} \tag{4.60}$$

f_{yb} is the nominal yield strength the anchor bolt

where $235\ \text{N/mm}^2 \le f_{yb} \le 640\ \text{N/mm}^2$

γ_2 is the partial safety factor for anchor bolt

5 ASSEMBLY FOR RESISTANCE

5.1 Column base

5.1.1 Column base with base plate

The calculation of the column base resistance, based on the plastic force equilibrium on the base plate and applied in EN1993-1-8:2006, is described in (Wald et al, 2008). Based on the combination of acting load, see Fig. 5.1, three patterns may be distinguished:

Pattern 1 <u>without tension in anchor bolts</u> occurs due to high normal force loading. The collapse of concrete appears before developing stresses in the tension part.

Pattern 2 <u>with tension in one anchor bolt row</u> arises when the base plate is loaded by small normal force compared to the ultimate bearing capacity of concrete. During collapse the concrete bearing stress is not reached. The breaking down occurs because of yielding of the bolts or because of plastic mechanism in the base plate.

Pattern 3 <u>with tension in both rows of anchor bolts</u> occurs when the base plate is loaded by tensile normal force. The stiffness is guided by yielding of the bolts or because of plastic mechanism in the base plate. This pattern occurs often in base plates designed for tensile force only and may lead to contact of baseplate to the concrete block.

The connection is loaded by axial force N_{Ed} and bending moment M_{Ed}, see Fig. 5.1. The position of the neutral axis is calculated according to the resistance of the tension part $F_{T,Rd}$. Then the bending resistance M_{Rd} is determined assuming a plastic distribution of the internal forces, see (Dewolf, Sarisley, 1980). For simplicity of the model, only the effective area is taken into account. The effective area A_{eff} under the base plate, which is taken as an active part of equivalent rigid plate, is calculated from an equivalent T-stub, with an effective width c, see Chapter 3.4.2. The compression force is assumed to act at the centre of the compressed part. The tensile force is located at the anchor bolts or in the middle when there are more rows or bolts, see (Thambiratnam, Paramasivam, 1986). Like for another cross sections of the composite structures there should be a closer look at the resistance for the ultimate limit state ULS and to the elastic behaviour under the serviceability limit state SLS. In the ultimate limit state the failure load of the system is important. Under service loads is checked the elastic behaviour and that the concrete cone will not fail. This would lead to cracks and with the time to a corrosion of the reinforcement of the concrete wall and finally to a failure of the construction.
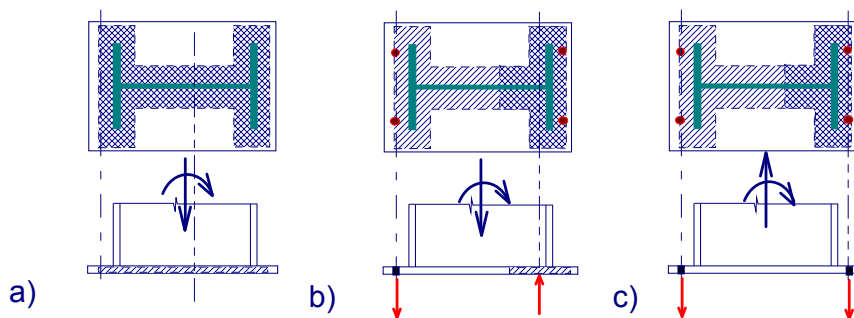

Fig. 5.1 The force equilibrium of the base plate a) no tension in anchor bolts,
b) one row of the anchor bolts in tension, c) two rows of the anchor bolts in tension
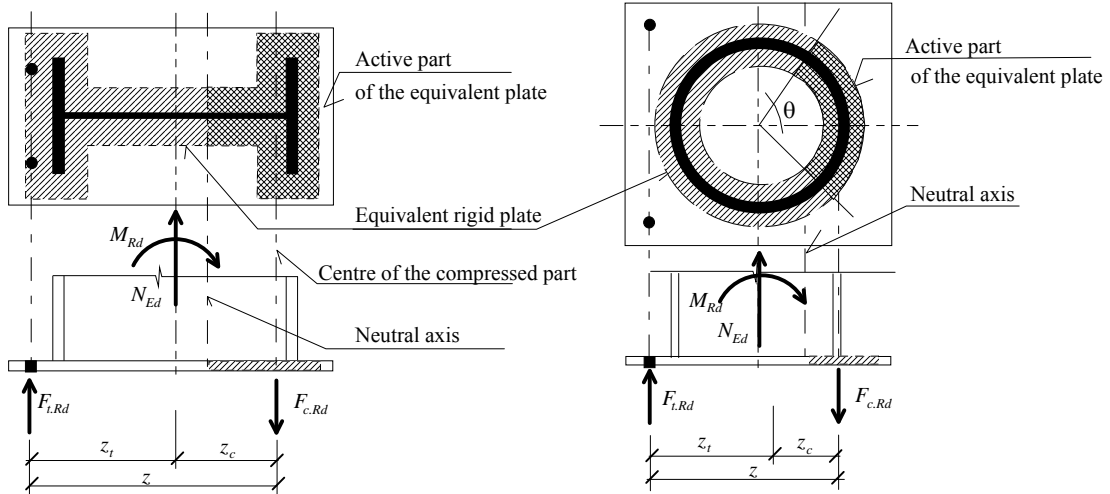
Fig. 5.2 Force equilibrium for the column base, one row of the anchor bolts in tension

The equilibrium of forces is calculated according to Fig. 5.2 as follows:

$$N_{Ed} = F_{c,Rd} + F_{t,Rd} \tag{5.1}$$

$$M_{Rd} = F_{c,Rd} \cdot z_c + F_{t,Rd} \cdot z_t \tag{5.2}$$

where

$$F_{c,rd} = A_{eff} \cdot f_{jd} \tag{5.3}$$

A_{eff} is effective area under the base plate.

The resistance of the compressed part $F_{c,Rd}$ and the resistance of the part in tension $F_{t,Rd}$ are determined in previous Chapters. If the tensile force in the anchor bolts according to Fig. 5.2 occur for

$$e = \frac{M_{Rd}}{N_{Ed}} \geq z_c \tag{5.4}$$

formulas for tension and compressed part is derived

$$\frac{M_{Rd}}{z} - \frac{N_{Ed} \cdot z_c}{z} \leq F_{c1,Rd} \tag{5.5}$$

$$\frac{M_{Rd}}{z} + \frac{N_{Ed} \cdot z_{c1}}{z} \leq F_{c,Rd} \tag{5.6}$$

Then, the column base moment resistance M_{Rd} under a constant normal force N_{Ed} is expressed as follow:

with tension force in the anchor bolts

$$M_{Rd} = \min \begin{cases} F_{t,Rd} \cdot z + N_{Ed} \cdot z_c \\ F_{c,Rd} \cdot z - N_{Ed} \cdot z_t \end{cases} \tag{5.7}$$

without tension force, both parts are compressed

$$M_{Rd} = \min \begin{cases} F_{c1,Rd} \cdot z + N_{Ed} \cdot z_c \\ F_{c,Rd} \cdot z - N_{Ed} \cdot z_{c1} \end{cases} \tag{5.8}$$

The procedure is derived for open section of I/H cross section. For rectangular hollow section RHS may be taken directly taking into account two webs. For circular/elliptical hollow sections CHS/EHS may be modified, see Fig. 5.2 and (Horová, 2011). Using sector coordinates depends the effective area $A_{eff} = 2\,\theta\,r\,c$ on the angle θ. The lever arm and the resistance of the component in compression is

$$z_c = r \cdot \cos\frac{\theta}{2} \tag{5.9}$$

$$F_{c,Rd} = F_{c1,Rd} = \pi \cdot r \cdot c \tag{5.10}$$

The resistance of the base plate connection under different loading is illustrated in M-N interaction diagram. In Fig. 5.3a there is an example of this diagram with its important points.
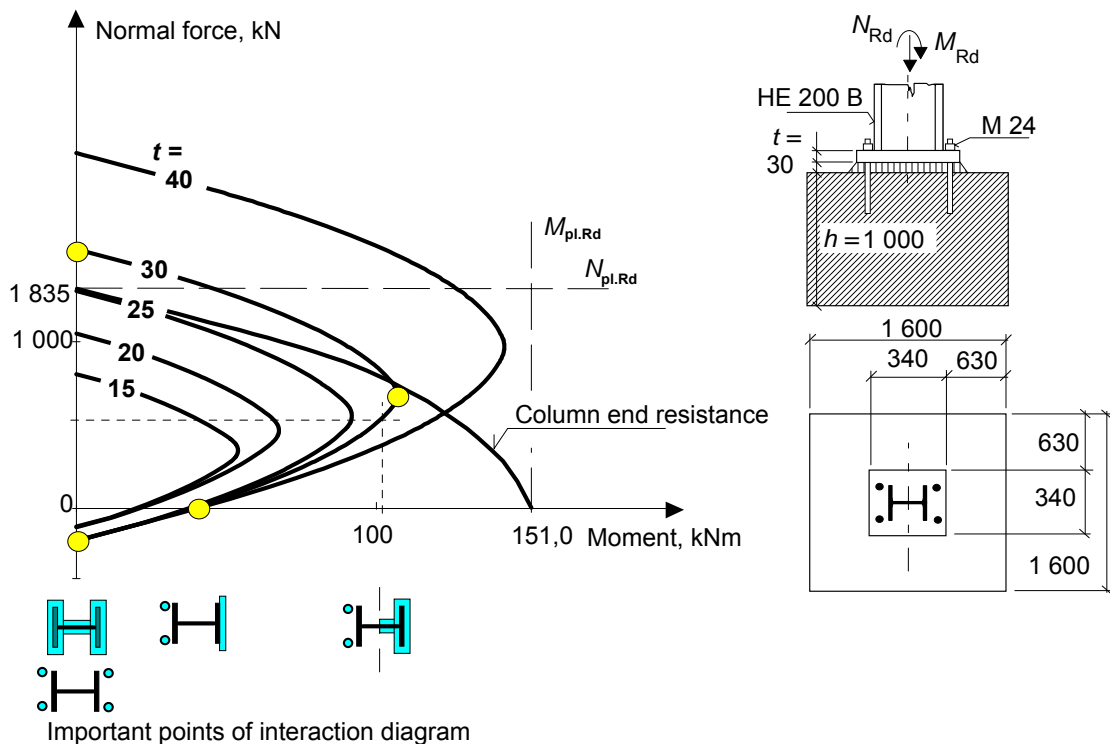
Fig. 5.3a An example of M-N interaction diagram for the base plate connection

5.1.2 Column base with anchor plate

The bending resistance of the base plate with anchor plate is assembled from the tensile/compression resistances of its component. The additional components to the column bases without the anchor plate is the anchor plate in bending and in tension. The procedure for evaluation of the resistance is the same in all connections loaded by bending moment and normal force.

First the resistance of the components in tension is evaluated: the base plate, the threaded studs, the anchor plate and the headed studs. The activated area in contact under the base and anchor plate is calculated from the equilibrium of internal forces for the tensile part resistance. From the known size of the contact area is calculated the lever arm and the

bending resistance of the column base for particular acting normal force by the same procedure like for column base with the base plate only without the anchor plate.

During design of the base plate with the anchor plate is the elastic-plastic stage at serviceability limit verified separately, similar to the composite steel and concrete beam design. If the headed and threaded studs are not over each another the resistance of the base plate is influenced by the resistance of the component the anchor plate in tension and related components like punching of treated studs. The elastic-plastic resistance at Serviceability limit state is calculated based on the bending resistance of the anchor plate only. Moment rotational diagram at Fig. 5.4b sums up the behaviour of column base which is influenced by the elastic bending of the anchor plate (1), its elastic-plastic bending (2) and its tension (3).
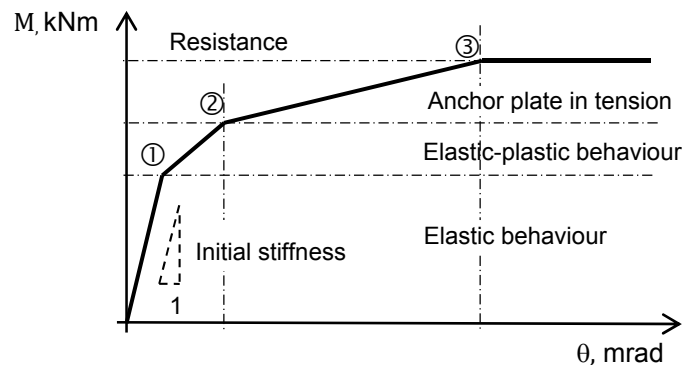
Fig. 5.3b Moment rotational diagram of column base with anchor plate

5.2   Simple steel to concrete joint

This joint typically represents a connection of a steel structure to a concrete wall. The anchor plate is loaded by shear load V_{Ed} and a bending moment $M_{y,Ed}$. The developed model assumes a stiff anchor plate and deformations due to the anchor plate are neglected. The connection between the girder and the anchor plate may be regarded as pinned, rigid or semi-rigid. For most structures the connection between the beam and the anchor plate may be assumed as pinned. In this case of a simple connection the anchor plate is only loaded by shear load and a corresponding bending moment caused by the eccentricity of the shear load. The connection between the girder and the anchor plate may be realised with butt straps or cams or any other simple connection, see Fig. 5.4.
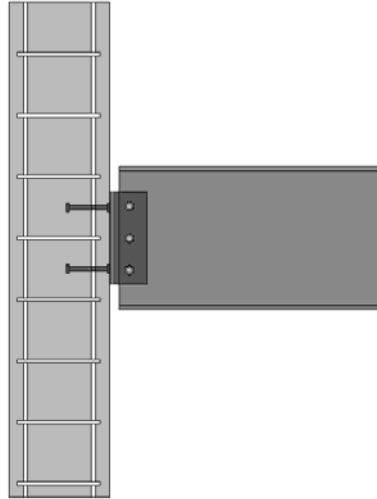
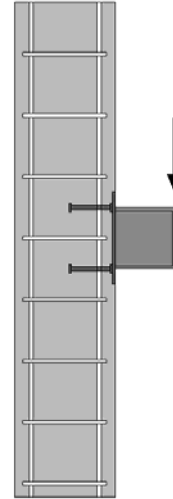Fig. 5.4a Simple joint with butt straps   Fig. 5.4b Simple joint with cams

If the connection between the girder and the anchor plate cannot be assumed as pinned, there might be larger bending moments in the joint. In this Chapter the system described is a pinned connection between the beam and the anchor plate with an eccentricity e_v. However if there is a bending moment derived in the global analysis, the eccentricity e_v may be assumed no longer a purely geometrical value anymore but is calculated by

$$e_v = \frac{M_{y,Ed}}{V_{Ed}}$$
(5.11)

The developed component model describes the structural behaviour of the simple joints. The joints are consisting of an anchor plate with headed studs with and without additional reinforcement in cracked as well as non-cracked concrete. To prove a sufficient resistance for the ultimate limit state, the following steps have to be done:

- evaluation of the tension force caused by the shear load,
- verification of the geometry of the tension zone,
- evaluation of the tension resistance,
- evaluation of the shear resistance,
- verification of interaction conditions.

In the following the mechanical joint model for the simple joints is described. Due to the eccentricity of the applied shear load a moment is acting on the anchor plate. This moment causes forces, which are shown in Fig. 5.5. The anchor row on the non-loaded side of the anchor plate is in tension. This anchor row represents the tension component of the joint $N_{Ed,2}$ and forms a vertical equilibrium with the compression force C_{Ed} under the anchor plate on the loaded side. The shear forces are carried by the headed studs, $V_{Ed,1}$ and $V_{Ed,2}$, and the friction between steel and concrete V_f.

The tension component of the joint, which is represented by the headed studs in tension or headed studs with stirrups in tension, in the case of using additional reinforcement, is described in Chapter 3. If no additional reinforcement is used, the following failure modes may occur: steel failure of the shaft, pull-out failure of the headed stud due to the high compression of the stud head on the concrete and concrete cone failure of the anchorage. When using additional reinforcement however, the stirrups contribute to the deformation and the resistance of the tension component. Besides the steel failure and the pull-out failure of the headed studs, a concrete failure due to yielding of the stirrups, an anchorage failure of the stirrups and a smaller

concrete cone failure may appear. A detailed description of these components is found in Chapter 3.
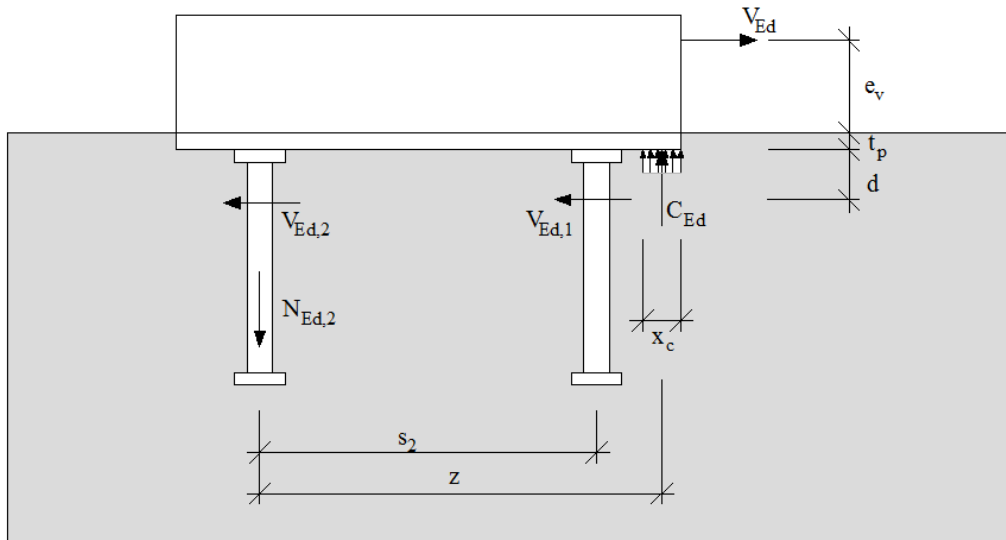

Fig. 5.5 Forces at the anchor plate caused by the shear force V_{Ed} and its eccentricity e_V

For the compression zone a rectangular stress block is assumed under the loaded side of the plate. The stresses in the concrete are limited according to EN1993 1-8 cl 6.2.5. The design bearing strength of the concrete is f_{jd}. When there is no grout and the anchor plate has a common geometry, f_{jd} may be assumed as $f_{jd} = 3f_{cd}$. The stress area A_c is given by the width of the anchor plate b and the length of the compression zone x_c perpendicular to the load, resulting from the equilibrium with the assumed tension force in the studs on the non-loaded side $N_{Ed,2}$. As the anchor plate is regarded as stiff, the compression zone starts at the edge of the plate. The stiffness of this component is assumed according to Chapter 3.

Equilibrium
$$\sum N: C_{Ed} = N_{Ed,2} \tag{5.12}$$

Compression force
$$C_{Ed} = f_{jd} \cdot x_c \cdot b$$
$$\text{for most cases } f_{jd} = 3 \, f_{cd} \tag{5.13}$$

The position of the shear load $V_{Ed,1}$ and $V_{Ed,2}$ has been derived according to the stress distribution given by the results of numerical calculations. There it is seen that the resulting shear force is placed with a distance of about d in average from the anchor plate, when d is the diameter of the headed stud. As a simplification of the mechanical joint model it is assumed that the shear forces of both anchor rows appear in the same line, see Fig. 5.6. In case of a high tension in the first row of studs only small additional shear forces $V_{Ed,2}$ is applied the 2nd stud row. The position of the friction force V_f is assumed between the concrete surface and the anchor plate.
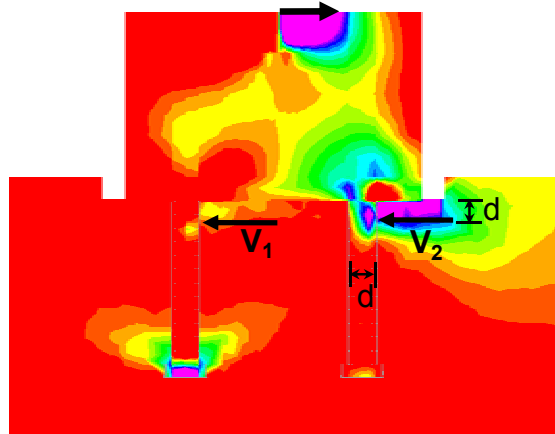
Fig. 5.6 Stress distribution σ_x in load direction

Forming the moment equilibrium according to (5.14), the size of the tension and the compression component of the joint is calculated. The rotational equilibrium is calculated for the point in the middle of the compression zone in one line with $V_{Ed,1}$ and $V_{Ed,2}$. The shear force is turning clockwise with a lever arm of $e_v + d + t_p$. The tension force $N_{Ed,2}$ is turning counter clockwise with a lever arm of z. The friction force is turning counter clockwise with a lever arm of d. The tension component carried by the second stud row $N_{Ed,2}$ is calculated with the following formula.

$$V_{Ed} \cdot (e_v + d + t_p) = N_{Ed,2} \cdot z + V_f \cdot d \tag{5.12}$$

$$N_{Ed,2} = \frac{V_{Ed} \cdot (e_v + d + t_p) - V_f \cdot d}{z} \tag{5.13}$$

If the pinned joint is loaded by diagonal pull, additional normal forces have to be considered in the moment equation, see Eq. (5.16). This equation requires, that the normal force does not lead to an uplift of the anchor plate. In this case both anchor rows would be subjected to tension forces and no shear resistance due to friction forces is carried by the pinned joint.

$$V_{Ed} \cdot (e_v + d + t_p) + N_{Ed} \cdot \left(z - \frac{s_2}{2}\right) = N_{Ed,2} \cdot z + V_f \cdot d \tag{5.14}$$

As already described above, the assumed tension load in the headed studs on the non-loaded side and the compression component form a vertical equilibrium. This approach requires an iterative process, as the area of the compression zone is dependent on the assumption for the tension load in the studs on the non-loaded side. But the shear resistance of the joint is not only limited by the acting moment. Therefore as a last step the resistance of the shear components have to be verified. The joint shear resistance is defined by the sum of the shear resistance of the studs and the friction between the concrete surface and the anchor plate, see Fig. 5.7 The resistance due to friction V_f is defined by the coefficient μ for friction between steel and concrete. In cl 6.2.2 of EN1993-1-8:2006 a friction coefficient of $\mu = 0.2$ is proposed. The stiffness is assumed as infinite, as the displacement is zero if the shear force is smaller than V_f.

Friction between steel and concrete V_f

1st stud row of headed studs in shear $V_{Ed,1}$

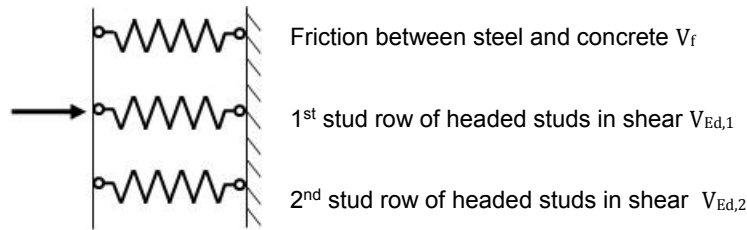2nd stud row of headed studs in shear $V_{Ed,2}$

Fig. 5.7 Shear components

After subtracting the component of the friction force, the rest of the applied shear load has to be carried by the headed studs. The total shear resistance depends on two possible failure modes due to shear: Steel failure of the headed studs as well as Concrete cone failure respectively pry-out failure. Also the distribution of the shear load among the anchor rows depends on the failure mode. Furthermore interaction between tension and shear loads in the stud row on the non-loaded side of the anchor plate has to be considered resulting in a reduced resistance of these studs. In case of a steel failure of the headed studs, it is assumed that at ultimate limit state the front anchor row is subjected to 100% of its shear resistance, as there are acting no tensional forces. The remaining part of the shear load is carried by the back row of anchors, depending on the interaction conditions. In contrast when verifying the anchorage for concrete failure, the shear load is distributed half to the front and half to the back row of anchors. Thereby the interaction condition for concrete failure has to be considered. The following interaction conditions are used:

Concrete failure $$n_N^{3/2} + n_V^{3/2} \leq 1 \qquad (5.15)$$

$$(5.16)$$

Steel failure $$n_N^2 + n_V^2 \leq 1$$

where

n_N is the minimum value for $\dfrac{N_{Ed,i}}{N_{Rd,i}}$

n_V is the minimum value for $\dfrac{V_{Ed,i}}{V_{Rd,i}}$

Additional verifications required

In the preceding description not all verifications are covered. Additional checks, which are not described in this manual have to be done:

- Verification of the steel components connected to the anchor plate.
- Calculation of the anchor plate. The calculated tension and compression forces causes bending moments in the anchor plate. The anchor plate must be able to carry these bending moments. The anchor plate has to be stiff and therefore in the plate no yielding is allowed.
- Additional checks for the reinforcement in the concrete wall to prevent local failure of the concrete due to the compression force with have to be done, see EN19921-1:2004.
- The concrete wall must be able to carry the loads transferred by the anchor plate.

The verification of the design resistance of the joint is described in the Table 5.1 in a stepwise manner.

Tab. 5.1 Verification of the design resistance of the joint

Step	Description	Formula	
		The eccentricity e_v and the shear force V_{Ed} are known.	
1	**Evaluation of the tension force caused by the shear load** Estimation of x_c and calculation of the tension component $N_{Ed,2}$.	z is depending on x_c $$N_{Ed,2} = \frac{V_{Ed} \cdot (e_v + d + t_p) - V_f \cdot d}{z}$$	
2	**Verification of compression height.** Check if the assumption for x_c is OK.	$$\sum N: C_{Ed} = N_{Ed,2} \qquad x_c = \frac{C_{Ed}}{b \cdot f_{jd}}$$ If x is estimated too small go back to Step 1 and try again. For most cases $f_{jd} = 3\,f_{cd}$	
3	**Evaluation of the tension resistance** Calculation of $N_{Rd,u}$	Without Stirrups $$N_{Rd,u} = \min \begin{cases} N_{Rd,u,s} \\ N_{Rd,p} \\ N_{Rd,u,c} \end{cases}$$	With Stirrups $$N_{Rd,u} = \min \begin{cases} N_{Rd,u,s} \\ N_{Rd,p} \\ \\ N_{Rd,cs} \\ N_{Rd,re,1} \\ N_{Rd,re,2} \end{cases}$$
4	**Calculation of the shear resistance**	$$V_{Rd,s} = 0.7 \cdot N_{Rd,u,s}$$ $$V_{Rd,cp} = k \ \min\left[N_{Rd,cs}, N_{Rd,re,1}, N_{Rd,re,2}, N_{Rd,u,group} \right]$$	
5	**Verification of interaction conditions**	Possible failure modes	
		Steel failure of the headed studs	Concrete failure
		$$V_{Ed,2} = V_{Ed} - V_{Rd,s} - V_f$$	$$V_{Ed,2} = \frac{V_{Ed} - V_f}{2}$$
		$$\left(\frac{N_{Ed,2}}{N_{Rd,u,s}}\right)^2 + \left(\frac{V_{Ed,2}}{V_{Rd,s}}\right)^2 \leq 1$$	$$\left(\frac{N_{Ed,2}}{N_{Rd,u}}\right)^{3/2} + \left(\frac{V_{Ed,2}}{V_{Rd,cp}}\right)^{3/2} \leq 1$$ $N_{Rd,u}$ is not including $N_{Rd,u,s}$
		Are both interaction equations OK?	
		YES	**NO**
		Design calculation finished	The load carrying capacity of the joint is not sufficient. The joint has to be improved.

5.3   Moment resistant steel to concrete joint

A representative spring and rigid link model was idealized for the behaviour of composite beam to reinforced concrete wall joint, subjected to hogging bending moment, which is illustrated in Fig. 5.8. The joint components are:

- longitudinal steel reinforcement in the slab, at Fig. component 1
- slip oft he composite beam ,component 2;
- beam web and flange, component 3;
- steel contact plate, component 4;
- components activated in the anchor plate connection, components 5 to 10 and 13 to 15;
- the joint link, component 11.
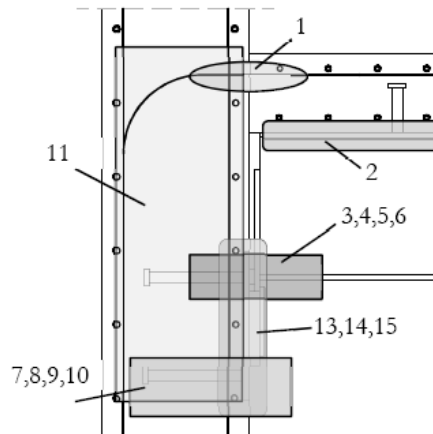
Fig. 5.8: Joint component model for the composite beam to reinforced concrete wall joint

In order to obtain the joint properties, the assembly of the components and of the joint models is described in the present section. For the joint under hogging bending moment, the assembly procedure was based on the mechanical model depicted in Fig. 5.8b. The determination of the joint properties to bending moment may be performed using a direct composition of deformations. The longitudinal steel reinforcement bar in slab, the slip of the composite beam, and the anchor plate components consider the models described in section 3. These models enable a good approximation to the real behaviour of the components, see (Henriques, 2008). The models may be described and composed also based on its stiffness coefficients as used in EN1993-1-8:2006.

The mechanical model represented in Fig. 5.9 presents only one row of components in tension and another in compression. This implies that the assembly procedure is much simpler, as no distribution of load is required amongst rows, as in steel/composite joint with two or more tension rows. Thus, the first step is the assembly of the components per row. Equivalent springs are defined per row, as represented in Fig. 5.9. The equivalent component/spring should perform as the group of components/springs it represents. The determination of its properties takes into consideration the relative position of the components: acting in series or in parallel. In the present case, either for the compression row either for the tension row, all joint components are acting in series. Thus, the determination of the properties of equivalent components/springs was performed as expressed in (5.17) for resistance $F_{eq,t}$ and $F_{eq,c}$, see (Henriques, 2008).
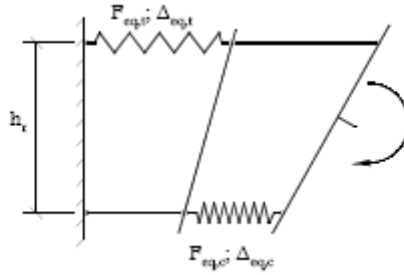
Fig. 5.9 Simplified joint model with assembly of components per row

$$F_{eq} = \min\{F_i \text{ to } F_n\} \tag{5.17}$$

where, the indexes i to n represent all components to consider either in tension either in compression, depending on the row under consideration.

Then, because only one tension row and one compression row was considered, the determination of the joint properties, M_j, Φ_j, becomes relatively easy. In order to determine the joint rotation, it is important to define the lever arm h_r. According to the joint configuration, it was assumed that the lever arm is the distance between the centroid of the longitudinal steel reinforcement bar and the mid thickness of bottom flange of the steel beam. The centroid of steel contact plate is assumed to be aligned with this reference point of the steel beam. Accordingly, the joint properties are obtained as follows:

$$F_{eq} = \min\{F_{eq,t}, F_{eq,c}, F_{JL}\} h_r \tag{5.18}$$

where, $F_{eq,t}$ and $F_{eq,c}$ are the equivalent resistance of the tension and compression rows, respectively, determined using Eq. (5.17).

6 ASSEMBLY FOR STIFFNESS

6.1 Column base

6.1.1 Column base with base plate

The calculation of stiffness of the base plate, given in (Wald et al, 2008), is compatible with beam to column stiffness calculation. The difference between these two procedures is in the fact that by the base plate joint the normal force has to be introduced, see (Ermopoulos, Stamatopoulos, 1996). In Fig. 6.1 there is the stiffness model which shows a way of loading, compression area under the flange, allocating of forces under the base plate, and a position of the neutral axes.
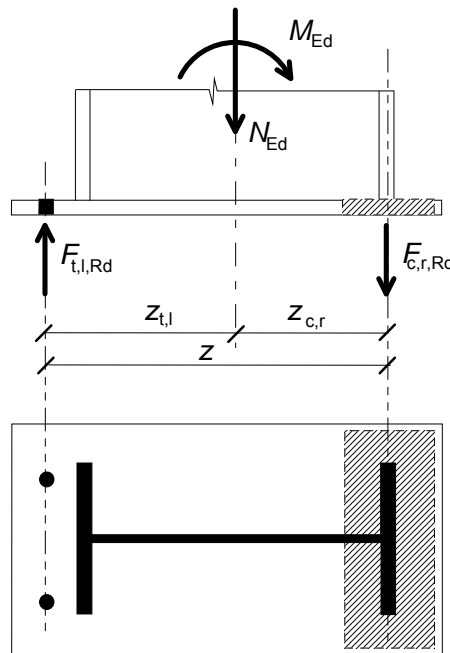
Fig. 6.1 The stiffness model of the base plate connection of the column base

By the calculation of the stiffness the effective area is only taken into account. The position of compression force $F_{c,Rd}$ is located at the centre of compression area. The tensile force $F_{t,Rd}$ is located at the anchor bolts. The rotational bending stiffness of the base plate is usually determined during proportional loading with constant eccentricity

$$e = \frac{M_{Ed}}{N_{Ed}} = \text{const.} \tag{6.1}$$

According to the eccentricity three possible basic collapse modes can arise with activation of anchor bolts, see (Wald et al, 2008). For large eccentricity with tension in one row of anchor bolts Pattern 1, see Fig. 6.2a, without tension in row of anchor bolts, small eccentricity, Pattern 2 in Fig. 6.2b, and with tension in both row of anchor bolts Pattern 3.

Pattern 1 with tension in one bolt row of anchor bolts arises when the base plate is loaded by small normal force compared to the ultimate bearing capacity of concrete. During collapse the concrete bearing stress is not reached. The breaking down occurs because of yielding of the bolts or because of plastic mechanism in the base plate.

Pattern 2 without tension in anchor bolts grows up during high normal force loading. The collapse of concrete appears before developing stresses in the tension part.

Pattern 3   with tension in one bolt row of anchor bolts arises when both bolt row of anchor bolts may be activated and column base is exposed to tension force in not so common, and the theorems may be derived similarly.
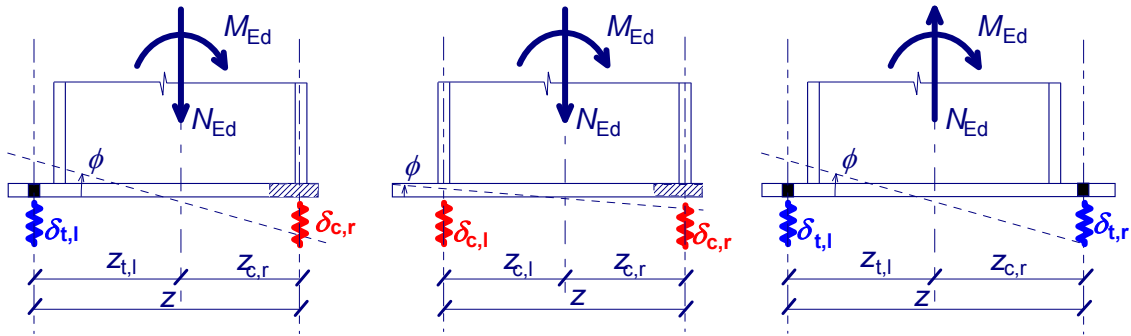

Fig. 6.2 The mechanical model of the base plate a) one anchor bolt row activated, b) no anchor bolt activated c) both anchor bolt rows activated

Deformations δ_t and δ_c of components depend on the stiffness of tension part k_t and the stiffness of the compression part k_c.

$$\delta_{t,l} = \frac{\frac{M_{Ed}}{z} - \frac{N_{Ed} z_t}{z}}{E\, k_t} = \frac{M_{Ed} - N_{Ed}\, z_t}{E\, z\, k_t} \tag{6.2}$$

$$\delta_{c,r} = \frac{\frac{M_{Ed}}{z} - \frac{N_{Ed} z_t}{z}}{E\, k_c} = \frac{M_{Ed} - N_{Ed}\, z_t}{E\, z\, k_c} \tag{6.3}$$

The rotation of the base plate could be determined from formulas above

$$\phi = \frac{\delta_{t,l} + \delta_{c,r}}{z} = \frac{1}{E\, z^2} \cdot \left(\frac{M_{Ed} - N_{Ed} \cdot z_c}{k_t} + \frac{M_{Ed} + N_{Ed} \cdot z_t}{k_c} \right) \tag{6.4}$$

From the rotation the initial stiffness is derived

$$S_{j,ini} = \frac{E\, z^2}{\frac{1}{k_c} + \frac{1}{k_t}} = \frac{E\, z^2}{\Sigma \frac{1}{k}} \tag{6.5}$$

Nonlinear part of the moment-rotation curve is given by coefficient μ, which express the ratio between the rotational stiffness in respect to the bending moment, see (Weynand et al, 1996) and EN1993-1-8:2006

$$\mu = \frac{S_{j,ini}}{S_j} = \left(\kappa\, \frac{M_{Ed}}{M_{Ed}} \right)^{\xi} \geq 1 \tag{6.6}$$

where

κ is coefficient introducing the beginning of non-linear part of curve, $\kappa = 1.5$

ξ is shape parameter of the curve, $\xi = 2.7$

The rotation stiffness is calculated as

$$S_j = \frac{E\, z^2}{\mu\, \Sigma \frac{1}{k}}$$

For above described components, the stiffness coefficients, showed in Fig. 6.3, is revised from bolt in tension k_b, base plate in bending k_p, and concrete in compression k_c.
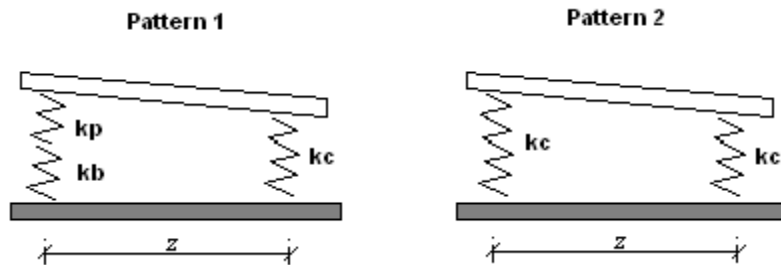

Fig. 6.3 The mechanical simulation with stiffness coefficients

As it is evident in Fig. 6.3, the stiffness of the tension part k_t consists of the stiffness of the base plate k_p and the stiffness of bolts k_b. With these parameters, S_j, μ, and M_{Rd}, we obtain the moment rotation curve, which is the best way how to describe behaviour of the base plate connection, see Fig. 6.4.

The procedure for evaluation of stiffens is derived for open section of I/H cross section. For rectangular hollow section RHS may be taken directly taking into account two webs. For circular/elliptical hollow sections CHS/EHS may be modified, see (Horová, 2011).
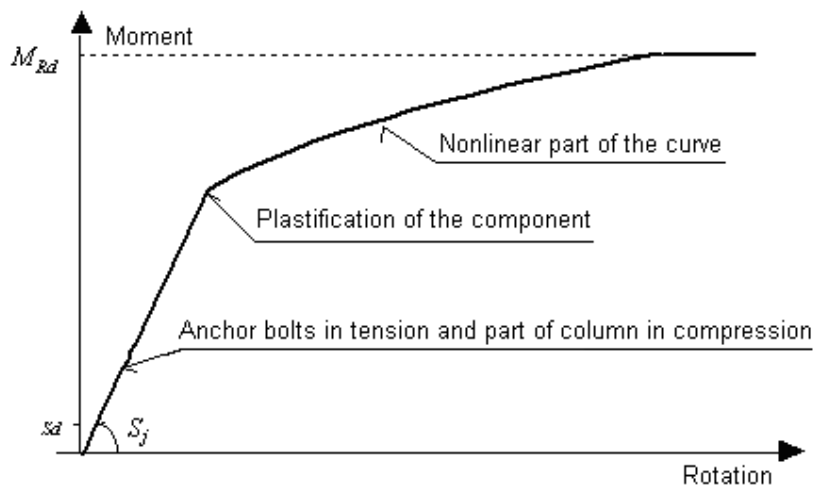
Fig. 6.4 Moment rotation curve for proportional loading

6.1.2   Column base with anchor plate

The bending stiffness of the base plate with anchor plate is assembled from the deformation stiffness's of its components, e.g. in the tensile part the base plate, the threaded studs, the anchor plate, and the headed studs and in the compressed part the concrete block in compression and base plate plus anchor plate in bending. The additional components are the anchor plate and treated studs. The deformation springs representing the individual components and its lever arms are summarized in Fig. 6.5. The effective stiffness coefficient, see Chapter 6.3 in EN1993-1-8:2005, is applied to transfer all deformational springs into the position of the threated stud.
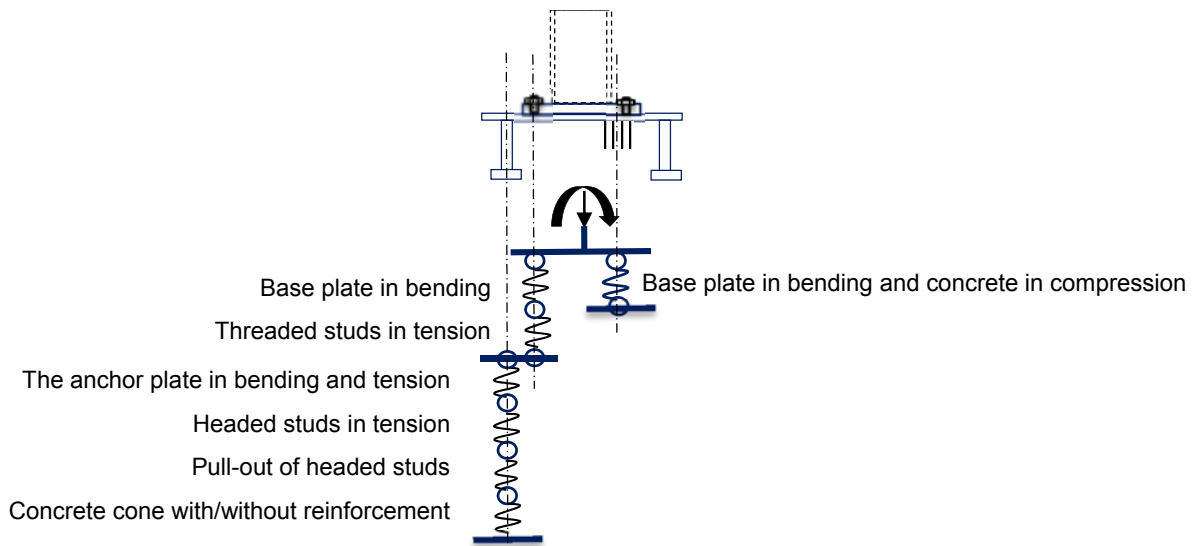
Fig. 6.5 Deformational springs representing in the model the components

6.2 Simple steel-to-concrete joint

The stiffness of the concrete components are not yet considered in the CEN/TS 1992-4-2 to calculate the deformation behaviour of the Simple joint. In the following the stiffness that have been developed within the INFASO project were applied to the Simple joint and from this the rotational stiffness of the joint is developed. A detailed description of this components may be found in Chapter 3. Thereby the rotational behaviour of the joint caused by the shear load V_{Ed} is calculated. It is assumed that in the case of a Simple joint the rotation does not influence the global analysis or the bending resistance of the joint to a high extend, see Fig. 6.6 and 6.7. The Simple joint is primarily a shear force connection and the rotation or the rotational stiffness of the joint is not relevant.
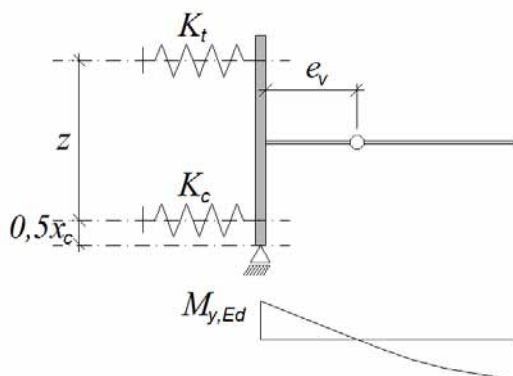
Fig. 6.6 Model for the global analysis of a simple joint between the beam and the anchor plate
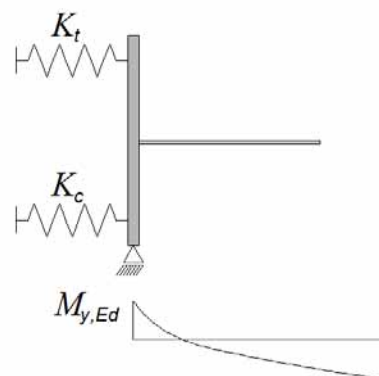
Fig. 6.7 Model for the global analysis of a rigid joint between the beam and the anchor plate

If the connection between the girder and the anchor plate cannot be assumed as pinned, there might be larger bending moments in the joint. In the following Chapters the system described is a simple connection between the beam and the anchor plate with an eccentricity e_v. However if there is a real bending moment derived in the global analysis, the eccentricity e_v may be assumed no longer a purely geometrical value anymore but is calculated by

$e_v = \dfrac{M_{y,Ed}}{V_{Ed}}$. In this case it is very important to determine the rotational stiffness of the joint because the rotational stiffness may influence the load distribution in the global analysis and the size of the bending moment of the joint, see Fig. 6.8. In order to model the rotational behaviour of the joint, at minimum two components are necessary, a tension component and a compression component. The tension component is represented by the headed stud in tension, see Chapter 3, and the compression component by the component concrete in compression. With these two components and the lever arm z and the rotational behaviour of the joint may be modelled.
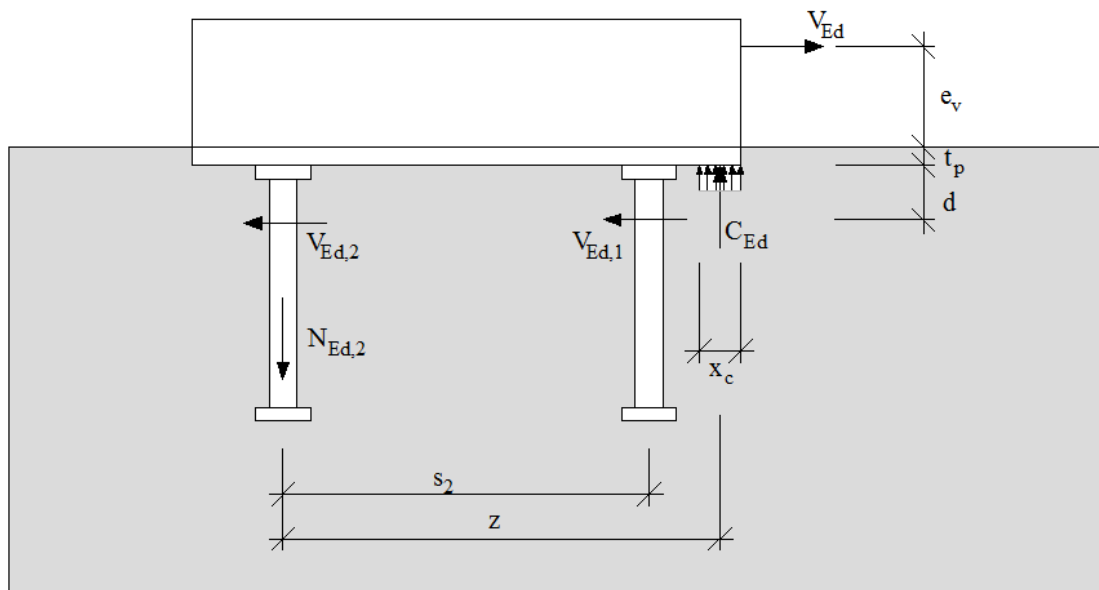
Fig. 6.8 Forces at the anchor plate caused by the shear force V_{Ed} and its eccentricity e_V

The shear load V_{Ed} causes a tension force $N_{Ed,2}$ in the headed stud on the non-loaded side of the anchor plat. In equilibrium with the tension force there is a compression force C_{Ed}. For the equilibrium of moments and forces also see Chapter 3.

This forces are leading to a deformation δ_T caused by the tension force on the non-loaded side of the anchor plate and a deformation δ_C caused by the compression force on the loaded side of the anchor plate, see Fig. 6.. With these two deformation values and the lever arm z the rotation of the stiff anchor plate may be calculated according to the following formula

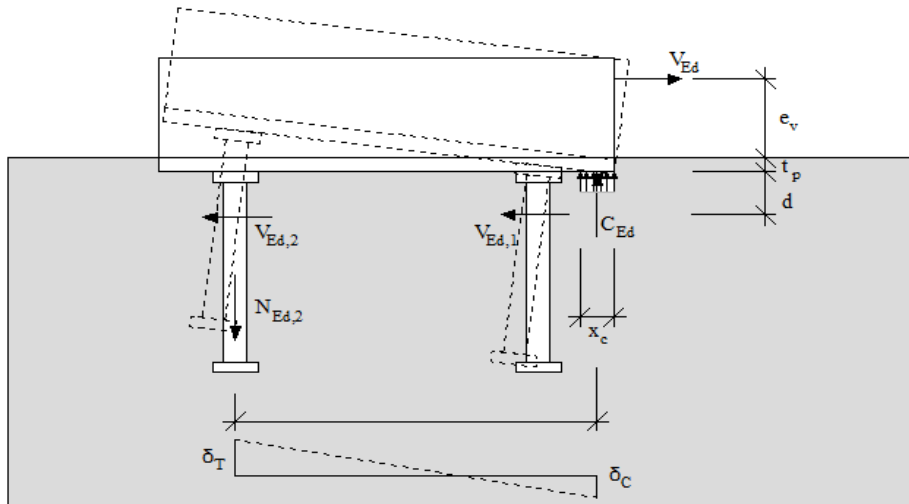$$\varphi = \frac{\delta_T + \delta_C}{z} \qquad (6.8)$$

Fig. 6.9 Rotation of the anchor plate caused by the shear load V_{Ed}

In the following an overview over the tension and over the compression component is given.

<u>The tension component</u>

The tension component is described in detail in Chapter 3. For these components two alternatives exist, one with additional stirrups and one without, see Fig. 6.10. For every alternative a model including several springs has been developed.
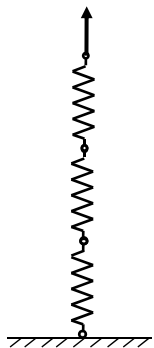
Headed studs in tension　　　　　　　　　　　　Headed studs with stirrups in tension

Steel failure in tension

Pull-out failure

Concrete cone failure
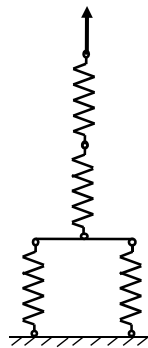
Steel failure in tension

Pull-out failure

Concrete cone failure
with stirrups in tension

Fig. 6.10 Spring model for headed stud in tension, with and without stirrups

Depending on, whether additional reinforcement is used or not, the deformations of the headed studs are defined as follow:

　　Headed studs in tension

$N = 0$ to $N = N_{u,c}$　　　　　and　$\delta_1 = \delta_{p1} + \delta_h$　　　　　　　　　　(6.9)

$N = N_{u,c}$ to $N = 0$　　　　　and　$\delta_2 = \delta_1(N_{u,c}) + \dfrac{N - N_{u,c}}{k_c}$　　　　　(6.10)

　　Headed studs with stirrups in tension

$N = 0$ to $N = N_{u,c}$　　　　　and　$\delta_1 = \delta_{p1} + \delta_h$　　　　　　　　　　(6.11)

$$N = N_{u,c} \text{ to } N = N_u \qquad \text{and} \quad \delta_2 = \delta_{p2} + \delta_h + (\delta_c + \delta_s) \tag{6.12}$$

$$N = N_u \text{ to } N = 0 \qquad \text{and} \quad \delta_3 = \delta_2(N_u) + \frac{N - N_u}{k_c} + \frac{N_u - N}{10\,000} \tag{6.13}$$

In both cases it is necessary to ensure that neither yielding nor pull-out failure of the headed studs is the decisive failure mode. The load-displacement behaviour after of these failure modes are not considered in the equations above.

The compression component

For the compression force the spring stiffness may be calculated as follows:

$$K_c = \frac{E_c \cdot \sqrt{A_{eff}}}{1.275} \tag{6.14}$$

The formula is taken from EN1993-1-8. The influence of the concrete stiffness is not very large on the rotational behaviour.

Determination of the lever arm z

Due to the equilibrium for each value of the shear load V_{Ed}, a corresponding tension force $N_{Ed,2}$ and the compression force C_{Ed} have to be calculated. As every value of V_{Ed} corresponds to a different compression force C_{Ed}, there is also a different height of the compression area x_c and another corresponding lever arm z. For example if a small V_{Ed} causes a small $N_{Ed,2}$ and C_{Ed}, the height of the compression zone x_c is small and the lever arm z is relatively large. If the shear load is increased, the size of the compression force rises and the height of the compression area x_c also grows, whereas the lever arm z decreases.

The changing of the lever arm z is easily taken into account in a computer based calculation. For a calculation without computer a constant lever arm should be assumed. For the most structures the best solution to determine the lever arm is to calculate the maximum resistance of the tension load of the headed studs. Based on this value the maximum compression force and the minimum z may be calculated. Only if the anchor plate is extreme small and the tension resistance is extremely large the lever arm should be determined in a different way.

The rotational stiffness

Not only the rotation caused by the shear load, but also the rotational stiffness of the joint is calculated. With the help of the rotational stiffness it is possible to model the joint in the global analysis assuming his realistic behaviour. The initial rotational stiffness $S_{j,ini}$ may be calculated according to EN1993-1-8. The following equation may be found in EN1993-1-8:2006, cl 6.3.1

$$S_{j,ini} = \frac{z^2}{\left(\dfrac{1}{K_T} + \dfrac{1}{K_c}\right)} \tag{6.15}$$

where

K_T is the stiffness of the tension component

K_c is the stiffness of the compression component

If no ductile behaviour is expected, the initial stiffness $S_{j,ini}$ is assumed up to the maximum load. In the case of ductility the stiffness S_j of the joint is changed according to the utilization level of the joint. Therefore the behaviour of the joint is represented by a moment-rotation curve with a trilinear shape, see equation 6.17. The determination of the associated factor μ is taken from

EN1993-1-8. It has to be mentioned that in this case large cracks that are undesirable might occur.

$$S_j = S_{j,ini}/\mu \qquad (6.16)$$

6.3 Moment resistant steel to concrete joint

For the joint under hogging bending moment, the assembly procedure was based on the mechanical model represented in Fig. 5.8a. The determination of the joint properties to bending moment is performed using two different approaches: the direct deformation superposition and model based on composition of stiffness coefficients by spring procedure.

The mechanical model represented in Fig. 5.8b presents only one row of components in tension and another in compression. The determination of the properties of equivalent components/springs was performed as expressed in (6.17), for deformation $\Delta_{eq,t}$ and $\Delta_{eq,c}$.

$$\Delta_{eq} = \sum_{i=1}^{n} \Delta_i \qquad (6.17)$$

where, the index i to n represent all components to consider either in tension either in compression, depending on the row under consideration. In order to determine the joint rotation, it is important to define the lever arm h_r. Accordingly, the joint properties are obtained as follows

$$\phi_j = \frac{\Delta_{eq,t} + \Delta_{eq,c} + \Delta_{JL}}{h_r} \qquad (6.18)$$

where

$\Delta_{eq,t}$ and $\Delta_{eq,c}$ are the equivalent deformation of the tension and compression rows, respectively, determined using (6.17).

7 GLOBAL ANALYSIS INCLUDING JOINT BEHAVIOUR

7.1 Structural analysis

The analysis of structures regarding the steel and composite joints modelling has been conventionally based on the concept of rigid, infinite rotational stiffness, or pinned, no rotational stiffness. However, it is well recognized that the real behaviour is often intermediate between these extreme situations, see (Jaspart, 2002). In these cases, the joints are designated as semi-rigid. In such joints, partial relative rotation between connected members is assumed, contrarily to the traditional concept of no or free rotation.

Consequently, the behaviour of the joint has a non-negligible influence on the structural analysis, see (Jaspart, 1997); and (Maquoi, Chabrolin, 1998) affecting: distribution of internal forces and deformations. In terms of resistance, the influence of the joint properties is obvious, as the structural capacity is limited if the joint is not fully capable of transmitting the internal forces, namely the bending moments. In such cases, the joint rotation capacity also becomes critical, defining the type of failure and the possibility to redistribute the internal forces. Thus, joints are keys parts of the structure, playing an important role in the behaviour of the structure. In what regards to the reinforced concrete joints, the structural analysis remains in the classical concept of rigid or pinned joints EN1992-1-1:2004. This is understandable due to the nature of the joints. In what concerns the steel-to-concrete joints, the joint behaviour is similar to steel

joints. In this way, the effect of the steel-to-concrete joint on the structural behaviour should be considered as in steel structures.

With the component method (Jaspart, 1997), the real behaviour of the steel/composite joints may be efficiently evaluated and characterized in terms of rotational stiffness, bending moment resistance and rotation capacity. Subsequently, their behaviour is introduced in the structural analysis. This allows integrating the joint design with the structural design. Such type of analysis is recommended by the codes, EN1993-1-8:2006 and EN1994-1-1:2010, and should follow the subsequent steps:

 – Characterization of the joint properties in terms of rotational stiffness, bending moment resistance and rotation capacity,
 – Classification of the joint,
 – Joint modelling on the structural model,
 – Joint idealization.

The joint classification as already been introduced in section 2.2 and consists in determining the boundaries for the conventional type of joint modelling regarding the stiffness, see Fig. 2.6, and the resistance, see Fig. 2.7. The classification of the joint determines the type of joint modelling that should be adopted for the structural analysis. For stiffness classification, the stiffness of the connected beam is used to define the boundaries. In terms of resistance, the classification is set according to the minimum capacity of the connected members. In terms of rotation capacity, the information available is quite limited. In the code EN1993-1-8:2006 only a qualitative classification is given which consists in the following: i) ductile joints (suitable for plastic analysis) – ductile components govern the behaviour of the joint; ii) semi-ductile joints components with limited deformation capacity govern the joint response; iii) and brittle joints (do not allow redistribution of internal forces) - brittle components control the joint response.

Tab. 7.1 Criteria to define the boundaries
for classification of beam-to-column steel and composite joints

Stiffness	
Rigid/Semi-rigid	$8\,E\,I_b/L_b$
Semi-rigid/Pinned	$0.5\,E\,I_b/L_b$
Resistance	
Full-strength/Partial-strength	Top of column: $\min\{M_{c,\,pl,Rd};\ M_{b,pl,Rd}\}$ Within column height: $\min\{2M_{c,pl,Rd};\ M_{b,pl,Rd}\}$
Partial-strength/Pinned	25% of Full-strength/Partial-strength

In the structural analysis, according to the stiffness and strength classification, three types of joint modelling are possible, as listed in Tab. 7.2. In the case of continuous joint, the full rotation continuity is guaranteed between the connected members. In the case of simple joint, all rotational continuity is prevented between the connected members.

Otherwise, the joint is semi-continuous. In relation to the physical representation of the joint in the structural model, different approaches may be used, as illustrated in Tab. 7.2. In Fig. 7.1a the actual behaviour of the joint is modelled: L-springs $S_{r,L}$ representing the connecting zone and S-springs $S_{r,S}$ representing the panel zone. The infinite rigid stubs assure that the flexibility of the joint will not be taken into consideration more than once. In Fig. 7.1b is presented a model to be used in the software which does not support flexural springs. Stubs with adequate bending stiffness $E\,I$ and resistance M, maintaining the clear separation between bending and shear influences are used to replace rotational springs. Finally, the concentrated model is represented in Fig. 7.1c. In this model, L-springs and S-springs are assembled into one single spring and displaced to the column axis S_c. The overall joint behaviour is then represented by a single rotational spring, two in the case of double sided joints. This simplified modelling solution is prescribed by EN1993-1-8:2006. The simplifications adopted are compensated in

the joint transformation. The joint transformation takes into account the shear force acting in the column, and the combination of the shear panel and connections in the joint spring at the beam-to-column axis intersection point, see (Huber et al, 1998).

Tab. 7.2 Criteria to define the boundaries for classification
of beam-to-column steel and composite joints EN1993-1-8:2006

Joint modelling	Joint Classification
Continuous	Full-strength and Rigid
Semi-continuous	Full-strength and Semi-rigid
	Partial-strength and Rigid
	Partial-strength and Semi-rigid
Simple	Pinned and Pinned
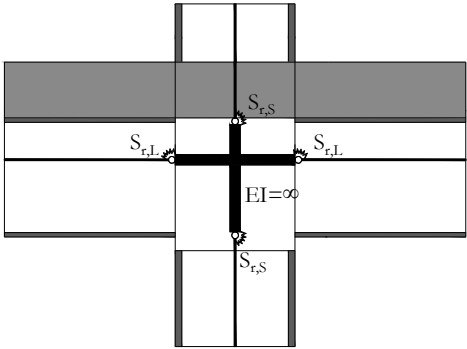
Fig. 7.1a Representation
of joint by infinite rigid stubs
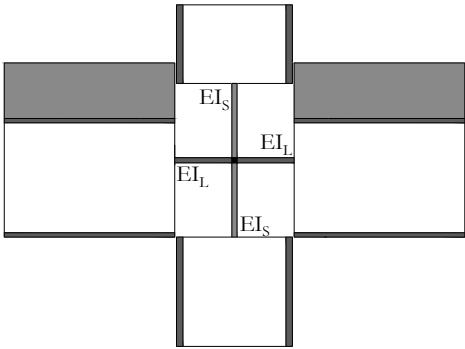
Fig. 7.1b Representation
of joint by deformable stubs
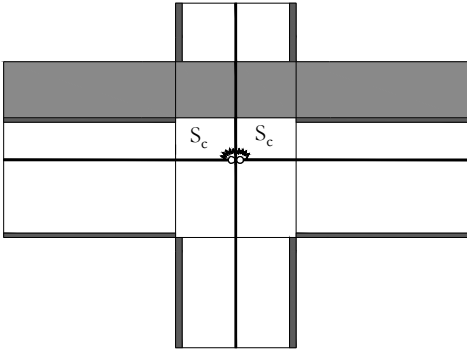
Fig. 7.1c Representation of joint by two rotational springs

The joint idealization consists in defining the type of flexural curve which will be attributed to the flexural spring representing the joint. The behaviour of the joints is typically nonlinear; however, its implementation in the flexural spring is not practical for everyday design. In this way, the behaviour of the joint may be simplified as schemed in Fig. 7.2. The selection of the appropriate curve depends on the type of analysis to perform: elastic, elastic-plastic, rigid-plastic. Accordingly the following behaviours may be assumed: i) linear elastic, Fig. 7.2a only requires rotational stiffness; ii) bi-linear or tri-linear elastic-plastic, Fig. 7.2b requires rotational stiffness, resistance and deformation capacity; iii) rigid plastic, Fig. 7.2c requires resistance and rotation capacity. In the case of semi-rigid joint, the joint rotational stiffness to be consider depends on the expected load on the joint, thus the following is considered: i) the acting bending moment is smaller than 2/3 of the joint bending moment resistance $M_{j,Rd}$ and the joint initial rotational stiffness $S_{j,ini}$ may be used; ii) in the other cases, the joint secant rotational stiffness S_j should be used. The latter is obtained dividing the joint initial stiffness $S_{j,ini}$ by the

stiffness modification coefficient η. The codes EN1993-1-8:2006 and EN1994-1-1:2010 provide the stiffness modification coefficient to consider according to the type of connection.
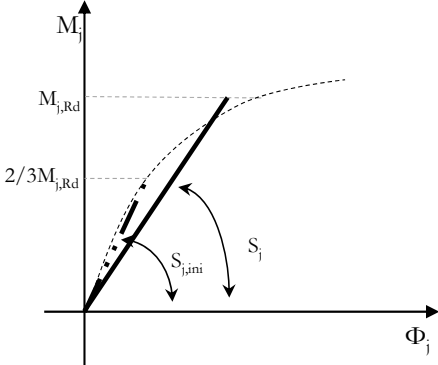

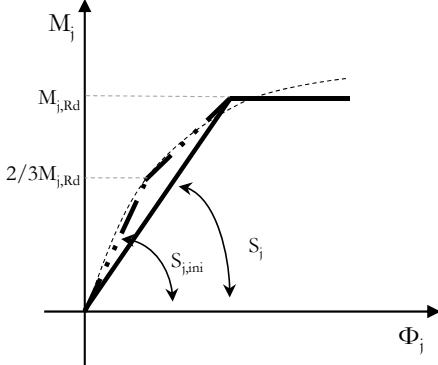Fig. 7.2a Linear elastic M-Φ curve idealized for the joint behaviour

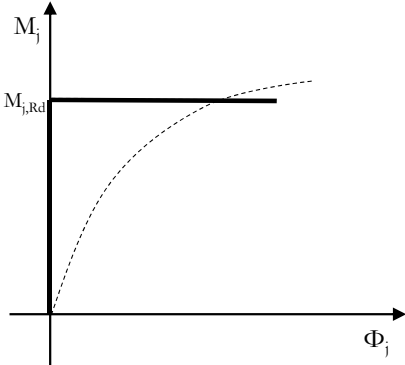Fig. 7.2b Bi-linear and tri-linear elastic-plastic M-Φ curve idealized for the joint behaviour

Fig. 7.2c Rigid plastic M-Φ curve idealized for the joint behaviour

The stiffness of a joint influences the deformability of the structure, which is reflected in the check for SLS. The influence of non-linear behaviour of joints in terms of ULS is more difficult to assess as it requires a non-linear analysis. The following example illustrates in a simplified way, the influence of joints in the behaviour of the structure. Considering the beam represented in Fig. 7.3, under a linear uniform load q and assuming rigid joints at both ends of the beam leads to the bending moment $M_{j,\infty}$ at both supports, and to the bending moment diagram represented by the dashed line. On the other hand, assuming at both ends of the beam a rotational stiffness of the joints S_j, then the bending diagram represented by the continuous line is obtained. This represents a bending moment re-distribution of ΔM that varies from 0 to $q\, L^2/12$. This re-distribution is also reflected in the vertical deflection of the beam, which may vary from $q\, L^4/(384\, EI)$ to $5\, q\, L^4/(384\, E\, I)$.
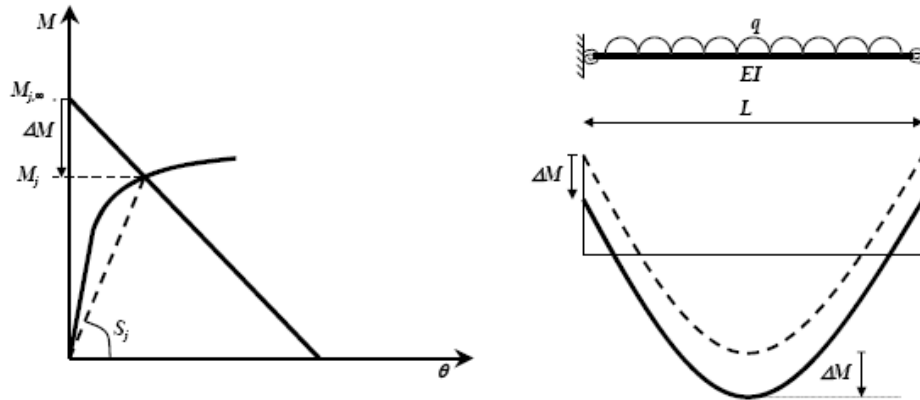
Fig. 7.3 Influence of a semi-rigid joint in the behaviour of the beam

The use of the concept of semi-rigid joints may has economic benefits, particularly in the optimization of moment connections. Possible savings due to semi-rigid design is 20 – 25 % in case of unbraced frames and 5 - 9 % in case of braced frames, see EN1990:2002.

7.2   Examples on the influence of joint behaviour

7.2.1   Reference building structures

In order to illustrate the influence of joint behaviour in the global analysis of structures, an example is provided in the following paragraphs. For complete details of the analysis see (Henriques, 2013). The building structures selected for the analysis considered two types of occupancy: office and car park. For the first type, the building structure erected in Cardington and subject to fire tests was chosen, see (Bravery 1993) and (Moore 1995). The building was designed to represent a typical multi-storey building for offices. For the car park building, the structure used in a recent RFCS project regarding Robustness in car park structures subject to a localized fire, see (Demonceau et al, 2012), was selected. Though the main characteristics of the reference building structures are used, modifications were performed whenever required to adapt the structures. Furthermore the performed calculations only considered the analysis of plane sub-structures which were extracted from the complete building structures. As higher variation of the structural system was found in the office building, two sub-structures were selected to represent this type of building while for the car park only one sub-structure was considered. The main characteristics and the adopted modifications of the referred building structures are summarized in the following paragraphs, see (Kuhlmann et al, 2012) and (Maquoi, 1998).

The office building structure

The main geometrical and mechanical properties of the office building are summarized in Tab. 3, together with the adopted modifications. The floor layout is illustrated in Fig. 7.4..

88

Tab. 7.3 The main properties and performed modifications
of the reference structure representing the office building type

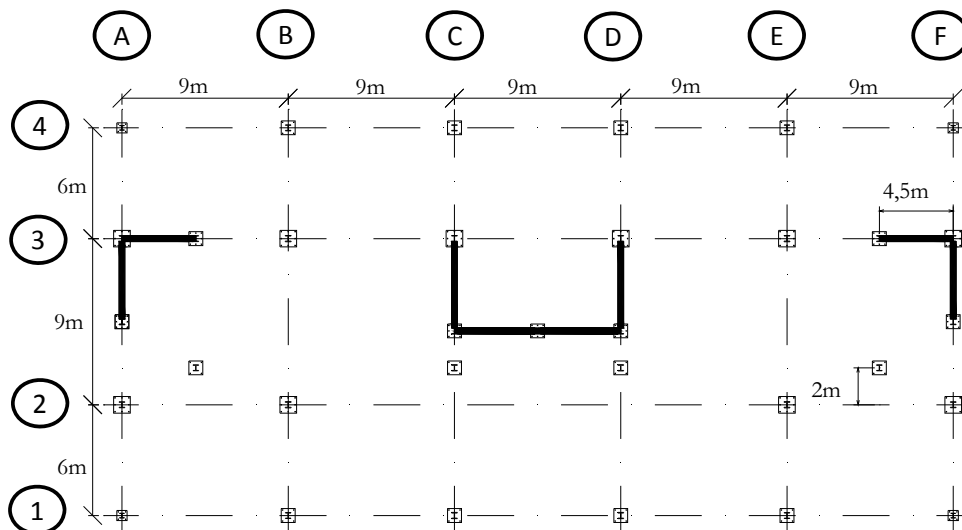| Reference Structure	Modifications
Nº of floors and height: 1 x 4.34 m + 7 x 4.14 m Nº of spans and length in longitudinal direction: 5 x 9 m Nº of spans in transversal direction: 2 x 6 m+1 x 9 m	No modifications
Columns: British steel profiles, grade S355, cross-section variation along height Beams: composite, British steel profiles + composite slab; grade S355 and grade S275; Lightweight concrete Bracing system: cross bracing flat steel	All British steel profiles were replaced by common European steel profiles with equivalent mechanical properties. Bracing systems were replaced by shear walls in order to introduce in the structural system, steel- to-concrete joints.
Beam-to-column joints: simple joints Column bases: continuous	The type of joint between horizontal members and vertical members was one of the key parameters of the study. The joint modelling was varied from continuous to simple. Column bases were assumed as simple joints.

Fig. 7.4 Floor layout of the reference structure representing the office building type

The car park building structure

This type of building represents the standard configuration of a car park structure in Europe. The main geometrical and mechanical properties of this type of building are summarized in Tab. 7.4. In this case, only a few modifications were required. Fig. 7.5 illustrates the floor layout.

Tab. 7.4 The main properties and performed modifications for the car park building type

Reference structure	Modifications
Nº of floors and height: 8 x 3 m Nº of spans and length in longitudinal direction: 6 x 10 m Nº of spans in transversal direction: 10 x 16 m	No modifications
Columns: steel profiles, grade S460, cross-section variation along height Beams: composite (steel profiles + composite slab); grade S355; normal weight concrete Bracing system: concrete core (assumed but not defined)	Dimensions given to the concrete core
Beam-to-column joints: semi-continuous joints Column bases: simple joints	No modifications
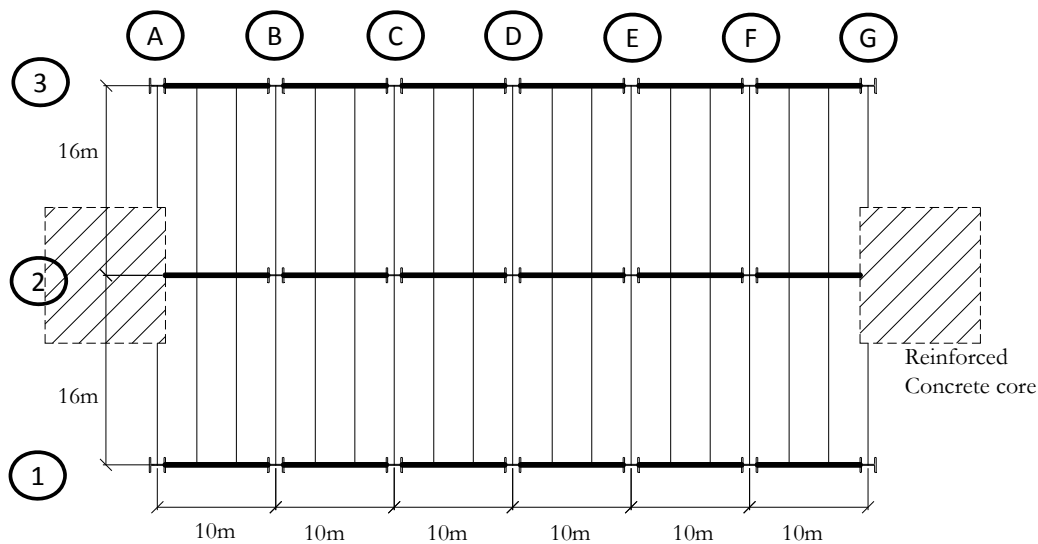
Fig. 7.5 Structural layout of the car park building type

7.2.2 Design

The structural calculations performed considered an elastic-plastic analysis. In all members and joints, except RC walls, plastic deformations were admissible. For sake of simplicity, the wall behaviour was always assumed elastic without limitation of capacity. However, it was considered that the steel-to-concrete joint includes the part of the wall surrounding the joint. Therefore, partially, hypothetic localized failure of the wall was considered. In terms of loading, two types of combinations were considered: i) Service Limit State; and ii) Ultimate Limit State.

In relation to the calculations, the strategy consisted in performing several numerical simulations where the beam-to-column and beam-to-wall joint properties were varied within the boundaries for joint classification. In addition, two cases considered the extreme situations of all joints either continuous or simple joints. For the other cases, the steel joints and steel-to-concrete joints are semi-continuous. In all calculations, the column bases joints were assumed simple. Tab. 7.5 lists the numerical simulations performed and identifies the joint properties considered in each case. Although the focus was on steel-to-concrete joints, steel joints were also considered to be semi-continuous so that the structural system was consistent.

The different cases presented in Tab. 7.5 considered the combination of different values of joint initial rotational stiffness and resistance capacity. In terms of rotation capacity, it was assumed that unlimited rotation capacity was available. A total of 10 cases were considered for each load combination.

Tab. 7.5 Definition of the cases for each load combination and each sub-structure

Case	Initial Rotational Stiffness			Bending Moment Resistance		
	Steel-to-concrete joint	Steel joint	Col. bases	Steel-to-concrete joint	Steel joint	Col. bases
1	R	R	P	FS	FS	P
2	R	SR: 0.5 (R/SR+SR/P)	P	FS	FS	P
3	SR: 2/3 (R/SR+SR/P)	SR: 0.5 (R/SR+SR/P)	P	FS	FS	P
4	SR: 1/3 (R/SR+SR/P)	SR: 0.5 (R/SR+SR/P)	P	FS	FS	P
5	SR: 2/3 (R/SR+SR/P)	SR: 0.5 (R/SR+SR/P)	P	PS: 2/3 (FS/PS+PS/P)	PS: 2/3 (FS/PS+PS/P)	P
6	SR: 1/3 (R/SR+SR/P)	SR: 0.5 (R/SR+SR/P)	P	PS: 2/3 (FS/PS+PS/P)	PS: 2/3 (FS/PS+PS/P)	P
7	SR: 2/3 (R/SR+SR/P)	SR: 0.5 (R/SR+SR/P)	P	PS: 1/3 (FS/PS+PS/P)	PS: 1/3(FS/PS+PS/P)	P
8	SR: 1/3 (R/SR+SR/P)	SR: 0.5 (R/SR+SR/P)	P	PS: 1/3 (FS/PS+PS/P)	PS: 1/3 (FS/PS+PS/P)	P
9	P	SR: 0.5 (R/SR+SR/P)	P	P	PS: 0.5 (FS/PS+PS/P)	P
10	P	P	P	P	P	P

R-Rigid; SR-Semi-rigid; P-Pinned; FS-Full-strength; PS-Partial-strength

7.2.3 Structural model

<u>Geometric and mechanical properties of members</u>

The three sub-structures selected for the structural calculations are illustrated in Fig. 7.6. The members' geometric dimensions and material properties are given in Tab. 7.6. For the bare steel cross-sections, the material behaviour was considered elastic-perfectly-plastic.

Tab. 7.6 Sub-structures members' geometric and material properties

Sub-structure	Members	Geometric	Material
I	Columns: AL-1 and 4	Bottom to 2nd floor: HEB320 2nd floor to Top: HEB260	S355 S355
	AL-2	Bottom to 2nd floor: HEB340 2nd floor to Top: HEB320	S355 S355
	Beams[*]	IPE360+Composite slab (h$_{slab}$ = 130mm) #Φ6//200mm	S355 LC35/38
	Walls	t$_w$ = 300mm vertical reinforcement Φ20//30cm horizontal Φ10//30cm	C30/37 S500
II	Columns	Bottom to 2nd floor: HEB 340 2nd floor to Top: HEB 320	S355 S355
	Beams[*]	IPE360+Composite slab (h$_{slab}$ = 130mm) #Φ6//200mm	S355 LC35/38
	Walls	t$_w$ = 300 mm vertical reinforcement Φ20//300 mm horizontal Φ10//300mm	C30/37 S500
III	Columns	Bottom to 2nd floor: HEB 550 2nd floor to 4th floor: HEB 400 4th floor to 6th floor: HEB 300 6th floor to 8th floor: HEB 220	S460 S460 S460 S460
	Beams[*]	IPE450+Composite slab (h$_{slab}$ = 120 mm) #Φ8//200 mm	S355 C25/30
	Walls	t$_w$ = 400 mm # Φ20//200 mm	C30/37 S500
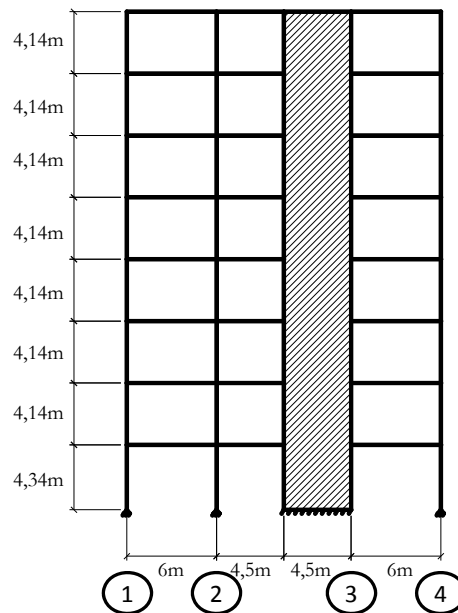
Fig. 7.6a Geometry of sub-structure I, office building alignment A
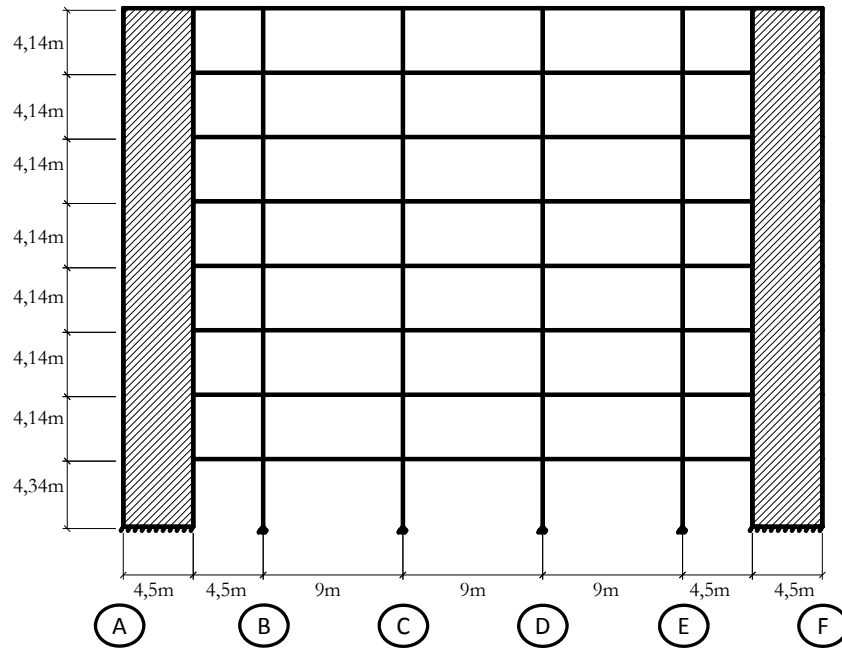
Fig. 7.6b Geometry of sub-structure II, Office building alignment 3
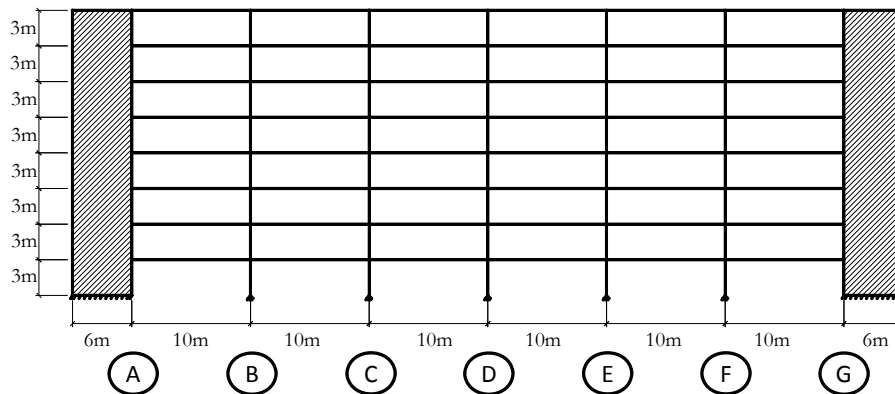
Fig. 7.6c Geometry of sub-structure III, car park building alignment 2

In order to simplify the structural modelling, the composite beams cross-section was replaced by equivalent rectangular cross-sections, see Table 7.7. Because of the different behaviour of the composite section under sagging and hogging bending moments, the equivalent beams cross-section (EqCS) varies within its length, as identified in Fig. 7.7. In terms of material properties, equivalent yield strength was also determined so that the equivalent cross-section attained a maximum bending moment equal to the resistance of the real composite cross-section.

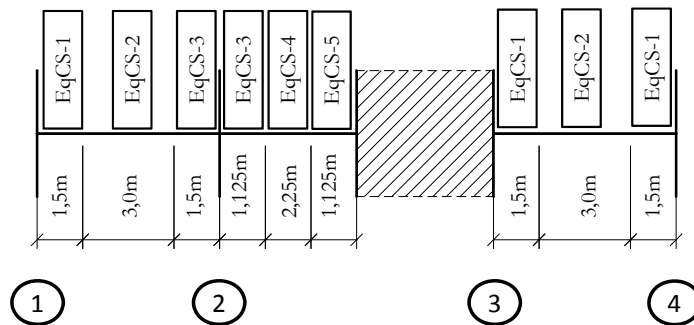| Sub-structure I				
Eq CS-1	Eq CS-2	Eq CS-3	Eq CS-4	Eq CS-5
$I=1.59 \times 10^8 mm^4$ $A=7034.56 mm^2$	$I=3.885 \times 10^8 mm^4$ $A=14512.67 mm^2$	$I=1.63 \times 10^8 mm^4$ $A=7087.57 mm^2$	$I=5.4975 \times 10^8 mm^4$ $A=12633.20 mm^2$	$I=1.58 \times 10^8 mm^4$ $A=7024.62 mm^2$
Equivalent rectangular cross-section dimension				
h=520.08mm b=13.53mm	h=566.78mm b=25.61mm	h=525.23mm b=13.49mm	h=580.67mm b=21.76mm	h=519.09mm b=13.53mm
Yield strength (f_y) of the equivalent rectangular cross-section to obtain the maximum bending moment ($M_{cb.max}$) of the composite beam cross-section				
$M_{cb.max}$ =351.41kN.m f_y=576.30N/mm^2	$M_{cb.max}$ =605.00kN.m f_y=441.31N/mm^2	$M_{cb.max}$ =358.94kN.m f_y=578.52N/mm^2	$M_{cb.max}$ =565.00kN.m f_y=462.12N/mm^2	$M_{cb.max}$ =349.98kN.m f_y=575.88N/mm^2
Sub-structure II				
Eq CS-1	Eq CS-2	Eq CS-3	Eq CS-4	Eq CS-5
$I=1.14 \times 10^8 mm^4$ $A=6012.32 mm^2$	$I=2.74 \times 10^8 mm^4$ $A=11207.20 mm^2$	$I=1.20 \times 10^8 mm^4$ $A=6101.78 mm^2$	$I=3.38 \times 10^8 mm^4$ $A=16431.90 mm^2$	$I=1.23 \times 10^8 mm^4$ $A=6141.54 mm^2$
Equivalent rectangular cross-section dimension				
h=476.37mm b=12.62mm	h= 541.42mm b= 20.70mm	h=486.39mm b= 12.54mm	h=496.74mm b= 33.08mm	h=490.57mm b= 12.52mm
f_y of the equivalent rectangular cross-section to obtain the M_{max} of the composite cross-section				
M_{max}=274.86kN.m f_y=575.81N/mm^2	M_{max}=470kN.m f_y=464.75N/mm^2	M_{max}=286.85kN.m f_y=579.90N/mm^2	M_{max}=631kN.m f_y=463.83N/mm^2	M_{max}=292.05kN.m f_y=581.62N/mm^2
Sub-structure III				
Eq CS-1	Eq CS-2	Eq CS-3		
$I=6.72 \times 10^8 mm^4$ $A=13192.32 mm^2$	$I=1.42 \times 10^9 mm^4$ $A=27012.63 mm^2$	$I=7.23 \times 10^8 mm^4$ $A=13600.91 mm^2$		
Equivalent rectangular cross-section dimension				
h=781.66mm b=16.88mm	h=794.22mm b=34.01mm	h=798.44mm b=17.00mm		
f_y of the equivalent rectangular cross-section to obtain the M_{max} of the composite cross-section				
M_{max}=988.86kN.m f_y=575.37N/mm^2	M_{max}=1338.00kN.m f_y=374.20N/mm^2	M_{max}=1057.61kN.m f_y=584.00N/mm^2		

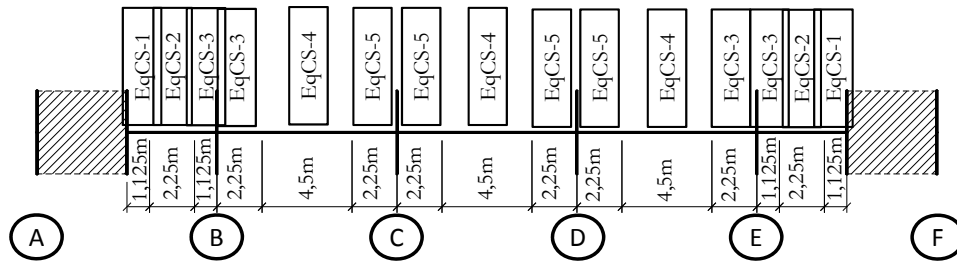Fig. 7.7a Identification of the equivalent cross-sections of the beams in sub-structure I

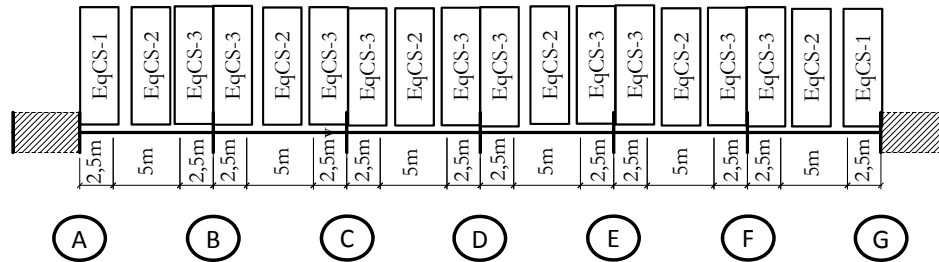Fig. 7.7b Identification of the equivalent cross-sections of the beams in sub-structure II

Fig. 7.7c Identification of the equivalent cross-sections of the beams in each sub-structure III

Joint properties

The boundaries values for classification of the joint in terms of rotational stiffness and resistance are listed in Tab. 7.8 for the three sub-structures. The joints were included in the structural models using concentrated flexural springs. For the partial-strength joints, a tri-linear behaviour was assigned, Fig. 7.8. The initial joint rotational stiffness is considered up to 2/3 of $M_{j,Rd}$, and then the joint rotation at $M_{j,Rd}$ is determined using the secant joint rotational stiffness. The latter is determined using a stiffness modification coefficient η equal to 2.

Tab. 7.8 The boundary values for classification of the joints in each sub-structure

	Joints	Rotational Stiffness		Bending Moment Resistance	
		R-SR [kNm/rad]	SR-P [kNm/rad]	FS-PS [kNm]	PS-P [kNm]
Sub-structure I	AL-1-right	108780.0	2782.5	351.4	87.9
	AL-2-left	108780.0	2782.5	358.9	89.7
	AL-2-right	205340.0	3710.0	358.9	89.7
	AL-3-left	205240.0	3710.0	345.0	87.5
	AL-3-right	108780.0	2782.5	351.4	85.9
	AL-4-left	108780.0	2782.5	351.4	87.9
Sub-structure II	AL-A-right	102293.3	2660.0	274.9	68.7
	AL-B-left	102293.3	2660.0	286.9	71.7
	AL-B-right	94640.0	2100.0	286.9	71.7
	AL-C-left to AL-D-right	94640.0	2100.0	292.1	73.0
	AL-E-left	94640.0	2100.0	286.9	71.7
	AL-E-right	102293.3	2660.0	286.9	71.7
	AL-F-left	102293.3	2660.0	274.9	68.7
Sub-structure III	AL-A-right	238560.0	7056.0	988.9	247.2
	AL-B-left	238560.0	7056.0	As below	As below
	AL-B-right to AL-F-left	238560.0	7591.5	b-6th: 1058.1 6th-T:380.4	b-6th: 264.3 6th-T: 95.1
	AL-F-right	238560.0	7056.0	As above	As above
	AL-G-left	238560.0	7056.0	988.9	247.2

R-Rigid; SR-Semi-rigid; P-Pinned; FS-Full-strength; PS-Partial-strength
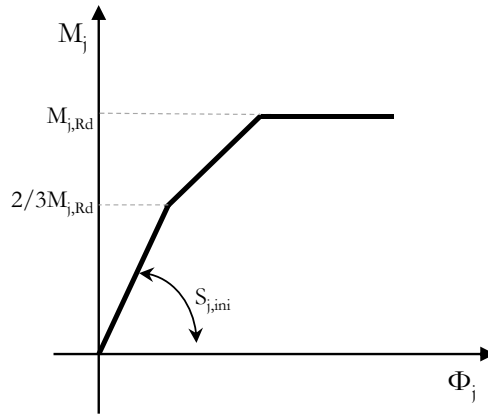
Fig. 7.8 Partial strength joint mechanical behaviour

Loading conditions

The loading considered in each sub-structure was determined for each load combination and varies with the structural conception and building occupancy. The loads and load combinations were defined according to EN1990:2002 and EN1991-1-1:2002. Note that for Sub-structure I and II, the wind action was also considered while for Sub-structure 3 no lateral action was assumed, this action was not quantified in (Demonceau et al, 2012) and it was considered that the stiffness of the wall will absorb it. In the office building structure, the slab works in the transverse direction, therefore the beams in the Sub-structure II are loaded with uniform distributed loads. For the other two sub-structures, the represented beams are the main beams so the loads are transmitted as concentrated loads, at the intersection of the secondary beams. In all cases the self-weight is considered.

Sub-structures finite element models

The structural calculations were performed in the finite element software (Abaqus 6.11, 2011). In Tab. 7.9 are listed the types of elements used to reproduce each component of the structural system (members and joints): i) beam elements for beams and columns, ii) shell/plate elements for the RC walls, and iii) spring elements to connect the structural members, in the different degrees of freedom.

Tab. 7.9 Types of finite elements attributed to each component, members and joints

Structural Model Component	Type of finite element	Description
Beams and Columns	Beam element	2-node linear beam element B31
Shear Walls	Shell element	4-node shell element S4R (general-purpose) with reduce integration and hourglass control
Beam-to-column and Beam-to-Wall Joints	Spring element	Non-linear spring element with single degree of freedom

The concentrated joint modelling was selected, where a flexural spring was used to represent the connection at each side of the column. As the parametric study was performed varying the properties of this flexural spring, it was assumed that this spring was already integrating the deformation of the column web panel and was already affected by the transformation parameter β, so that an iterative calculation was avoid. As the main goal is to analyse the influence of the joint and to obtain some structural requirements to the steel-to-concrete joints, the joint springs are located at the axis of the columns, and the eccentricity associated to the height of this member is neglected. . In what concerns the other degrees of freedom, namely axial and shear direction of the beam, translation springs are used to connect the members.

96

In this way, in each connection, between structural members, three springs are used, one for each relevant degree of freedom.

The use of the above described types of elements was previously validated against academic problems (Simoes da Silva et al, 2010). Simultaneously, the calibration of the required mesh refinement was performed. Tab. 7.10 summarizes the mesh refinement to consider in the different members of the structural models simulated and discussed in the next section.

Tab. 7.10 Summary of the mesh refinement for each member of the structural model

Member	Number of elements or mesh size
Beams	40
Columns	10
Shear walls	400 mm x 400 mm

The performed numerical calculations are two dimensional; therefore, no out-of-plane deformations occur. Both material and geometrical non-linearities are taken into account. Furthermore, the analysis neglects any possible in-plane buckling phenomena. The structural capacity is in this way only limited by the maximum resistance of the members and joints cross-sections. Finally, in what concerns to the simulation of the column loss, the procedure consisted in replacing the support of the relevant column by the reactions forces obtained in a previous calculation during the application of the real loading, and then to reduce them to zero.

7.2.4   Analysis and discussion for Service Limit State

The structure under service limit state (SLS) has to guarantee the comfort of the users. If in terms of loading this limit state is less demanding, in terms of deformation requirements it is often the most limiting state, and therefore, design guiding. For this load condition, the analysis of the steel-to-concrete joint properties is performed using the two following parameters: beams deflection and structure lateral deformation. For the latter, only Substructures I and II are considered, as no horizontal load (namely wind load) was considered in the analysis of Sub-structure III.

Fig. 7.10 illustrates how the beams deflection was considered. The maximum values obtained for each case are listed in Table 7.11, in a beam connected to a RC member, columns in grey, and in a beam only supported by steel columns. According to the Portuguese National Annex to EN1993-1-1:2006 the limit value $\delta_{max} = L/300$ was calculated and is included in the table. It is observed that in Sub-structures I and II, the values are distant from this limit, even if the beams deformation achieves 20 mm in the sub-structure II with simple joints, the value is still 33% below the limit. The beam deformations in sub-structure III are closer to the limit value but still, this value is not exceeded for any of the cases. In Fig. 7.11 are represented the beams deformations for the cases corresponding to the maximum and minimum deflections, for the beams implementing steel-to-concrete joints. These is seen as the envelope of the beams deformation, as these cases consider the two extreme situations in what respects the joint properties: i) continuous (Rigid + Full Strength); and ii) simple (Pinned). Using the beam deformation mode corresponding to the maximum beam deflection, the deformation corresponding to the code limit was extrapolated and is also included in the figure. The figure illustrates the above observations, confirming Substructure III closer to the limit.
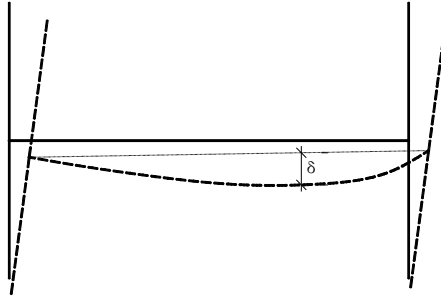
Fig. 7.9 Representation of the considered beams deflection

Tab. 7.11 Maximum beams deformation under service limit state [mm]

Case	Sub-structure I		Sub-structure II		Sub-structure III		Joint Properties	
	Beam 1-2	Beam 3-4	Beam C-D	Beam A-B	Beam C-D	Beam F-G		
1	2.6	3.0	5.5	0.3	21.7	7.7	R	FS
2	3.3	3.2	7.8	0.3	22.9	12.7		
3	3.3	3.5	7.8	0.4	23.4	12.6		
4	3.3	3.6	7.8	0.4	23.7	12.6		
5	3.3	3.5	7.8	0.4	23.7	14.1		
6	3.3	3.6	7.8	0.4	24.1	14.1	↓	↓
7	3.3	3.5	7.8	0.4	24.7	18.8		
8	3.3	3.6	7.8	0.4	25.2	18.8		
9	3.2	4.6	7.8	0.6	28.1	15.1		
10	6.1	6.1	20.5	1.5	31.8	27.1	P	P
δ_{max} [mm]	20	20	30	15	33.3	33.3		

R-Rigid; P-Pinned; FS-Full-strength
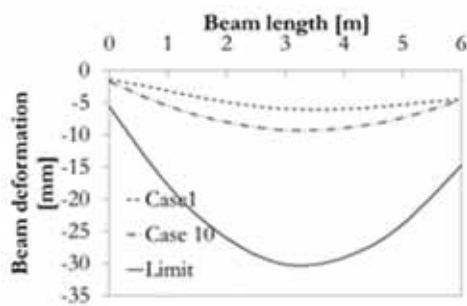
a) Sub-structure I
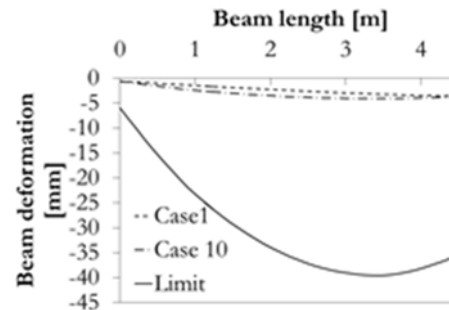
b) Sub-structure II
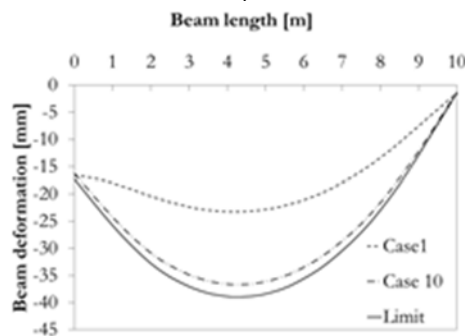
c) Sub-structure III

Fig. 7.10 Beam deformations envelop and limit according to PNA to EN1993-1-1:2006 supported by a steel-to-concrete joint

Besides the beams deformation, the lateral stiffness of the sub-structures is also affected by the joint properties. In Tab. 7.12 are listed the maximum top floor displacements obtained for each case and for Sub-structures I and II. The design limit $d_{h,top,limit}$ according to Portuguese National Annex to EN1993-1-1:2006 is also included. As for the beams deflections, it is observed that the observed values are distant from the code limit. Note that as long as the joints are continuous or semi-continuous, the top floor displacement suffers small variations. This is due to the dominant contribution of the RC wall to the lateral stiffness of the sub-structures. In Fig. 7.11 are represented the sub-structures lateral displacement envelops and the code limit. In Sub-structure II, because two RC walls contribute to the lateral stiffness of the sub-structure, the variation between minimum and maximum is quite reduced.

Tab. 7.12 Top floor lateral displacement for Sub-structures I and II [mm]

Case	Sub-structure I	Sub-structure II	Joint Properties	
1	26.7	13.5	R	FS
2	27,6	14.0		
3	28.3	14.1		
4	28.6	14.2		
5	28.3	14.1		
6	28.6	14.2	↓	↓
7	28.3	14.1		
8	28.6	14.2		
9	31.4	14.8		
10	36.0	16.2		
$d_{h.top.limit}$ [mm]	94.3	94.3	P	P

R-Rigid; P-Pinned; FS-Full-strength

Sub-structure I   Sub-structure II
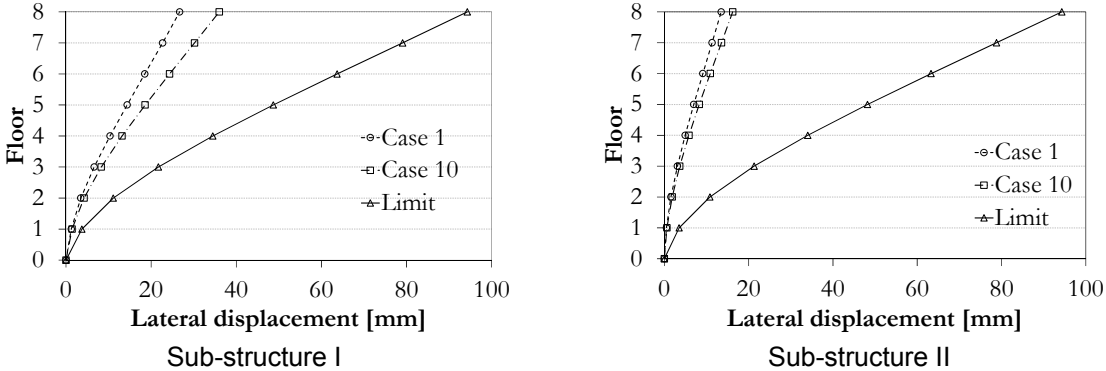
Fig. 7.11 Lateral displacements envelops

In what concerns the steel-to-concrete joints, under service limit state, the bending moment developed in the joints and the required joint rotation are represented in Fig. 7.12. In Fig. 7.13 the ratio between the bending moment developed in the joints and the joint or beam bending moment capacity is represented. For none of the cases, the joints under SLS attained the maximum bending moment resistance of the joint. As for the deformations, Sub-structure III is the most demanding to the joints. In case 7, almost 70% of the joint bending moment capacity is activated. Because the assumed joint resistance is lower, in case 7 and 8 the percentage of bending moment activated is higher. In Fig. 7.13 is shown the maximum joint rotations observed for each sub-structure and for each case. For the cases where the joints are modelled as pinned, the joint rotation required is naturally higher, but never greater than 11 mrad. In the other cases, the joint rotation is quite low, below 3.2 mrad, which is expectable as not plastic deformation of the joints occurs.
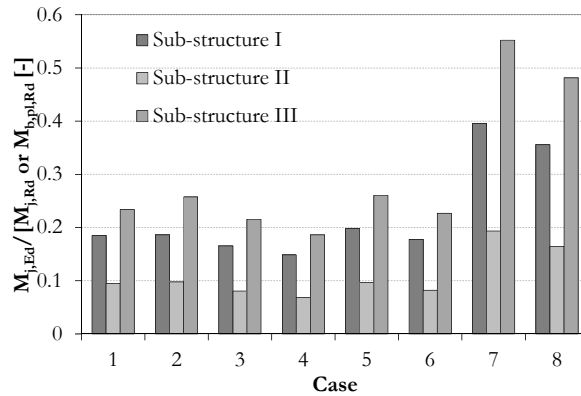
Fig. 7.12 Ratio between acting bending moment and bending moment capacity
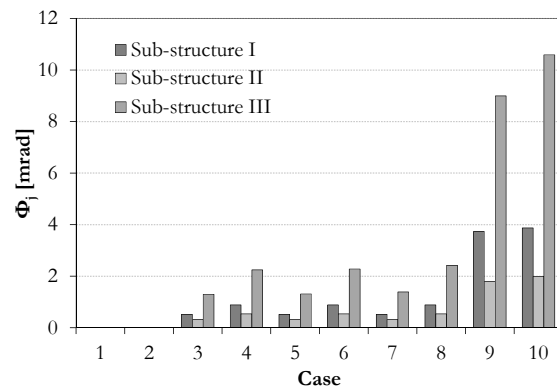of joint/beam under SLS

Fig. 7.13   Joint rotation under SLS

7.2.5   Analysis and discussion for Ultimate Limit State

At Ultimate Limit State (ULS), joints should perform so that the structural integrity is not lost. This requires to the joints either resistance either deformation capacity, allowing the redistribution of internal forces within the structure. In order to quantify such structural demands to the steel-to-concrete joints, calculations considering the load combinations of this limit state are performed. In Fig. 7.14 are summarized the maximum loads obtained on these joints M_j, N_j, V_j. In all cases, hogging bending moment and the axial compression are reported. Though, it should be referred that axial tension is observed in bottom floors of the sub-structures; however, in average, the maximum value does not exceed 10 kN.

Tab. 7.13 Top floor lateral displacement for Sub-structures I and II

Joint Location	Sub-structure I			Sub-structure II			Sub-structure III			Joint Properties	
	AL-3-L	AL-3-R	AL-3-L	AL-F-L	AL-A-R	AL-F-L	AL-G-L	AL-A-R	AL-A-L		
Case	M_j [kNm]	N_j [kN]	V_j [kN]	M_j [kNm]	N_j [kN]	V_j [kN]	M_j [kNm]	N_j [kN]	V_j [kN]		
1	169.0	68.5	181.1	64.7	31.8	72.9	441.1	387.6	345.8	R	FS
2	170.0	61.7	183.3	65.	33.4	73.9	539.5	406.4	371.4		
3	151.2	62.3	178.3	54.2	31.5	70.8	406.4	392.6	362.3		
4	136.2	62.8	174.3	46.2	30.1	68.7	350.4	382.1	355.6		
5	151.2	62.3	178.3	54.2	31.5	70.8	432.1	384.0	381.6	↓	↓
6	136.3	62.8	174.3	46.2	30.1	68.7	376.1	372.5	376.1		
7	138.0	62.1	174.8	54.8	33.0	71.3	401.9	381.3	394.5		
8	121.7	62.4	170.5	46.6	31.6	69.2	344.7	371.9	388.9		
9	0	65.9	138.9	0	21.0	56.5	0	282.4	346.5		
10	0	43.3	134.0	0	51.7	59.4	0	346.7	370.9	P	P

AL-Alignment; L – Left hand side; R- right hand side; R – Rigid; P – Pinned; FS – Full Strength

Fig. 7.14 shows the ratio between acting bending moment and the bending moment capacity of the steel-to-concrete joints or of the beams, in the case of full strength joints. As expected, for this limit state the ratio increases in comparison to the service limit state though, in none of the cases the full capacity of joints is activated. The higher ratios are observed in Sub-structures I and III, for the cases with lower bending moment resistance.

In Fig. 7.15 are plotted the maximum joint rotations observed in the different calculations. The maximum required joint rotation is approximately 20 mrad for the case studies where the steel-to-concrete joints are modelled as simple joints.
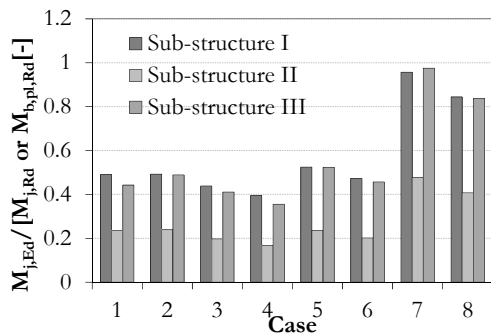

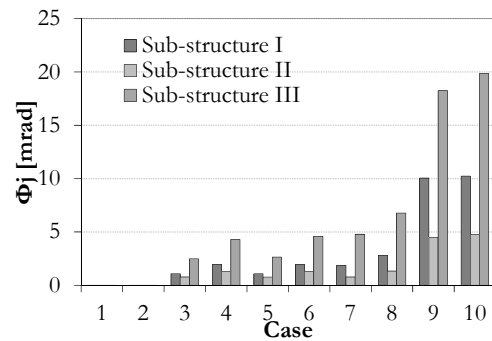Fig. 7.14 Ratio between acting bending moment and bending moment capacity of joints, and beam at ULS

Fig. 7.15 Maximum joint rotation at ULS

8 TOLERANCES

8.1 Standardized tolerances

The European standard EN1090-2:2008 describes the geometric tolerances in Chapter 11. Limits of geometric deviations contained therein are independent from the execution classes and they are divided into two types.

Essential tolerances called those which are necessary for the mechanical resistance and stability of the completed structure.

Functional tolerances have decisive influence on other criteria such as fit-up and appearance. The permitted limits of deviations are defined for two tolerance classes in generally. Stricter limits apply to class 2. Is not a class set, tolerance class 1 applies.

The essential tolerances, as well as the functional tolerances are normative.

With regard to the connections of steel structures in concrete components, essential tolerances are limited in Chapter 11.2.3.2 for foundation bolts and other supports and in Chapter 11.2.3.3 for column bases. There, with regard to their desired location, permissible deviations of a group of anchor bolts and instructions for the required hole clearance are specified for base plates.

More interesting for connections with embedded anchor plates in concrete structures are the functional tolerances given in Annex D Tab. 2.20, see Fig. 8.1.

The European standard EN13670:2011 Execution of concrete structures contains in Chapter 10 also information to geometrical tolerances, which are for buildings of importance, such as structural safety. Two tolerance classes are defined, in which in generally the tolerance class 1 (reduced requirements) applies. The application of the tolerance class 2 is intended mainly in connection with structural design according to EN1992-1-1:2004 Appendix A. Fig. 8.2 (Fig. 2 in EN13670:2011) provides limits of permissible deviations from the vertical of walls and pillars. Deviations of these components have decisive influence on the steel structures to be connected there (if required).
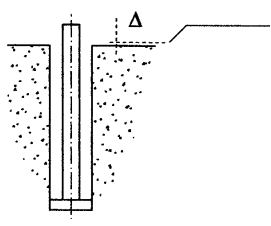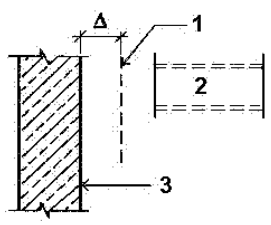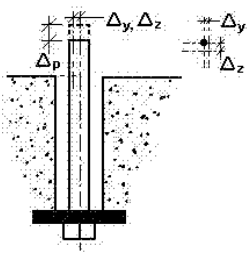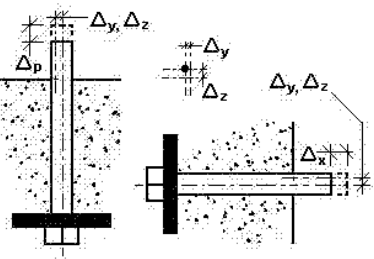
102
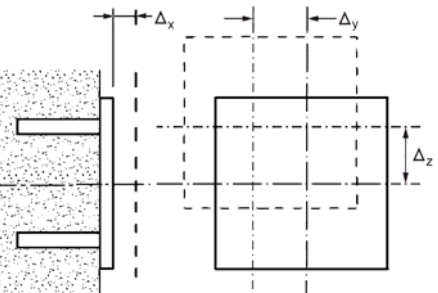
No	Criterion		Parameter	Permitted deviation Δ
1	Foundation level 		Deviation Δ from specified level	-15 mm ≤ Δ ≤ +5 mm
2	Vertical wall 	Kay 1 Specified position 2 Steel component 3 Supporting wall	Deviation Δ from specified position at support point for steel component	Δ = ± 25 mm
3	Pre-set foundation bolt where prepared for adjustment 		Deviation Δ from specified location and protrusion : - Location at tip - Vertical protrusion Δ_p NOTE The permitted deviation for location of the centre of a bolt group is 6 mm.	Δ_y, Δ_z = ± 10 mm -5 mm ≤ Δ_p ≤ 25 mm
4	Pre-set foundation bolt where not prepared for adjustment 		Deviation Δ from specified location, level and protrusion: - Location at tip - Vertical protrusion Δ_p - Vertical protrusion Δ_x NOTE The permitted deviation for location also applies to the centre of bolt group.	Δ_y, Δ_z = ± 3 mm -5 mm ≤ Δ_p ≤ 45 mm -5 mm ≤ Δ_x ≤ 45 mm
5	Steel anchor plate embedded in concrete 		Deviations Δ_x, Δ_y, Δ_z from the specified location and level	Δ_x, Δ_y, Δ_z = ± 10 mm

Fig. 8.1 Functional tolerances – concrete foundations and support,
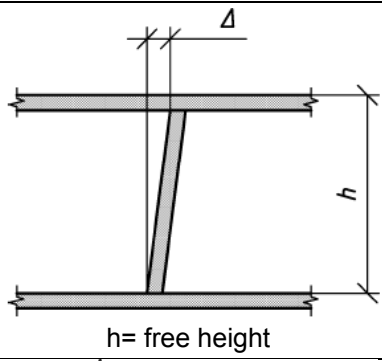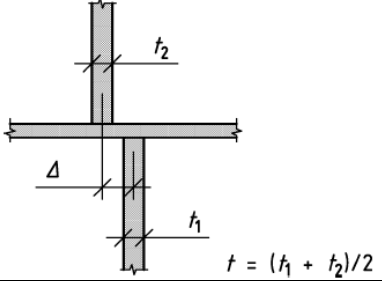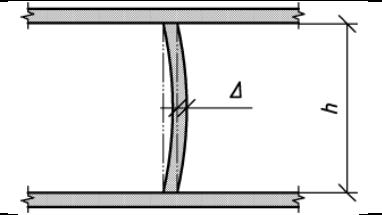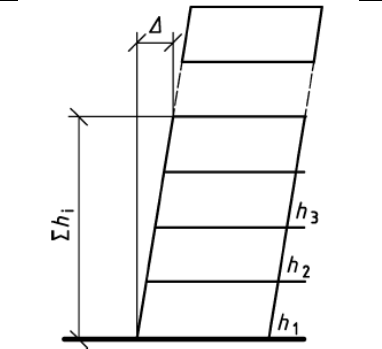**Tab. D.2.20 in EN1090-2:2008**

No	Type of deviation	Description	Permitted deviation Δ Tolerance class 1
a	h= free height	Inclination of a column or wall at any lever in a single or a multi-storey building $h \leq 10\,m$ $h > 10\,m$	The larger of $15\,mm\ or\ h/400$ $25\,mm\ or\ h/800$
b	$t = (t_1 + t_2)/2$	Deviation between centres	The larger of $t/300$ or 15 mm But not more than 30 mm
c		Curvature of a column or wall between adjacent storey levels	The larger of $t/30$ or 15 mm But not more than 30 mm
d	$\sum h_i$=sum of height of storeys considered	Location of a column or a wall at any storey level, from a vertical line through its intended centre at base level in a multi-storey structure n is the number of storeys where $n > 1$	The smaller of $50\,mm$ or $$\frac{\sum h_i}{(200n^{\frac{1}{2}})}$$

Fig. 8.2 Permissible deviations from the vertical of walls and pillars,
abridged **Fig. 2 in EN13670:2011**

Geometric tolerances, which are in terms of suitability for use and the accuracy of fit for the building of importance, are regulated in the informative Annex G, unless regulated otherwise, the tolerances of Annex G apply, see Fig. 8.3. It is assumed that tolerances contained therein relate to geometrical sizes, which have only a limited influence on the bearing capacity. Fig. 8.1 shows the permissible deviations of built in components in all directions, compare EN1090-2:2008 D. 2.20 line 5.
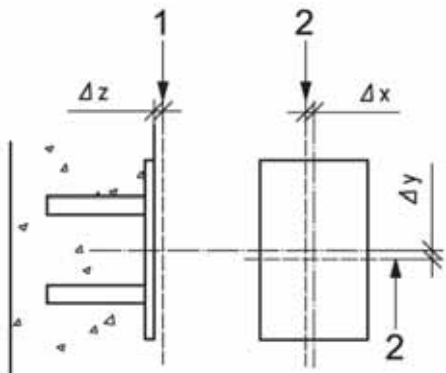
No	Type of deviation	Description	Permitted deviation Δ
d	1 normal position in plane 2 normal position in depth	Anchoring plates and similar inserts Deviation in plane Deviation in depth	Δ_x, $\Delta_y = \pm 20$ mm $\Delta_z = \pm 10$ mm

Fig. 8.3 Permitted deviations for holes and inserts,
abridged **Fig. G.6 in EN13670:2011**

An assessment of the impact of the tabular listed permissible limits on connections with embedded anchor plates will be in the next Chapter 8.2.

8.2 Recommended tolerances

For deviations from fixtures (anchoring) of the target location, relatively low values are allowed in the previously mentioned standards, ±10 mm in each direction, see EN1090-2:2008, or ± 20 mm in the plains and ± 10 mm perpendicular to the surface, see EN13670:2011. Tolerances for angular misalignments of the anchor plates to their installation levels are not available.

However, in EN 13670 Fig. 2d for multi-story buildings clearly greater deviations of the upper floors to the vertical are allowed. For example, the permissible horizontal displacement of the top-level of a floor from the target location is for a seven-story building with a floor height of 3.50 m.

$$\sum h_i \, / \, (200 \; n^{1/2}) = 46 \text{ mm} \qquad (8.1)$$

If the building is made of prefabricated concrete elements, the concrete anchor plate - even with exact location within the individual component - may exhibit the same displacement from the target location as the above shown deviations.

Therefore, the deviations defined directly for anchor plates by ± 10 mm seem to be hardly feasible. Much larger deviations have to be expected. If necessary, special tolerances for the location of the built in components have to be defined. EN13670:2011 describes another principle of tolerance definition, in which the allowable deviation of any point of construction compared to a theoretical target location over a fixed value is defined in Chapter 10.1 cl 5. A recommendation for the maximum permissible deviation is ± 20 mm.

Definitely, connecting elements between steel and concrete structures must be able to compensate tolerances. Considering the previous explanations, a development of joints for taking deviations of the anchor plate from the theoretical target location of ± 20 to 25 mm is recommended. Fig. 8.4 and 8.5 show exemplary a connections with and without the possibility to compensate geometrical derivations.
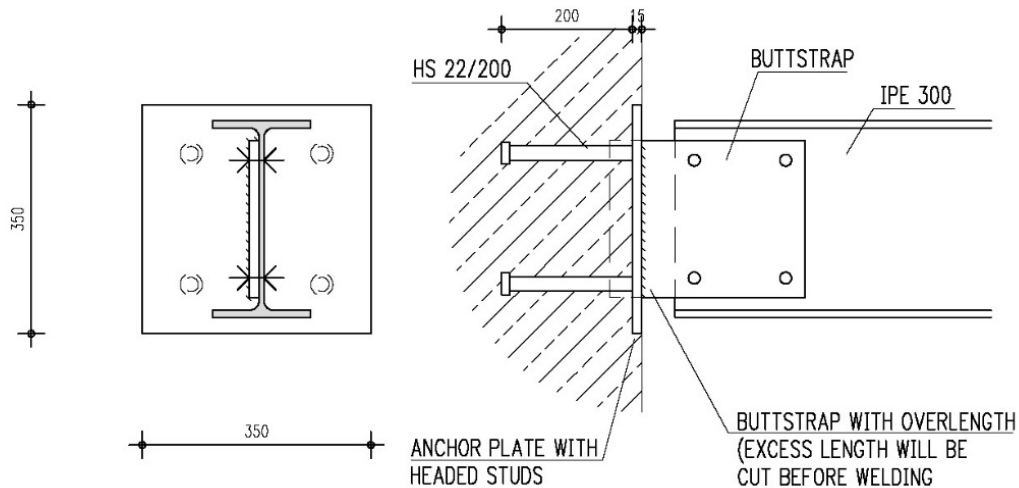
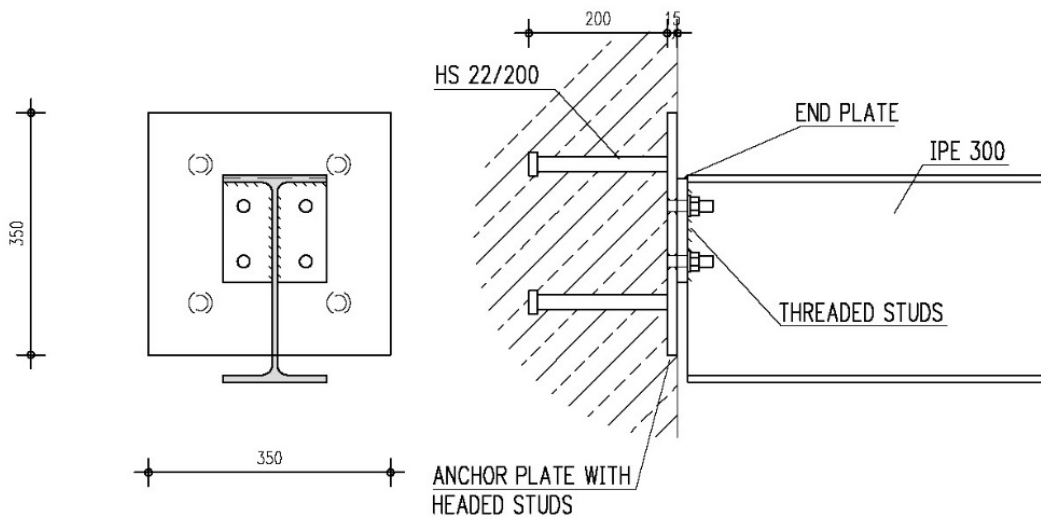Fig. 8.4 Joint <u>with</u> possibility of adjustment

Fig. 8.5 Joint <u>without</u> possibility of adjustment

The following methods is used to compensate certain displacements of build in components to the target location. Depending on the loading, priority direction of the loads, the most appropriate solution has to be chosen.

<u>Tolerance absorption in the longitudinal direction of the profile</u>

    Bolted connection with end plate and scheduled filler plates
    Bolted connection with base plate and grouting
    Cleat / console
    Beam / pillar scheduled with overlength; adjustment and welding on site
    Buttstrap with overlength; adjustment and welding on site
    Buttstrap with slot holes

<u>Tolerance absorption perpendicular to the longitudinal direction of profile:</u>

    Additional steel plate with threaded bolts; welded on site; beam / pillar with end plate
    Anchor plate with threaded bolts; head plate with oversized holes
    Buttstrap; welding on site

9 WORKED EXAMPLES

9.1 Pinned base plate

Check the resistance of the column base. The column of HE 200 B section, a concrete foundation size 850 x 850 x 900 mm, a base plate thickness 18 mm, steel S 235 and concrete C 12/15, $\gamma_{Mc} = 1.50$, $\gamma_{M0} = 1.00$.
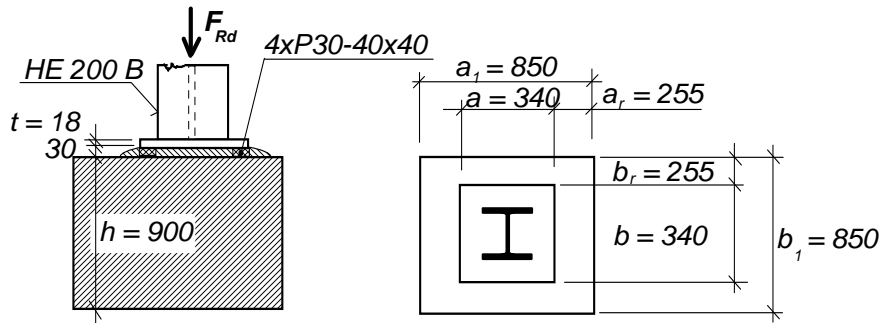

Fig. 9.1 Designed column base

Step 1 Concrete design strength

The stress concentration factor should be calculated, see Chap. 3.3. The minimum values for a_1 (or b_1) are taken into account

$$a_1 = b_1 = \min \left\{ \begin{array}{c} a + 2\,a_r = 340 + 2 \cdot 255 = 850 \\ 3\,a = 3 \cdot 340 = 1\,020 \\ a + h = 340 + 900 = 1\,240 \end{array} \right\} = 850 \text{ mm}$$

The condition $a_1 = b_1 = 850 > a = 340$ mm is satisfied, and therefore

$$k_j = \sqrt{\frac{a_1 \cdot b_1}{a \cdot b}} = \sqrt{\frac{850 \cdot 850}{340 \cdot 340}} = 2.5$$

The concrete design strength is calculated from the equation

$$f_{jd} = \frac{\beta_j\,F_{Rd,u}}{b_{eff}\,l_{ef}} = \frac{\beta_j\,A_{c0}\,f_{cd}\sqrt{\dfrac{A_{c1}}{A_{c0}}}}{A_{c0}} = \beta_j\,f_{cd}\,k_j = 0.67 \cdot \frac{12.0}{1.5} \cdot 2.5 = 13.4 \text{ MPa}$$

Step 2 Flexible base plate

The flexible base plate is replaced by a rigid plate, see the following picture Fig. 9.2.

The strip width is

$$c = t\sqrt{\frac{f_y}{3 \cdot f_{jd} \cdot \gamma_{M0}}} = 18 \cdot \sqrt{\frac{235}{3 \cdot 13.4 \cdot 1.00}} = 43.5 \text{ mm}$$
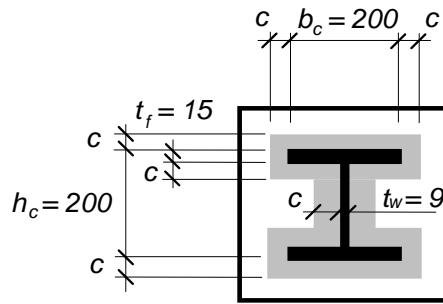
Fig. 9.2 Effective area under the base plate

The effective area of the base plate of H shape is calculated as a rectangular area minus the central areas without contact such that;

$$A_{eff} = \min(b; b_c + 2c) \cdot \min(a; h_{ef} + 2c)$$
$$- \max[\min(b; b_c + 2c) - t_w - 2c; 0] \cdot \max(h_c - 2t_f - 2c; 0)$$

$$A_{eff} = (200 + 2 \cdot 43.5) \cdot (200 + 2 \cdot 43.5)$$
$$- (200 + 2 \cdot 43.5 - 9 - 2 \cdot 43.5) \cdot (200 - 2 \cdot 15 - 2 \cdot 43.5)$$

EN1993-1-8
cl 6.2.5

$$A_{eff} = 82\,369 - 15\,853 = 66\,516 \text{ mm}^2$$

Step 3 Design resistance

The design resistance of the column base in compression is

$$N_{Rd} = A_{eff} \cdot f_{jd} = 66\,516 \cdot 13.4 = 891 \cdot 10^3 \text{N}$$

EN1993-1-8
cl 6.2.5

Comments

The design resistance of the column footing is higher than the resistance of the column base

$$N_{pl,Rd} = \frac{A_c \cdot f_y}{\gamma_{M0}} = \frac{7808 \cdot 235}{1.00} = 1\,835 \cdot 10^3 \text{N} > N_{Rd}$$

EN1993-1-1
cl 6.2.4

where A_c is area of the column. The column base is usually designed for column resistance, which is determined by column buckling resistance.

It is expected, that the grout will not affect the column base resistance. The grout has to be of better quality or the thickness has to be smaller than

$$0.2 \min(a; b) = 0.2 \cdot 340 = 68 \text{ mm}$$

EN1993-1-8
cl 6.2.5

The steel packing or the levelling nuts is placed under the base plate during the erection. It is recommended to include the packing/nuts in the documentation

9.2 Moment resistant base plate

In the following example the calculation of the moment resistance and the bending stiffness of the column base at Fig. 9.3 is shown. The Column HE 200 B is loaded by a normal force $F_{Sd} = 500$ kN. The concrete block C25/30 of size 1 600 x 1 600x 1000 mm is designed for particular soil conditions. The base plate is of 30 mm thickness and the steel strength is S235. Safety factors are considered as $\gamma_{Mc} = 1.50$; $\gamma_{Ms} = 1.15$, $\gamma_{M0} = 1.00$; and $\gamma_{M2} = 1.25$. The connection between the base plate and the concrete is carried out through four headed studs of 22 mm diameter and an effective embedment depth of 150 mm, see Fig. 9.3. The diameter of the head of the stud is 40 mm. The supplementary reinforcement for each headed stud consists of two legged 12 mm diameter stirrups on each side of the stud. Consider $f_{uk} = 470$ MPa for studs and design yield strength of the supplementary reinforcement

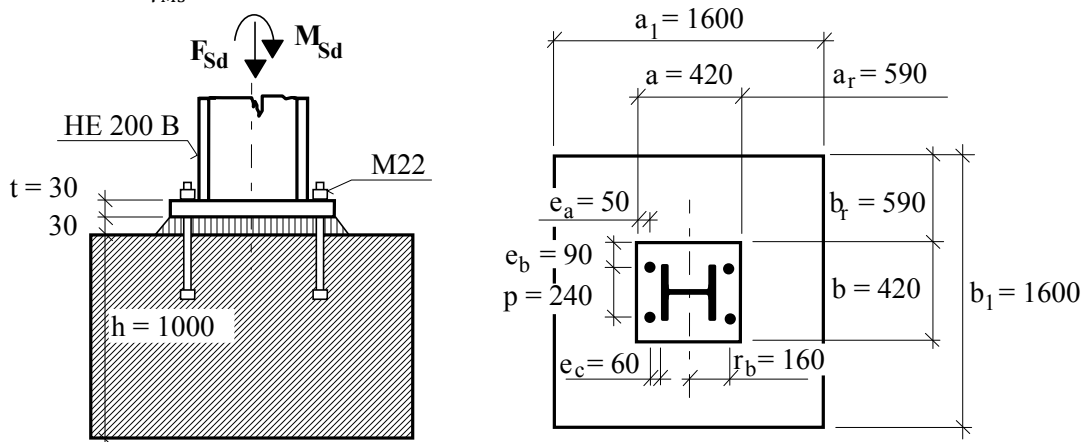as $f_{yd,re} = \dfrac{f_{yk,re}}{\gamma_{Ms}} = \dfrac{500}{1.15} = 435$ MPa.

Fig. 9.3 Designed column base

Step 1 Base plate resistance

1.1 Component base plate in bending and headed studs in tension

Lever arm, for fillet weld $a_{wf} = 6$ mm is

$$m = 60 - 0.8 \cdot a_{wf} \cdot \sqrt{2} = 60 - 0.8 \cdot 6 \cdot \sqrt{2} = 53.2 \text{ mm}$$

The minimum T-stub length in base plates where the prying forces not taken into account, is

$$l_{eff,1} = \min \begin{Bmatrix} 4\,m + 1.25\,e_a = 4 \cdot 53.2 + 1.25 \cdot 50 = 275.3 \\ 2\,\pi\,m = 2\,\pi \cdot 53.2 = 334.3 \\ b \cdot 0.5 = 420 \cdot 0.5 = 210 \\ 2\,m + 0.625\,e_a + 0.5\,p = 2 \cdot 53{,}2 + 0.625 \cdot 50 + 0.5 \cdot 240 = 257.7 \\ 2\,m + 0.625\,e_a + e_b = 2 \cdot 53.2 + 0.625 \cdot 50 + 90 = 227.7 \\ 2\,\pi\,m + 4\,e_b = 2\,\pi \cdot 53.2 + 4 \cdot 90 = 694.3 \\ 2\,\pi\,m + 2\,p = 2\,\pi \cdot 53.2 + 2 \cdot 240 = 814.3 \end{Bmatrix}$$

$l_{eff,1} = 210$ mm

The effective length of headed studs L_b is taken as

$$L_b = \min(h_{eff};\ 8 \cdot d) + t_g + t + \frac{t_n}{2} = 150 + 30 + 30 + \frac{19}{2} = 219.5 \text{ mm}$$

The resistance of T - stub with two headed studs is

$$F_{T,1-2,Rd} = \frac{2\ L_{eff,1}\ t^2\ f_y}{4\ m\ \gamma_{M0}} = \frac{2 \cdot 210 \cdot 30^2 \cdot 235}{4 \cdot 53.2 \cdot 1.00} = 417.4 \text{ kN}$$

The resistance is limited by tension resistance of two headed studs M 22, the area in tension $A_s = 303$ mm.

$$F_{T,3,Rd} = 2 \cdot B_{t,Rd} = 2 \cdot \frac{0.9 \cdot f_{uk} \cdot A_s}{\gamma_{M2}} = 2 \cdot \frac{0.9 \cdot 470 \cdot 303}{1.25} = 205.1 \text{ kN}$$

1.2 Component base plate in bending and concrete block in compression

To evaluate the compressed part resistance is calculated the connection factor as

$$a_1 = b_1 = \min \left\{ \begin{matrix} a + 2.\,a_r = 420 + 2 \cdot 590 = 1\ 600 \\ 3a = 3 \cdot 420 = 1260 \\ a + h = 420 + 1\ 000 = 1\ 420 \end{matrix} \right\} = 1\ 260 \text{ mm}$$

and $a_1 = b_1 = 1\ 260 > a = b = 420$ mm

The above condition is fulfilled and

$$k_j = \sqrt{\frac{a_1 \cdot b_1}{a \cdot b}} = \sqrt{\frac{1\ 260 \cdot 1\ 260}{420 \cdot 420}} = 3.00$$

The grout is not influencing the concrete bearing resistance because

$$0.2 \cdot \min(a; b) = 0.2 \cdot \min(420;\ 420) = 84 \text{ mm} > 30 \text{ mm} = t_g$$

The concrete bearing resistance is calculated as

$$f_{jd} = \frac{2}{3} \cdot \frac{k_j \cdot f_{ck}}{\gamma_{Mc}} = \frac{2}{3} \cdot \frac{3.00 \cdot 25}{1.5} = 33.3 \text{ MPa}$$

From the force equilibrium in the vertical direction $F_{Sd} = A_{eff} \cdot f_{jd} - F_{t,Rd}$, the area of concrete in compression A_{eff} in case of the full resistance of tension part is calculated

$$A_{eff} = \frac{F_{Sd} + F_{Rd,3}}{f_{jd}} = \frac{500 \cdot 10^3 + 205.1 \cdot 10^3}{33.3} = 21\ 174 \text{ mm}^2$$

The flexible base plate is transferred into a rigid plate of equivalent area. The width of the strip c around the column cross section, see Fig. 9.4, is calculated from

$$c = t\sqrt{\frac{f_y}{3 \cdot f_{jd} \cdot \gamma_{M0}}} = 30 \cdot \sqrt{\frac{235}{3 \cdot 33.3 \cdot 1.00}} = 46.0 \text{ mm}$$
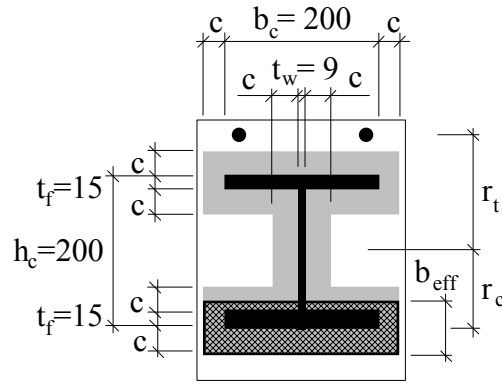
Fig. 9.4 The effective area under the base plate

1.3 Assembly for resistance

The active effective width is calculated as

$$b_{eff} = \frac{A_{eff}}{b_c + 2\,c} = \frac{21\,174}{200 + 2 \cdot 46.0} = 72.5 \text{ mm} < \ t_f + 2\,c = 15 + 2 \cdot 46.0 = 107.0 \text{ mm}$$

The lever arm of concrete to the column axes of symmetry is calculated as

$$r_c = \frac{h_c}{2} + c - \frac{b_{eff}}{2} = \frac{200}{2} + 46.0 - \frac{72.5}{2} = 109.8 \text{ mm}$$

The moment resistance of the column base is $M_{Rd} = F_{T,3,Rd} \cdot r_t + A_{eff} \cdot f_{jd} \cdot r_c$

$$M_{Rd} = 205.1 \cdot 10^3 \cdot 160 + 21\,174 \cdot 33.3 \cdot 109.8 = 110.2 \text{ kNm}$$

Under acting normal force $N_{Sd} = 500$ kN the moment resistance in bending is

$M_{Rd} = 110.2$ kNm.

1.4 The end of column resistance

The design resistance in poor compression is

$$N_{pl,Rd} = \frac{A \cdot f_y}{\gamma_{M0}} = \frac{7808 \cdot 235}{1.00} = 1\,835 \cdot 10^3 N > \ N_{Rd} = 500 \text{kN}$$

The column bending resistance

$$M_{pl,Rd} = \frac{W_{pl} \cdot f_{yk}}{\gamma_{M0}} = \frac{642.5 \cdot 10^3 \cdot 235}{1.00} = 151.0 \text{ kNm}$$

The interaction of normal force reduces moment resistance

$$M_{Ny,Rd} = M_{pl,Rd} \frac{1 - \dfrac{N_{Sd}}{N_{pl,Rd}}}{1 - 0.5\,\dfrac{A - 2\,b\,t_f}{A}} = 151.0 \cdot \frac{1 - \dfrac{500}{1\,835}}{1 - 0.5\,\dfrac{7\,808 - 2 \cdot 200 \cdot 15}{7\,808}} = 124.2 \text{ kNm}$$

The column base is designed on acting force only (not for column resistance).

Step 2 Base plate stiffness

2.1 Component base plate in bending and headed stud in tension

The component stiffness coefficients for headed studs and base plate are calculated

$$k_b = 2.0 \cdot \frac{A_s}{L_b} = 2.0 \cdot \frac{303}{219.5} = 2.8 \text{ mm}$$

$$k_p = \frac{0.425 \cdot L_{beff} \cdot t^3}{m^3} = \frac{0.425 \cdot 210 \cdot 30^3}{53.2^3} = 16.0 \text{ mm}$$
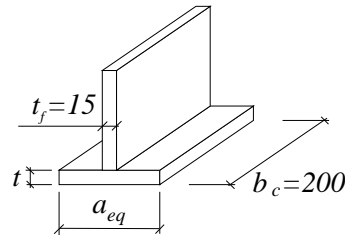
Fig. 9.5 The T stub in compression

2.2 Component base plate in bending and concrete block in compression

For the stiffness coefficient the T-stub in compression, see Fig. 9.5, is

$$a_{eq} = t_f + 2.5 \, t = 15 + 2.5 \cdot 30 = 90 \text{ mm}$$

$$k_c = \frac{E_c}{1.275 \cdot E_s} \cdot \sqrt{a_{eq} \cdot b_c} = \frac{31\,000}{1.275 \cdot 210\,000} \cdot \sqrt{90 \cdot 200} = 15.5 \text{ mm}$$

2.3 Assembly of component tensile stiffness coefficient to base plate stiffness

The lever arm of component in tension z_t and in compression z_c to the column base neutral axes is

$$z_t = \frac{h_c}{2} + e_c = \frac{200}{2} + 60 = 160 \text{ mm}$$

$$z_c = \frac{h_c}{2} - \frac{t_f}{2} = \frac{200}{2} - \frac{15}{2} = 92.5 \text{ mm}$$

The stiffness coefficient of tension part, headed studs and T stub, is calculated as

$$k_t = \frac{1}{\frac{1}{k_b} + \frac{1}{k_p}} = \frac{1}{\frac{1}{2.8} + \frac{1}{16.0}} = 2.4 \text{ mm}$$

For the calculation of the initial stiffness of the column base the lever arm is evaluated

$$z = z_t + z_c = 160 + 92.5 = 252.5 \text{ mm} \qquad \text{and}$$

$$a = \frac{k_c \cdot z_c - k_t \cdot z_t}{k_c + k_t} = \frac{15.5 \cdot 92.5 - 2.4 \cdot 160}{15.5 + 2.4} = 58.6 \text{ mm}$$

The bending stiffness is calculated for particular constant eccentricity

$$e = \frac{M_{Rd}}{F_{Sd}} = \frac{110.2 \cdot 10^6}{500 \cdot 10^3} = 220.4 \text{ mm}$$

as

$$S_{j,ini} = \frac{e}{e+a} \cdot \frac{E_S \cdot z^2}{\mu \sum_i \frac{1}{k_i}} = \frac{220.4}{220.4 + 58.6} \cdot \frac{210\,000 \cdot 252.5^2}{1 \cdot \left(\frac{1}{2.4} + \frac{1}{15.5}\right)} = 21.981 \cdot 10^9 \text{ Nmm/rad}$$

$$= 21\,981 \text{ kNm/rad}$$

Step 3 Anchorage resistance and stiffness

As discussed in Chapter 3 Concrete components, the stiffness of anchorage is determined for separate components, failure modes, and then combined together. In this case, the anchorage is considered as a group of four headed studs with nominal stud diameter of 22 mm arranged in a way displayed in Fig. 9.6. Furthermore, supplementary reinforcement with the arrangement shown in Fig. 9.6 is considered.

Due to moment loading on the anchor group generated by the lateral loads only one side studs will be subjected to tension loads. Therefore in the following example, two studs are considered while evaluating the behaviour of the anchor group. Here, diameter of the reinforcing bar is considered as 12 mm and the effective embedment depth of the stud is considered as 150 mm, distance from of the head to the concrete surface.
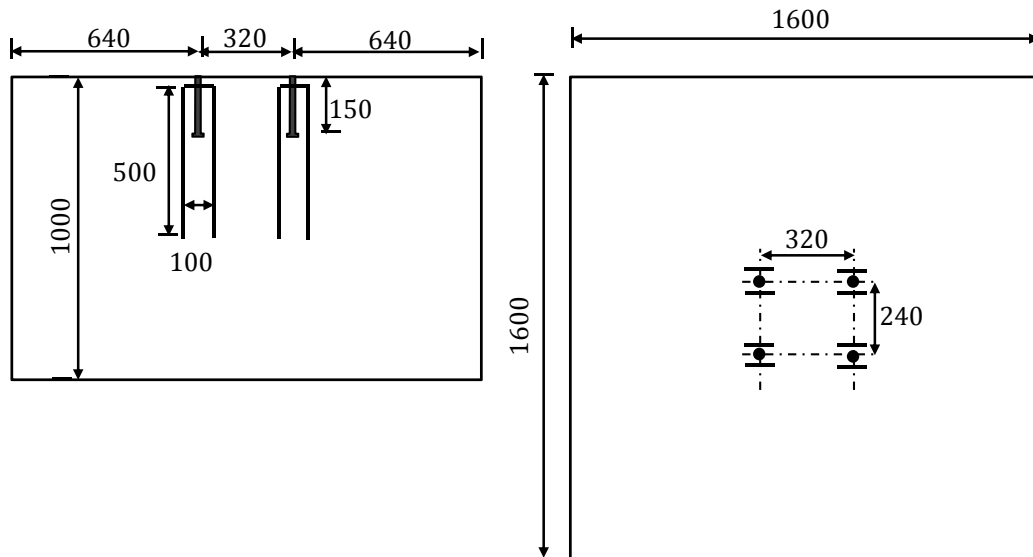

Fig. 9.6 Headed studs and supplementary reinforcement configuration

3.1 Component S – Steel failure of headed stud

Component S comprises of evaluating the design load-displacement response of the headed studs under tensile loading, when they undergo steel failure. Only two anchors will be considered in tension. From Eq. (3.3) and (3.4) is calculated the load and the stiffness as

$$N_{Rd,s} = \frac{n \cdot \pi \cdot d_{s,nom}^2 \cdot f_{uk}}{4 \cdot \gamma_{Mp}} = \frac{2 \cdot \pi \cdot 22^2 \cdot 470}{4 \cdot 1.5} = 238\,216 \text{ N} = 238.2 \text{ kN}$$

$$k_{s1} = \frac{A_{s,nom} E_s}{L_h} = \frac{n \cdot \pi \cdot d_{s,nom}^2}{4} \cdot \frac{E_s}{L_h} = \frac{2 \cdot \pi \cdot 22^2 \cdot 210\,000}{4 \cdot 150} =$$

$$= 1\,064\,371 \frac{\text{N}}{\text{mm}} = 1\,064.4 \frac{\text{kN}}{\text{mm}}, \text{ for } N_{act} < 238.2 \text{ kN}$$

$$k_{s2} = 0; \ N_{act} = 238.2 \text{ kN}$$

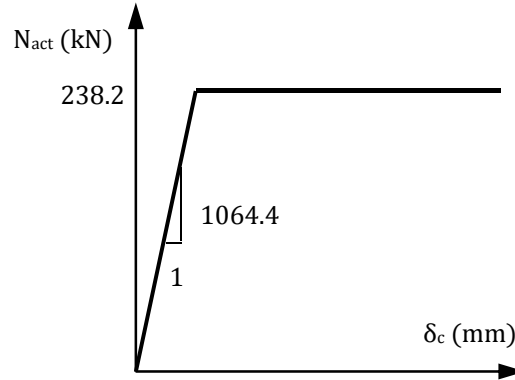Hence, the load-displacement curve for the spring is obtained as shown in Fig. 9.7.

Fig. 9.7 Load-displacement behaviour of spring representing component S

3.2 Component C – Concrete cone failure

Component CC comprises of evaluating the design load-displacement response of the headed studs under tensile loading, when they undergo concrete cone failure. The critical edge distance $c_{cr,N} = 1.5\,h_{ef} = 225$ mm. Using Eqs (3.7) through (3.9), it is

$$N_{Rd} = N_{Rk,c}^0 \cdot \psi_{A,N} \cdot \psi_{s,N} \cdot \psi_{re,N} / \gamma_{Mc}$$

$$N_{Rk,c}^0 = k_1 \cdot h_{ef}^{1.5} \cdot f_{ck}^{0.5} = 12.7 \cdot 150^{1.5} \cdot 25^{0.5} \text{ N} = 116,7 \text{ kN}$$

$$\psi_{A,N} = \frac{A_{c,N}}{A_{c,N}^0} = \frac{(1.5 \cdot 150 + 240 + 1.5 \cdot 150) \cdot (1.5 \cdot 150 + 1.5 \cdot 150)}{9 \cdot 150^2} = \frac{690 \cdot 450}{9 \cdot 150^2} = 1.53$$

Since maximum edge distance, $c < c_{cr,N} = 225$ mm, hence $\psi_{s,N} = 1.0$

There is no closely spaced reinforcement, hence, $\psi_{re,N} = 1.0$

Therefore, $N_{Rd,c} = 116.7 \cdot 1.53 \cdot 1.0 \cdot \frac{1.0}{1.5} = 119.0$ kN

The stiffness of the descending branch $k_{c,de}$ for the design is described with the following function

$$k_{c,de} = \alpha_c \sqrt{f_{ck}\,h_{ef}} \cdot \psi_{A,N} \cdot \psi_{s,N} \cdot \psi_{re,N} = -537\sqrt{25 \cdot 150} \cdot 1.53 \cdot 1.0 \cdot 1.0 = -50.31 \frac{\text{kN}}{\text{mm}}$$

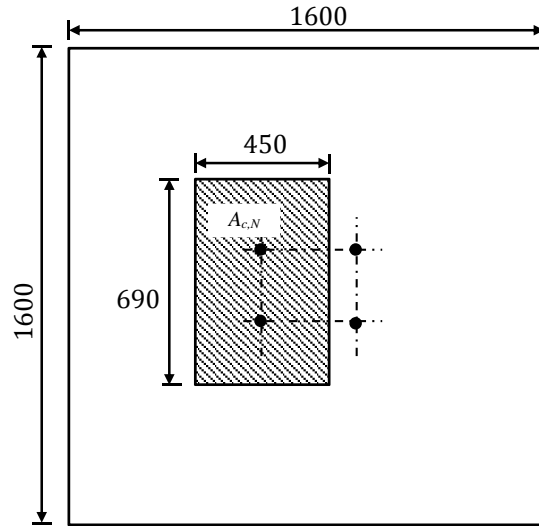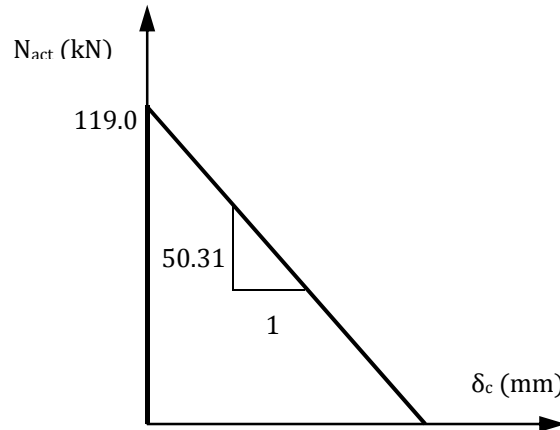The displacement corresponding to zero load is $\frac{119.0}{50,31} = 2.37$ mm

Fig. 9.8 Evaluation of group effect

The load-displacement curve for the spring is shown in Fig. 9.9.

Fig. 9.9 Load-displacement behaviour of spring representing component CC

3.3 Component RS – Steel failure of stirrups

Component RS comprises of evaluating the design load-displacement response of the stirrups, when they undergo steel failure. The design load for yielding of the stirrups is given as Eq. (3.17)

$$N_{Rd,s,re} = A_{s,re} \cdot f_{yd,re} = n_{re} \cdot \pi \cdot \left(d_{s,re}^2 / 4\right) \cdot f_{yd,re}$$

For each stud, two stirrups with two legs on either side of the headed stud are provided. Therefore, for two headed studs in tension, the total number of the legs of the stirrups in tension is 8. Hence,

$$N_{Rd,s,re} = 8 \cdot \left(\frac{\pi}{4} \cdot 12^2\right) \cdot 435 = 393.6 \text{ kN}$$

$$\delta_{Rd,s,re} = \frac{2 \cdot N_{Rd,s,re}^2}{\alpha_s \cdot f_{ck} \cdot d_{s,re}^4 \cdot n_{re}^2} = \frac{2 \cdot 393\,578^2}{12\,100 \cdot 25 \cdot 12^4 \cdot 8^2} = 0.77 \text{ mm}$$

Stiffness as a function of displacement is given as Eq. (3.18)

115

$$k_{s,re1} = \frac{\sqrt{n_{re}^2 \cdot \alpha_s \cdot f_{ck} \cdot d_{s,re}^4}}{\sqrt{2 \cdot \delta}} = \frac{\sqrt{8^2 \cdot 12\,100 \cdot 25 \cdot 12^4}}{\sqrt{2 \cdot \delta}} = \frac{448\,023}{\sqrt{\delta}} \text{ N/mm}$$

for $\delta < \delta_{Rd,s,re}$

$k_{s,re2} = 0$ for $\delta \geq \delta_{Rd,s,re}$

The load-displacement curve for the spring is shown in Fig. 9.10
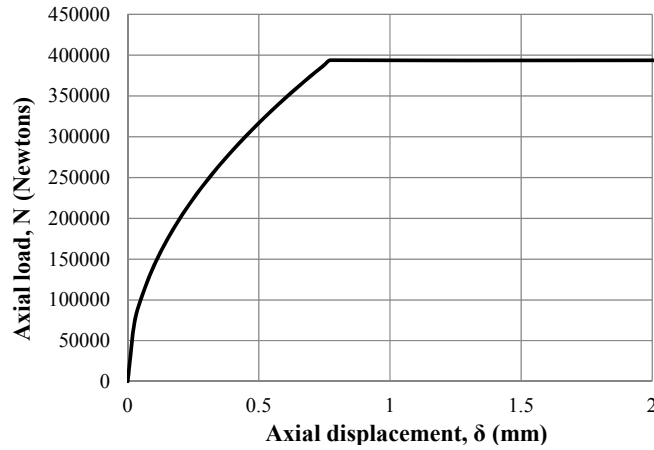
Fig. 9.10 Load-displacement behaviour of spring representing component RS

3.4 Component RB – Bond failure of stirrups

Component RB comprises of evaluating the design load-displacement response of the stirrups under tensile loading, when they undergo bond failure. The design anchorage capacity of the stirrups is given by Eq. (3.21). Assuming a cover of 25 mm to stirrups and considering the distance between the stud and the stirrup as 50 mm, l_1 is calculated as CEN/TC1992-4-1:2009

$$l_1 = 150 - 25 - 0.7 \cdot 50 = 90 \text{ mm}$$

Considering f_{bd} for C25/30 grade concrete is $2.25 \cdot \frac{1.8}{1.5} \cdot 1.0 \cdot 1.0 = 2.7$ N/mm², see Eq (8.2) cl 8.4.2.(2) in EN1992:2004, it is

$$N_{Rd,b,re} = \sum n_{re} \cdot l_1 \cdot \pi \cdot d_{s,re} \cdot \frac{f_{bd}}{\alpha} = 8 \cdot 90 \cdot \pi \cdot 12 \cdot \frac{2.7}{0.49} = 149\,565 \text{ N} = 149.6 \text{ kN}$$

The corresponding displacement is obtained using Eq. (3.20) as

$$\delta_{Rd,b,re} = \frac{2 \cdot N_{Rd,b,re}^2}{\alpha_s \cdot f_{ck} \cdot d_{s,re}^2 \cdot n_{re}^2} = \frac{2 \cdot 149\,565^2}{12100 \cdot 25 \cdot 12^4 \cdot 8^2} = 0.11 \text{ mm}$$

It may be noted that since $N_{Rd,b,re} < N_{Rd,s,re}$, bond failure of stirrups is the governing failure mode for the stirrups.

Stiffness as a function of displacement is given as

$$k_{b,re1} = \frac{\sqrt{n_{re}^2 \cdot \alpha_s \cdot f_{ck} \cdot d_{s,re}^4}}{\sqrt{2\delta}} = \frac{\sqrt{8^2 \cdot 12\,100 \cdot 25 \cdot 12^4}}{\sqrt{2\delta}} = \frac{448\,023}{\sqrt{\delta}} \text{N/mm}$$

for $\delta < \delta_{Rd,b,re}$

$k_{b,re2} = 0$ for $\delta \geq \delta_{Rd,b,re}$

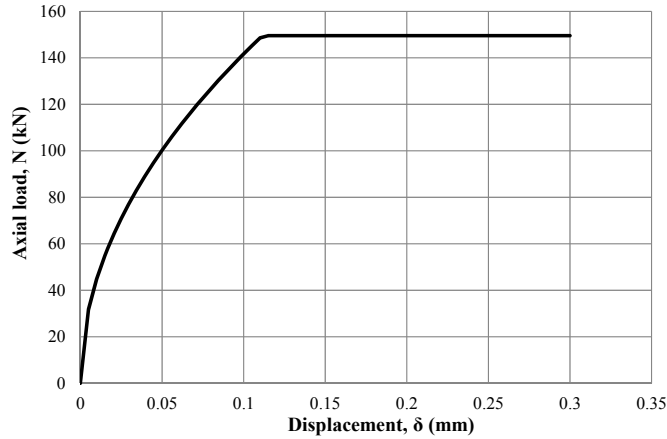The load-displacement curve for the spring is shown in Fig. 9.11.

Fig. 9.11 Load-displacement relation of spring representing component RB

3.5 Component P - Pull out failure of the headed stud

For the first range, $N > N_{Rd,c}$ using Eqs (3.26) through (3.30), it is

$$k_p = \alpha_p \cdot \frac{k_a \cdot k_A}{k_2}$$

$a = 0.5 \cdot (d_h - d_s) = 0.5 \cdot (40 - 22) = 9 \text{ mm}$

$$k_a = \sqrt{\frac{5}{a}} \geq 1.0; \text{hence, } k_a = 1.0$$

DM I
Eq. (3.26)

$$k_A = 0.5 \cdot \sqrt{d_s^2 + m \cdot (d_h^2 - d_s^2)} - 0.5 \cdot d_h = 0.5 \cdot \sqrt{22^2 + 9 \cdot (40^2 - 22^2)} - 0.5 \cdot 40 =$$
$$= 31.30$$

DM I
Eq. (3.29)

$k_2 = 600$ (assuming uncracked concrete)

DM I
Eq. (3.28)

$$k_p = \alpha_p \cdot \frac{k_a \cdot k_A}{k_2} = 0.25 \cdot \frac{1.0 \cdot 31.30}{600} = 0.0130$$

Thus, using Eq. (3.24), it is

DM I
Eq. (3.30)

$$\delta_{Rd,p,1} = k_p \cdot \left(\frac{N_{Rd,c}}{A_h \cdot f_{ck} \cdot n}\right)^2 = 0.0130 \cdot \left(\frac{119.0 \cdot 10^3}{\frac{\pi}{4} \cdot (40^2 - 22^2) \cdot 25 \cdot 2}\right)^2 = 0.096 \text{ mm}$$

In second range, using Eq. (3.25), it is

DM I
Eq. (3.24)

$$\delta_{Rd,p,2} = 2k_p \cdot \left(\frac{\min\left(N_{Rd,p}; N_{Rd,re}\right)}{A_h \cdot f_{ck} \cdot n}\right)^2 - \delta_{Rd,p,1}$$

Eq. (3.31) yields

$N_{Rd,p} = n \cdot p_{uk} \cdot A_h / \gamma_{Mc}$

DM I
Eq. (3.25)

$N_{Rd,re} = \min(N_{Rd,s,re}; N_{Rd,b,re}) = \min(393.6; 149.6) = 149.6 \text{ kN}$

The typical value of p_{uk} is considered as $12 f_{ck} = 12 \cdot 25 = 300$ MPa. Hence, it is

$$N_{Rd,p} = 2 \cdot 300 \cdot \frac{\pi}{4} \cdot \frac{(40^2 - 22^2)}{1.5} = 350.6 \text{ kN}$$

$$\delta_{Rd,p,2} = 2 \cdot 0.0130 \cdot \left(\frac{149\,565}{\frac{\pi}{4} \cdot (40^2 - 22^2) \cdot 25 \cdot 2} \right)^2 - 0.096 = 0.21 \text{ mm}$$

The stiffness as a function of displacement is obtained using equations (3.34) and (3.35) as:

$$k_{p,1} = \sqrt{\frac{\left(\frac{\pi}{4} \cdot (40^2 - 22^2) \cdot 25 \cdot 2 \right)^2}{0.0130 \cdot \delta_{act}}} = \frac{384\,373}{\sqrt{\delta_{act}}}$$

<div style="text-align:right">DM I
Eq. (3.34)</div>

$$k_{p,2} = \sqrt{\frac{\left(\frac{\pi}{4} \cdot (40^2 - 22^2) \cdot 25 \cdot 2 \right)^2}{2 \cdot 0.0130 \cdot \delta_{act}^2} (\delta_{act} + 0.096)} = \frac{271\,792}{\delta_{act}} \cdot \sqrt{\delta_{act} + 0.096}$$

<div style="text-align:right">DM I
Eq. (3.35)</div>

The load-displacement curve for the spring is shown in Fig. 9.12.
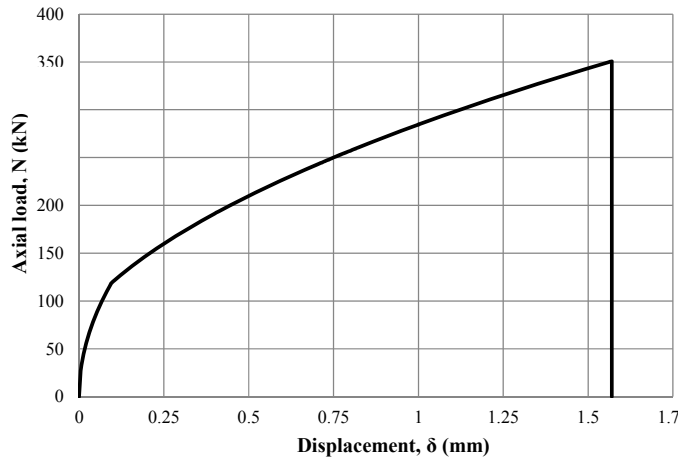
Fig. 9.12 Load-displacement behaviour of spring representing component P

3.6 Interaction of components Concrete and Stirrups

Once the concrete breakout occurs, the load is transferred to the stirrups and the load shared by concrete decreases with increasing displacement. The load carried by the combined component concrete + stirrups corresponding to any given displacement is given by Eq. (3.59) as

$$N_{act} = N_{Rd,c} + k_{c,de}\, \delta + \min\left(n_{re}\, d_{s,re}^2 \sqrt{\frac{\alpha_s\, f_{ck}\, \delta}{2}}; \; N_{Rd,s,re}; \; N_{Rd,b,re}\right)$$

<div style="text-align:right">DM I
Eq. (3.59)</div>

Hence, for a given displacement δ [mm] the load [kN] carried by combined concrete and stirrups is given as

$$N_{act} = 119.0 - 50.31 \cdot \delta + \min(448.023\sqrt{\delta}; \; 393.6; \; 149.6)$$

<div style="text-align:right">DM I
Eq. (3.59)</div>

The load-displacement curve for the spring is shown in Fig. 9.13.
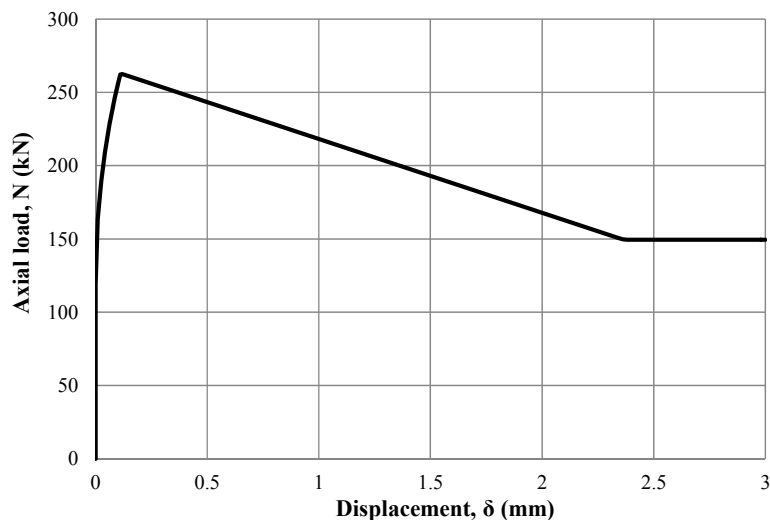
Fig. 9.13 Load-displacement behaviour of spring representing combined component concrete and stirrups

Interaction of all components:

The combined load-displacement behaviour combining all the components is displayed in Figure 9.14
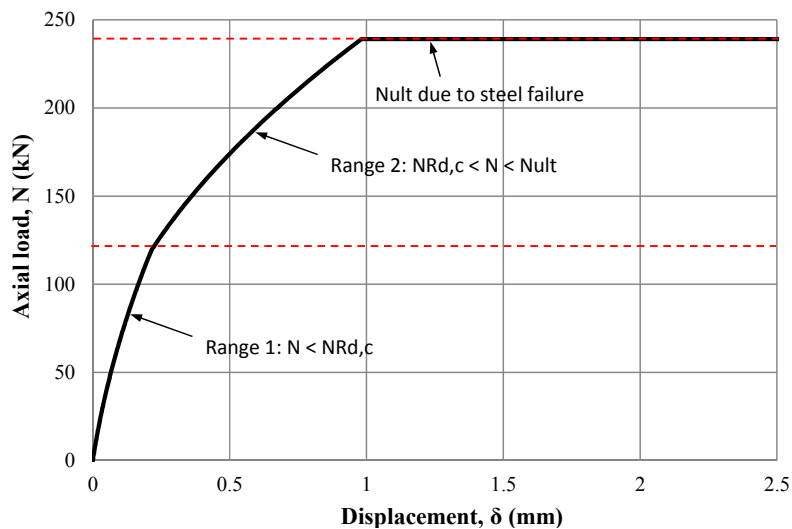
Fig. 9.144 Load-displacement behaviour obtained by combining all the components

Notes

- The resistance of the anchoring by the headed studs is limited by its threaded part, which represents a ductile behaviour.
- The resistance of the base plate is limited by the tension resistance of two headed studs M 22, 205.1 kN. Under the serviceability limit state SLS is required resistance of the concrete cone,119.0 kN. The elastic behaviour is expected till the 2/3 of the bending resistance of the base plate, which comply, $2/3 \cdot 417.4 = 314.3$ kN.
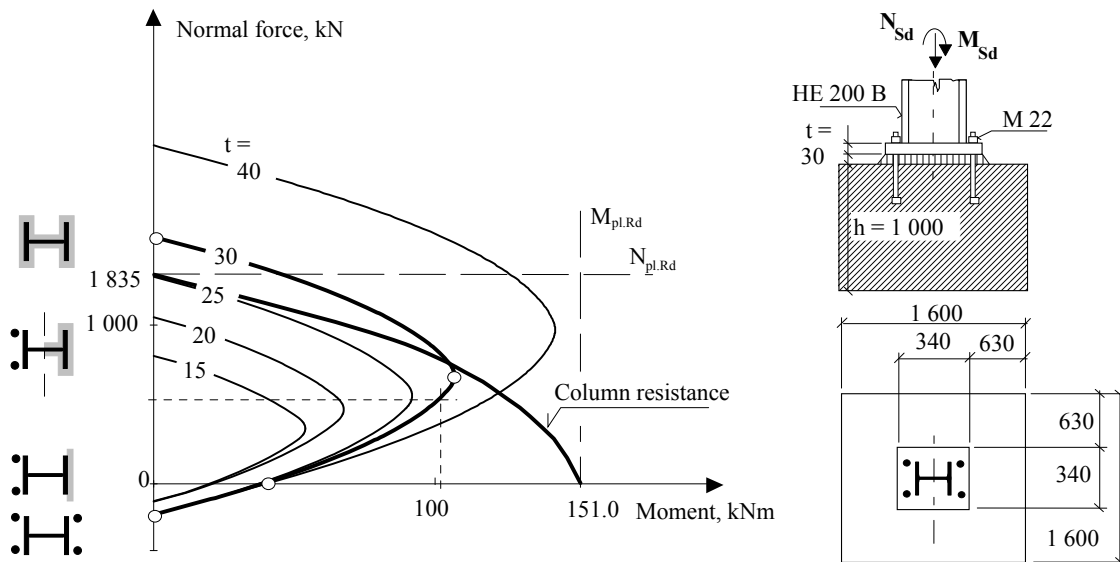
Fig. 9.155a The column base resistance is compared to the column resistance
for different base plate thickness

- The column base resistance is compared to the column resistance for different base plate thickness, see Fig. 9.15a. For plate P 30 are shown the major points of the diagram, e.g. the pure compression, the highest bending resistance, in case of coincidence of the neutral axis and the axis of symmetry of cross-section, the pure bending and the pure tension.
- A conservative simplification may be applied by placing the concrete reaction on the axes of the compressed flange only see Fig. 9.15b. This model is uneconomical and not often used for prediction of resistance, but applied for stiffness prediction.
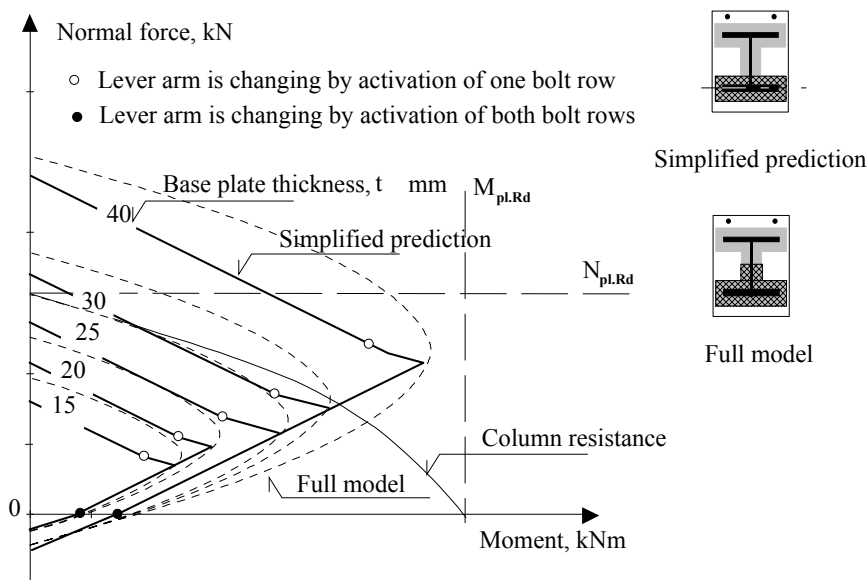
Fig. 9.16b The column base resistance calculated by the simplified prediction,
the contact force under the compressed flange only,
is compared to the application of the of the full contact area

- The stiffness of the anchoring by the headed studs corresponds to the expected stiffness calculated by a simplified conservative method based on the embedded effective length. The component stiffness coefficients for headed studs is estimated

as

$$k_b = 2.0 \cdot \frac{A_s}{L_b} = 2.0 \cdot \frac{A_s}{\min(h_{eff}; 8 \cdot d)} = 2.0 \cdot \frac{303}{150} = 4.04 \text{ mm}$$

and the deformation for acting force 300 kN is $\delta_{300} = \frac{F_{Ed}}{E \ k_b} = \frac{300}{210\,000 \cdot 4.04} = 0.35$ mm.

For headed stud is predicted, see Fig. 9.13, more precise value reached 0.22 mm.

- The classification of the column base according to its bending stiffness is evaluated in comparison to column bending stiffness. For column length $L_c = 4$ m and its cross-section HE 200 B is relative bending stiffness

$$\overline{S}_{j,ini} = S_{j,ini} \cdot \frac{L_c}{E_s \cdot I_c} = 21.981 \cdot 10^9 \cdot \frac{4000}{210\,000 \cdot 56.96 \cdot 10^6} = 7.53$$

EN1993-1-8

cl 6.3

The designed column base is sway for braced as well as non-sway frames because

$$\overline{S}_{j,ini} = 7.53 < 12 = \overline{S}_{j,ini,EC3,n}; \ \overline{S}_{j,ini} = 7.53 < 30 = \overline{S}_{j,ini,EC3,s}$$

- The influence of tolerances and size of welds, see EN 1090-2 and Chapter 8, is not covered in above calculation.

9.3 Stiffened base plate

Calculate the moment resistance of the column base shown in Fig. 9.17. Column HE 200 B is loaded by normal force F_{Sd} = 1 100 kN. Concrete block C16/20 of size 1 600 x 1 600 x 1000 mm is design for particular soil conditions. Base plate of thickness 30 mm, steel S235, γ_{Mc} = 1.50; γ_{M0} = 1.00; and γ_{M2} = 1.25.
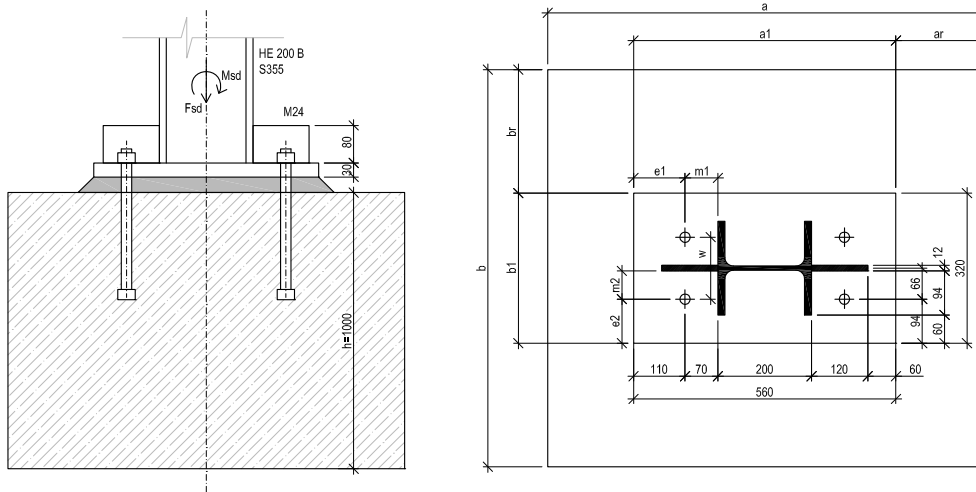
Fig. 9.17 Designed column base

Step 1 Component in tension

Resistance of component base plate in bending and headed studs in tension. Anchor stud lever arm, for fillet weld $a_{wf} = 6$ mm is

$$m = 70 - 0.8 \cdot a_{wf} \cdot \sqrt{2} = 70 - 0.8 \cdot 6 \cdot \sqrt{2} = 63.2 \text{ mm}$$

DM I
Fig. 4.4

The T-stub length, in base plates are the prying forces not taken into account, is:

$$l_{eff,1} = \min \begin{cases} 4\,m + 1.25\,e_1 = 4 \cdot 63.2 + 1.25 \cdot 110 = 390.3 \\ 2\pi\,m = 2\,\pi \cdot 63.2 = 397.1 \\ b \cdot 0.5 = 320 \cdot 0.5 = 160 \\ 2\,m + 0.625\,e_1 + 0.5\,w = 2 \cdot 63.2 + 0.625 \cdot 110 + 0{,}5 \cdot 132 = 261.2 \\ 2\,m + 0.625\,e_1 + e_2 = 2 \cdot 63.2 + 0.625 \cdot 110 + 94 = 289.2 \\ 2\,\pi\,m + 4\,e_2 = 2\,\pi \cdot 63.2 + 4 \cdot 94 = 773.1 \\ 2\,\pi\,m + 2\,w = 2\,\pi \cdot 63.2 + 2 \cdot 132 = 661.1 \end{cases}$$

EN1993-1-8
6.2.6.4

$$l_{eff,1} = 160 \text{ mm}$$

The effective length of headed studs L_b is taken as

DM I
Fig. 4.1

$$L_b = 8 \cdot d + t_g + t + \frac{t_n}{2} = 8 \cdot 24 + 30 + 30 + \frac{19}{2} = 261.5 \text{ mm}$$

The resistance of T - stub with two headed studs is

$$F_{T,1-2,Rd} = \frac{2\,L_{eff,1}\,t^2 f_y}{4\,m\,\gamma_{M0}} = \frac{2 \cdot 160 \cdot 30^2 \cdot 235}{4 \cdot 63.2 \cdot 1.00} = 267.7 \text{ kN}$$

The resistance is limited by tension resistance of two headed studs M 24 with the area in tension $A_s = 353$ mm

$$F_{T,3,Rd} = 2 \cdot B_{t,Rd} = 2 \cdot \frac{0.9 \cdot f_{ub} \cdot A_s}{\gamma_{M2}} = 2 \cdot \frac{0.9 \cdot 360 \cdot 353}{1.25} = 183.0 \text{ kN}$$

Step 2 Component in compression

The connection concentration factor is calculated as

$$a_1 = \min \begin{Bmatrix} a_1 + 2\,a_r = 560 + 2 \cdot 520 = 1\,600 \\ 3\,a_1 = 3 \cdot 560 = 1\,680 \\ a_1 + h = 560 + 1\,000 = 1\,560 \end{Bmatrix} = 1\,560 \text{ mm}$$

$$b_1 = \min \begin{Bmatrix} b_1 + 2b_r = 320 + 2 \cdot 640 = 1\,600 \\ 3\,b_1 = 3 \cdot 320 = 960 \\ b_1 + h = 320 + 1\,000 = 1\,320 \end{Bmatrix} = 960 \text{ mm}$$

and $a_1 = 1560 > a_1 = 560$ mm $\quad b_1 = 960 > b_1 = 320\,a_1$

The above condition is fulfilled and

$$k_j = \sqrt{\frac{a_1 \cdot b_1}{a \cdot b}} = \sqrt{\frac{1\,560 \cdot 960}{560 \cdot 320}} = 2.89$$

The grout is not influencing the concrete bearing resistance because

$$0.2 \cdot \min(a; b) = 0.2 \cdot \min(560;\ 320) = 64 \text{ mm} > 30 \text{ mm} = t_g$$

The concrete bearing resistance is calculated as

$$f_{jd} = \frac{2}{3} \cdot \frac{k_j \cdot f_{ck}}{\gamma_{Mc}} = \frac{2}{3} \cdot \frac{2.89 \cdot 16}{1.5} = 20.6 \text{ MPa}$$

From the force equilibrium in the vertical direction $F_{Sd} = A_{eff} \cdot f_{jd} - F_{t,Rd}$, is calculated the area of concrete in compression A_{eff} in case of the full resistance of tension part.

$$A_{eff} = \frac{F_{Sd} + F_{Rd,3}}{f_{jd}} = \frac{1\,100 \cdot 10^3 + 183 \cdot 10^3}{20.6} = 62\,282 \text{ mm}^2$$

The flexible base plate is transferred into a rigid plate of equivalent area. The width of the strip c around the column cross section, see Fig. 9.18, is calculated from

$$c = t \sqrt{\frac{f_y}{3 \cdot f_{jd} \cdot \gamma_{M0}}} = 30 \cdot \sqrt{\frac{235}{3 \cdot 20.6 \cdot 1.00}} = 58.5 \text{ mm}$$
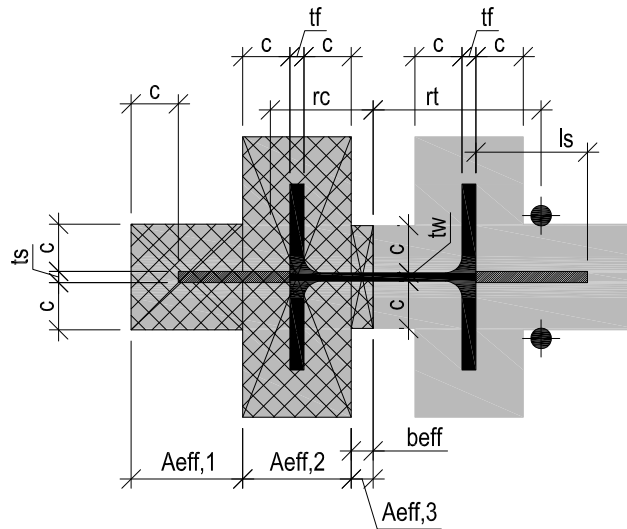
Fig. 9.18 The effective area under the base plate

The effective area is

$$A_{eff,1} = l_s \cdot (2c + t_s) = 120 \cdot (2 \cdot 58.5 + 12) = 15\ 480\ \text{mm}^2$$

$$A_{eff,2} = (2c + 200) \cdot (2c + t_f) = (2 \cdot 58.5 + 200) \cdot (2 \cdot 58.5 + 15) = 41\ 844\ \text{mm}^2$$

$$A_{eff,3} = A_{eff} - \left(A_{eff,1} + A_{eff,2}\right) = 62\ 282 - (15\ 480 + 41\ 844) = 4\ 958\ \text{mm}^2$$

The active effective width is calculated from known area in compression

$$b_{eff} = \frac{A_{eff,3}}{2\,c + t_w} = \frac{4\ 958}{2 \cdot 58.5 + 9} = 39.3\ \text{mm}$$

Step 3 Assembly for resistance

The gravity centre of effective area

$$x_t = \frac{A_{eff,1} \cdot x_{t1} + A_{eff,2} \cdot x_{t2} + A_{eff,3} \cdot x_{t3}}{A_{eff}}$$

$$= \frac{15\ 480 \cdot \frac{l_s}{2} + 41\ 844 \cdot \left(l_s + \frac{2c + t_f}{2}\right) + 4\ 958 \cdot \left(l_s + 2c + t_f + \frac{b_{eff}}{2}\right)}{62\ 282}$$

$$= \frac{15\ 480 \cdot 60 + 41\ 844 \cdot \left(120 + \frac{2 \cdot 58.5 + 15}{2}\right) + 4\ 958 \cdot \left(120 + 2 \cdot 58.5 + 15 + \frac{39.3}{2}\right)}{62\ 282}$$

$$= 161.5\ \text{mm}$$

The lever arm of concrete to the column axes of symmetry is calculated as

$$r_c = \frac{h_c}{2} + 120 + c + \left(b_{eff} - \frac{53}{2}\right) - x_t = \frac{200}{2} + 120 + 58.5 + (39.3 - 26.5) - 161.5 =$$

124

$= 129.8$ mm

The lever arm of concrete to the column axes of symmetry is calculated as

$$r_t = \frac{h_c}{2} + 70 + (\frac{53}{2} - b_{eff}) = 170 + (26.5 - 39.3) = 157.2 \text{ mm}$$

Moment resistance of column base is

$$M_{Rd} = F_{T,3,Rd} \cdot r_t + A_{eff} \cdot f_{jd} \cdot r_c$$

$$M_{Rd} = 183 \cdot 10^3 \cdot 157.2 + 62\,282 \cdot 20.6 \cdot 129.8 = 195.3 \text{ kNm}$$

Under acting normal force $N_{Sd} = 1\,100$ kN is the moment resistance

$$M_{Rd} = 195.3 \text{ kNm}$$

Step 4 Resistance of the end of column

The design resistance in poor compression is

$$N_{pl,Rd} = \frac{A \cdot f_y}{\gamma_{M0}} = \frac{(A_{HE200B} + 2 \cdot l_s \cdot t_s) \cdot 235}{1.00} = \frac{(7\,808 + 2 \cdot 120 \cdot 12) \cdot 235}{1.00} = 2\,511.7 \text{ kN}$$

$$> N_{Rd} = 1\,100 \text{ kN}$$

and column bending resistance

$$M_{pl,Rd} = \frac{W_{pl} \cdot f_{yk}}{\gamma_{M0}}$$

$$W_{pl} = W_{pl,s} + W_{pl,HEB} = 2 \cdot l_s \cdot t_s \cdot z_s + 642.5 \cdot 10^3 = 2 \cdot 12 \cdot 120 \cdot 160 + 642.5 \cdot 10^3 =$$

$$= 1\,103.3 \cdot 10^3 \text{ mm}^3$$

$$M_{pl,Rd} = \frac{W_{pl} \cdot f_{yk}}{\gamma_{M0}} = \frac{1\,103.3 \cdot 10^3 \cdot 235}{1.00} = 259.3 \text{ kNm}$$

The interaction of normal force reduces moment resistance

$$M_{Ny,Rd} = M_{pl,Rd} \frac{1 - \frac{N_{Sd}}{N_{pl,Rd}}}{1 - 0.5 \frac{A - 2\,b\,t_f}{A}} = 259.3 \cdot \frac{1 - \frac{1\,100}{2\,511.7}}{1 - 0.5 \frac{7\,808 - 2 \cdot 200 \cdot 15}{7\,808}} = 164.8 \text{ kNm}$$

The column base is designed on acting force even for column resistance.

Note

The resistance of the base plate is limited by the tension resistance of two headed studs M 24; 183.0 kN. The elastic behaviour is expected till the 2/3 of the bending resistance of the base plate; $2/3 \cdot 267.7 = 178.5$ kN, which comply for the bending moment at SLS about $195.3 \cdot 178.5/183.0$ kNm.

9.4   Column base with anchor plate

Evaluate the resistance of the column base shown in Fig. 9.19 using component method. The Column HE 200 B is loaded by the normal force F_{Ed} = 45 kN and by the bending moment M_{Ed} = 20 kNm. The concrete block designed for the particular soil conditions is made out of concrete strength C30/37 and has dimensions of 1600 x 1600 x 1000 mm. The base plate thickness is 30 mm and the anchor plate 10 mm. The steel grade is S355 and the safety factors are considered as γ_{Mc} = 1.50; γ_{M0} = 1.00 and γ_{M2} = 1.25.
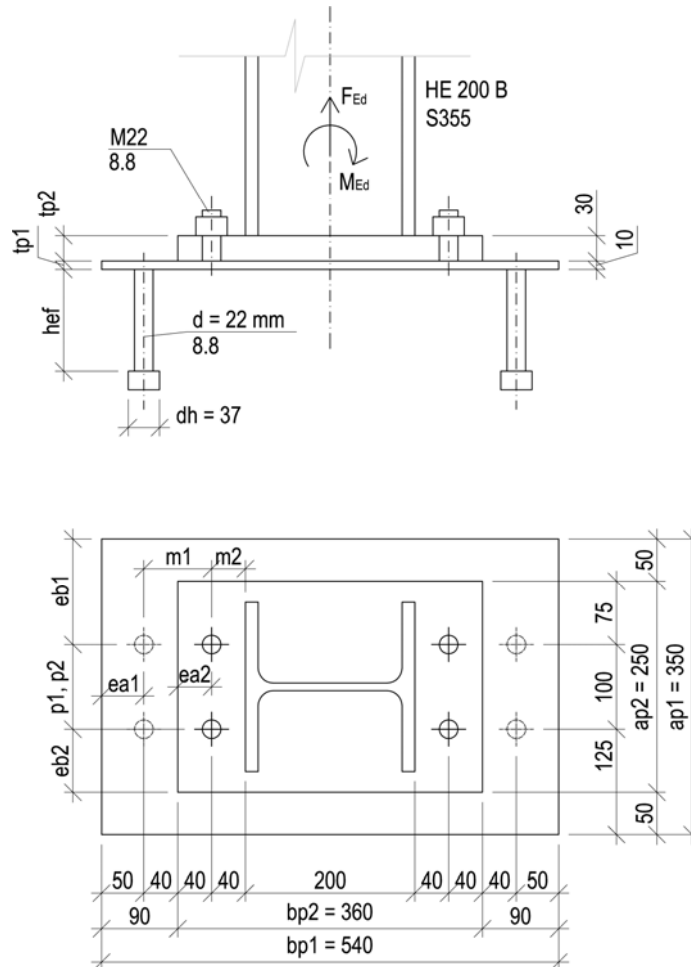
Fig. 9.19 Designed column base with anchor plate

Procedure

The calculation follows the Component method procedure for the column bases:

1 Components in tension
    1.1. Threaded studs in tension
    1.2. Punching of the anchor plate under threaded studs
    1.3. Base plate in bending
    1.4. Threaded studs in shear and bearing
    1.5. Headed studs in tension
    1.6. Punching of the anchor plate above the headed studs

Step 1 Components in tension

<u>Step 1.1 Threaded studs in tension</u>

The resistance of the component threaded studs in tension, with d = 22 mm, strength 8.8, f_{ub} = 800 N/mm², with number of studs is n = 2, area of one stud is A_s = 303 mm² and coefficient k_2 = 0.9, is

$$F'_{t,Rd,2} = \frac{n \cdot k_2 \cdot A_s \cdot f_{ub}}{\gamma_{M2}} = \frac{2 \cdot 0.9 \cdot 303 \cdot 800}{1.25} = 349.1 \text{ kN}$$

EN1993-1-8

Tab. 3.41

The resistance of one stud is 174.5 kN.

<u>Step 1.2 Punching of the anchor plate under threaded studs</u>

The resistance in punching of the anchor plate, for f_u = 510 MPa and the effective width of studs weld a_w = 1 mm, is

$$F_{p,Rd,V} = \frac{n \cdot A_v \cdot f_{uk}}{\sqrt{3} \cdot \gamma_{M2}} = \frac{n \cdot t_{p1} \cdot l_{v,eff,1} \cdot f_{uk}}{\sqrt{3} \cdot \gamma_{M2}} = \frac{n \cdot t_{p1} \cdot 2\,\pi \cdot \left(a_w + \frac{d_{stud}}{2}\right) \cdot f_{uk}}{\sqrt{3} \cdot \gamma_{M2}} =$$

$$= \frac{2 \cdot 10 \cdot 2\pi \cdot \left(1 + \frac{22}{2}\right) \cdot 510}{\sqrt{3} \cdot 1.25} = 355.2 \text{ kN}$$

The resistance of one stud is 177.6 kN.

Step 1.3 Base plate in bending

The base plate has thickness t_{p2} = 30 mm, width a_{p2} = 250 mm, yield strength f_{yk} = 355 N/mm², m_2 = 33.2 mm, e_{a2} = 40 mm, e_{b2} = 75 mm, and p_2 = 100 mm, see in Fig. 9.18. Headed stud lever arm for fillet weld a_{wf} = 6 mm is

$$m = 40 - 0.8 \cdot a_{wf} \cdot \sqrt{2} = 40 - 0.8 \cdot 6 \cdot \sqrt{2} = 33.2 \text{ mm}$$

The T-stub length, in base plate are the prying forces not taken into account, is

$$l_{eff,2} = \min \begin{cases} 4\,m + 1.25\,e_a = 4 \cdot 33.2 + 1.25 \cdot 40 = 182.9 \\ 2\,\pi\,m = 2\,\pi \cdot 33.2 = 208.7 \\ b \cdot 0.5 = 250 \cdot 0.5 = 125.0 \\ 2\,m + 0.625\,e_a + 0.5\,p = 2 \cdot 33.2 + 0.625 \cdot 40 + 0.5 \cdot 100 = 141.4 \\ 2\,m + 0.625\,e_a + e_b = 2 \cdot 33,2 + 0.625 \cdot 40 + 75 = 166.4 \\ 2\,\pi\,m + 4\,e_b = 2\pi \cdot 33.2 + 4 \cdot 75 = 508.7 \\ 2\,\pi\,m + 2\,p = 2\,\pi \cdot 33.2 + 2 \cdot 100 = 408.7 \end{cases}$$

$$l_{eff,2} = 125 \text{ mm}$$

Resistance of rigid plate T-stub in bending is verified for three possible failure modes

Mode 1

$$F_{T,1,Rd,2} = \frac{4 \cdot l_{eff,2} \cdot m_{pl,1,Rd,2}}{m} = \frac{4 \cdot l_{eff,2} \cdot \frac{t_{p,2}^2 \cdot f_{yk}}{4 \cdot \gamma_{M0}}}{m} = \frac{4 \cdot 125 \cdot \frac{30^2 \cdot 355}{4 \cdot 1.0}}{33.2} = 1\,202.5 \text{ kN}$$

Mode 2

$$F_{T,2,Rd,2} = \frac{2 \cdot l_{eff,2} \cdot m_{pl,2,Rd,2} + \sum F_{t,Rd} \cdot n}{m + n} = \frac{2 \cdot l_{eff,2} \cdot \frac{t_{p,2}^2 \cdot f_{yk}}{4 \cdot \gamma_{M0}} + \sum F_{t,Rd} \cdot n}{m + n} =$$

$$= \frac{2 \cdot 125 \cdot \frac{30^2 \cdot 355}{4 \cdot 1.0} + 349 \cdot 10^3 \cdot 40}{33.2 + 40} = 463.5 \text{ kN}$$

Mode 3

$$\sum F_{t,Rd} = \min(F'_{t,Rd}; \; F_{p,Rd,V}) = \min(349.1; 355.2) = 349.1 \text{ kN}$$

$$F_{T,3,Rd,2} = \sum F_{t,Rd} = 349.1 \text{ kN}$$

Decisive is Mode 3 with failure in threaded studs in tension $F_{t,3,Rd}$ = 349.1 kN.

Step 1.4 Threaded studs in shear and bearing

Threaded studs have diameter d = 22 mm, d_0 = 24 mm, base plate thickness t_{p2} = 30 mm, coefficient e_1 = 40 mm, e_2 = 75 mm, tensile strength f_u = 510 N/mm², f_{ub} = 800 N/mm², area of one stud A_s = 303 mm²; α_v = 0.6; γ_{M2} = 1.25 see in Fig. 9.18.

$$F_{v,Rd} = \frac{n \cdot \alpha_v \cdot f_{ub} \cdot A_s}{\gamma_{M2}} = \frac{2 \cdot 0.6 \cdot 800 \cdot \pi \cdot \left(\frac{22}{2}\right)^2}{1.25} = 291.9 \text{ kN}$$

The resistance of one stud is 146.0 kN.

$$F_{b,Rd,2} = \frac{n \cdot k_1 \cdot \alpha_b \cdot f_u \cdot d \cdot t}{\gamma_{M2}} = \frac{2 \cdot 2.5 \cdot 0.56 \cdot 510 \cdot 22 \cdot 30}{1.25} = 754.0 \text{ kN}$$

The resistance of one stud is 377.0 kN.

where

$$k_1 = \min\left\{2.8 \frac{e_2}{d_0} - 1.7; 2.5\right\} = \min\left\{2.8 \frac{75}{24} - 1.7; 2.5\right\} = \min\{7.05; 2.5\} = 2.5$$

$$\alpha_b = \min\left\{\frac{f_{ub}}{f_u}; 1.0; \frac{e_1}{3d_0}\right\} = \min\left\{\frac{800}{510}; 1.0; \frac{40}{3 \cdot 24}\right\} = \min\{1.57; 1.0; 0.56\} = 0.56$$

Step 1.5 Headed studs in tension

The resistance of headed studs in tension, of diameter d = 22 mm and material 8.8, with tensile strength f_{ub} = 800 N/mm², two studs n = 2 and coefficient k_2 = 0.9; is

$$F'_{t,Rd} = \frac{n \cdot k_2 \cdot A_s \cdot f_{ub}}{\gamma_{M2}} = \frac{2 \cdot 0.9 \cdot \pi \cdot \left(\frac{22}{2}\right)^2 \cdot 800}{1.25} = 437.9 \text{ kN}$$

The resistance of one stud is 219.0 kN.

Step 1.6 Punching of the anchor plate above the headed studs

The resistance in punching of the anchor plate, for $f_u = 510$ N/mm^2 and the effective width of studs weld $a_w = 1$ mm, is

$$F_{p,Rd,V} = \frac{n \cdot A_v \cdot f_{uk}}{\sqrt{3} \cdot \gamma_{M2}} = \frac{n \cdot t_{p1} \cdot l_{v,eff,1} \cdot f_{uk}}{\sqrt{3} \cdot \gamma_{M2}} = \frac{n \cdot t_{p1} \cdot 2 \, \pi \cdot \left(a_w + \frac{d_{stud}}{2}\right) \cdot f_{uk}}{\sqrt{3} \cdot \gamma_{M2}} =$$

$$= \frac{2 \cdot 10 \cdot 2\pi \cdot \left(1 + \frac{22}{2}\right) \cdot 510}{\sqrt{3} \cdot 1.25} = 355.2 \text{ kN}$$

The resistance of one headed stud is 177.6 kN.

Step 1.7 Concrete cone failure without reinforcement

The resistance of concrete cone failure without reinforcement, for the concrete block made out of concrete strength C30/37, $f_{ck} = 30$ N/mm^2, $k_1 = 12.7$; and length of headed studs $h_{ef} = 200$ mm, is

$$N_{Rd} = N_{Rk,c}^0 \cdot \psi_{A,N} \cdot \psi_{s,N} \cdot \psi_{re,N} / \gamma_{Mc}$$

$$N_{Rk,c}^0 = k_1 \cdot h_{ef}^{1.5} \cdot f_{ck}^{0.5} = 12.7 \cdot 200^{1.5} \cdot 30^{0.5} \text{ N} = 196.8 \text{ kN}$$

$$\psi_{A,N} = \frac{A_{c,N}}{A_{c,N}^0} = \frac{420\,000}{360\,000} = 1.17$$

$$A_{c,N}^0 = s_{cr,N}^2 = \left(2 \, c_{cr,N}\right)^2 = \left(2 \, (1.5 \cdot h_{ef})\right)^2 = \left(2(1.5 \cdot 200)\right)^2 = 360\,000 \text{ mm}^2$$

$$A_{c,N} = \left((1.5 \cdot h_{ef}) \cdot 2\right) \cdot (1.5 \cdot h_{ef} + p + 1.5 \cdot h_{ef}) =$$

$$= \left((1.5 \cdot 200) \cdot 2\right) \cdot (1.5 \cdot 200 + 100 + 1.5 \cdot 200) = 420\,000 \text{ mm}^2$$

Since maximum edge distance is $c < c_{cr} = 1.5 \, h_{ef} = 300$ mm and $\psi_{s,N} = 1.0$

There is no closely spaced reinforcement and $\psi_{re,N} = 1.0$

$$N_{Rk,c} = 196.8 \cdot 1.17 \cdot 1.0 \cdot 1.0 = 230.3 \text{ kN}$$

$$N_{Rd,c} = \frac{N_{Rk,c}}{\gamma_{Mc}} = \frac{230.3}{1.5} = 153.5 \text{ kN}$$

Step 1.8 Concrete cone failure with reinforcement

For concrete cone failure with reinforcement, with diameter of headed studs d = 22 mm and diameter of stirrups $d_s = 8$ mm, is factor for support of reinforcement

$$\psi_{supp} = 2.5 - \frac{x}{h_{ef}} = 2.5 - \frac{\frac{d}{2} + d_{s,a} + \frac{d_{s,t}}{\tan 35°}}{h_{ef}} = 2.5 - \frac{\frac{d}{2} + \left(5 \cdot \frac{d_s}{2} - \frac{d}{2}\right) + \frac{\left(\frac{d_s}{2} + 10\right)}{\tan 35°}}{h_{ef}} =$$

$$= 2.5 - \frac{\frac{22}{2} + \left(5 \cdot \frac{8}{2} - \frac{22}{2}\right) + \frac{\left(\frac{8}{2} + 10\right)}{\tan 35°}}{200} = 2.3$$

and resistance

$$N_{Rd,max} = \frac{\psi_{supp} \cdot N_{Rk,c}}{\gamma_{Mc}} = \frac{2.3 \cdot 230.2}{1.5} = 353.0 \text{ kN}$$

with

$$k_{c,de} = \alpha_c \cdot \sqrt{f_{ck} \cdot h_{ef}} \cdot \psi_{A,N} \cdot \psi_{s,N} \cdot \psi_{re,N} = -537 \cdot \sqrt{30 \cdot 200} \cdot 1.17 \cdot 1.0 \cdot 1.0 =$$

$$= -48.7 \text{ kN/mm}$$

where
α_c = -537 is factor of component concrete break out in tension

Yielding of reinforcement will occur for

$$N_{Rd,1} = N_{Rd,s,re} + N_{Rd,c} + \delta_{Rd,s} \cdot k_{c,de} =$$

$$= A_{s,re} \cdot \frac{f_{yk,s}}{\gamma_{Ms}} + N_{Rd,c} + \frac{2 \cdot N_{Rd,s,re}^2}{\alpha_s \cdot f_{ck} \cdot d_{s,re}^4 \cdot (n \cdot n_{re})^2} \cdot k_{c,de} =$$

$$= n \cdot n_{re} \cdot \pi \cdot \left(\frac{d_{s,re}^2}{4}\right) \cdot \frac{f_{yk,s}}{\gamma_{Ms}} + N_{Rd,c} + \frac{2 \cdot \left(n \cdot n_{re} \cdot \pi \cdot \left(\frac{d_{s,re}^2}{4}\right) \cdot \frac{f_{yk,s}}{\gamma_{Ms}}\right)^2}{\alpha_s \cdot f_{ck} \cdot d_{s,re}^4 \cdot (n \cdot n_{re})^2} \cdot k_{c,de} =$$

$$= 2 \cdot 4 \cdot \pi \cdot \left(\frac{8^2}{4}\right) \cdot \frac{500}{1.15} + 153.5 + \frac{2 \cdot \left(2 \cdot 4 \cdot \pi \cdot \left(\frac{8^2}{4}\right) \cdot \frac{500}{1.15}\right)^2}{12100 \cdot 30 \cdot 8^4 \cdot (2 \cdot 4)^2} \cdot (-48.7) =$$

$$= 174.8 + 153.5 + 0.642 \cdot (-48.7) = 297.0 \text{ kN}$$

where
α_s = 12 100   is factor of the component stirrups
n_{re} = 4   is total number of legs of shafts
$N_{Rd,s,re}$ is design tension resistance of the stirrups for tension failure [N]
$d_{s,re}$ = 8 mm   is nominal diameter of the stirrup
d_p = 25 mm   is the covering
$f_{yk,s}$ = 500 N/mm²   is design yield strength of the stirrups
γ_{Ms} = 1.15   is the partial safety factor
l_1 is anchorage length [mm]

Anchorage failure resistance of the of reinforcement is

$$N_{Rd,2} = N_{Rd,b,re} + N_{Rd,c} + \delta_{Rd,b} \cdot k_{c,de} = \sum n_{re} \cdot l_1 \cdot \pi \cdot d_{s,re} \cdot \frac{f_{bd}}{\alpha} + N_{Rd,c} + \delta_{Rd,b} \cdot k_{c,de} =$$

$$= n \cdot n_{re} \cdot l_1 \cdot \pi \cdot d_s \cdot \frac{f_{bd}}{\alpha} + N_{Rd,c} + \frac{2 \cdot N_{Rd,b,re}^2}{\alpha_s \cdot f_{ck} \cdot d_{s,re}^4 \cdot n_{re}^2} \cdot k_{c,de} =$$

$$= n \cdot n_{re} \cdot \left(h_{ef} - d_p - d_{s,t} - \frac{d_{s,a}}{1.5} \right) \cdot \pi \cdot d_s \cdot \frac{2.25 \cdot \eta_1 \cdot \eta_2 \cdot f_{ctk;0,05}}{\alpha \cdot \gamma_{Mc}} + N_{Rd,c}$$

$$+ \frac{2 \cdot \left(n \cdot n_{re} \cdot l_1 \cdot \pi \cdot d_s \cdot \frac{f_{bd}}{\alpha} \right)^2}{\alpha_s \cdot f_{ck} \cdot d_{s,re}^4 \cdot n_{re}^2} k_{c,de} =$$

$$= n \cdot n_{re} \cdot \left(h_{ef} - d_p - \left(\frac{d_s}{2} + 10 \right) - \frac{\left(5 \cdot \frac{d_s}{2} - \frac{d}{2} \right)}{1.5} \right) \cdot \pi \cdot d_s \cdot \frac{2.25 \cdot \eta_1 \cdot \eta_2 \cdot f_{ctk;0,05}}{\alpha \cdot \gamma_{Mc}} + N_{Rd,c} +$$

$$\frac{2 \cdot \left(n \cdot n_{re} \cdot \left(h_{ef} - d_p - \left(\frac{d_s}{2} + 10 \right) - \frac{\left(5 \cdot \frac{d_s}{2} - \frac{d}{2} \right)}{1.5} \right) \cdot \pi \cdot d_s \cdot \frac{2.25 \cdot \eta_1 \cdot \eta_2 \cdot f_{ctk;0,05}}{\alpha \cdot \gamma_{Mc}} \right)^2}{\alpha_s \cdot f_{ck} \cdot d_{s,re}^4 \cdot n_{re}^2} \cdot k_{c,de} =$$

$$= 2 \cdot 4 \cdot \left(200 - 25 - \left(\frac{8}{2} + 10 \right) - \frac{\left(5 \cdot \frac{8}{2} - \frac{22}{2} \right)}{1.5} \right) \cdot \pi \cdot 8 \cdot \frac{2.25 \cdot 1.0 \cdot 1.0 \cdot 2.0}{0.49 \cdot 1.5} + 153.5$$

$$+ \frac{2 \cdot \left(2 \cdot 4 \cdot \left(200 - 25 - \left(\frac{8}{2} + 10 \right) - \frac{\left(5 \cdot \frac{8}{2} - \frac{22}{2} \right)}{1.5} \right) \cdot \pi \cdot 8 \cdot \frac{2.25 \cdot 1.0 \cdot 1.0 \cdot 2.0}{0.49 \cdot 1.5} \right)^2}{12100 \cdot 30 \cdot 8^4 \cdot (2 \cdot 4)^2} \cdot (-48.7)$$

$$= 190.8 + 153.5 + 0.765 \cdot (-48.7) = 307.0 \text{ kN}$$

where

l_1 is anchorage length [mm]

d_s is diameter of stirrups [mm]

$\alpha = 0.7 \cdot 0.7 = 0.49$ is factor for hook effect and large concrete cover

f_{bd} is for C30/37 grade concrete is $2.25 \cdot \frac{2.0}{1.5} \cdot 1.0 \cdot 1.0 = 3.0$ N/mm²

$\eta_1 = 1.0$ is coefficient of bond conditions for vertical stirrups

             and 0.7 for horizontal stirrups

$\eta_2 = 1.0$ is coefficient of bond conditions for dimension ≤ 32 mm

             and $(132 - d_s)/100$ for dimension ≥ 32 mm

The resistance of concrete cone failure with reinforcement is

$$\min\left(N_{Rd,max}; N_{Rd,1}; N_{Rd,2} \right) = \min(353.0; 297.0; 307.0) = 297.0 \text{ kN}$$

<u>Step 1.9 Pull-out failure of headed studs</u>

The resistance of pull-out failure of headed studs, with diameter of stud d = 22 mm, diameter of stud's head d_h = 37 mm, concrete C30/37 with compressive strength f_{ck} = 30 N/mm² and the characteristic ultimate bearing pressure at ultimate limit state under the headed of stud $p_{uk} = 12 \cdot f_{ck}$ N/mm², is

$$N_{Rk,p} = n \cdot p_{uk} \cdot A_h = n \cdot 12 \cdot f_{ck} \cdot \frac{\pi}{4} \cdot \left(d_h^2 - d^2\right) = 2 \cdot 12 \cdot 30 \cdot \frac{\pi}{4} \cdot (37^2 - 22^2) = 500.5 \text{ kN}$$

$$N_{Rd,p} = \frac{N_{Rk,p}}{\gamma_{Mc}} = \frac{500.5}{1.5} = 333.7 \text{ kN}$$

The resistance of one stud is 166.8 kN

<u>Step 1.10 T stub of the anchor plate in bending</u>

The resistance of component T-stub of the anchor plate in bending has thickness t_{p1} = 10 mm, yield strength f_{yk} = 355 N/mm², distance of threaded and headed stud m_1 = 80 mm, e_{a1} = 50 mm, e_{b1} = 125 mm and p_1 = 100 mm, see in Fig. 9.18.

Due to small thickness of the anchor plate are the prying forces for evaluation of the effective length of T stub taken into account as

Resistance of anchor plate T-stub in tension is verified for three failure modes, see in Fig. 9.19. For effective length of the T stub

$$l_{eff,1} = \min \begin{cases} 4\ m_1 + 1.25\ e_{a1} = 4 \cdot 80 + 1.25 \cdot 50 = 382.5 \\ 2\ \pi\ m_1 = 2\ \pi \cdot 80 = 502.7 \\ 5\ n_1\ d_1 \cdot 0.5 = 220 \cdot 0.5 = 110.0 \\ 2\ m_1 + 0.625\ e_{a1} + 0.5\ p_1 = 2 \cdot 80 + 0.625 \cdot 50 + 0.5 \cdot 100 = 241.3 \\ 2\ m_1\ + 0.625\ e_{a1} + e_{b1} = 2 \cdot 80 + 0.625 \cdot 50 + 93.8 = 285.0 \\ \pi\ m_1 + 2\ e_{b1} = \pi \cdot 80 + 2 \cdot 93.8 = 721.4 \\ \pi\ m_1 + p_1 = \ \pi \cdot 80 + 100 = 351.3 \end{cases}$$

$l_{eff,1} = 110.0$ mm
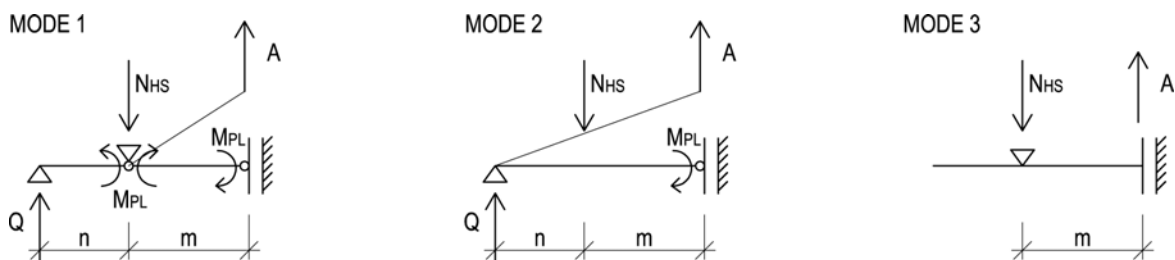
Fig. 9.19 T-stub in tension and forces in the individual failure modes

Mode 1

$$F_{T,1,Rd,ap} = \frac{4 \cdot l_{eff,1} \cdot m_{pl,Rd,1}}{m} = \frac{4 \cdot l_{eff,1} \cdot \frac{t_{p,1}^2 \cdot f_{yk}}{4 \cdot \gamma_{M0}}}{m} = \frac{4 \cdot 110.0 \cdot \frac{10^2 \cdot 355}{4 \cdot 1.0}}{80} = 48.8 \text{ kN}$$

Mode 2

$$F_{T,2,Rd,ap} = \frac{2 \cdot l_{eff,1} \cdot m_{pl,2,Rd,2} + \sum F_{t,Rd} \cdot n}{m + n} = \frac{2 \cdot l_{eff,1} \cdot \frac{t_{p,1}^2 \cdot f_{yk}}{4 \cdot \gamma_{M0}} + \sum F_{t,Rd} \cdot n}{m + n} =$$

$$= \frac{2 \cdot 110.0 \cdot \frac{10^2 \cdot 355}{4 \cdot 1.0} + 297.0 \cdot 10^3 \cdot 50}{80 + 50} = 129.1 \text{ kN}$$

Mode 3

$$\sum F_{t,Rd} = \min\left(F'_{t,Rd1}; F_{p,Rd,V,1}; N_{Rd,1}; N_{Rd,p}\right) = \min(437.9; 355.2; 297.0; 333.7)$$

$$= 297.0 \text{ kN}$$

$$F_{T,3,Rd,ap} = \sum F_{t,Rd} = 297.0 \text{ kN}$$

Mode 1 is decisive for the thin plate, 48.8 kN, see in Fig. 9.20.
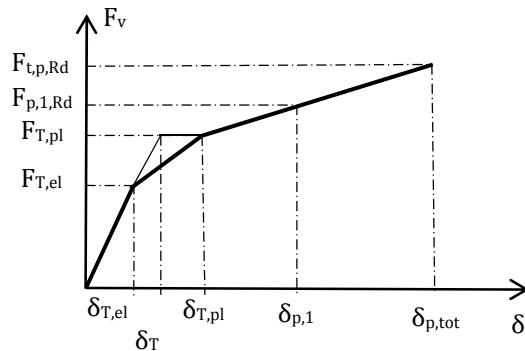
Fig. 9.20 Vertical forces F_v and vertical deformation δ of T stub

Step 1.11 Anchor plate in tension

The anchor plate in tension resistance is

$$F_{t,apRd} = A_{ap,1} \cdot \frac{f_{yk}}{\gamma_{M0}} = t_{p,1} \cdot b_{ap,eff} \cdot \frac{f_{yk}}{\gamma_{M0}} = 10 \cdot 2 \cdot \left(22 + 2 \cdot \sqrt{2} \cdot 1\right) \cdot \frac{355}{1.0} = 176.3 \text{ kN}$$

where

$$b_{ap,eff} = n_1 \cdot \left(d_1 + 2 \cdot \sqrt{2} \cdot a_w\right)$$

studs weld effective thickness a_w = 1 mm

Step 1.12 Headed studs in shear

The shear resistance of headed studs, with material 8.8, strength f_{ub} = 800 N/mm², α_v = 0.6; γ_{M2} = 1.25; is

$$F_{v,Rd} = \frac{n \cdot \alpha_v \cdot f_{ub} \cdot A_s}{\gamma_{M2}} = \frac{2 \cdot 0.6 \cdot 800 \cdot \pi \cdot \left(\frac{22}{2}\right)^2}{1.25} = 291.9 \text{ kN}$$

EN1993-1-8

Tab. 3.41

The resistance of one stud is 146.0 kN.

Step 1.13 Pry-out failure of headed stud

The resistance in pry-out failure of headed studs for is

$$V_{Rd,CP} = 2 \cdot N_{Rd,c} = 2 \cdot 153.5 = 307.0 \text{ kN}$$

DM I

Ch. 3.2

Step 1.14 Reduction of resistance in the vertical/horizontal direction

For the calculation of plastic deformation is used model of continues beam with three plastic hinges at supports and under applied load, see in Fig. 9.21.
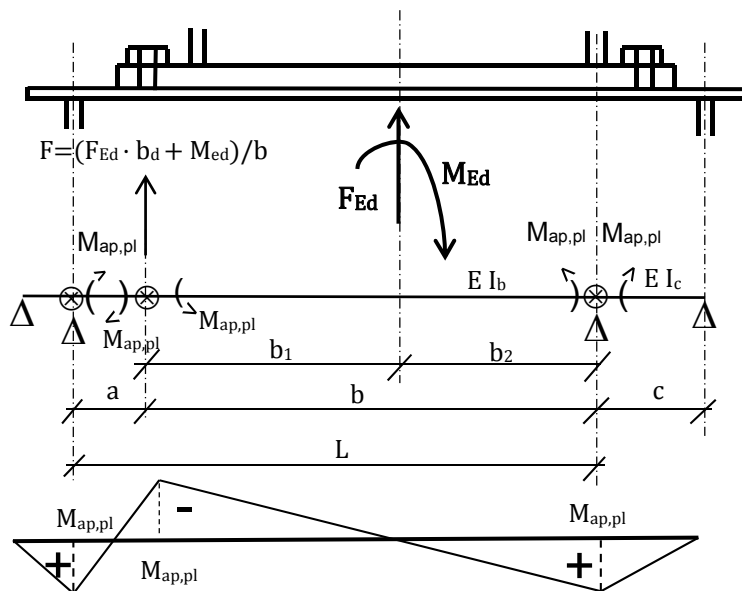
Fig. 9.21 Model of continues beam with three plastic hinges

$$A = \min\left(F_{T,1,Rd,1}; \; F_{T,2,Rd,1}; \; F_{T,3,Rd,1}\right) = \min\left(48.8; \; 126.1; 296.7\right) = 48.8 \text{ kN}$$

DM I

Ch. 4.4

$$Q = \frac{l_{eff,1} \cdot m_{pl,Rd,1}}{n} \cdot 2 = \frac{l_{eff,1} \cdot \dfrac{t_{p,1}^2 \cdot f_{yk}}{4 \cdot \gamma_{M0}}}{n} \cdot 2 = \frac{110.0 \cdot \dfrac{10^2 \cdot 355}{4 \cdot 1.0}}{50} \cdot 2 = 39.1 \text{ kN}$$

$$N_{HS,T} = A + Q = 48.8 + 39.1 = 87.9 \text{ kN}$$

Plastic deformation is calculated, see Fig. 9.21, for moment resistance

$$M_{pl} = \frac{b_{p1} \cdot t_{p1}^2}{4} \cdot \frac{f_{yk}}{\gamma_{M0}} = \frac{350 \cdot 10^2}{4} \cdot \frac{355}{1} = 3.1 \text{ kNm}$$

$$I_c = \frac{1}{12} \cdot b_{p1} \cdot t_{p1}^3 = \frac{1}{12} \cdot 350 \cdot 10^3 = 29.2 \cdot 10^3 \text{ mm}^4; \ I_b = \infty$$

$$\delta_T = \frac{1}{E \, I_b} \cdot \frac{1}{6} \cdot b^2 \cdot M_{pl} + \frac{1}{E \, I_c} \cdot \frac{1}{3} \cdot b \cdot c \cdot M_{pl} =$$

$$= \frac{1}{210\,000 \cdot \infty} \cdot \frac{1}{6} \cdot 232.5^2 \cdot 3106 + \frac{1}{210\,000 \cdot 29.2} \cdot \frac{1}{3} \cdot 232.5 \cdot 127.5 \cdot 3106 = 0 + 5.2$$

$$= 5.2 \text{ mm}$$

with distance between threaded stud and headed stud $a = 80$ mm as

$$\delta_{T,pl} = 1.48 \, \delta_T = 7.8 \text{ mm}$$

$$\delta_{p,tot} = \delta_{T,pl} + \sqrt{a_{ap}^2 - a^2} = \sqrt{(a + \Delta a)^2 - a^2} = \delta_{T,pl} + \sqrt{\left(a + \frac{a \cdot F_{p,Rd}}{t_{p1} \cdot b_{ap,eff} \cdot E}\right)^2 - a^2} =$$

$$= \delta_{T,pl} + \sqrt{\left(a + \frac{a \cdot \dfrac{A \cdot f_{y,p}}{\gamma_{M0}}}{t_{p1} \cdot b_{ap,eff} \cdot E}\right)^2 - a^2} = \delta_{T,pl} + \sqrt{\left(a + \frac{a \cdot \dfrac{t_{p1} \cdot b_{p,eff} \cdot f_{y,p}}{\gamma_{M0}}}{t_{p1} \cdot b_{ap,eff} \cdot E}\right)^2 - a^2} =$$

DM I
Eq. (4.43)

$$= 7.8 + \sqrt{\left(80 + \frac{80 \cdot 8.88 \cdot \dfrac{355}{1.0}}{210 \cdot 10^3}\right)^2 - 80^2} = 13.9 \text{ mm}$$

For the plastic deformation at resistance of the anchor plate punching under the threaded studs $F_{p,Rd}$ = 176.28 kN and $F_{p,Rd,V} = A + \dfrac{F_{p,Rd} \cdot \delta_{p,tot}}{(a + \Delta a)} = 79.0$ kN

The acting horizontal force for this deformation is

$$F_{p,Rd,H} = \frac{F_{t,p,Rd} \cdot a}{\delta_{p,tot}} = \frac{79.0 \cdot 80}{13.9} = 454.3 \text{ kN}$$

For the resistance of headed studs in shear V_{Rd} = 291.9 kN is assumed the linear proportion between the axial and horizontal forces, see in Fig. 9.22. The resistance in tension is calculated as

$$F_{p,1,Rd} = F_{T,pl} + \frac{F_{t,p,Rd} - F_{T,pl}}{F_{p,Rd,H}} \cdot V_{Rd} = 48.8 + \frac{79.0 - 48.8}{454.3} \cdot 291.9 = 68.2 \text{ kN}$$

and deformation for $F_{p,1,Rd}$ = 68.2 kN, see in Fig. 9.20, is

$$\delta_{p,1} = \delta_{T,pl} + \frac{F_{p,1,Rd} - F_{T,pl}}{F_{t,p,Rd} - F_{T,pl}} \cdot \delta_{p,tot} = 7.8 + \frac{68.2 - 48.8}{79.0 - 48.8} \cdot 13.9 = 16.7 \text{ mm}$$
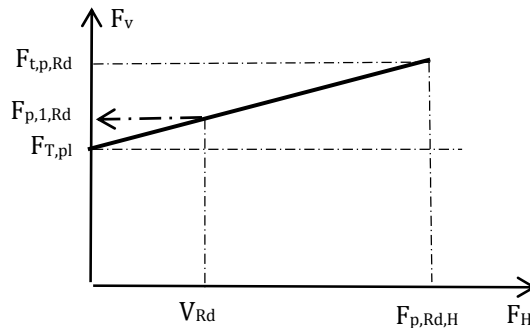
Fig. 9.22 Acting vertical F_v and horizontal F_H forces to the anchor plate

The acting force in headed studs in case of the membrane action in the anchor plate

$$N_{HS,1} = A + Q = 68.2 + 39.1 = 107.3 \text{ kN}$$

Step 1.15 Interaction in shear and tension for treaded and headed studs

For the threaded studs is the interaction in shear and tension

$$\frac{F_{v,Ed}}{F_{v,Rd}} + \frac{F_{t,Ed}}{1.4 \cdot F_{t,Rd}} \leq 1$$

$$\frac{291.9}{291.9} + \frac{(107.3 - 48.8) \cdot \left(\frac{220 + 165.9}{140 + 165.9}\right)}{1.4 \cdot 349.1} \leq 1.00$$

1.15 is not ≤ 1

For the headed studs is the interaction in shear and tension

$$\frac{F_{v,Ed}}{F_{v,Rd}} + \frac{F_{t,Ed}}{1.4 \cdot F_{t,Rd}} \leq 1$$

$$\frac{291.9}{291.9} + \frac{107.3 - 48.8}{1.4 \cdot 437.9} \leq 1$$

1.10 is not ≤ 1

For anchoring of headed stud in concrete is the interaction in shear and tension

$$\left(\frac{F_{v,Ed}}{F_{v,Rd}}\right)^{\frac{3}{2}} + \left(\frac{F_{t,Ed}}{F_{t,Rd}}\right)^{\frac{3}{2}} \leq 1$$

$$\left(\frac{291.9}{306.1}\right)^{\frac{3}{2}} + \left(\frac{107.3 - 48.8}{296.7}\right)^{\frac{3}{2}} \leq 1$$

1.02 is not ≤ 1

The full capacity in shear is not achieve due to headed stud resistance. By reducing the acting forces to 80 % it is for interaction of the threaded stud

$$\frac{233.5}{291.9} + \frac{(107.3 - 48.8) \cdot \left(\frac{220 + 165.9}{140 + 165.9}\right)}{1.4 \cdot 349.1} \leq 1$$

$0.95 \leq 1$

and for the headed stud

$$\frac{233.5}{291.9} + \frac{107.3 - 48.8}{1.4 \cdot 437.9} \leq 1$$

$0.86 \leq 1$

and for anchoring of headed stud in concrete

$$\left(\frac{233.5}{306.1}\right)^{\frac{3}{2}} + \left(\frac{107.3 - 48.8}{296.7}\right)^{\frac{3}{2}} \leq 1$$

$0.71 \leq 1$

Step 2 Component in compression

The component base plate in bending and concrete block in compression is calculated for the strength of the concrete block, C30/37, $f_{ck} = 30$ N/mm², and $\gamma_{Mc} = 1.5$.

The connection concentration factor is

$$a_1 = \min \begin{cases} a_1 + 2\,a_r = 250 + 2 \cdot 675 = 1\,600 \\ 3\,a_1 = 3 \cdot 250 = 750 \\ a_1 + h = 250 + 1\,000 = 1\,250 \end{cases} = 750 \text{ mm}$$

$$b_1 = \min \begin{cases} b_1 + 2b_r = 360 + 2 \cdot 620 = 1\,600 \\ 3\,b_1 = 3 \cdot 360 = 1080 \\ b_1 + h = 360 + 1\,000 = 1\,360 \end{cases} = 1\,080 \text{ mm}$$

and $a_1 = 750 > a_1 = 250$ mm $\quad b_1 = 1080 > b_1 = 360$ mm

The above condition is fulfilled and

$$k_j = \sqrt{\frac{a_1 \cdot b_1}{a \cdot b}} = \sqrt{\frac{1\,080 \cdot 750}{250 \cdot 360}} = 3.00$$

The concrete bearing resistance is calculated as

$$f_{jd} = \frac{2}{3} \cdot \frac{k_j \cdot f_{ck}}{\gamma_{Mc}} = \frac{2}{3} \cdot \frac{3.00 \cdot 30}{1.5} = 40.0 \text{ N/mm}^2$$

From the force equilibrium in the vertical direction $F_{Sd} = A_{eff} \cdot f_{jd} - F_{t,Rd}$, is calculated the area of concrete in compression A_{eff} in case of the full resistance of tension part

$$A_{eff} = \frac{F_{Sd} + F_{Rd,3}}{f_{jd}} = \frac{-45 \cdot 10^3 + 107.3 \cdot 10^3}{40.0} = 1\,557 \text{ mm}^2$$

The flexible base plate is transferred into a rigid plate of equivalent area. The width of the strip c around the column cross section, see Fig. 9.23a, is calculated from

$$c = (t_{p1} + t_{p2}) \sqrt{\frac{f_y}{3 \cdot f_{jd} \cdot \gamma_{M0}}} = (30 + 10) \cdot \sqrt{\frac{355}{3 \cdot 40.0 \cdot 1.00}} = 68.8 \text{ mm}$$
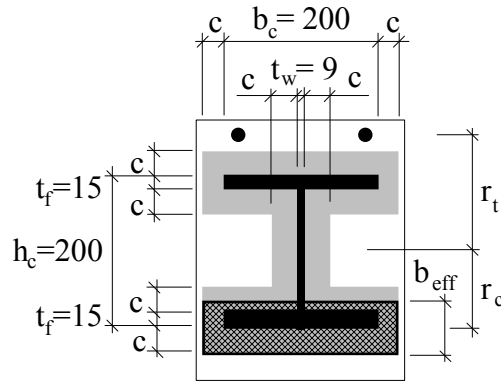
Fig. 9.23a The effective area under the base plate

Step 3 Assembly for resistance

Step 3.1 Column base resistance

The active effective width is calculated as

$$b_{eff} = \frac{A_{eff}}{a_{p2} + 2\,t_{p1}} = \frac{1\,557}{270} = 5.8\text{ mm} < t_f + 2\,c = 15 + 2 \cdot 68.8 = 152.6\text{ mm}$$

The lever arm of concrete to the column axes of symmetry, see Fig. 9.23b, is calculated as

$$r_c = \frac{h_c}{2} + c - \frac{b_{eff}}{2} = \frac{200}{2} + 68.8 - \frac{5.8}{2} = 165.9\text{ mm}$$

The moment resistance of the column base is $M_{Rd} = F_{T,min} \cdot r_t + A_{eff} \cdot f_{jd} \cdot r_c$

$$F_{T,min} = 107.3 \cdot \frac{220 + 165.9}{140 + 165.9} = 135.3\text{ kN}$$

$$M_{Rd} = 135.3 \cdot 10^3 \cdot 140 + 1\,557 \cdot 40 \cdot 165.9 = 29.3\text{ kNm}$$

Under acting normal force $N_{Sd} = -45$ kN the moment resistance in bending is $M_{Rd} = 29.3$ kNm.
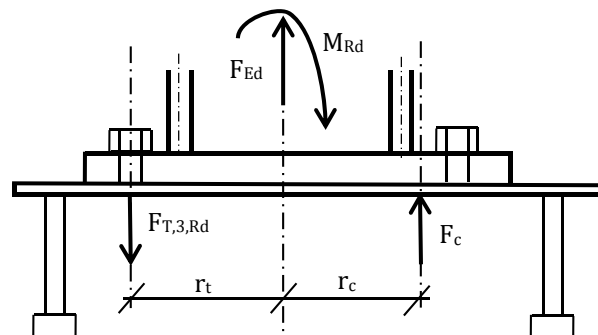
Fig. 9.23b The lever arm of concrete and threaded stud to the column axes

3.2 End of column resistance

The design resistance in poor compression is

$$N_{pl,Rd} = \frac{A \cdot f_y}{\gamma_{M0}} = \frac{7808 \cdot 355}{1.00} = 2\,772 \cdot 10^3\,N > N_{Rd} = -45\,kN$$

The column bending resistance

$$M_{pl,Rd} = \frac{W_{pl} \cdot f_{yk}}{\gamma_{M0}} = \frac{642.5 \cdot 10^3 \cdot 355}{1.00} = 228.1\,kNm$$

The interaction of normal force reduces moment resistance (this interaction is valid for compression load only)

$$M_{Ny,Rd} = M_{pl,Rd} \frac{1 - \frac{N_{Sd}}{N_{pl,Rd}}}{1 - 0.5\frac{A - 2\,b\,t_f}{A}} = 228.1 \cdot \frac{1 - \frac{0}{2772}}{1 - 0.5\frac{7\,808 - 2 \cdot 200 \cdot 15}{7\,808}} = 258.0\,kNm$$

$$M_{Ny,Rd} = 228.1\,kNm$$

The column base is designed on acting force only not for column resistance.

Step 3.3 Elastic resistance for Serviceability limit state

The resistance of the base plate is limited by the T stub resistance, 48.8 kN. The elastic-plastic behaviour is expected by reaching the bending resistance of the anchor plate T stub; 87.9 kN, which comply for the bending moment at SLS as 22.7 kNm.

Step 4 Connection stiffness

4.1 Component´s stiffness

The component´s stiffness coefficients are calculated as in Worked example 9.2. The additional component is the anchor plate in bending and in tension and the component threaded stud. In compression are transferring the forces both plates under the column, the base and anchor plates.

The component base plate in bending and the threaded studs in tension

The stiffness coefficient for the threaded stud is assumed as

$$k_{b2} = 2.0 \cdot \frac{A_s}{L_b} = 2.0 \cdot \frac{303}{49.5} = 12.2\,mm$$

The component stiffness coefficients for base plate is calculated as

$$k_{p2} = \frac{0.425 \cdot L_{beff} \cdot t^3}{m^3} = \frac{0.425 \cdot 125 \cdot 30^3}{33.2^3} = 39.2\,mm$$

Component base and anchor plates and concrete block in compression
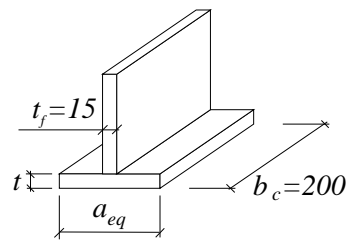
Fig. 9.23c The T stub in compression

The stiffness coefficient for concrete block in compression, see Fig. 9.23c, is calculated for $a_{eq} = t_f + 2.5\,t = 15 + 2.5 \cdot 40 = 115$ mm

where thickness $t = t_1 + t_2$ = 10 + 30 = 40 mm

$$k_c = \frac{E_c}{1.275 \cdot E_s} \cdot \sqrt{a_{eq} \cdot b_c} = \frac{33\,000}{1.275 \cdot 210\,000} \cdot \sqrt{115 \cdot 200} = 18.7 \text{ mm}$$

<div align="right">EN1993-1-8
Tab. 6.11</div>

Component anchor plate in bending and in tension

The component stiffness coefficients for anchor plate is calculated from the bending of the anchor plate as

$$k_{p1} = \frac{0.85 \cdot L_{beff} \cdot t^3}{m^3} = \frac{0.85 \cdot 110.0 \cdot 10^3}{(80 - 2 \cdot \frac{22}{2})^3} = 0.5 \text{ mm}$$

<div align="right">EN1993-1-8
Tab. 6.11</div>

Component headed stud in tension

The component stiffness coefficients for headed studs is calculated as

$$k_{b1} = \frac{n \cdot A_{s,nom}}{L_b} = \frac{2 \cdot \frac{\pi \cdot 22^2}{4}}{8 \cdot 22} = 4.3 \text{ mm}$$

<div align="right">EN1993-1-8
Tab. 6.11</div>

4.2 Assembly for stiffness

The coefficients of the initial stiffness in elongation are assembled to rotational stiffness as in Worked example 9.2. The additional component is the anchor plate in bending and in tension only.
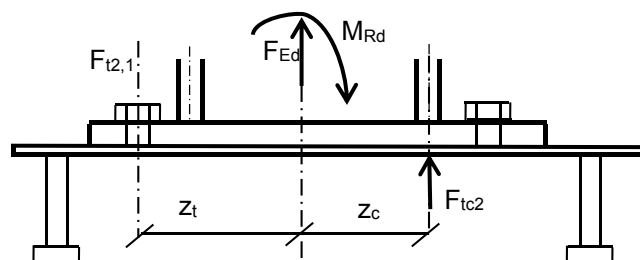
Fig. 9.23d The lever arm in tension and compression

The lever arm of components, see Fig. 9.23d, in tension z_t and in compression z_c to the column base neutral axes are

$$z_t = \frac{h_c}{2} + e_c = \frac{200}{2} + 40 = 140 \text{ mm}$$

$$z_c = \frac{h_c}{2} - \frac{t_f}{2} = \frac{200}{2} - \frac{15}{2} = 92.5 \text{ mm}$$

The stiffness of tension part, studs, T stubs and concrete parts, is calculated from the stiffness coefficient for base plate and threaded studs

$$k_{t2} = \frac{1}{\frac{1}{k_{b2}} + \frac{1}{k_{p2}}} = \frac{1}{\frac{1}{12.2} + \frac{1}{39.2}} = 9.33 \text{ mm}$$

from the stiffness coefficient for anchor plate and headed studs

$$k_{t1} = \frac{1}{\frac{1}{k_{p1}} + \frac{1}{k_{b1}}} = \frac{1}{\frac{1}{0.5} + \frac{1}{4.3}} = 0.43 \text{ mm}$$

based on eccentricity

$$k_{t1,eff} = \frac{z}{z + 80} \cdot k_{t1} = \frac{232.5}{312.5} \cdot 0.43 = 0.32 \text{ mm}$$

where

$$z = z_t + z_c = 140 + 92.5 = 232.5 \text{ mm}$$

with the effective stiffness coefficient in tension in position of threaded stud

$$k_t = \frac{1}{\frac{1}{k_{t1}} + \frac{1}{k_{t2}}} = \frac{1}{\frac{1}{0.32} + \frac{1}{9.33}} = 0.31 \text{ mm}$$

For the calculation of the initial stiffness of the column base the lever arm is evaluated

$$z = 232.5 \text{ mm} \qquad \text{and}$$

$$a = \frac{k_c \cdot z_c - k_t \cdot z_t}{k_c + k_t} = \frac{18.7 \cdot 92.5 - 0.31 \cdot 140}{18.7 + 0.31} = 88.7 \text{ mm}$$

The bending stiffness is calculated for particular constant eccentricity

$$e = \frac{M_{Rd}}{F_{Sd}} = \frac{20 \cdot 10^6}{45 \cdot 10^3} = 444 \text{ mm}$$

as

$$S_{j,ini} = \frac{e}{e+a} \cdot \frac{E_S \cdot z^2}{\mu \sum_i \frac{1}{k_i}} = \frac{444}{444 + 88.7} \cdot \frac{210\,000 \cdot 232.5^2}{1 \cdot \left(\frac{1}{0.31} + \frac{1}{18.7}\right)} = 2\,888 \cdot 10^6 \text{ Nmm/rad}$$

$$= 2\,888 \text{ kNm/rad}$$

Summary

Moment rotational diagram at Fig. 9.23e sums up the behaviour of column base with anchor plate for loading with constant eccentricity.
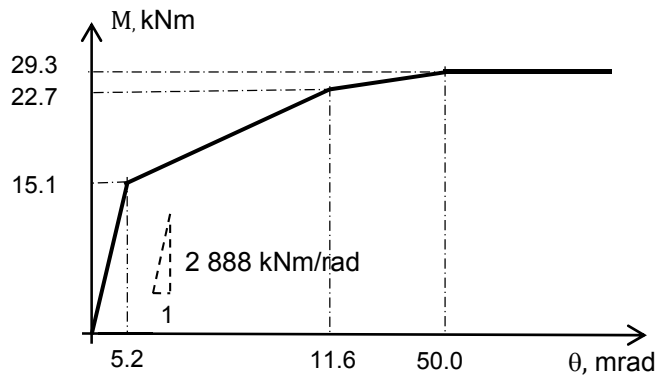
Fig. 9.23e Moment rotational diagram of column base with anchor plate
for loading with constant eccentricity

144

9.5 Simple steel to concrete joint

In this example the calculation of a simple steel-to-concrete joint is demonstrated. A girder is connected to a concrete wall by a simple joint. The load capacity of the joint will be raised by the use of additional reinforcement. The example does only include the design calculation of the joint. The verification of the concrete wall is not included and the local failure of the concrete wall due to the tension force caused by the eccentricity of the shear load is not considered.

Overview about the system

In this example a steel platform is installed in an industrial building. The main building is made of concrete. The system consists of concrete walls and concrete girders. An extra platform is implemented in the building in order to gain supplementary storage room.

The platform consists of primary and secondary girders. The primary girders are made of HE400A and they are arranged in a grid of 4.00 m. On one side they are supported on the concrete wall, on the other side they are supported by a steel column. The concrete wall and the steel beam are connected by a pinned steel-to-concrete joint.
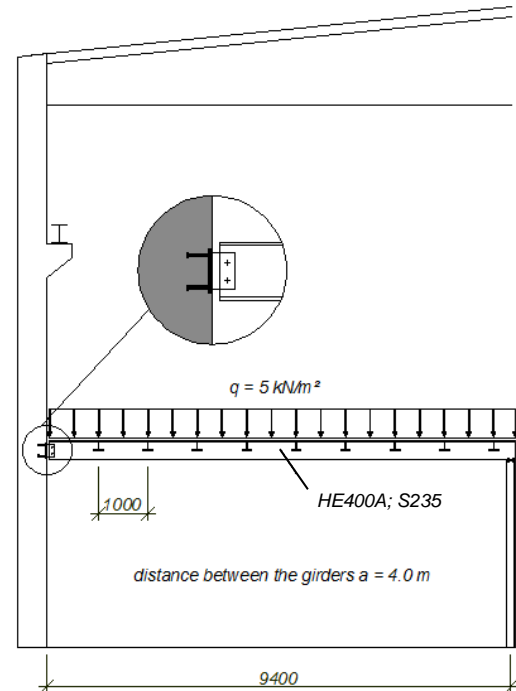
Fig. 9.24 Side view on structure

Structural system and design of the girder

The structural system of the primary girder is a simply supported beam with an effective length of 9.4 m. The cross section of the girder is HE400A. The girder carries load applied to a width a = 4.0 m which is the distance to the next girder, see Fig. 9.25
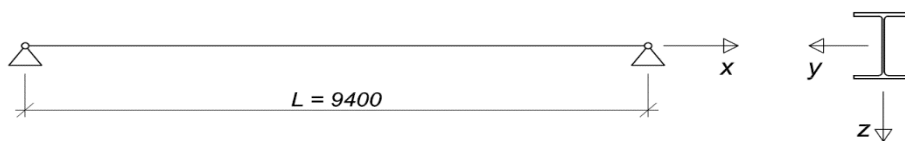
Fig. 9.25 structural system

Load on the girder

Self-weight of the girder with connection	2.0 kN/m
Floor and other girders	$4.0 \text{ m} \cdot 1.0 \frac{\text{kN}}{\text{m}^2} = 4.0 \text{ kN/m}$
Dead load	6.0 kN/m

Live load $\qquad$ $4.0 \text{ m} \cdot 5.0 \frac{\text{kN}}{\text{m}^2} = 20.0 \text{ kN/m}$

Design forces

Maximum shear load

$$V_{z,Ed} = 9.4 \text{ m} \cdot \frac{1.35 \cdot 6.0 \frac{\text{kN}}{\text{m}} + 1.5 \cdot 20.0 \frac{\text{kN}}{\text{m}}}{2} = 179 \text{ kN} \approx 180 \text{ kN}$$

Maximum bending moment

$$M_{y,Ed} = (9.4 \text{ m})^2 \cdot \frac{1.35 \cdot 6.0 \frac{\text{kN}}{\text{m}} + 1.5 \cdot 20.0 \frac{\text{kN}}{\text{m}}}{8} = 420 \text{ kNm}$$

Verification of the girder section

Next to the joint $\qquad$ $V_{z,Ed} = 180 \text{ kN} \leq V_{pl,z,Rd} = 777.8 \text{ kN}$

In the middle of the girder $\qquad$ $M_{y,Ed} = 420 \text{ kNm} \leq M_{pl,y,Rd} = 602.1 \text{ kNm}$

The girder is stabilized against lateral torsional buckling by the secondary girders, which have a distance of 1.0 m. Lateral torsional buckling is not examined in this example. The example only includes the design calculation of the joint. The verification of the concrete wall is not included.

Overview of the joint
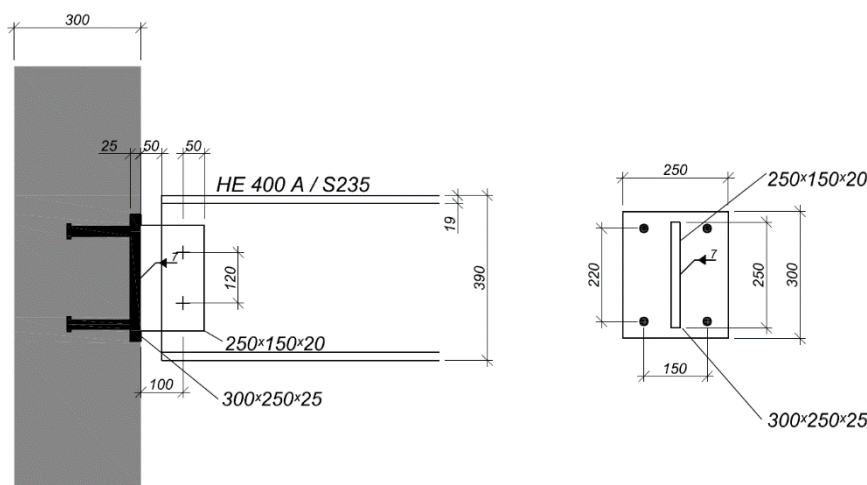
Fig. 9.26 Joint geometry
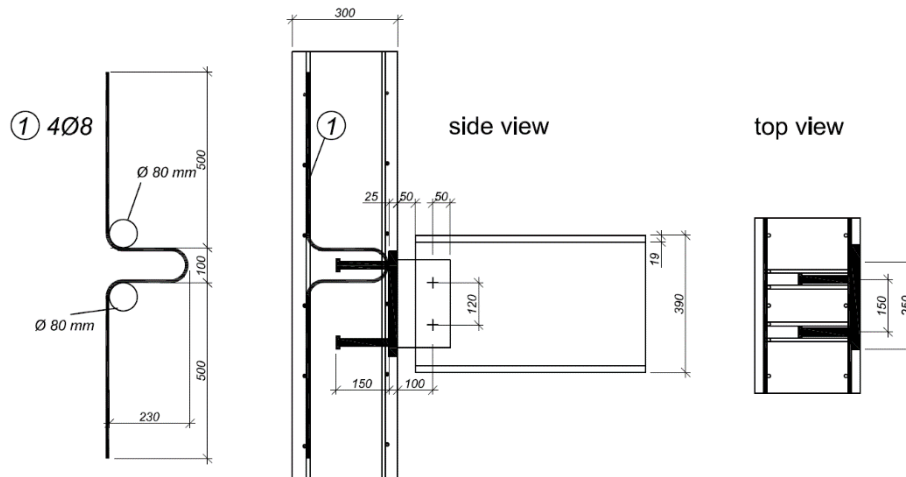
Fig. 9.27 Reinforcement

In the following an overview of the joint geometry is given.

Connected girder	HE400A, S235
Concrete	C30/37 ($f_{ck,cube}$ = 37 N/mm², cracked)
Stirrups	4 x 8 mm / B500A (two per headed stud)
Butt straps:	150 x 250 x 20 mm / S235
Anchor plate	300 x 250 x 25 mm / S235
Headed Studs	d = 22 mm
	h = 150 mm / S235J2 + C470
Bolt connection	2 x M24 10.9
Shear load of the joint	V_{Ed} =180 kN

Connection between the girder HE400A and the anchor plate

The small torsion moment caused by the eccentricity between the girder and the butt straps is transferred into the girder HE400A and from this primary girder to the secondary girders. The eccentric connection induces bending and shear stresses in the butt strap. In the following they are determined:

$$M_{Ed} = V_{Ed} \cdot 0.1 = 18 \text{ kNm}$$

$$\tau_V = 1.5 \cdot \frac{V_{Ed}}{A_V} = 1.5 \cdot \frac{180}{5000} = 54.0 \leq 135.6 \text{ N/mm}^2$$

$$\sigma = \frac{M_{Ed}}{W} = \frac{18}{\dfrac{250^2 \cdot 20}{6}} = 86.4 \leq 235.0 \text{ N/mm}^2$$

The maximum forces don`t appear at the same place.

Edge distances: $e_1 = 65 \text{ mm} > 1.2 \cdot d_0 = 1.2 \cdot 26 = 31.2 \text{ mm}$

$e_2 = 50 \text{ mm} > 1.2 \cdot d_0 = 1.2 \cdot 26 = 31.2 \text{ mm}$

$p_1 = 120 \text{ mm} > 2.2 \cdot d_0 = 2.2 \cdot 26 = 57.2 \text{ mm}$

Shear resistance of the bolts:

EN 3-1-8

Table 3.3

147

$$F_{v,Rd} = \alpha_V \cdot A_S \cdot \frac{f_{ub}}{\gamma_{M2}} = 0.6 \cdot 353 \cdot \frac{1000}{1.25} = 169.4 \text{ kN}$$

$$V_{Rd,1} = n_V \cdot F_{v,Rd} = 2 \cdot 169.4 = 338.8 \text{ kN}$$

Bearing resistance of the butt strap:

$$V_{Rd,2} = 286.8 \text{ kN}$$

$$F_{b,Rd} = \frac{k_1 \cdot \alpha_b \cdot f_u \cdot d \cdot t}{\gamma_{M2}} = \frac{2.5 \cdot 0.83 \cdot 360 \cdot 24 \cdot 20}{1.25} = 286.8 \text{ kN}$$

$$k_1 = \min\left[2.8\frac{e_2}{d_0} - 1.7; 1.4\frac{p_2}{d_0} - 1.7; 2.5\right] = \min[3.68; -; 2.5]$$

$$\alpha_b = \min\left[\frac{e_1}{3 \cdot d_0}; \frac{f_{ub}}{f_u}; 1.0\right] = \min[0.83; 2.78; 1.0]$$

Bearing resistance of the beam web:

$$V_{Rd,3} = 190.1 \text{ kN}$$

$$F_{b,Rd} = \frac{k_1 \cdot \alpha_b \cdot f_u \cdot d \cdot t}{\gamma_{M2}} = \frac{2.5 \cdot 1.0 \cdot 360 \cdot 24 \cdot 11}{1.25} = 190.1 \text{ kN}$$

$$k_1 = \min\left[2.8\frac{e_2}{d_0} - 1.7; 1.4\frac{p_2}{d_0} - 1.7; 2.5\right] = \min[3.68; -; 2.5]$$

$$\alpha_b = \min\left[\frac{e_1}{3 \cdot d_0}; \frac{f_{ub}}{f_u}; 1.0\right] = \min[-; 2.78; 1.0]$$

$$V_{Rd} = \min[V_{Rd,1}; V_{Rd,2}; V_{Rd,3}] = 190.1 \text{ kN} \geq V_{Ed} = 180 \text{ kN}$$

Welding of the butt straps to the anchor plate

A welding seam all around with $a_w = 7$ mm is assumed. Following stresses in the welding seam can be determined:

$$a_w = 2 \cdot 7 = 14 \text{ mm}$$

$$l_{eff} = 250 \text{ mm}$$

$$W_{el,w} = \frac{a_w \cdot l_{w,eff}^2}{6} = \frac{14 \cdot 250^2}{6} = 145.8 \cdot 10^3 \text{ mm}^2$$

$$\sigma_{w,Rd} = \frac{f_u}{\beta_w \cdot \gamma_{M2}} = \frac{360}{0.8 \cdot 1.25} = 360 \text{ N/mm}^2$$

Shear stresses caused by shear load and eccentricity:

$$\tau_{II} = \frac{V_{ED}}{2 \cdot a_w \cdot l_{w,eff}} = \frac{180}{2 \cdot 7 \cdot 250} = 51.4 \text{ N/mm}^2$$

$$\sigma_w = \frac{M_{Ed}}{W} = \frac{18}{145.8} = 123.5 \text{ N/mm}^2$$

$$\sigma_\perp = \tau_\perp = \sigma_w \cdot \sin 45° = 123.5 \cdot \sin 45° = 87.3 \leq \frac{0.9 \cdot f_u}{\gamma_{M2}} = 259.2 \text{ N/mm}^2$$

Interaction caused by bending and shear stresses:

$$\sigma_{w,Ed} = \sqrt{\sigma_\perp^2 + 3(\tau_\perp^2 + \tau_{II}^2)} = \sqrt{87.3^2 + 3(87.3^2 + 51.4^2)} = 195.0 \leq \sigma_{w,Rd} = 360 \text{ N/mm}^2$$

148

Design of the connection to the concrete

The anchor plate has the geometry 300 x 250 x 25 mm S235

Headed studs $d = 22$ mm

$h = 150$ mm S350 C470

Stirrups (for each headed stud) $4 \cdot 8$ mm B 500 A

The verification of the design resistance of the joint is described in a stepwise manner. The eccentricity e_v and the shear force V_{Ed} are known.

Step 1 Evaluation of the tension force caused by the shear load

If the joint is loaded in shear the anchor row on the non-loaded side of the anchor plate is subjected to tension. In a first step the tension load has to be calculated. Therefore the height of the compression area has to be assumed.

Shear load of the connection $V_{Ed} = 180$ kN

Resistance due to friction $V_f = C_{Ed} \cdot 0.2 = N_{Ed,2} \cdot 0.2$

Thickness plate $t_p = 25$ mm

Diameter anchor $d = 22$ mm

Eccentricity $e_v = 100$ mm

Calculation of $N_{Ed,2}$

$$N_{Ed,2} = \frac{V_{Ed} \cdot (e_v + d + t_p) - V_f \cdot d}{z}$$

$$N_{Ed,2} \cdot (1 + \frac{0.2 \cdot d}{z}) = \frac{V_{Ed} \cdot (e_v + d + t_p)}{z}$$

The height of the compression zone is estimated to $x_c = 20$ mm

With x_c the lever arm

$$z = 40 + 220 - \frac{x}{2} = 40 + 220 - \frac{20}{2} = 250 \text{ mm}$$

and

$$N_{Ed,2}(1 + \frac{0.2 \cdot 22}{250}) = \frac{V_{Ed} \cdot (100 + 22 + 25)}{250}$$

From this the tension force result $N_{Ed,2} = 104.0$ kN

Step 2 Verification of the geometry of the compression zone

The tension component of the joint $N_{Ed,2}$ forms a vertical equilibrium with the compression force C_{Ed} under the anchor plate on the loaded side. The next step of the calculation is to prove that the concrete resistance is sufficient for the compression force and that the assumption of the compression area was correct.

Calculation of the compression force

$$\sum N : C_{Ed} = N_{Ed,2} = 104.0 \text{ kN}$$

Height of the compression zone is

$$f_{cd} = f_{ck} \cdot \frac{\alpha}{\gamma_{Mc}} = 17 \text{ N/mm}^2$$

where $\alpha = 0.85$

The compression forces are causing a bending moment in the anchor plate. To make sure that the anchor plate is still elastic, only the part of the anchor plate is activated which is activated with elastic bending only.

Fig. 9.28 Effective with

$$b_{eff} = t_{bs} + 2 \cdot t_p \cdot \sqrt{\frac{f_y}{3 \cdot f_{jd} \cdot \gamma_{M0}}}$$

$$= 20 + 2 \cdot 25 \cdot \sqrt{\frac{235}{3 \cdot 17 \cdot 1.0}} = 127 \text{ mm}$$
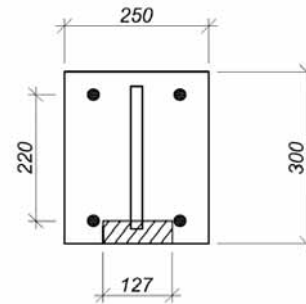
$$x_c = \frac{C_{Ed}}{b \cdot 3 \cdot f_{cd}} = \frac{104.0}{127 \cdot 3 \cdot 17} = 16 \text{ mm}$$

Instead of the regular width b of the anchor plate the effective width b_{eff} is used. The calculated $x_c = 16$ mm is smaller than the predicted value of $x_c = 20$ mm. That means that the lever arm was estimated slightly too small. This is on the safe side, so the calculation may be continued.

Step 3 Evaluation of the tension resistance

3.1 Steel failure of the fasteners

Calculation of the characteristic failure load of the headed studs on the non-loaded side:

$$N_{Rd,s} = n_a \cdot A_s \cdot \frac{f_{uk}}{\gamma_{Mp}} = 2 \cdot 380 \frac{470}{1.5} \cdot 10^{-3} = 238.1 \text{ kN}$$

where
Characteristic ultimate strength $\quad\quad\quad f_{uk} = 470 \text{ N/mm}^2$
Characteristic yield strength $\quad\quad\quad\quad f_{yk} = 350 \text{ N/mm}^2$
Number of headed studs in tension $\quad\quad n_a = 2$

Cross section area of one shaft $\quad\quad\quad A_s = \pi \cdot \frac{d^2}{4} = 380 \text{ mm}^2$

Partial safety factor $\quad\quad\quad\quad\quad\quad\quad \gamma_{Mp} = 1.2 \cdot \frac{f_{uk}}{f_{yk}} = 1.5$

3.2 Pull-out failure

If the concrete strength is too low or the load bearing area of the headed stud is too small, pull-out failure might occur.

$$N_{Rd,p} = n \cdot \frac{p_{uk}}{\gamma_{Mc}} \cdot A_h = n \cdot \frac{p_k \cdot f_{ck}}{\gamma_{Mc}} \cdot \frac{\pi}{4} \cdot \left(d_h^2 - d_{s,nom}^2\right) = 2 \cdot \frac{12 \cdot 30}{1.5} \cdot \frac{\pi}{4} \cdot (35^2 - 22^2) = 279.4 \text{ kN}$$

where
Factor considering the head pressing $\quad\quad p_k = 12 \cdot f_{ck}$
Partial safety factor $\quad\quad\quad\quad\quad\quad\quad \gamma_{Mc} = 1.5$

3.3 Concrete cone failure

A pure concrete cone failure should not occur because of the reinforcement, but this failure load has to be calculated so that the resistance may be combined with the resistance of the stirrups.

$$N_{Rd,c} = N_{Rk,c}^0 \cdot \Psi_{A,N} \cdot \Psi_{s,N} \cdot \Psi_{re,N}/\gamma_{Mc}$$

$$N_{Rk,c}^0 = k_1 \cdot h_{ef}^{1.5} \cdot f_{ck}^{0.5} = 12.7 \cdot 165^{1.5} \cdot 30^{0.5} = 147.4 \text{ kN}$$

$$\Psi_{A,N} = \frac{A_{c,N}}{A_{c,N}^0} = \frac{319\ 275}{245\ 025} = 1.3$$

$$A_{c,N}^0 = s_{cr,N}^2 = (2\ c_{cr,N})^2 = (2\ (1.5 \cdot h_{ef}))^2 = (2(1.5 \cdot 165))^2 = 245\ 025 \text{ mm}^2$$

$$N_{Rk,c} = 147.4 \cdot 1.3 \cdot 1.0 \cdot 1.0 = 191.6 \text{ kN}$$

$$N_{Rd,c} = \frac{N_{Rk,c}}{\gamma_{Mc}} = \frac{191.6}{1.5} = 127.7 \text{ kN}$$

where

Effective anchorage depth $\quad\quad\quad\quad\quad h_{ef} = h_n + t_{AP} - k = 165 \text{ mm}$

Factor for close edge $\quad\quad\quad\quad\quad\quad\quad \Psi_{s,N} = 1.0$

Factor for small reinforcement spacing $\quad \Psi_{re,N} = 1.0$

Actual projected area $\quad\quad\quad\quad\quad\quad A_{c,N} = (2 \cdot 1.5 \cdot h_{ef}) \cdot (2 \cdot 1.5 \cdot h_{ef} + s_1) =$
$$= (2 \cdot 1.5 \cdot 165) \cdot (2 \cdot 1.5 \cdot 165 + 150) = 319\ 275 \text{ mm}^2$$

Partial safety factor $\quad\quad\quad\quad\quad\quad\quad \gamma_{Mc} = 1.5$

3.4 Concrete cone failure with reinforcement

With reinforcement one of the three below described failure modes will occur.

3.5 Concrete failure

$$N_{Rk,cs} = \Psi_{supp} \cdot N_{Rk,u,c} = 2.26 \cdot 191.6 = 433.0 \text{ kN}$$

$$N_{Rd,cs} = \frac{N_{Rk,cs}}{\gamma_{Mc}} = \frac{433.0}{1.5} = 288.7 \text{ kN}$$

where

Factor for support of reinforcement $\quad\quad\quad \Psi_{supp} = 2.5 - \frac{x}{h_{ef}} = 2.26$

Distance between the anchor axis and the crack on the surface

$$x = \frac{d_{nom}}{2} + d_{s,a} + \frac{d_{s,t}}{\tan 35°} = 40 \text{ mm}$$

Distance of hanger reinforcement to the face of the anchor shaft

$$d_{s,a} = 5 \cdot \frac{d_s}{2} - \frac{d}{2} = 9 \text{ mm}$$

Distance axis of the reinforcement to the concrete surface

$$d_{s,t} = \frac{d_s}{2} + 10 = 14 \text{ mm}$$

Partial safety factor $\quad\quad \gamma_{Mc} = 1.5$

3.6 Yielding of reinforcement

$$N_{Rd,re,1} = N_{Rd,s,re} + N_{Rd,c} + \delta_{Rd,s,re} \cdot k_{c,de}$$
$$N_{Rd,re,1} = 174.8 + 127.7 + 0.642 \cdot -49.1 = 271.0 \text{ kN}$$

where
Normal force of hanger reinforcement

$$N_{Rd,s,re} = A_{s,y} \cdot \frac{f_{s,y,k}}{\gamma_{Ms}} = n_{re} \cdot \pi \cdot \left(\frac{d_{s,re}^2}{4}\right) \cdot \frac{f_{yk}}{\gamma_{Ms}} = 8 \cdot \pi \cdot \left(\frac{8^2}{4}\right) \cdot \frac{500}{1.15} = 174.8 \text{ kN}$$

Deformation of reinforcement at yielding

$$\delta_{Rds,re} = \frac{2 \cdot \left(A_{s,y} \cdot f_{s,yd}\right)^2}{\alpha_s \cdot f_{ck} \cdot d_{s,re}^4 \cdot (n \cdot n_{re})^2} = \frac{2 \cdot (174.8 \cdot 10^3)^2}{12100 \cdot 30 \cdot 8^4 \cdot (2 \cdot 4)^2} = 0.642 \text{ mm}$$

Stiffness concrete break out

$$k_{c,de} = \alpha_c \cdot \sqrt{f_{ck} \cdot h_{ef}} \cdot \psi_{A,N} \cdot \psi_{s,N} \cdot \psi_{re,N} = -537 \cdot \sqrt{30 \cdot 165} \cdot 1.3 \cdot 1.0 \cdot 1.0 = -49.1 \text{ kN/mm}$$

Partial safety factor $\quad \gamma_{Ms} = 1.15$

3.7 Anchorage failure of the reinforcement

$$N_{Rd,re,2} = N_{Rd,b,re} + N_{Rd,c} + \delta_{Rd,b,re} \cdot k_{c,de}$$

$$N_{Rd,re,2} = 147.7 + 127.7 + 0.459 \cdot -49.1 = 252.8 \text{ kN}$$

where

Anchorage force of all hanger legs

$$N_{Rd,b,re} = n \cdot n_{re} \cdot l_1 \cdot \pi \cdot d_s \cdot \frac{f_{bd}}{\alpha}$$

$$N_{Rd,b,re} = 2 \cdot 4 \cdot 120 \cdot \pi \cdot 8 \cdot \frac{3.0}{0.49} \cdot 10^{-3}$$

$$= 147.7 \text{ kN}$$

Anchorage length of the hanger

$$l_1 = h_{ef} - d_p - d_{s,t} - \frac{d_{s,a}}{1.5} = 165 - 25 - 14 - \frac{9}{1,5} =$$

$$= 120 \text{ mm}$$

Dist. hanger reinforcement to the face of the anchor shaft:

$$d_{s,a} = 5 \cdot \frac{d_s}{2} - \frac{d}{2} = 5 \cdot \frac{8}{2} - \frac{22}{2} = 9 \text{ mm}$$

Dist. axis of the reinforcement to the concrete surface

$$d_{s,t} = \frac{d_s}{2} + 10 = 14 \text{ mm}$$

Bond strength

$$f_{bd} = 2.25 \cdot \eta_1 \cdot \eta_2 \cdot \frac{f_{ctk}}{\gamma_{Mc}} = 2.25 \cdot 1 \cdot 1 \cdot \frac{2}{1.5} = 3.0 \text{ N/mm}^2$$

where η_1 is coefficient of bond conditions, $\eta_1 = 1.0$ for vertical stirrups and 0.7 for horizontal stirrups, $\eta_2 = 1.0$ for dimension ≤ 32 mm and (132 - dimension)/100 for dimension ≥ 32 mm

Hook $\quad \alpha = 0.49$

Def. of the reinforcement at bond failure

$$\delta_{Rd,b,re} = \frac{2 \cdot \left(N_{Rd,b,re}\right)^2}{\alpha_s \cdot f_{ck} \cdot d_{s,re}^4 (n \cdot n_{re})^2} = \frac{2 \cdot (147.7 \cdot 10^3)^2}{(12100 \cdot 30 \cdot 8^4 \cdot (2 \cdot 4)^2)} = 0.459 \text{ mm}$$

Partial safety factor $\gamma_{Mc} = 1.5$

The decisive component of the three failure modes of the concrete cone failure with reinforcement is the anchorage failure of the reinforcement. The anchors have a tension resistance of $N_{Rd,u} = N_{Rd,re,2} = 252.8$ kN

Step 4 Evaluation of the shear resistance

4.1 Steel failure of the fasteners

$$F_{v,Rd} = \frac{n_{a,v} \cdot 0.6 \cdot f_{uk} \cdot A_s}{\gamma_{M2}} = \frac{2 \cdot 0.6 \cdot 470 \cdot \pi \cdot \left(\frac{22}{2}\right)^2}{1.25} = 171.5 \text{ kN}$$

4.2 Pry-out failure

$$V_{Rd,CP} = k_3 \cdot N_{Rd,u,cc+group} = 2 \cdot 184.9 = 369.9 \text{ kN}$$

where

Min. component concrete failure

$$N_{Rd+group} = \min\left[N_{Rd,cs}; N_{Rd,s,re}; N_{Rd,b,re}; N_{Rd,u,c,group}\right]$$
$$\min[288.7 \text{ kN}; 271.0 \text{ kN}; 252.8 \text{ kN}, 184.9 \text{ kN}]$$

Partial safety factor $\quad \gamma_{Mc} = 1.5$

According to the Technical Specifications the factor k_3 is taken as 2.0. There are not yet made examinations how the resistance $V_{Rd,CP}$ may be calculated taking account of the reinforcement. Therefore $N_{Rd,u,cc+hr}$ is determined as the minimum value of the concrete cone failure with reinforcement ($N_{Rk,u,max}$, $N_{Rd,u,1}$, $N_{Rd,u2}$) and the concrete cone failure of the whole anchor group without considering additional reinforcement ($N_{Rd,u,c}$). $N_{Rd,u,c}$ is calculated in the following.

$$N_{Rk,u,c,group} = N^0{}_{u,c} \cdot \frac{A_{c,N}}{A^0{}_{c,N}} \cdot \Psi_{s,N} \cdot \Psi_{re,N} \cdot \Psi_{ec,N}$$

$$N_{Rk,u,c,group} = 147.4 \cdot \frac{461175}{245025} \cdot 1.0 \cdot 1.0 \cdot 1.0 = 277.4 \text{ kN}$$

$$N_{Rd,u,c,group} = \frac{N_{Rk,u,c}}{\gamma_{Mc}} = \frac{277.4 \text{ kN}}{1.5} = 184.9 \text{ kN}$$

where

$$N^0{}_{u,c} = k_1 \cdot f_{ck}{}^{0.5} \cdot h_{ef}{}^{1.5} = 12.7 \cdot 30^{0.5} \cdot 165^{1.5} \cdot 10^{-3} = 147.4 \text{ kN}$$

Effective anchorage depth $\qquad h_{ef} = h_n - t_{AP} = 150 - 10 + 25 = 165 \text{mm}$
Factor for close edge $\qquad \Psi_{s,N} = 1.0$
Factor for small reinforcement spacing $\qquad \Psi_{re,N} = 1.0$
Factor for eccentricity of loading $\qquad \Psi_{ec,N} = 1.0$
Reference projected area $\qquad A^0{}_{c,N} = s_{crN}{}^2 = 495^2 = 245025 \text{ mm}^2$
Actual projected area $\qquad A_{c,N} = (s_{crN} + s_2) \cdot (s_{crN} + s_1)$
$\qquad\qquad\qquad\qquad = (495 + 220) \cdot (495 + 150) =$
$\qquad\qquad\qquad\qquad 461175 \text{ mm}^2$

Step 5 Verification of interaction conditions

5.1 Interaction of tension and shear for steel failure

Shear load in the headed studs on the non-loaded side is

$$V_{Ed,2} = V_{Ed} - V_{Rd,s} - V_f = 180 - 190.1 - 20.8 = -31.0 \text{ kN}$$

All loads is taken by the front anchor. No load for the back anchor and

$$\left(\frac{N_{Ed,2}}{N_{Rd,s}}\right)^2 + \left(\frac{V_{Ed,2}}{V_{Rd}}\right)^2 \leq 1$$

$$\left(\frac{104.0}{238.1}\right)^2 + \left(\frac{0}{171.5}\right)^2 = 0.19 \leq 1$$

5.2 Interaction of tension and shear for concrete failure

Shear load in the headed studs on the non-loaded side is

$$V_{Ed,2} = \frac{V_{Ed} - V_f}{2} = \frac{180 - 20}{2} = 80 \text{ kN}$$

$$\left(\frac{N_{Ed,2}}{N_{Rd,u}}\right)^{3/2} + \left(\frac{V_{Ed,2}}{V_{Rd}}\right)^{3/2} \leq 1$$

DM I

(5.15)

$$\left(\frac{104.0}{252.8}\right)^{3/2} + \left(\frac{80}{184.9}\right)^{3/2} = 0.57 \leq 1$$

Note

Without the additional reinforcement there would be a brittle failure of the anchor in tension in concrete. The resistance of pure concrete cone failure with reinforcement is nearly two times the size of the resistance without reinforcement. With the additional reinforcement there is a ductile failure mode with reserve capacity.

9.6 Moment resistant steel to concrete joint

The steel-to-concrete connection is illustrated in Fig. 9.27. It represents the moment-resistant support of a steel-concrete-composite beam system consisting of a hot rolled or welded steel profile and a concrete slab, which can either be added in situ or by casting semi-finished precast elements. Beam and slab are connected by studs and are designed to act together. Whereas the advantage of the combined section is mostly seen for positive moments, where compression is concentrated in the slab and tension in the steel beam, it may be useful to use the hogging moment capacity of the negative moment range either as a continuous beam, or as a moment resistant connection. In this case, the reinforcement of the slab is used to raise the inner lever arm of the joint. The composite beam is made of a steel profile IPE 300 and a reinforced concrete slab with a thickness of 160 mm and a width of 700 mm. The concrete wall has a thickness of 300 mm and a width of 1 450 mm. The system is subjected to a hogging bending moment $M_{E,d}$ = 150 kNm. Tabs 9.1 and 9.2 summarize data for the steel-to-concrete joint.
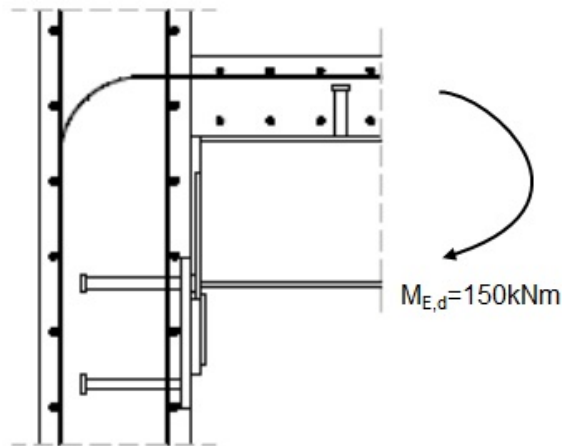
Fig. 9.27: Geometry of the moment resisting joint

Tab. 9.1 Geometry for the steel-to-concrete joint

Geometry								
RC wall			**RC Slab**			**Anchors**		
t [mm]	300		t [mm]	160		d [mm]	22	
b [mm]	1450		b [mm]	700		d_h [mm]	35	
h [mm]	1600		l [mm]	1550		l_a [mm]	200	
Reinforcement			**Reinforcement**			h_{ef} [mm]	215	
Φ_v [mm]	12		Φ_l [mm]	16		n_v	2	
n_v	15		n_l	6		e_1 [mm]	50	
s_v [mm]	150		s_l [mm]	120		p_1 [mm]	200	
Φ_h [mm]	12		Φ_t [mm]	10		n_h	2	
n_h	21		nt	14		e_2 [mm]	50	
s_h [mm]	150		s_t [mm]	100		p_2 [mm]	200	
			$c_{tens,bars}$ [mm]	30				
			r_{hook} [mm]	160				
Console 1			**Console 2**			**Anchor plate**		
t [mm]	20		t [mm]	10		t_{ap} [mm]	15	
b [mm]	200		b [mm]	170		b_{ap} [mm]	300	
h [mm]	150		h [mm]	140		l_{ap} [mm]	300	
Shear Studs			**Steel beam**	**IPE 300**		**Contact Plate**		
d [mm]	22		h [mm]	300		t [mm]	10	
h_{cs} [mm]	100		b [mm]	150		b_{cp} [mm]	200	
N_f	9		t_f [mm]	10.7		l_{cp} [mm]	30	
s [mm]	140		t_w [mm]	7.1		$e_{1,cp}$ [mm]	35	
a [mm]	270		As [mm²]	5381		$e_{b,cp}$ [mm]	235	
h_c [mm]	90					b_{ap} [mm]	300	

155

The part of the semi-continuous joint configuration, within the reinforced concrete wall, adjacent to the connection, is analyzed in this example. This has been denominated as "Joint Link". The main objective is to introduce the behaviour of this component in the global analysis of the joint which is commonly disregarded.

Tab. 9.2 Material of the steel-to-concrete joint

Concrete wall		Concrete slab		Rebars wall	
$f_{ck,cube}$ [Mpa]	50	$f_{ck,cube}$ [Mpa]	37	f_{syk} [MPa]	500
$f_{ck,cyl}$ [Mpa]	40	$f_{ck,cyl}$ [Mpa]	30	f_u [Mpa]	650
E [GPa]	36	E [GPa]	33		
f_{ctm} [Mpa]	3.51	f_{ctm} [Mpa]	2.87		
Rebars Slab		Steel Plates		Anchors	
f_{syk} [Mpa]	400	f_{syk} [Mpa]	440	f_{syk} [Mpa]	440
f_u [Mpa]	540	f_u [Mpa]	550	f_u [Mpa]	550
ε_{sry} [‰]	2	Steel Profile		Shear Studs	
ε_{sru}	75	f_{syk} [Mpa]	355	f_{syk} [Mpa]	440
		f_u [Mpa]	540	f_u [Mpa]	550

The design value of the modulus of elasticity of steel E_s may be assumed to be 200 GPa.
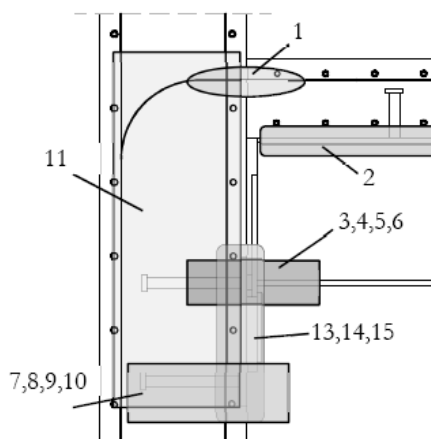
Fig. 9.28 Activated joint components

In order to evaluate the joint behaviour, the following basic components are identified, as shown in Fig. 9.28:

- longitudinal steel reinforcement in the slab, component 1
- slip of the composite beam, component 2;
- beam web and flange, component 3;
- steel contact plate, component 4;
- components activated in the anchor plate connection, components 5 to 10 and 13 to 15;
- the joint link, component 11.

Step 1 Component longitudinal reinforcement in tension

In this semi-continuous joint configuration, the longitudinal steel reinforcement bar is the only component that is able to transfer tension forces from the beam to the wall. In addition, the experimental investigations carried (Kuhlmann et al., 2012) revealed the importance of this component on the joint response. For this reason, the accuracy of the model to predict the joint response will much depend on the level of accuracy introduced in the modelling of this component. According to ECCS Publication Nº 109 (1999), the behaviour of the longitudinal steel reinforcement in tension is illustrated in Fig. 9.29.

156
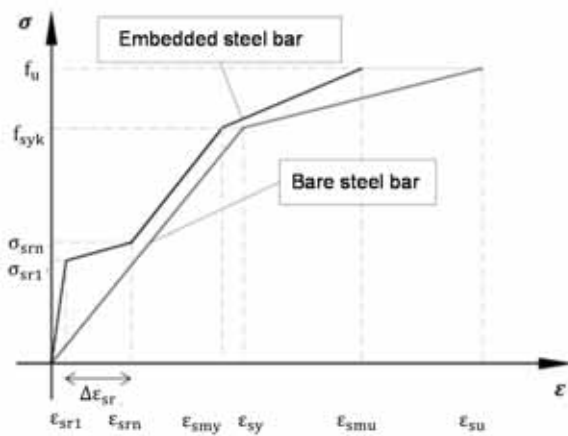
σ_{sr1}	stress of the embedded steel at the first crack
ε_{sr1}	strain of the embedded steel at the first crack
σ_{srn}	stress of the embedded steel at the last crack
ε_{srn}	strain of the embedded steel at the last crack
f_{syk}	yielding stress of the bare bar
ε_{sy}	strain at yield strength of the bare bar
ε_{smy}	strain at yield strength of the embedded bar
f_u	ultimate stress of the bare steel
ε_{su}	strain of the bare bar at ultimate strength
ε_{smu}	strain at ultimate strength of the embedded bar

Fig. 9.29 Stress-strain curve for steel reinforcement in tension

The resistance of the component may then be determined as follows

$$F_{s,r} = A_{s,r} \, f_{yr}$$

Since concrete grades of wall and slab are different it is possible to evaluate separately the stress-strain curve of the two elements. While the concrete is uncracked, the stiffness of the longitudinal reinforcement is considerably higher when compared with bare steel. Cracks form in the concrete when mean tensile strength of the concrete f_{ctm} is achieved. The stress in the reinforcement at the beginning of cracking (σ_{sr1}) is determined as follows.

$$\sigma_{sr1,d,SLAB} = \frac{\sigma_{sr1,SLAB}}{\gamma_{Ms}} = \frac{f_{ctm,SLAB} \cdot k_c}{\gamma_{Ms} \cdot \rho} \left[1 + \rho \frac{E_s}{E_c} \right] = \frac{2.87 \cdot 0.39}{1.15 \cdot 0.010} [1 + 0.010 \cdot 6.06]$$
$$= 97.1 \text{ Nmm}^{-2}$$
ECCS (1999)

$$\sigma_{sr1,d,WALL} = \frac{\sigma_{sr1,WALL}}{\gamma_{Ms}} = \frac{f_{ctm,WALL} \cdot k_c}{\gamma_{Ms} \cdot \rho} \left[1 + \rho \frac{E_s}{E_c} \right] = \frac{3.51 \cdot 0.39}{1.15 \cdot 0.010} [1 + 0.010 \cdot 6.06]$$
$$= 118.7 \text{ Nmm}^{-2}$$

where: f_{ctm} is the tensile strength of the concrete; E_s and E_c are the elastic modulus of the steel reinforcement bar and concrete, k_c is a factor which allows using the properties of the steel beam section and ρ is the ratio between the area of steel reinforcement and the area of concrete flange expressed as follows:

$$k_c = \frac{1}{1 + \frac{t_{slab}}{2 \cdot z_0}} = \frac{1}{1 + \frac{160}{2 \cdot 51.8}} = 0.39$$
ECCS (1999)

$$\rho = \frac{A_{s,r}}{A_{c,slab}} = \frac{n_l \cdot \pi \cdot \Phi_l^2/4}{b_{eff,slab} \cdot t_{slab}} = \frac{1\,206.4}{700 \cdot 160} = 0.010$$

where: $A_{c,slab}$ is the area of the effective concrete slab; $A_{s,r}$ is the area of the longitudinal reinforcement within the effective slab width (in this example the width of the slab is fully effective); t_{slab} is the thickness of the concrete flange and z_0 is the vertical distance between the centroid of the uncracked concrete flange and uncracked unreinforced composite section, calculated using the modular ration for short-term effects, E_s/E_c.

$$z_0 = x_{c,h} - \frac{t_{slab}}{2} = \left[\frac{b_{eff} \cdot \frac{E_c}{E_s} \cdot t_{slab} \cdot \frac{t_{slab}}{2} + \left(t_{slab} + \frac{h_{IPE300}}{2} \right) \cdot A_{IPE300}}{b_{eff} \cdot t_{slab} \cdot \frac{E_c}{E_s} + A_{IPE300}} \right] - \frac{t_{slab}}{2} = 51.8 \text{ mm}$$
CEB-FIB Model Code (1990)

157

where
$x_{c,h}$ is the dimension of the component concrete block in compression.

According to CEB-FIB Model Code (1990), the stress $\sigma_{srn,d}$ and the increment of the reinforcement strain $\Delta\varepsilon_{sr}$ are given by

$$\Delta\varepsilon_{sr,SL} = \frac{f_{ctm,SL} \cdot k_c}{\gamma_S \cdot E_s \cdot \rho} = 0.00045 \qquad\qquad \Delta\varepsilon_{sr,WA} = \frac{f_{ctm,WA} \cdot k_c}{\gamma_S \cdot E_s \cdot \rho} = 0.00056$$

$$\varepsilon_{sr1,SL} = \frac{\sigma_{sr1,d,SL}}{E_s} - \Delta\varepsilon_{sr,SL} = 3.0 \cdot 10^{-5} \qquad\qquad \varepsilon_{sr1,WA} = \frac{\sigma_{sr1,d,WA}}{E_s} - \Delta\varepsilon_{sr,WA} = 3.6 \cdot 10^{-5}$$

$$\sigma_{srn,d,SL} = 1.3 \cdot \sigma_{sr1,d,SL} = 126.2 \text{Nmm}^{-2} \qquad\qquad \sigma_{srn,d,WA} = 1.3 \cdot \sigma_{sr1,d,WA} = 154.3 \text{Nmm}^{-2}$$

$$\varepsilon_{srn,SL} = \varepsilon_{sr1,SL} + \Delta\varepsilon_{sr,SL} = 4.9 \cdot 10^{-4} \qquad\qquad \varepsilon_{srn,WA} = \varepsilon_{sr1,WA} + \Delta\varepsilon_{sr,WA} = 5.9 \cdot 10^{-4}$$

The yield stress and strain, f_{syk} and ε_{smy} are given by

$$f_{syk,d} = \frac{f_{syk}}{\gamma_S} = \frac{400}{1.15} = 347.8 \text{Nmm}^{-2}$$

$$\varepsilon_{smy,SL} = \frac{f_{syk,d} - \sigma_{srn,d,SL}}{E_s} + \varepsilon_{sr1,SL} + \Delta\varepsilon_{sr,SL} = 1.6 \cdot 10^{-3}$$

$$\varepsilon_{smy,WA} = \frac{f_{syk,d} - \sigma_{srn,d,WA}}{E_s} + \varepsilon_{sr1,WA} + \Delta\varepsilon_{sr,WA} = 1.6 \cdot 10^{-3}$$

The ultimate strain ε_{srmu} is determined as follows, where the tension stiffening is also taken into account. The factor $\beta_t = 0.4$ takes into account the short-term loading; and for high-ductility bars, δ is taken equal to 0.8.

$$\varepsilon_{smu,SL} = \varepsilon_{sy} - \beta_t \Delta\varepsilon_{sr,SL} + \delta\left(1 - \frac{\sigma_{sr1,d,SL}}{f_{syk,d}}\right)\left(\varepsilon_{su} - \varepsilon_{sy}\right) = 4.4 \cdot 10^{-2}$$

$$\varepsilon_{smu,WA} = \varepsilon_{sy} - \beta_t \Delta\varepsilon_{sr,WA} + \delta\left(1 - \frac{\sigma_{sr1,d,WA}}{f_{syk,d}}\right)\left(\varepsilon_{su} - \varepsilon_{sy}\right) = 4.0 \cdot 10^{-2}$$

where: ε_{sy} and $f_{syk,d}$ are the yield strain and stress of the bare steel reinforcement bars, respectively; ε_{su} is the ultimate strain of the bare steel reinforcement bars.

Assuming the area of reinforcement constant, the force-deformation curve is derived from the stress-strain curve, where the reinforcement deformation should be evaluated as described above.

$$\Delta = \varepsilon \cdot l$$

The elongation length (l) to consider is equal to sum of the L_t (related to the slab) with h_c (related to the wall). Only in the determination of the ultimate deformation capacity, the length of the reinforcement bar is considered higher than this value, as expressed in the following:

$\rho < 0.8\,\%$	$\Delta_{sru} = 2\,L_t\,\varepsilon_{srmu}$
$\rho \geq 0.8\,\%$ and $a \leq L_t$	$\Delta_{sru} = (h_c + L_t)\,\varepsilon_{srmu}$
$\rho \geq 0.8\,\%$ and $a > L_t$	$\Delta_{sru} = (h_c + L_t)\varepsilon_{srmu} + (a - L_t)\,\varepsilon_{srmu}$

where is

$$L_t = \frac{k_c \cdot f_{ctm} \cdot \Phi}{4 \cdot \tau_{sm} \cdot \rho} = \frac{0.39 \cdot 2.87 \cdot 16}{4 \cdot 5.16 \cdot 0.01} = 81 \text{ mm}$$

In the above expression, L_t is defined as the transmission length and represents the length of the reinforcement from the wall face up to the first crack zone which should form close to the joint. The parameter a is the distance of the first shear connector to the joint and h_c

is the length of the reinforcement up to the beginning of the bend. τ_{sm} is the average bond stress, given by

$$\tau_{sm} = 1.8 \cdot f_{ctm}$$

Forces can be evaluated considering minimum values of tensions found for slab and wall. Table 9.3 summarizes the results for the stress-strain and force-displacement curves.

Tab. 9.3 Force-displacement relation for longitudinal reinforcement in tension

σ_{SL} [N/mm²]	ε_{SL} [-]	σ_{WA} [N/mm²]	ε_{WA} [-]	F [kN]	Δ_r [mm]
97.1	$3.0 \cdot 10^{-5}$	118.7	$3.6 \cdot 10^{-5}$	117.1	0.0
126.2	$4.9 \cdot 10^{-4}$	154.3	$5.9 \cdot 10^{-4}$	152.3	0.1
347.8	$1.6 \cdot 10^{-3}$	347.8	$1.6 \cdot 10^{-3}$	419.6	0.3
469.5	$4.4 \cdot 10^{-2}$	469.5	$4.0 \cdot 10^{-2}$	566.5	5.7

Step 2 Component slip of composite beam

The slip of composite beam is not directly related to the resistance of the joint; however, the level of interaction between the concrete slab and the steel beam defines the maximum load acting on the longitudinal reinforcement bar. In EN 1994-1-1: 2010, the slip of composite beam component is not evaluated in terms of resistance of the joint, but the level of interaction is considered on the resistance of the composite beam. However, the influence of the slip of the composite beam is taken into account on the evaluation of the stiffness and rotation capacity of the joint. The stiffness coefficient of the longitudinal reinforcement should be affected by a reduction factor k_{slip} determined according to Chap. 3.7.

According to (Aribert, 1995) the slip resistance may be obtained from the level of interaction as expressed in the following. Note that the shear connectors were assumed to be ductile allowing redistribution of the slab-beam interaction load.

$$F_{slip} = N \cdot P_{RK}$$

Where: *N* is the real number of shear connectors; and P_{RK} is characteristic resistance of the shear connectors that can be determined according to EN1994-1-1:2010 as follows

$$P_{RK} = \min\left(\frac{0.8 \cdot f_u \cdot \pi \cdot d^2}{\gamma_{MV} \cdot 4} ; \frac{0.29 \cdot \alpha \cdot d^2 \sqrt{f_{ck} \cdot E_{cm}}}{\gamma_{MV}}\right)$$

with

$$3 \leq \frac{h_{sc}}{d} \leq 4 \qquad\qquad \alpha = 0.2\left(\frac{h_{sc}}{d} + 1\right)$$

$$\frac{h_{sc}}{d} > 4 \qquad\qquad \alpha = 1$$

where f_u is the ultimate strength of the steel shear stud; d is the diameter of the shear stud; f_{ck} is the characteristic concrete cylinder resistance; E_{cm} is the secant modulus of elasticity of the concrete; h_{sc} is the height of the shear connector including the head; γ_V is the partial factor for design shear resistance of a headed stud.

$$P_{RK} = \min\left(\frac{0.8 \cdot 540 \cdot \pi \cdot 22^2}{1.25 \cdot 4} ; \frac{0.29 \cdot 1 \cdot 22^2 \cdot \sqrt{30 \cdot 33)}}{1.25}\right) = \min(486.5; \ 111.0) = 111.0 \text{ kN}$$

$$F_{slip} = 9 \cdot 111.0 = 999.0 \text{ kN}$$

Concerning the deformation of the component, assuming an uniform shear load distribution along the beam, an equal distribution of the load amongst the shear studs is expected.

The stiffness of the component is obtained as a function of the number of shear studs and of the stiffness of a single row of shear studs, as follows

$$k_{slip} = N \cdot k_{sc} = 900 \text{ kN/mm}$$

where the stiffness of one shear connector k_{sc} may be considered equal to 100 kN/mm, see cl A.3(4) in EN 1994-1-1:2010.

Step 3 Component beam web and flange in compression

According to EN1993-1-8:2006, the resistance can be evaluated as follows

$$M_{c,Rd} = \frac{W_{pl} \cdot f_{syk}}{\gamma_{M0}} = \frac{628\,400 \cdot 355}{1.0} = 223.0 \text{ kN}$$

$$F_{c,fb,Rd} = \frac{223\,000}{(300 - 10.7)} = 771.1 \text{ kN}$$

The stiffness of this component may be neglected.

Step 4 Component steel contact plate in compression

According to EN1994-1-1:2010, the resistance can be evaluated as follows and the stiffness is infinitely rigid compared to rest of the connection.

$$F_{cp} = f_{y,cp} \, A_{eff,cp} = 440 \cdot 200 \cdot 30 = 2\,640 \text{ kN}$$

Step 5 Component T-stub in compression

According to EC 1993-1-8:2006, the bearing width c can be calculated using the hypothesis of cantilever beam for all directions. It is an iterative process as the bearing width and the concrete bearing strength f_j are mutually dependent.

$$c = t_{ap} \cdot \sqrt{\frac{f_y}{3 \cdot f_{jd} \cdot \gamma_{M0}}} \qquad\qquad f_{jd} = \frac{\beta_j \, F_{Rd,u}}{b_{eff} \, l_{eff}} = \frac{\beta_j \, A_{c0} \, f_{cd} \sqrt{\frac{A_{c1}}{A_{c0}}}}{A_{c0}} = \beta_j \, f_{cd} \, k_j$$

where β_j is the foundation joint material coefficient and F_{Rdu} is the concentrated design resistance force. Assuming an uniform distribution of stresses under the equivalent rigid plate and equal to the bearing strength of the concrete, the design compression resistance of a T-stub should be determined as follows

$$F_{C,Rd} = f_{jd} \cdot b_{eff} \cdot l_{eff}$$

where b_{eff} and l_{eff} are the effective width and length of the T-stub flange, given by

$$A_{eff} = \min(2c + b_{cp}; b_{ap}) \cdot (c + l_{cp} + \min(c; \ e_{1,cp})) = 69.4 \cdot 239.4 = 16625.9 \text{ mm}^2$$

and f_{jd} is the design bearing strength of the joint.

Thus, c = 19.7 mm; f_{jd} = 84.9 MPa; l_{eff} = 69.4mm; b_{eff} = 239.4 mm; F_c = 1411.0 kN

The initial stiffness $S_{ini,j}$ may be evaluated as follows

$$S_{ini,j} = \frac{E_c \sqrt{A_{eff}}}{1.275}$$

c is given by $c = 1.25 \cdot t_{ap}$ and b_{eff} and l_{eff} are given by

$$A_{eff} = \min(2.5 \, t_{ap} + b_{cp}; b_{ap}) \cdot (1.25 \, t_{ap} + l_{cp} + \min(1.25 \, t_{ap}, e_{1,cp})) = 67.5 \cdot 237.5 = 16\,031 \text{ mm}^2$$

Thus, $c = 18.7$ mm; $l_{eff} = 67.5$ mm; $b_{eff} = 237.5$ mm and $S_{ini,j} = 3\,575.0$ kN/mm

This value of the initial stiffness could be used for the calculation of the component of displacement related to the T-stub in compression.

Step 6 Joint Link

In the proposed model based on the STM principles, the properties of this diagonal spring are determined as follows:

- The resistance is obtained based on the strut and nodes dimension and admissible stresses within these elements, given in Tab. 3.2.
- The deformation of the diagonal spring is obtained by assuming a non-linear stress-strain relation for the concrete under compression, as defined in (Henriques, 2013).

In terms of resistance, the model is characterized by the resistance of the nodes at the edge of the diagonal strut. Accordingly, the maximum admissible stresses, see Tab. 3.2, and the geometry of these nodes define the joint link load capacity. It is recalled that failure is governed by the nodal regions and disregarded within the strut. Hence, the resistance of the nodes is obtained as follows.

6a)   Node N1

The geometry of the node is defined in one direction by the bend radius of the longitudinal reinforcement and by the strut angle θ with the dimension a Fig. 9.30. In the other direction (along the width of the wall), assuming the distance between the outer longitudinal overestimates the resistance of this node, since the analytical approach assumes that the stresses are constant within the dimension brb and the stress field "under" the hook and along this dimension is non-uniform.
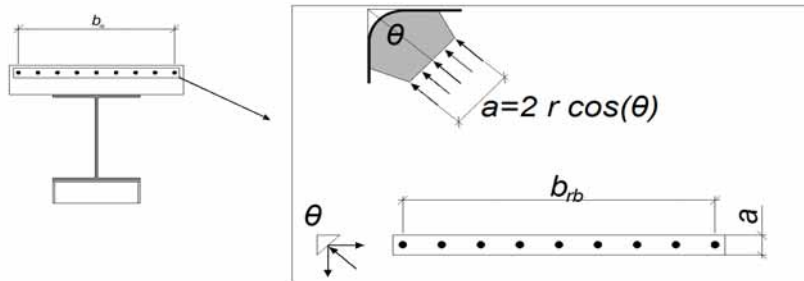

Fig. 9.30 Definition of the width of node N1

According to Henriques (2013), in order to obtain a more accurate approach, an analytical expression was derived to estimate an effective width "under" each reinforcement bar where constant stresses can be assumed. The basis of this analytical expression was a parametrical study performed by means of numerical calculations.
In order to obtain an expression which could approximate the effective width with sufficient accuracy, a regression analysis, using the data produced in the parametric study, was performed The effective width $b_{eff,rb}$ of the reinforcement is calculated as a function of the reinforcement bar diameter d_{rb}, the spacing of bars s_{rb} and strut angle θ as follows

$s_{rb} \geq 80$ mm $\qquad b_{eff,rb} = n \cdot 2.62 \cdot d_{rb}^{0.96} \cdot (\cos \theta)^{-1.05}$

$s_{rb} < 80$ mm $\qquad b_{eff,rb} = n \cdot 2.62 \cdot d_{rb}^{0.96} \cdot (\cos \theta)^{-1.05} \cdot \left(\frac{s_{rb}}{80}\right)^{0.61}$

As in this case $s_{rb} > 80$ mm

$$\theta = \arctan\left(\frac{z}{b}\right) = \arctan\left(\frac{406.65}{300 - \frac{16}{2} - \frac{10}{2} - 30 \cdot 2}\right) = 1.06 \text{ rad}$$

$$a = 2 \cdot r_{hook} \cdot \cos(\theta) = 2 \cdot 160 \cdot \cos(1.06) = 155.97 \text{ mm}$$

$$b_{eff,rb} = 6 \cdot 2.62 \cdot d_{rb}^{0.96} \cdot (\cos\theta)^{-1.05} = 478.054 \text{ mm}$$

The node dimensions are determined from

$$A_{N1} = b_{eff,rb} \cdot 2 \cdot r \cdot \cos\theta$$

where A_{N1} is the cross-section area of the diagonal concrete strut at node N1. Finally, the resistance of the node is given by

$$F_{r,N1} = A_{N1} \cdot 0.75 \cdot \nu \cdot f_{cd} = 1\,252.7\text{kN} \qquad\qquad \nu = 1 - \frac{f_{ck,cyl}}{250} = 0.84$$

6b) Node N2

The geometry of the node, on the concrete strut edge, is defined by the projection of the dimensions of the equivalent rigid plate, representing the anchor plate subjected to compression, in the direction of the concrete strut, see Fig. 9.31.
The node dimensions are determined from

$$A_{N2} = \frac{l_{eff}}{\cos\theta} \cdot b_{eff} = 35\,041.3 \text{ mm}^2$$

where: A_{N2} is the cross-section area of the diagonal concrete strut at node N2 where the admissible stresses have to be verified; l_{eff} and b_{eff} are the dimensions of the equivalent rigid plate determined according to the effective T-stub in compression. Considering the admissible stresses and the node dimensions, the resistance of the node is obtained

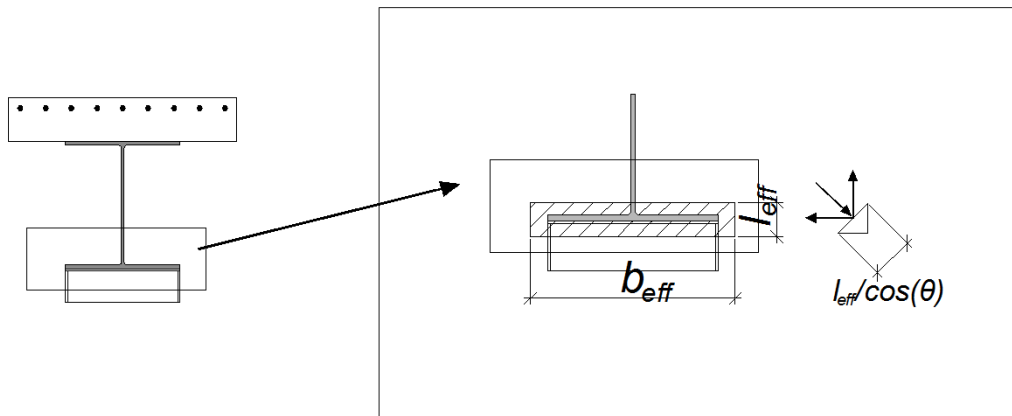$$F_{r,N2} = A_{N2} \cdot 3 \cdot \nu \cdot f_{cd} = 2\,354 \text{ kN}$$

Fig. 9.31 Definition of the width of node N2

6c) Joint link properties

The minimum resistance of the two nodes, N1 and N2, gives the resistance of the joint link in the direction of the binary force generated by the bending moment applied to the joint. Projecting the resistance in the horizontal direction, yields

$$F_{C-T,JL} = F_{r,N1} \cdot \cos\theta = 610.6 \text{ kN}$$

According to (Henriques 2013), the deformation of the joint link is given by

$$\Delta_{JL} = \left(6.48 \cdot 10^{-8} \cdot F^2{}_{C-T,JL} + 7.47 \cdot 10^{-5} \cdot F_{C-T,JL} \right) \cdot \cos \theta$$

Thus, considering 10 load steps, Tab. 9.4 summarizes the force-displacement curve.

Tab. 9.4 Force-displacement for the Joint Link component

F_h [kN]	Δ_h [mm]
0.0	0.00
61.1	0.00
122.1	0.00
183.2	0.01
244.2	0.01
305.3	0.01
366.3	0.02
427.4	0.02
488.5	0.03
549.5	0.03
610.6	0.03

Step 7 Assembly of joint

The simplified mechanical model represented in Fig. 9.32 consists of two rows, one row for the tensile components and another for the compression components. It combines the tension and compression components into a single equivalent spring per row.
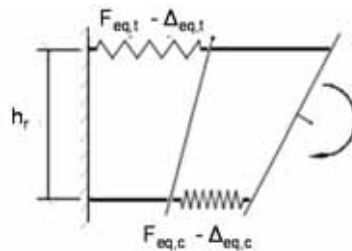

Fig. 9.32: Simplified joint model with assembly of components per row

The properties of the equivalent components/springs are calculated, for resistance, $F_{eq,t}$ and $F_{eq,c}$, and deformation, $\Delta_{eq,t}$ and $\Delta_{eq,c}$, as follows

$$F_{eq} = \min(F_i \text{ to } F_n)$$

$$\Delta_{eq} = \sum_{i=1}^{N} \Delta_i$$

where index i to n represents all relevant components, either in tension or in compression, depending on the row under consideration.

According to the joint configuration, it is assumed that the lever arm is the distance between the centroid of the longitudinal steel reinforcement bar and the middle plane of the bottom flange of the steel beam. The centroid of the steel contact plate is assumed aligned with this reference point of the steel beam. Hence, the bending moment and the corresponding rotation follow from

$$M_j = \min(F_{eq,T}; F_{eq,C}; F_{JL}) \cdot h_r \qquad \Phi_j = \frac{\Delta_{eq,T} + \Delta_{eq,C} + \Delta_{JL}}{h_r}$$

Thus

$F_{t,max} =$ 566.5 kN   Longitudinal rebar
$F_{c,max} =$ 610.6 kN   Joint link

163

$F_{eq} =$ 566.5 kN
$h_r =$ 406.65 mm
$M_j =$ 230.36 KNm

Table 9.5 summarizes the main results in order to calculate the moment rotation curve, where Δ_r is the displacement of the longitudinal steel reinforcement, Δ_{slip} is related to the slip of composite beam through to the coefficient k_{slip}, Δ_{T-stub} is the displacement of the T-stub in compression and ΔJL is the displacement of the joint link.

Tab. 9.5 Synthesis of results

F [kN]	Δ_r [mm]	Δ_{slip} [mm]	Δ_{T-stub} [mm]	Δ_{JL} [mm]	Δ_t [mm]	Φ [mrad]	M_j [kNm]
0.0	0.00	0.00	0.00	0.00	0.00	0.00	0.00
117.1	0.01	0.13	0.03	0.00	0.17	0.40	47.64
152.3	0.09	0.17	0.04	0.01	0.30	0.73	61.93
419.6	0.27	0.47	0.12	0.02	0.88	2.06	170.63
566.5	5.68	0.63	0.16	0.03	6.36	15.53	230.36

Note

The resulting moment-rotation behaviour is shown in Fig. 9.33. The system is able to resist the applied load.
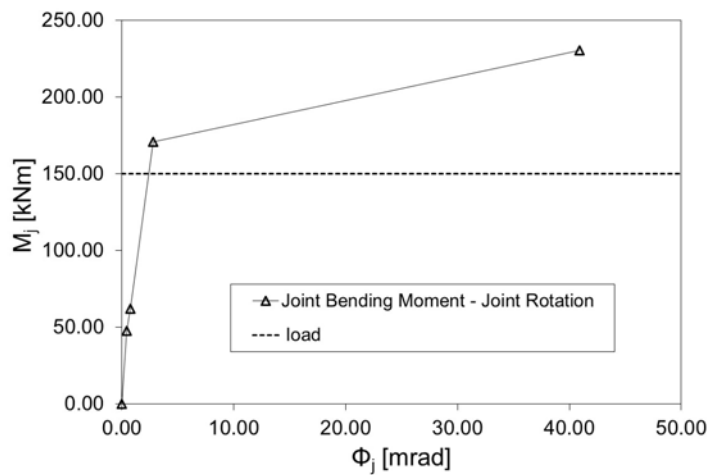

Fig. 9.33 Joint bending moment-rotation curve M_j - Φ_j

9.7 Portal frame

This example illustrates the design of a portal frame designed of columns with cross section HEB 180 and of a rafter with cross section IPE 270, as illustrated in Fig. 9.33. The stiffness of the connections and column bases is considered under design. The steel grade is S235JR, f_y = 235 N/mm² and the profiles are class 1 sections. Safety factors are considered as γ_{M0} = 1.0 and γ_{M1} = 1.1.

Fig. 9.34 highlights position of loads and Tab. 9.2 synthetizes the loads values, while load case combinations are summarized in Tab. 9.3.
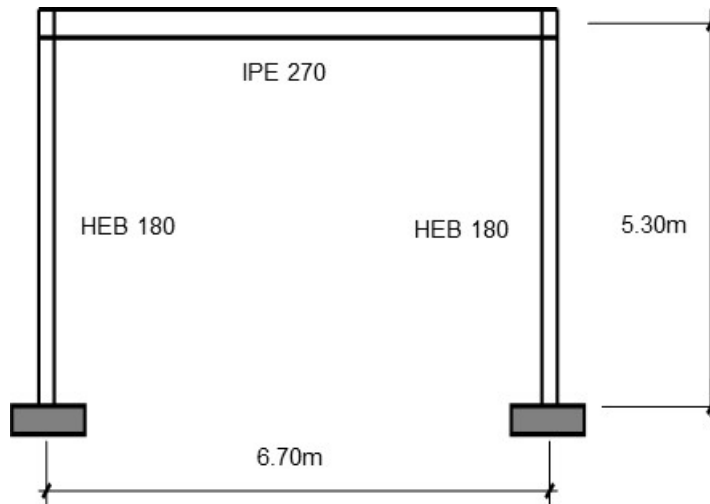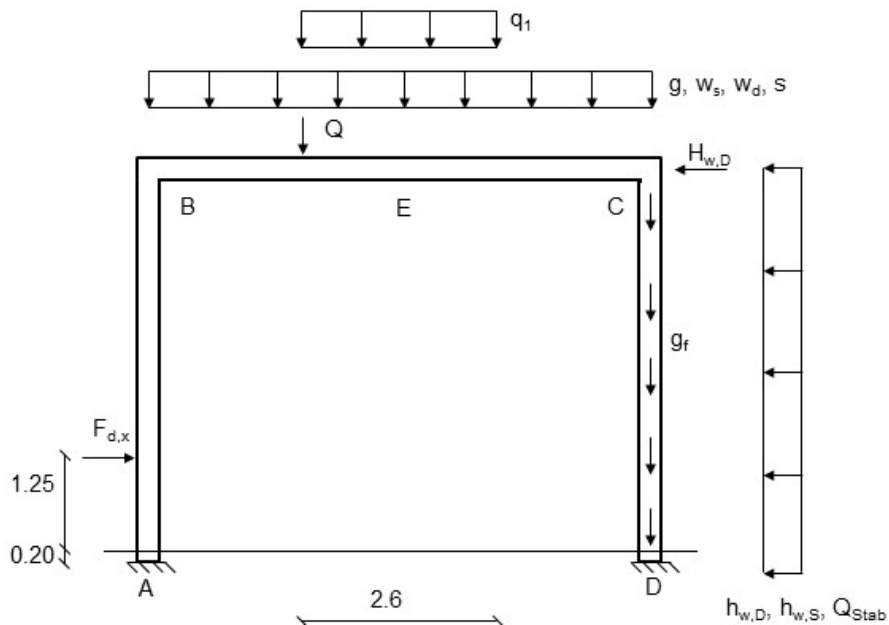

Fig. 9.33 Designed portal frame

Fig. 9.34 Acting loads

165

<div align="center">Tab. 9.2 Applied loads</div>

<u>Self-weight + dead loads</u>
$g_F = 0.5 \cdot 5.3 \approx 2.7$ kN/m
$g = 4.8$ kN/m
$s = 5.0$ kN/m
$q_1 = 3.0$ kN/m. b = 2.6m (equipment)
$Q_1 = 9.8$ kN
$w_D = 0.8$ kN/m
$w_S = -3.9$ kN/m

Imperfection $r_2 = 0.85$, n = 2

<u>Wind</u>
$h_{w.D} = 0.8 \cdot 0.65 \cdot 5.3 = 2.7$ kN/m
$H_{w.D} = 0.4 \cdot 0.8 \cdot 0.65 \cdot 5.3 = 1.1$ kN
$h_{w.S} = 0.5 \cdot 0.65 \cdot 5.3 = 1.7$ kN/m

<u>Impact load</u> (EN1991-1-7:2006)
$F_{d.x} = 100$ kN (h=1.45m)

max $Q_{Stab} \approx (48+58)\ 0.85/200 < 0.5$ kN
(added in the wind load case)

<div align="center">Tab. 9.3 Load case combinations</div>

LC 1 $(g+g_f) \cdot 1.35$
LC 2 $(g+g_f) \cdot 1.35 + s \cdot 1.5$
LC 3 $(g+g_f) \cdot 1.35 + s \cdot 1.5 + q_1 \cdot 1.5 \cdot 0.7$
LC 4 $(g+g_f) \cdot 1.35 + s \cdot 1.5 + (w+w_D) \cdot 1.5 \cdot 0.6 + q_1 \cdot 1.5 \cdot 0.7$
LC 5 $(g+g_f) \cdot 1.35 + s \cdot 1.5 \cdot 0.5 + (w+w_D) \cdot 1.5 + q_1 \cdot 1.5 \cdot 0.7$
LC 6 $(g+g_f) \cdot 1.35 + s \cdot 1.5 - (w+w_D) \cdot 1.5 \cdot 0.6 + q_1 \cdot 1.5 \cdot 0.7$
LC 7 $(g+g_f) \cdot 1.35 + s \cdot 1.5 \cdot 0.5 - (w+w_D) \cdot 1.5 + q_1 \cdot 1.5 \cdot 0.7$
LC 8 $(g+g_f) \cdot 1.0 + (w+w_S) \cdot 1.5$
LC 9 $(g+g_f) \cdot 1.0 + q_1 \cdot 1.0 +$ truck $+ s \cdot 0.2$ (exceptional combination – impact load)

The main steps in order to verify a steel portal frame are the following:
Step 1   Global analysis of the steel structure, with fully restrained column bases. Provide internal forces and moments and the corresponding displacements under several loading condition.
Step 2   Verification of single elements
Step 3   Verification of the column-beam joint, in terms of stiffness and resistance.
Step 4   Verification of column base joint, taking into account an impact load
Step 5   Updating of internal forces and moments of the system considering the effective stiffness of the restraints

<u>Step 1 Global analysis</u>
From a 1st order elastic analysis the internal force diagrams envelope due to vertical and horizontal loads, Fig. 9.35 to 9.36 are obtained. Fig. 9.37 illustrates the structural displacement in case di wind load, in direction x. For each combination is necessary to check whether 2nd order effects should be taken into account in the structural analysis by the following simplified expression for beam-and-column type plane frames

$$\alpha_{cr} = \left(\frac{H_{Ed}}{V_{Ed}}\right) \cdot \left(\frac{h_i}{\delta_{H,Ed}}\right)$$

EN 1993-1-1
cl 5.2.1

where:
H_{Ed} is the total horizontal reaction at the of the storey
V_{Ed} is the total vertical reaction at the bottom of the storey
$\delta_{H,Ed}$ is the relative horizontal displacement of the top storey
h_i is the height of the storey
In this case, α_{cr} is always greater than 10 and thus the first order analysis is enough.
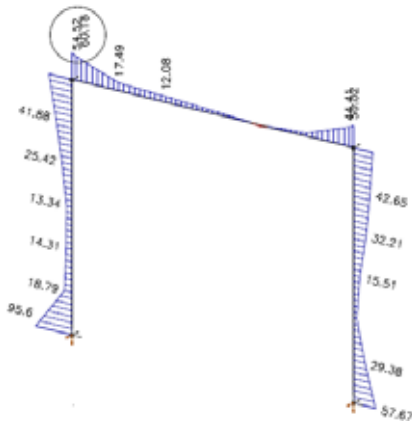
Fig. 9.35 System with max bending
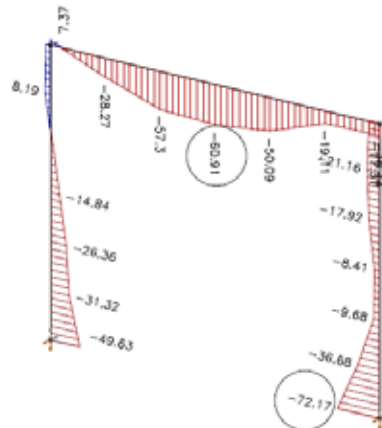moment from all combinations [kNm]

Fig. 9.36 System with min bending
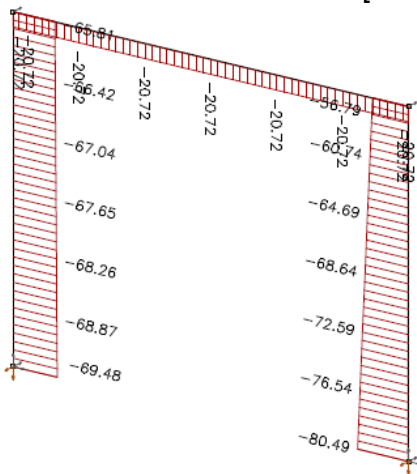moment from all combinations [kNm]

Fig. 9.37 System with min axial force
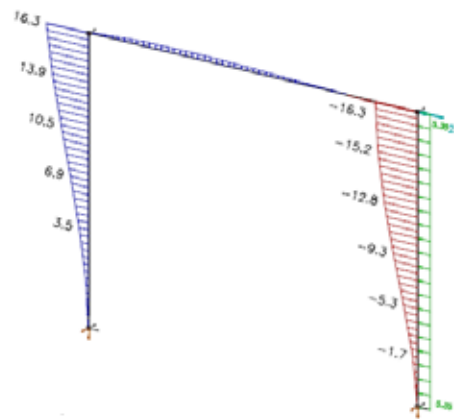from all combinations [kN]

Fig. 9.38 Deformation
for wind in x-direction [mm]

Maximal deformation under variable load is 17 mm at the top.

Step 2 Verification of elements
Verifications are performed using the EC3 Steel Member Calculator for iPhone.

Column HEB 180 is verified as

Acting forces from LC 6	Critical section resistance	Buckling resistance	Verification
$N_{min,d}$ = -80 kN	$N_{c,Rd}$ = -1533 kN	$N_{b,y,Rd}$ = -1394 kN	$\varepsilon\,(N+M_y+V) \leq 1$ 0.477
$M_{Ay,d}$ = 51 kNm	$M_{yAy,c,Rd}$ = 113.1 kNm	$N_{b,z,Rd}$ = 581 kN	$\varepsilon\,(M_b + N_{by}\,(6.61)) \leq 1$
$M_{B'y,d}$ = 45 kNm	$V_{c,Rd}$ = 274 kN	$M_{b,Rd}$ = 102.8 kNm	**0.265**

Beam IPE 270 is verified as

Acting force from LC 4	Critical cection resistance	Buckling resistance	Verification
$N_{min,d}$ = -19 kN	$N_{c,Rd}$ = 1079.7 kN		$\varepsilon\,(N+M_y+V) \leq 1$ **0.536**
$M_{Ey,d}$ = 61 kNm	$M_{y,c,Rd}$ = 113.7 kNm	$M_{b,Rd}$ = 103,4 kNm	$\varepsilon\,(M_b) + N_{by}\,(6,61)) \leq 1$
$M_{B''y,d}$ = -51 kNm	$V_{c,Rd}$ = 300.4 kN		**0.265**

167

Step 3 Design of beam to column joint
The connection is illustrated in Fig. Fig. 9.39. The end plate has a height of 310 mm, a thickness of 30 mm and a width of 150 mm with 4 bolts M20 10.9.
Design Values

$M_{y,Rd}$ = -70.7 kNm > -54.5 kNm (at x = 0.09 of supports axis)
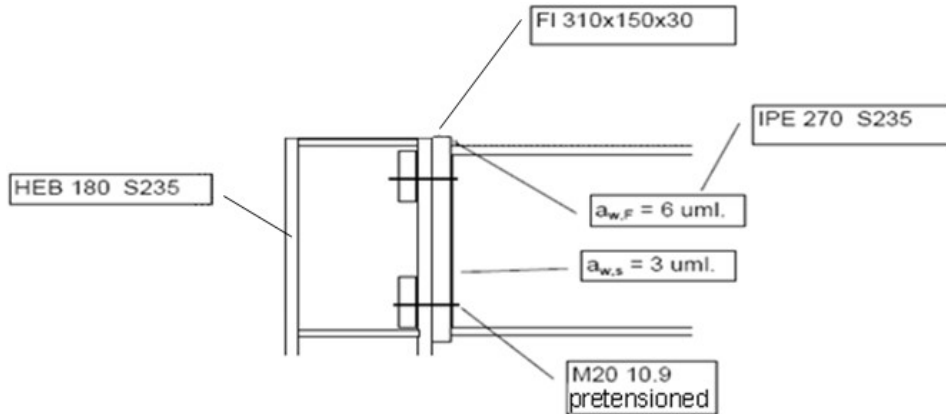$V_{z,Rd}$ = 194 kN

Fig. 9.39 Design of beam-to-column joint

The verification is performed using the ACOP software. The resulting bending moment – rotation curve is represented in Fig. 9.40.
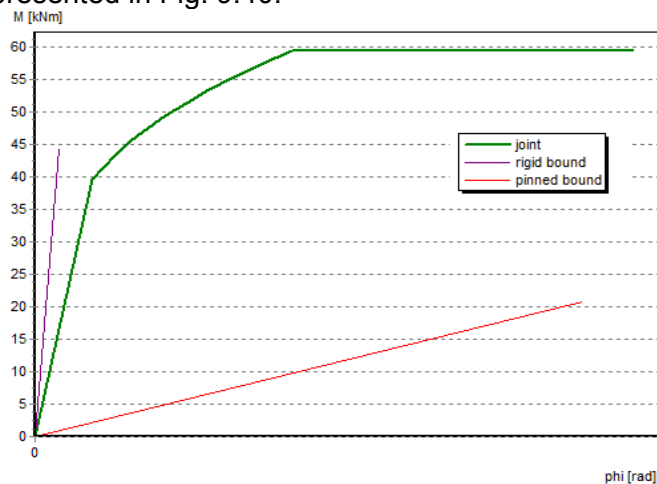
Fig. 9.40 The bending moment to rotation curve M_j - Φ_j

Step 4 Verification of the column base joint
Main Data
-       Base plate of 360 x 360 x 30 mm, S235
-       Concrete block of size 600 x 600 x 800 mm, C30/37
-       Welds $a_{w,Fl}$ = 7 mm, $a_{w,St}$ = 5 mm
-       The support with base plate is in a 200 mm deep of the foundation.
Design Values

Characteristic	LC	$N_{x,d}$ [kN]	$M_{y,d}$ [kNm]
N_{min}	6	-80	51
M_{max}	9	-31.6	95.6

Fig. 9.41 represents the designed column base. In the verification procedure, the following step are accomplished:

a) calculation of the resistance of component base plate in bending and anchor bolts in tension;
b) evaluation of the area of concrete in compression,
c) calculation of the strip *c* around the column cross section,
d) calculation of moment resistant of column base,
e) check of the end of column,
f) evaluation of the bending stiffness component stiffness;,
g) evaluation of the stiffness of tension part, bolts and T stub,
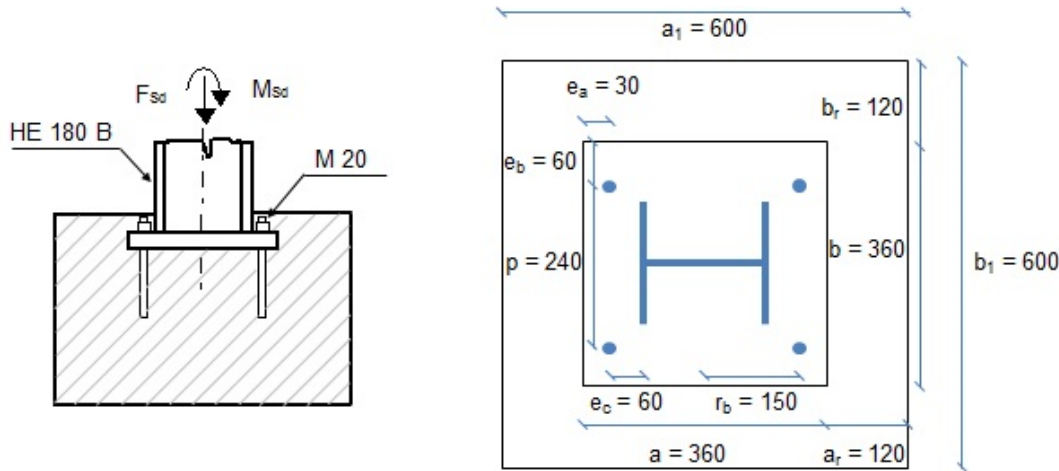h) evaluation of the bending stiffness.

Fig. 9.41 Designed column base

4a)   Resistance of component base plate in bending and anchor bolts in tension
For anchor bolt lever arm, for fillet weld a_{wf} = 7 mm, it is
$$m = 60 - 0.8 \cdot a_{wf} \cdot \sqrt{2} = 60 - 0.8 \cdot 7 \cdot \sqrt{2} = 52.1 \text{ mm}$$

The T - stub length, in base plates are the prying forces not taken into account, is
$$l_{eff,1} = \min \begin{cases} 4 \cdot m + 1.25 \cdot e_a = 4 \cdot 52.1 + 1.25 \cdot 30 = 245.9 \\ 4 \cdot \pi \cdot m = 4 \cdot \pi \cdot 52.1 = 654.7 \\ 0.5\,b = 0.5 \cdot 360 = 180 \\ 2 \cdot m + 0.625 \cdot e_a + 0.5 \cdot p = 2 \cdot 52.1 + 0.625 \cdot 30 + 0.5 \cdot 240 = 243 \\ 2 \cdot m + 0.625 \cdot e_a + e_b = 2 \cdot 52.1 + 0.625 \cdot 30 + 60 = 183 \\ 2 \cdot \pi \cdot m + 4 \cdot e_b = 2 \cdot \pi \cdot 52.1 + 4 \cdot 60 = 567.4 \\ 2 \cdot \pi \cdot m + 2 \cdot p = 2 \cdot \pi \cdot 52.1 + 2 \cdot 240 = 807.4 \end{cases} =$$

$$l_{eff,1} = 180 \text{ mm}$$

The effective length of anchor bolt L_b is taken as
$$L_b = 8 \cdot d + t = 8 \cdot 20 + 30 = 190 \text{ mm}$$

The resistance of T - stub with two anchor bolts is
$$F_{T,1-2,Rd} = \frac{2 \cdot L_{eff,1} \cdot t^2 \cdot f_y}{4 \cdot m \cdot \gamma_{M0}} = \frac{2 \cdot 180 \cdot 30^2 \cdot 235}{4 \cdot 52.1 \cdot 1} = 365.4 \cdot 10^3 \text{N}$$

while the tension resistance of two anchor bolts M 20 for the area of threaded part of bolt
$$A_s = 314 \text{ mm}$$
$$F_{T,3,Rd} = 2 \cdot B_{t,Rd} = 2 \cdot \frac{0.9 \cdot f_{ub} \cdot A_s}{\gamma_{M2}} = \frac{0.9 \cdot 360 \cdot 314}{1.25} = 162.8 \cdot 10^3 \text{N}$$

4b)To evaluate the compressed part resistance is calculated the connection concentration factor as

DM I
Fig. 4.4

EN1993-1-8
6.4.6.5

DM I
Fig. 4.1

EN1993-1-8
cl 6.2.4.1

$$a_1 = b_1 = \min \begin{Bmatrix} a + 2 \cdot a_r = 360 + 2 \cdot 120 = 600 \\ 3 \cdot a = 3 \cdot 360 = 1\,080 \\ a + h = 360 + 800 = 116 \end{Bmatrix} = 600 \text{ mm}$$

and

$a_1 = b_1 = 600 \text{ mm} > \max(a, b)$

The above condition is fulfilled and

$$k_j = \sqrt{\frac{a_1 \cdot b_1}{a \cdot b}} = \sqrt{\frac{600 \cdot 600}{360 \cdot 360}} = 1.67$$

The grout is not influencing the concrete bearing resistance because

$0.2 \min (a; b) = 0.2 \cdot \min (360; 360) = 72 \text{ mm} > 30 \text{ mm} = t$

The concrete bearing resistance is calculated as

$$f_{j,d} = \frac{2}{3} \cdot \frac{k_j \cdot f_{ck}}{\gamma_{Mc}} = \frac{2}{3} \cdot \frac{1.67 \cdot 30}{1.5} = 22.3 \text{ MPa}$$

for each load case, from the force equilibrium in the vertical direction $F_{Sd} = A_{eff} f_j - F_{t,Rd}$, is calculated the area of concrete in compression A_{eff} in case of the full resistance of tension part.

$$A_{eff-LC6} = \frac{F_{Sd-LC6} + F_{Rd,1}}{f_{jd}} = \frac{80 \cdot 10^3 + 365.4 \cdot 10^3}{22.3} = 19\,973.1 \text{ mm}^2$$

$$A_{eff-LC9} = \frac{F_{Sd-LC9} + F_{Rd,1}}{f_{jd}} = \frac{31.6 \cdot 10^3 + 365.4 \cdot 10^3}{22.3} = 17\,802.7 \text{ mm}^2$$

4c)   The flexible base plate is transferred into a <u>rigid plate of equivalent area</u>.

The width of the strip *c* around the column cross section, see Fig. 9.40, is calculated from

$$c = t \cdot \sqrt{\frac{f_y}{3 \cdot f_{jd} \cdot \gamma_{M0}}} = 30 \cdot \sqrt{\frac{235}{3 \cdot 22.3 \cdot 1}} = 56.2 \text{ mm}$$
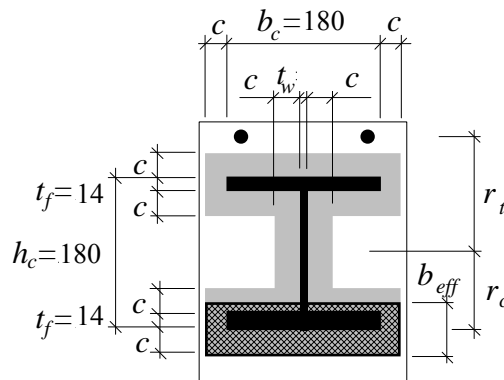
Fig. 9.42 The effective area under the base plate

4d)   The active effective width is calculated from known area in compression

$$b_{eff-LC6} = \frac{A_{eff-LC6}}{b_c + 2 \cdot c} = \frac{19\,937.1}{180 + 2 \cdot 57.2} = 68.3 \text{ mm} < t_f + 2 \cdot c = 14 + 2 \cdot 56.2 = 126.4 \text{ mm}$$

$$b_{eff-LC9} = \frac{A_{eff-LC9}}{b_c + 2 \cdot c} = \frac{17\,802.7}{180 + 2 \cdot 57.2} = 60.9 \text{ mm} < t_f + 2 \cdot c = 14 + 2 \cdot 56.2 = 126.4 \text{ mm}$$

The lever arms of concrete to the column axes of symmetry is calculated as

$$r_{c-LC6} = \frac{h_c}{2} + c - \frac{b_{eff-LC6}}{2} = \frac{180}{2} + 56.2 - \frac{68.3}{2} = 112.1 \text{ mm}$$

$$r_{c-LC9} = \frac{h_c}{2} + c - \frac{b_{eff-LC9}}{2} = \frac{180}{2} + 56.2 - \frac{60.9}{2} = 115.8 \text{ mm}$$

Moment resistances of column base are

$$M_{Rd-LC6} = F_{T,1,Rd} \cdot r_t + A_{eff-LC6} \cdot f_{jd} \cdot r_{c-LC6} = 104.7 \text{ kNm}$$

$$M_{Rd-LC9} = F_{T,1,Rd} \cdot r_b + A_{eff-LC9} \cdot f_{jd} \cdot r_{c-LC9} = 100.8 \text{ kNm}$$

4e)The <u>end of column</u> needs to be checked. The design resistance in pure compression is

$$N_{pl,Rd} = \frac{A \cdot f_y}{\gamma_{M0}} = \frac{6\,525 \cdot 235}{1.0} = 1\,533.4 \text{ kN}$$

and column bending resistance

$$M_{pl,Rd} = \frac{W_{pl} \cdot f_y}{\gamma_{M0}} = \frac{481 \cdot 10^3 \cdot 235}{1.0} = 113.1 \text{ kNm}$$

The interaction of normal force changes moment resistance

$$M_{Ny,Rd} = M_{pl,Rd} \cdot \frac{1 - \dfrac{N_{Sd}}{N_{pl,Rd}}}{1 - 0.5 \cdot \dfrac{A - 2 \cdot b \cdot t_f}{A}} = 113.0 \cdot \frac{1 - \dfrac{80}{1\,533.4}}{1 - 0.5 \cdot \dfrac{6\,525 - 2 \cdot 180 \cdot 14}{6\,525}} = 120.9 \text{ kNm}$$

4f) To evaluate the <u>bending stiffness </u>the particular component stiffness is calculated

$$k_b = 2.0 \cdot \frac{A_s}{L_b} = 2.0 \cdot \frac{314}{190} = 3.3 \text{ mm}$$

$$k_p = \frac{0.425 \cdot L_{beff} \cdot t^3}{m^3} = \frac{0.425 \cdot 180 \cdot 30^3}{52.1^3} = 14.6 \text{ mm}$$
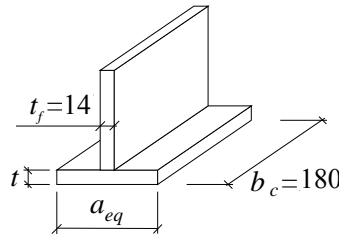

Fig. 9.43 The T stub in compression

The concrete block stiffness is evaluated based on T-stub in compression, see Fig. 9.43

$$a_{eq} = t_f + 2.5 \cdot t = 14 \cdot 2.5 \cdot 30 = 89 \text{ mm}$$

$$k_c = \frac{E_c}{1.275 \cdot E_s} \cdot \sqrt{a_{eq} \cdot b_c} = \frac{33\,000}{1.275 \cdot 210000} \cdot \sqrt{89 \cdot 180} = 15.6 \text{ mm}$$

4g) The <u>lever arm of component</u> in tension z_t and in compression z_c to the column base
   neutral axes is

$$r_t = \frac{h_c}{2} + e_c = \frac{180}{2} + 60 = 150 \text{ mm}$$

$$z_c = \frac{h_c}{2} - \frac{t_f}{2} = \frac{180}{2} + \frac{14}{2} = 83 \text{ mm}$$

The stiffness of tension part, bolts and T stub, is calculated as

$$k_t = \frac{1}{\dfrac{1}{k_b} + \dfrac{1}{k_p}} = \frac{1}{\dfrac{1}{3.3} + \dfrac{1}{14.6}} = 2.7 \text{ mm}$$

4h) For the calculation of the <u>initial stiffness</u> of column base is evaluated the lever arm

$$r = r_t + z_c = 150 + 83 = 233 \text{ mm}$$

and

$$a = \frac{k_c \cdot r_{c1} - k_t \cdot r_t}{k_c + k_t} = \frac{15.6 \cdot 83 - 2.7 \cdot 150}{15.6 + 2.7} = 43.26 \text{ mm}$$

The bending stiffness is calculated for particular constant eccentricity

$$e_{LC-6} = \frac{M_{Rd-LC6}}{F_{Sd-LC6}} = \frac{104.7 \cdot 10^6}{80.0 \cdot 10^3} = 1\,308.8 \text{ mm}$$

$$e_{LC-9} = \frac{M_{Rd-LC9}}{F_{Sd-LC9}} = \frac{100.8 \cdot 10^6}{31.6 \cdot 10^3} = 3\,189.9 \text{ mm}$$

as

$$S_{j,ini-LC6} = \frac{e_{LC-6}}{e_{LC-6} + a} \cdot \frac{E_s \cdot r^2}{\mu \sum_i \frac{1}{k_i}} = \frac{1\,308.8}{1\,308.8 + 3\,189.9} \cdot \frac{210\,000 \cdot 233^2}{1 \cdot \left(\frac{1}{2.7} + \frac{1}{15.6}\right)} = 25\,301 \text{ kNm/rad}$$

$$S_{j,ini-LC9} = \frac{e_{LC-9}}{e_{LC-9} + a} \cdot \frac{E_s \cdot r^2}{\mu \sum_i \frac{1}{k_i}} = \frac{3\,189.9}{3\,189.9 + 3\,189.9} \cdot \frac{210\,000 \cdot 233^2}{1 \cdot \left(\frac{1}{2.7} + \frac{1}{15.6}\right)} = 25\,846 \text{ kNm/rad}$$

These values of stiffness do not satisfy the condition about the rigid base

$$S_{j,ini} \geq 30\,E \cdot I_b / L_b = 45\,538 \text{ kNm/rad}$$

Step 5 Updating of internal forces and moments
Steps 1 to 4 should be evaluated again considering internal forces obtained from a structural analysis taking into account the stiffness of column base, see Fig. 9.44. Tab. 9.4 summarizes results of the structural analysis of the two meaning full combinations N_{min} and M_{max}.
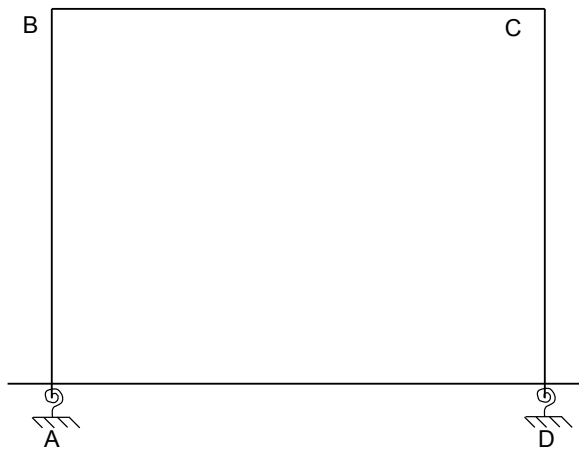

Fig. 9.44 Structural system with rotational springs

Tab. 9.4 Comparison of internal forces between the model with rigid column base joint and the model with the actual stiffness

Load case	Column base stiffness	Point A		Point B		Point C		Point D	
		N [kN]	M [kNm]	N [kN]	M [kNm]	N [kN]	M [kNm]	N [kN]	M [kNm]
6	Rigid	-57.0	1.6	-54.0	27.7	-56.0	49.3	-80.0	51.0
	Semi-rigid	-56.9	3.1	-53.3	24.3	-57.1	-40.7	-80.8	48.4
9	Rigid	-31.6	95.6	-29	-18.7	-29.0	-36.0	-47.0	32.6
	Semi-rigid	-30.5	87.3	-27.9	-17.7	-30.9	-40.6	-48.4	34.7

For the LC6 has been implemented a structural model with two rotational springs equal to $25\,301$ kNm/rad. For the LC9 the adopted rotational stiffness was equal to $25\,846$ kNm/rad. Due to the proximity of the stiffness value calculated in Step 4. it was reasonable to assumed in a simplified manner. The lower value of the stiffness in order to update the internal forces of the system.

As shown in the above table, the differences in terms of internal forces are negligible and therefore the single elements and the beam to column joint is considered verified. Tab. 9.4 synthetizes the updated properties of the column base joint.

Tab. 9.4 Updated properties of the column base joint

Load case	Column base stiffness	A_{eff} [mm²]	b_{eff} [mm]	r_c [mm]	M_{rd} [kNm]	$S_{j.ini}$ [kNm/rad]
6	Rigid	19 973.1	68.3	112.1	104.7	25 301
	Semi-rigid	20 008.0	68.4	112.0	104.8	25 268
9	Rigid	17 802.7	60.9	115.8	100.8	25 846
	Semi-rigid	17 757.0	60.7	115.8	100.7	25 344

The designed column base fulfils the asked requirements as shown in the Tab. 9.4.

10 SUMMARY

This design manual summarises the reached knowledge in the RFCS Project RFSR-CT-2007-00051 New Market Chances for Steel Structures by Innovative Fastening Solutions between Steel and Concrete (INFASO). The material was prepared in cooperation of two teams of researchers one targeting on fastening technique modelling and others focusing to steel joint design from Institute of Structural Design and Institute of Construction Materials, Universität Stuttgart, Department of Steel and Timber Structures, Czech Technical University in Prague, and practitioners Gabinete de Informática e Projecto Assistido Computador Lda., Coimbra, Goldbeck West GmbH, Bielefeld, stahl+verbundbau GmbH, Dreieich and European Convention for Constructional Steelwork, Bruxelles.

The model of three types of steel to concrete connections with the headed studs on anchor plate are introduced. There are based on component method and enable the design of steel to concrete joints in vertical position, e.g. beam to column or to wall connections, and horizontal ones, base plates. The behaviour of components in terms of resistance, stiffness, and deformation capacity is summed up for components in concrete and steel parts: header studs, stirrups, concrete in compression, concrete panel in shear, steel reinforcement, steel plate in bending, threaded studs, anchor plate in tension, beam web and flange in compression and steel contact plate.

In the Chapters 5 and 6 are described the possibility of assembly of components behaviour into the whole joint behaviour for resistance and stiffness separately. The presented assembly enables the interaction of normal forces, bending moments and shear forces acting in the joint. The global analyses in Chapter 7 is taken into account the joint behaviour. The connection design is sensitive to tolerances, which are recapitulated for beam to column connections and base plates in Chapter 8. The worked examples in Chapter 9 demonstrates the application of theory to design of pinned and moment resistant base plates, pinned and moment resistance beam to column connections and the use of predicted values into the global analyses.

References

<u>Standards and guidelines</u>

CEB-FIP Model Code 1990, Comité Euro-International du Béton, Lausanne, 1993.

CEN/TS1992-4-1, *Design of fastenings for use in concrete – Part 4-2, Headed fasteners* Technical Specification, CEN, Brussels, 2009.

EN1090-2, *Execution of steel structures and aluminium structures, Part 2, Technical requirements for steel structures.* CEN, Brussels, 2008.

EN13670, *Execution of concrete structures*, CEN, Brussels, 2011.

EN1990, Eurocode 0: *Basis of structural design*, CEN, Brussels, 2002.

EN1991-1-1, *Eurocode 1: Actions on structures, Part 1.1, General actions, Densities, self-weight, imposed load for buildings*, CEN, Brussels, 2002.

EN1991-1-1, *Eurocode 1: Actions on structures, Part 1.7, General actions, Densities, self-weight, imposed load for buildings*, CEN, Brussels, 2006.

EN1992-1-1, Eurocode 2, Design of concrete structures, Part 1-7, *General actions - Accidental actions*, CEN, Brussels, 2004.

EN1993-1-1, Eurocode 3, Design of steel structures, Part 1-1, *General rules and rules for buildings*, CEN, Brussels, 2010.

EN1993-1-8, Eurocode 3, Design of steel structures, Part 1-8, *Design of joints*, CEN, Brussels, 2006.

EN1994-1-1, Eurocode 4, Design of composite steel and concrete structures, Part 1-1, *General rules and rules for buildings*, CEN, 2010.

EN206-1, Concrete - Part 1, *Specification, performance, production and conformity*, CEN, Brussels, 2000.

FIB Bulletin 58, *Design of anchorages in concrete,* Guide to good practice, International federation for structural concrete, Lausanne, 2011.

<u>Textbooks and publications</u>

Aribert, J. M., *Influence of Slip on Joint Behaviour*, Connections in Steel Structures III, Behaviour, Strength and Design, Third International Workshop, Trento, 1995.

Astaneh A. et al., *Behaviour and design of base plates for gravity, wind and seismic loads,* In AISC, National Steel Construction Conference, Las Vegas, 1992.

Bouwman L.P., Gresnigt A.M., Romeijn A., *Research into the connection of steel base plates to concrete foundations*, TU-Delft Stevin Laboratory report 25.6.89.05/c6, Delft.

Bravery P.N.R., *Cardington Large Building Test Facility*, Construction details for the first building. Building Research Establishment, Internal paper, Watford (1993) 158.

British Steel plc, *The behaviour of multi-storey steel framed buildings in fire*, European Joint Research Programme, Swinden Technology Centre, South Yorkshire, 1999.

Demonceau J., *Steel and composite building frames: Sway-response under conventional loading and development of membrane effects in beam further to an exceptional actions.* PhD Thesis, University of Liege, Liege, 2008.

Demonceau J.F., Huvelle C., Comeliau L., Hoang L.V., Jaspart J.P., Fang C. et al, *Robustness of car parks against localised fire,* European Comission, Final Report RFSR-CT-2008-00036, Brussels, 2012.

Da Silva L. Simoes, Towards a consistent design approach for steel joints undergeneralized

loading, *Journal of Constructional Steel Research*, 64 (2008) 1059–1075.

De Wolf J. T., Sarisle, E. F., Column base plates with axial loads and moments, *Journal of Structural Division ASCE,* 106 (1980) 2167-2184.

Di Sarno L, Pecce M.R., Fabbrocino G., Inelastic response of composite steel and concrete base column connections, *Journal of Constructional Steel Research* 63 (2007) 819–832.

ECCS, European Convention for Constructional Steelwork, *Design of Composite Joints for Buildings.* Publication 109, TC11, Composite Structures, Belgium, 1999.

Ermopoulos J. Ch., Stamatopoulos G. N., Mathematical Modelling of Column Base Plate Connections, *Journal of Constructional Steel Research,* 36 (1996) 79-100.

Gresnigt N., Romeijn A., Wald F., Steenhuis M., Column Bases in Shear and Normal Force*, Heron* (2008) 87-108.

Heinisuo M., Perttola H., Ronni H., Joints between circular tubes, *Steel Construction*, 5(2) (2012) 101-107.

Henriques J., Behaviour of joints: simple and efficient steel-to-concrete joints, PhD Thesis, University of Coimbra, 2013.

Hofmann J. Behaviour *and design of anchorages under arbitrary shear load direction in uncracked concrete*, (Tragverhalten und Bemessung von Befestigungen unter beliebiger Querbelastung in ungerissenem Beton), PhD Thesis, IWB, University of Stuttgart, 2005.

Horová K., Wald F., Sokol Z., *Design of Circular Hollow Section Base Plates,* in Eurosteel 2011 6th European Conference on Steel and Composite Structures. Brussels, 2011 (1) 249-254.

Huber G., Tschemmernegg F., Modeling of Beam-to- Column Joints: Test evaluation and practical application, *Journal of Constructional Steel Research* 45 (1998) 119-216.

Jaspart J.P., Design of structural joints in building frames, *Prog. Struct. Engng Mater.*, 4 (2002) 18–34.

Jaspart J.P., *Recent advances in the field of steel joints - column bases and further configurations for beam-to-column joints and beam splices,* Professorship Thesis, Department MSM, University of Liege, Belgium, 1997.

Johansen K. W., *Pladeformler*, Kobenhavn, Pol. Forening, 1949.

Kuhlmann U. , Hofman J., Wald F., da Silva L., Krimpmann M., Sauerborn N. et al, *New market chances for steel structures by innovative fastening solutions between steel and concrete INFASO,* Final report EUR 25100 EN, European Commission, 2012.

Mallée R., Silva J. F., *Anchorage in Concrete Construction*, Ernst and Sohn Verlag, Darmstadt, 2006, ISBN 978-433-01143-0.

Maquoi R., Chabrolin B., *Frame Design Including Joint Behaviour*, ECSC, Report 18563. Luxembourg. Office for Official Publications of the European Communities, 1998.

Melchers R. E., Column-base response under applied moment, J*ournal of Constructional Steel Research* 23 (1992) 127-143.

Metric studs, Nelson stud welding specification, 2009, http://www.nelsonstud.com.

Metric studs, Nelson stud welding stud and ferrule catalog, 2013, http://www.nelsonstud.com.

Moore D.B. *Steel fire tests on a building framed. Building Research Establishment*, No. PD220/95, Watford (1995) 13.

Nakashima S., *Experimental behaviour of steel column-base connections*, Report, Osaka Institute of Technology, 1996.

Nakashima S., Mechanical Characteristics of Exposed Portions of Anchor Bolts in Steel Column Bases under Combined Tension and Shear. *Journal of Constructional Steel Research,* 46, (1998) 206-277.

Pallarés I., Hajjar J. F., Headed Steel Stud Anchors in Composite Structures: Part I – Shear, Part II – Tension and Interaction, The Newmark Structural Engineering Laboratory, NSEL-013, April 2009.

Penserini P., Colson A., Ultimate limit strength of column-base connections, *Journal of Constructional Steel Research* 14 (1989) 301-320.

Pertold J, Xiao R.Y, Wald F, Embedded steel column bases: I. Experiments and numerical simulation, *Journal of Constructional Steel Research*, *56 (3) 2000, 253-270.*

Pertold J, Xiao R.Y, Wald F, Embedded steel column bases: II. Design model proposal, *Journal of Constructional Steel Research*, *56 (3) 2000, 271-286.*

Pitrakkos T., Tizani W., Experimental behaviour of a novel anchored blind-bolt in tension Engineering Structures, 49, 2013, 905-919.

Romeijn A., The fatigue behaviour of multiplanar tubular joints*, Heron* 39 (1994) 3-14.

Simoes da Silva L., Simoes R., Gervasio H., *Design of Steel Structures, Eurocode 3: Design of steel structures, Part 1-1 General rules and rules for buildings.* ECCS Eurocode Design Manuals, 2010.

Steenhuis M., Wald F., Sokol Z., Stark J.W.B., Concrete in Compression and Base Plate in Bending*, Heron* 53 (2008) 51-68.

Thambiratnam, D. P., Paramasivam P., Base plates under axial load and moment, *Journal of Structural Engineering* 112 (1986) 1166-1181.

Wald F., Bouguin V., Sokol Z., Muzeau J.P., Component Method for Base Plate of RHS, Proceedings of the Conference Connections in Steel Structures IV: Steel Connections in the New Millenium, October 22-25, Roanoke 2000, s. IV/8- IV/816.

Wald F., Sokol Z., Jaspart J.P., Base Plate in Bending and Anchor Bolts in Tension, *Heron* 53 (2008) 21-50.

Wald F., Sokol Z., Steenhuis M. and Jaspart, J.P., Component Method for Steel Column Bases, *Heron* 53 (2008) 3-20.

Weynand K., Jaspart J.-P. Steenhuis M., *The stiffness model of revised Annex J of Eurocode 3*, in Connections in Steel Structures III, Pergamon, New York, 1996, 441-452.

Wilkinson T., Ranzi G., Williams P., Edwards M. Bolt prying in hollow section base plate connections*, in Sixth International Conference on Advances in Steel Structures and Progress in Structural Stability and Dynamics*, Hong Kong, 2009, ISBN 978-988-99140-5-9.

Software

Abaqus 6.11, *Theory Manual and Users Manuals*. Dassault Systemes Simulia Corp., 2011.

ACOP software, http://amsections.arcelormittal.com.

EC3 Steel Member Calculator for iPhone, CMM, Associacao Portuguesa de Construcao Metalica e Mista, https://itunes.apple.com/us/app/ec3-steel-member-calculator.

Sources

This Design manual I was prepared based on Final report (Kuhlmann et al, 2012). The following Figs were worked up according the Eurocodes and its background materials: EN1090-2:2008 Figs 8.1-8.3, EN1992-1-1:2004 Fig. 3.5, CEB-FIP:1990 Fig. 4.11, (Gresnight et al, 2008) Fig. 4.20, (Steenhuis et al, 2008) Figs 3.6-3.9, (Wald et al, 2008) Figs 4.1-4.8.

List of partners working on the dissemination project RFS2-CT-2012-00022 Valorisation of knowledge for innovative fastening solution between steel and concrete:

Ulrike Kuhlmann, Jakob Ruopp
  Institute of Structural Design
  University Stuttgart
  Pfaffenwaldring 7
  70569 Stuttgart
  Germany

Jan Hofmann, Akanshu Sharma
  Institute of Construction Materials
  University Stuttgart
  Pfaffenwaldring 4
  70569 Stuttgart
  Germany

František Wald, Šárka Bečková, Ivo Schwarz
  Czech Technical University in Prague
  Department of Steel and Timber Structures
  Thákurova 7
  16629 Praha
  Czech Republic

Luis Simões da Silva, Helena Gervásio, Filippo Gentili
  GIPAC – Gabinete de Informática e Projecto Assistido Computador Lda.
  Trav. Padre Manuel da Nóbrega 17
  3000-323 Coimbra
  Portugal

Markus Krimpmann
  Goldbeck West GmbH
  Ummelner Str. 4-6
  33649 Bielefeld
  Germany

Jörg van Kann
  stahl+verbundbau GmbH
  Im Steingrund 8
  63303 Dreieich
  Germany

Véronique Dehan
  ECCS - European Convention for Constructional Steel work
  AVENUE DES OMBRAGES 32
  1200 Bruxelles
  Belgium